2004

The role of a subsurface lime-fly ash barrier in the mitigation of acid sulphate soils

Laura J. Banasiak
University of Wollongong, lbanasia@uow.edu.au

THE ROLE OF A SUBSURFACE LIME-FLY ASH BARRIER IN THE MITIGATION OF ACID SULPHATE SOILS

A thesis submitted in fulfillment of the requirements for the award of the degree

MASTERS OF ENGINEERING - RESEARCH

From

UNIVERSITY OF WOLLONGONG

By

LAURA JOAN BANASIAK

B. Env. Sci. (Hons)

FACULTY OF ENGINEERING

2004

DECLARATION

I, Laura J. Banasiak, declare that this thesis, submitted in fulfilment of the requirements for the award of Masters of Civil Engineering, in the Faculty of Engineering, University of Wollongong, is wholly my own work unless otherwise referenced or acknowledged. This document has not been submitted for any qualifications at any other academic institution.

Laura B. Banasiak

21 December 2004

ACKNOWLEDGEMENTS

The success of this research can be partly attributed to the assistance of many people. Firstly, I would like to thank Professor Buddhima Indraratna, my supervisor, for his constant support and encouragement. He has assisted me in acquiring additional skills and knowledge relating to my research and has been a constant source of information and his expertise has been beneficial to my progress. I now have a greater sense of confidence in regards to my academic abilities.

I would also like to thank Roy Lawrie (NSW Department of Agriculture), David Clark and Robert Clark (Clarks Mining Services), John Boers (J. & M. Boers) for their technical advice and in-field assistance. Thank you to the staff led by Graham Lancaster at the Southern Cross University Environmental Analysis Laboratory for performing part of the water chemical testing. Thankyou to Greg Thompson and staff of Allen, Price and Associates for the surveying of the lime-fly ash barrier field site.

Thanks to the technical staff and students at the University of Wollongong, Faculty of Engineering for their assistance. Special thanks go to Bob Rowlan for his tireless help, knowledge and long days in the field and to Joanne George for her constant support in the Environmental Engineering Laboratory. I would also like to thank Ian Kirby, Ian Bridge, Ian Frew, Norm Gal, Mark Rigoni, Marcus Morgan and Alexandra Golab.

Without the support of local landholders this project would not have been possible. I would like to thank Neil and Kay Lord, Harris, the Forsyth Family for generously providing me with field sites.

Thank you to all my family for their support and encouragement throughout the completion of this thesis. Special thanks to my grandma and field work helper Joan Cowell who helped me and provided me with constant entertainment that made fieldwork more enjoyable. My grandpa Bill Cowell also deserves special thanks for his nifty gadgets that made field work just that little bit easier.

ABSTRACT

The effectiveness of using a sub-surface lime-fly ash barrier to reduce the oxidation of a pyritic soil layer and to improve groundwater and surface water quality was investigated for land affected by acid sulphate soils near Berry in southeastern NSW, Australia. Prior to the installation of the lime-fly ash barrier, groundwater and surface water analyses indicated a highly acidic environment. High concentrations of dissolved aluminium, total iron and sulphate in the groundwater were a result of falling groundwater tables and biotic oxidation. Traditional management techniques of ground water manipulation, via floodgates or weirs, would be rendered ineffective in arresting biotic oxidation where the pyrite layer is submerged.

The study combined field and laboratory analysis in order to determine the feasibility of the lime-fly ash barrier at the study site. A comprehensive field study incorporated the installation of piezometers and observation wells to determine the level of the phreatic surface along with the monitoring of water quality parameters at the site of the lime-fly ash barrier, and also floodgate sites and the site of the self-regulating tilting weir. The installation of the lime-fly ash barrier was undertaken by the pumping of a slurry through boreholes via pressure pumping.

The subsurface lime-fly ash barrier, as an acid sulphate soil remediation technique, was shown to significantly improve groundwater quality. Groundwater pH increased to values between 4.5 and 5.5. The concentration of the pyritic oxidation products, acidic cations Al^{3+} and Fe^{total}, basic cations Ca^{2+} and Mg^{2+} and anions Cl^- and SO_4^{2-}, also, on average decreased in the groundwater after the installation of the lime-fly ash barrier. A comparison between the average groundwater table elevations before and after the installation of the barrier also indicated a perched water table, which would reduce the exposure of pyritic soil to oxygen, and in turn reduce pyritic oxidation and the generation of acidic products.

The Lime-fly ash barrier is effective in remediating acid sulphate soils in areas in which floodgates and weirs cannot be installed. A comparison of the result shows that the lime-fly ash barrier had greater success in increasing the groundwater pH than

the self-regulating tilting weir. The lime-fly ash barrier treats acid sulphate soils and the related environmental problems before they occur, whereas, the floodgates treat the pyrite oxidation products generated after they have been discharged into the flood mitigation drains. Significantly greater concentrations of Al^{3+}, Fe^{total} and SO_4^{2-} were found in the groundwater at the floodgate sites.

TABLE OF CONTENTS

LIST OF FIGURES

LIST OF TABLES

LIST OF PLATES

Chapter 1 Introduction

1.1 General Background

The presence of acid sulphate soils and their associated problems have been largely ignored or unrecognised in the past, despite the fact that they were identified by Australian soil scientists as early as 1963 (Walker, 1963). Artificial drainage has increased the distribution, magnitude and frequency of acid generation from oxidised acid sulphate soils which has in turn increased the rate of estuarine acidification by many orders of magnitude, a rate greater than that which may have occurred under natural drought/flood cycles (Lin *et al.*, 1995a).

The Shoalhaven floodplains are the most southern (35°S) of Australia's twelve floodplains known to have acid sulphate soils (Willett *et al.*, 1992). This region is very low lying with the pyritic soil layer within close proximity to the surface organic layer (Pease, 1994). For this reason, the pyrite layer is usually submerged contradicting the low pH levels that were recorded throughout the year of research (Pease, 1994). While the submergence of the pyrite layer by elevating the groundwater table via weir operation can successfully reduce new acid formation, the biological oxidation of pyrite under submerged conditions can still prevail if the organic content and the sulphidic constituents in clayey soils are high.

1.2 Purpose of Study

Previous acid sulphate soil management strategies have involved restoring the phreatic zone above the pyritic layer through the installation of weirs within the drain to decrease the production of acidic oxidation products and reduce the transport of these products to the drains. The amount of new acid produced was reduced, however the large amount of acid previously generated within the soil profile was not investigated. This current research involves an alternative practical solution, namely lime barrier creation. Research completed by Blunden (2000) validated the use of static weirs to raise groundwater levels as a method of submerging the potential acid sulphate soil layers, thereby significantly lowering the amount of oxygen reacting with pyrite, hence, decreasing acid production. However, in very low-lying areas of the Shoalhaven Floodplain where the water table is relatively high, a significant

amount of acid is still being formed. The use of static weirs is not practical in such low-lying areas, because any further increase in groundwater table elevation would create accessibility problems.

Recent studies conducted at the University of Wollongong (Rudens, 2001) suggest that in acidic groundwater conditions with relatively high organic matter, the bacterium *Thiobacillus ferrooxidans* can directly oxidise pyrite under submerged conditions. Preliminary small-scale experiments suggest that lateral injection of lime-fly ash slurry to create an alkaline barrier above the pyrite layers may reduce the bacterial activity, while simultaneously neutralising the acid already produced.

Preliminary tests indicate the presence of relatively shallow pyrite layers, which need to be treated by means other than groundwater table manipulation. The rate of acid formation by biotic oxidation can be many factors greater than conventional oxidation reactions; hence, in low-lying areas of high organic content, lime-fly ash injection to create alkaline barriers above the potential acid sulphate soils layers is to be investigated. Therefore, the purpose of this study is to examine the effect of a lime-fly ash barrier on the groundwater and drain water acidity and to compare this with sites remediated by other techniques, such as weirs and modified floodgates.

1.3 Research Aims

The specific aims of this research were to:

- Undertake a comprehensive literature review on acid sulphate soils and an analysis on the use of grouting techniques to remediate acid sulphate soils.

- Introduce an alternative practical solution (lime-fly ash barrier installation) to the remediation of acid sulphate soils in low-lying areas, which based on preliminary studies at the University of Wollongong, has shown good potential as an effective way of controlling the soil and groundwater acidity.

- Investigate the impact of the barrier on groundwater and surface water quality and compare this with results obtained from sites with other remediate structures i.e. weirs and modified floodgates.

1.4 Thesis Structure

This thesis is divided into four sections, as outlined below:

1.4.1 Part I: Literature Review

Chapter 2 presents a literature review, which outlines the important aspects of acid sulphate soils. The physical and chemical properties of acid sulphate soils are detailed, as well as pyrite oxidation and acid production. The environmental impacts of pyrite oxidation and resulting acid production and on-ground management and acid sulphate soils remediation strategies are described. Chapter 2 also describes the analytical and numerical solutions for modelling the oxidation of pyrite and other sulphidic materials and reviews previous acid sulphate soil rehabilitation research and management strategies relevant to this current study.

In Chapter 3 a detailed description of the theory related to the lime-injection technique is given. The principles of grouting theory are introduced and the properties and requirements of grouts relevant to this study are considered.

1.4.2 Part II: Field trial of Sub-surface Lime-Fly ash Barrier

Chapter 4 describes the location and geomorphology of the study sites and the climatic conditions of the area and identifies the methods of soil physical and chemical analysis that were employed in this study. The equipment used to monitor the physical and chemical characteristics of the groundwater and surface water at the study sites and the climatic conditions of the area obtained over the entire study period are also described in Chapter 4.

In Chapter 5, the methodology involved in the installation of the Lime-Fly ash Barrier is outlined. The equipment used in the injection process is described and the

evaluation of the barrier in the field via trench investigations and observation wells is reviewed.

1.4.3 The impact of the Sub-Surface Lime-Fly ash Barrier on groundwater and surface water quality

The groundwater elevation data measured at the lime-fly ash barrier study site is presented in Chapter 6. The elevation of the groundwater table in relation to the location of the acid sulphate soil layer is addressed and a comparison between the pre- and post-barrier groundwater table elevation characteristics are also described.

The influence of the barrier on the groundwater and surface water forms a major part of this research. In Chapter 7, groundwater and surface water quality properties that were measured before and after the installation of the lime-fly ash barrier are described and analysed. Changes in groundwater and surface water quality at the floodgate and weir sites are described in Chapter 8. Chapter 9 compares the water quality properties measured at the lime-fly ash barrier site and the floodgate/weir sites.

1.4.4 Conclusions and Recommendations

Chapter 10 presents the findings of this research in relation to the effectiveness of a sub-surface lime-fly ash barrier in remediating acid sulphate soils. Recommendations for future research are also discussed.

Chapter 2 Literature Review

2.1 Introduction

This Chapter is divided into three sections. The first section describes the processes involved in the formation of pyrite and acid sulphate soils. The physical and chemical properties of acid sulphate soils are also detailed, along with environmental and engineering problems associated with the oxidation of pyrite. The second section describes the use of lime and fly ash in soil improvement. The final section of this chapter reviews previous on-ground management and acid sulphate soil remediation strategies conducted in Australia. The principle of tidal buffering is introduced, as is the use of permeable reactive barriers. Research shows that regardless of previous efforts, an alternative management strategy is necessary to combat the problems associated with acid sulphate soils. Chapter 3.0 expands on this by describing the principles involved in this study.

2.2 Introduction to Acid Sulphate Soils

Dent and Pons (1995) state that acid sulphate soils are the 'nastiest soils in the world'. Acid sulphate soils (ASS) are basically soils containing appreciable amounts of sulphide minerals, which have been allowed to oxidise by exposure to air and have become acidic. The common form of sulphide mineral is pyrite (FeS_2), however other sulphidic compounds such as iron monosulphide (FeS), greigite (Fe_3S_4) and various organic sulphides, may also exist in small concentrations (Bloomfield, 1973; Bush and Sullivan, 1996). Under reducing conditions, acid sulphate soils remain chemically inert, and on oxidation, complex chemical changes take place, generating acidic drainage, often abnormally high in trace metals such as aluminium, which leaches from the soil and into estuaries (Dent, 1986).

Increased population pressure has led to the rapid reclamation of coastal land and has resulted in the environmental degradation of estuarine ecosystems due to the development of acid sulphate soils (Lin *et al.*, 1995a). In NSW and other parts of the Australian coastal zone, natural controls have caused major accumulation of pyrite in Holocene sediments of estuarine flood plains. Due to the depositional environment in which they form, subsurface concentrations in Australia are commonly above the

management action criteria of $0.55S_{cr}\%$ set by Stone *et al.* (1998). Some of these areas have been drained over many years for agricultural grazing and cropping, and enhancement of these drainage systems for flood mitigation since the 1950s appears to have increased the degradation of the estuaries. The problems from acid sulphate soils are now being exacerbated by other activities such as engineering constructions, extractive industries, urban developments and some aquaculture projects. For many estuaries, during some rainfall/flood events, the limit of the neutralising capacity for the acid output is now being greatly exceeded (Lin *et al*, 1995b).

While pyrite oxidation is influenced by anthropogenic activities, natural control on pyrite oxidation may take place in any area of acid sulphate soils that has an extremely dry climate or has at least experienced a significant period of low rainfall in the past. Acid sulphate materials produced during prolonged drought episodes are not re-pyritised to a significant extent in the reduced conditions existing during the subsequent periods of high rainfall. The acidified pyritic layer can act as a storage sink of acid sulphate materials, which can be moved upwards by capillary action and acidify the non-pyritic topsoils (Lin *et al*, 1995b).

The term 'potential acid sulphate soils' has been used to distinguish unoxidised acid sulphate soils (pyrite remains in soil due to its reducing environment) from developed acid sulphate soils (pyrite is oxidised due to oxidising environment) (Lin and Melville, 1993). Potential acid sulphate soils are usually waterlogged soil that is unoxidised. Any disturbance that admits oxygen will lead to the development of actual acid sulphate layers. It is often assumed that potential acid sulphate soils are completely innocuous to the environment if kept under water. Actual acid sulphate soils overlay potential acid sulphate soils in Australian coastal environments.

2.2.1 Formation of Pyrite

The world pattern has been driven mainly by postglacial sea level change. The last glacial maximum was at least 18000 years B.P. and the current sea levels have been relatively stable for the last 3000 years (Thom and Chappell, 1975; Roy, 1984; Woodroffe *et al.*, 2000). The rise in sea during this period created conditions conducive to pyrite formation and resulted in extensive deposits of sulphidic

sediments (Woodroffe *et al.*, 2000). Each regional pattern is also determined by its unique sedimentary and geomorphological history. In tidal swamp and marsh, bacteria (*Desulfovibrio desulfuricans*) decomposing the abundant organic matter reduce SO_4^{2-} from the tidewater and Fe (III) oxides from the sediment. The main end product is pyrite, FeS_2 that may attain concentrations of 15% by mass or 100kg/m^3 of mud where sedimentation is slow (Dent and Pons, 1995). Pyrite itself may occur as loose assemblages of individual crystals or as dense, spherical clusters (framboids) commonly 10-20μm diameter (Ritsema *et al.*, 2000).

The recovery of sea level in the Holocene was accompanied by the building up of 'bottomless' sulphide clays where sedimentation kept pace with the rising sea level and pyrite accumulated under mangroves and reed swamp. Under more recent, more stable sea levels, there has been a rapid seaward growth of deltas and infilling of estuaries, producing thin (<3m thick) sulphide clays in enclosed, brackish water swamps, overlying non-sulphide tidal flat deposits. Some of these Holocene sulphide sediments have been drained naturally or through changes in the distributary channels in deltas (Dent and Pons, 1995). Holocene-age (<10000 years BP) sulphide sediments were formed in estuarine lowlands throughout the world following the last major sea-level rise (Berner, 1984).

Pyrite forms during shallow burial via the reaction of detrital iron minerals with H_2S. The H_2S in turn, is produced by the reduction of interstitial dissolved sulphate by bacteria using sedimentary organic matter as a reducing agent and energy source. The major factors controlling how much pyrite can form in sediment are the amounts of organic matter and reactive iron minerals deposited in sediment, and the availability of dissolved sulphate (Berner, 1984). Pyrite is formed in low energy estuarine systems by a bacterial catalysed reaction requiring a reducing environment, a source of sulphate, presence of labile organic matter and a source of iron (Dent, 1986). High temperatures of the tropics and subtropics, particularly in location of large tidal exchange, allow maximal pyrite accumulation (Lin *et al.*, 1995a).

The first step in the overall process of sedimentary pyrite formation is the bacterial reduction of sulphate. This process occurs only under anoxic conditions. Dissolved

oxygen migrates into the sediment from the overlying water via molecular diffusion, wave and current stirring, or bioturbational irrigation but is consumed by oxic bacteria, living near the sediment-water interface, which use the oxygen to convert organic matter to CO_2. This prevents the O_2 from penetrating far into the sediment and as a result, anoxic conditions necessary for bacterial sulphate reduction result below a depth normally of a few centimetres (Berner, 1984). The major factors controlling the rate of bacterial sulphate reduction in normal marine sediments (those deposited in oxygenated bottom waters) is the amount and especially the reactivity of organic matter deposited in the sediment and the availability of dissolved sulphate.

The common factors in the formation of pyrite are (i) a supply of SO_4^{2-}, usually from tidewater, which is reduced to sulphides by bacteria decomposing the organic matter; and (ii) a supply of Fe from the conditions, which are most abundantly fulfilled in tidal swamps and salt marshes. Pyrite formation requires decomposable organic matter and SO_4^{2-} to produce H_2S, Fe to produce metastable Fe sulphides, and an oxidant such as molecular O_2 to transform H_2S to elemental sulphur S that can react with the metastable sulphides to form FeS_2 (Ritsema *et al.*, 2000). The chemical reaction can only take place under anoxic environments and with a sufficient supply of organic matter and dissolved sulphate thus allowing the reduction of sulphate to sulphides (mainly pyrite) through the action of sulphate-reducing bacteria (Pons, 1973; Berner, 1984; Dent, 1986).

Pyrite formation is also limited by the amount and reactivity of detrital (not total iron deposited) iron minerals added to the sediment. In terrigenous marine sediments deposited under normal oxygenated conditions, the iron minerals are sufficiently abundant and reactive. Therefore, they don't pose a serious threat. In highly calcareous sediments (derived from the skeletal debris of marine organisms) there is insufficient iron to bring about appreciable pyrite formation (calcareous skeletal debris is much lower in iron than terrigenous material). Even in the presence of high organic matter concentrations and abundant H_2S, if CaCO3 dominates the sediment, the pyrite concentration is low (Berner, 1984).

The process of pyrite accumulation in acid sulphate soils is shown in the following figure.

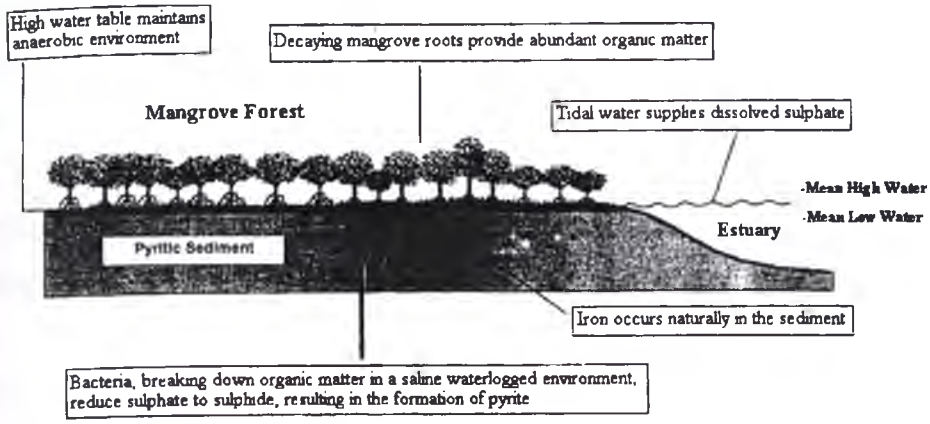

Figure 2.1: Environmental Conditions required for pyrite accumulation (Naylor et al., 1995)

The overall chemical reaction can be expressed by the following equation (Dent, 1986):

$$\underbrace{Fe_2O_{3(s)}}_{\text{iron}} + \underbrace{4SO_{4\ (aq)}^{2-}}_{\text{sulfate}} + \underbrace{8CH_2O}_{\text{organic matter}} + \tfrac{1}{2}O_2 \xrightarrow{\text{bacterial driven with reducing conditions}} \underbrace{FeS_{2(s)}}_{\text{pyrite}} + \underbrace{8HCO_3^-}_{\text{bicarbonate}} + 4H_2O \qquad (2.1)$$

It has been suggested that hydrogen sulphide must be firstly formed and then reacted with iron oxides to produce pyrite (Equation 2.2 and 2.3) (Bohn et al., 1989). Equation 2.3 differs from Equation 2.1 in that iron monosulphides is shown to form.

$$SO_{4(aq)}^{2-} + 2CH_2O_{(s)} \xrightarrow{\text{bacteria}} H_2S_{(g)} + 2HCO_{3(aq)} \qquad (2.2)$$

$$3H_2S_{(g)} + 2FeOOH_{(s)} \longrightarrow FeS_{(s)} + FeS_{2(s)} + 4H_2O_{(l)} \qquad (2.3)$$

Quantitative estimates of the rate of FeS_2 accumulation range between $7x10^{-8}$ to $5x10^{-1}$ mol S/dm^3/yr (Ritsema *et al.*, 2000).

In localities far removed from terrigenous clays or silts, and where the sediments instead consist almost entirely of calcium carbonate derived from the skeletal debris of marine organisms, there is insufficient iron to bring about appreciable pyrite formation. Iron is commonly found within coastal clay soils and is supplied in iron

oxides including oxyhydroxides such as goethite, FeOOH, and hydroxides and oxides such as hematite, Fe_2O_3 (Blunden, 2000). Fanning (1993) suggested that oyster communities commonly form on mangrove brace roots of Rhizophora by utilising bicarbonate. The remnants of these oyster shells provide the main buffering store for most acid sulphate soils in the form of calcium carbonate. In terms of neutralisation capacity, they make up no more than 0.5% by mass of sulphur (Dent, 1993). Even in the presence of high organic matter concentrations and abundant H_2S, if $CaCO_3$ dominates the sediment the pyrite concentration is low (Berner, 1984).

In summary, pyrite formation results from the reaction of H_2S, from bacterial sulphate reduction, with reactive detrital iron minerals. In freshwater sediments this process is limited by low concentrations of dissolved sulphate. As a result, little pyrite is formed and there is no simple correlation between organic carbon and pyrite sulphur. In normal marine sediments (those deposited in oxygen-containing bottom waters), pyrite formation is limited mainly by the amount and reactivity of organic matter buried in the sediment, and as a result pyrite sulphur and organic carbon correlate positively with one another (Berner, 1984).

2.2.2 Distribution of Acid Sulphate Soils

Acid sulphate soils are widely distributed in the coastal marshy areas of many locations in the world (Calvert and Ford, 1973). van Breeman (1980) estimated that there are 12-14 million ha of acid sulphate soils worldwide by restricting a survey to Holocene coastal plains and tidal swamp sediments. They are concentrated in otherwise densely settled coastal floodplains, mostly in the tropics, where development pressures are intense and little suitable alternatives land for expansion of farming or urban and industrial development exists. Two-thirds of the known extent is in Vietnam, Thailand, Indonesia, Malaysia and northern Australia (Ritsema *et al.*, 2000). Table 2.1 shows the worldwide distribution of acid sulphate soils (Brinkman, 1982).

Table 2.1: Calculated worldwide distribution of acid sulphate soils (Brinkman, 1982)

Region	Area of ASS ($x10^6$ ha)
Africa	3.7
Asia	6.7
Latin America	2.1
Australia	1.0

These estimates however appear to be modest. According to Lin and Melville (1992) the Australian coastal zone has about 1.2 x 10^6 ha of sulphidic sediments, containing ~10^9 t of pyrite. However, Naylor *et al.* (1995) mapped landform elements likely to contain acid sulphate soils for the coast of New South Wales. These maps showed that New South Wales has 0.4-0.6 x 10^6 ha of acid sulphate soils. If the extent of acid sulphate soils throughout Northern Australia is similar to that in New South Wales, then more than 3 x 10^6 ha of acid sulphate soils may exist in Australia (White *et al.*, 1997).

Acid sulphate soils exhibit enormous spatial variations that are tied to the dynamic estuarine, deltaic and floodplain environments of which they are a part. The conditions suitable for the formation of pyrite in sediments lend clues to the location of acid sulphate soils in the coastal zone (Naylor *et al.*, 1995). Acid sulphate soils occur in wave protected mangroves and marshes, outer barrier tidal lakes, and backswamp areas where the accumulation of organic matter and reduced sediments can occur (Naylor *et al.*, 1995). Tidal flushing adds low concentrations of dissolved oxygen necessary to complete pyritisation of sulphate and remove bicarbonates, thereby maintaining favourable slightly acidic conditions (van der Kevie, 1973; Pons *et al.*, 1982).

The rate of sedimentation in coastal environments may also have an impact on the location of acid sulphate soils. Pons and van Breeman (1982) suggest that a slow sedimentation rate is likely to form high pyritic concentrations due to the kinetics of pyrite formation. Rapid sedimentation may hinder the transformation of monosulphides to pyrite (Goldhabar and Kaplan, 1982; Lin and Melville, 1994).

The catchments of most rivers along the coast of New South Wales are reasonably small as a result of the close proximity to the Eastern Range. Estuarine sediments (due to low sedimentation rates in the estuarine embayments) are often sulphide-rich with reduced S contents exceeding 2 per cent (Lin, 1999). Sulphidic sediments have been found in most estuarine lowlands and coastal embayments along the eastern (Walker, 1972) and northern Australian coasts, as well as in parts of Western Australia, South Australia and Victoria (Berner, 1984). Acid sulphate soil has been reported to occur in only a few Australian inland areas where pedogenesis has been influenced by iron sulphide-rich rock (Davison *et al.*, 1985; Kraus, 1998). The distribution of acid sulphate soils along the coast of New South Wales is shown in Figure 2.2).

They also exhibit very significant temporal variability, not least in their defining characteristics of acidity and related toxicities. Acid sulphate soils export their problems in drainage and floodwaters; consequently, both reliable static soil survey and dynamic chemical/hydrological modelling are required to provide useful information for soil environmental management (Ritsema *et al.*, 2000).

2.3 Properties of Acid Sulphate Soils

This section describes the processes involved in the oxidation of pyrite and the physical and chemical characteristics of acid sulphate soils. It also illustrates the impact of acid generated from acid sulphate soils on the soil, groundwater and surface water environment.

2.3.1 Oxidation of Pyrite

The chemical, physical and biological reactions, and the interactions between these processes that occur during the oxidation of pyrite in acid sulphate soils are complex and not well understood (Dent, 1986). It is recognised that the accumulation of acid sulphates in soil profiles is brought about by the bacterial and chemical oxidation of sulphides in pyrite (FeS_2) (Calvert and Ford, 1973).

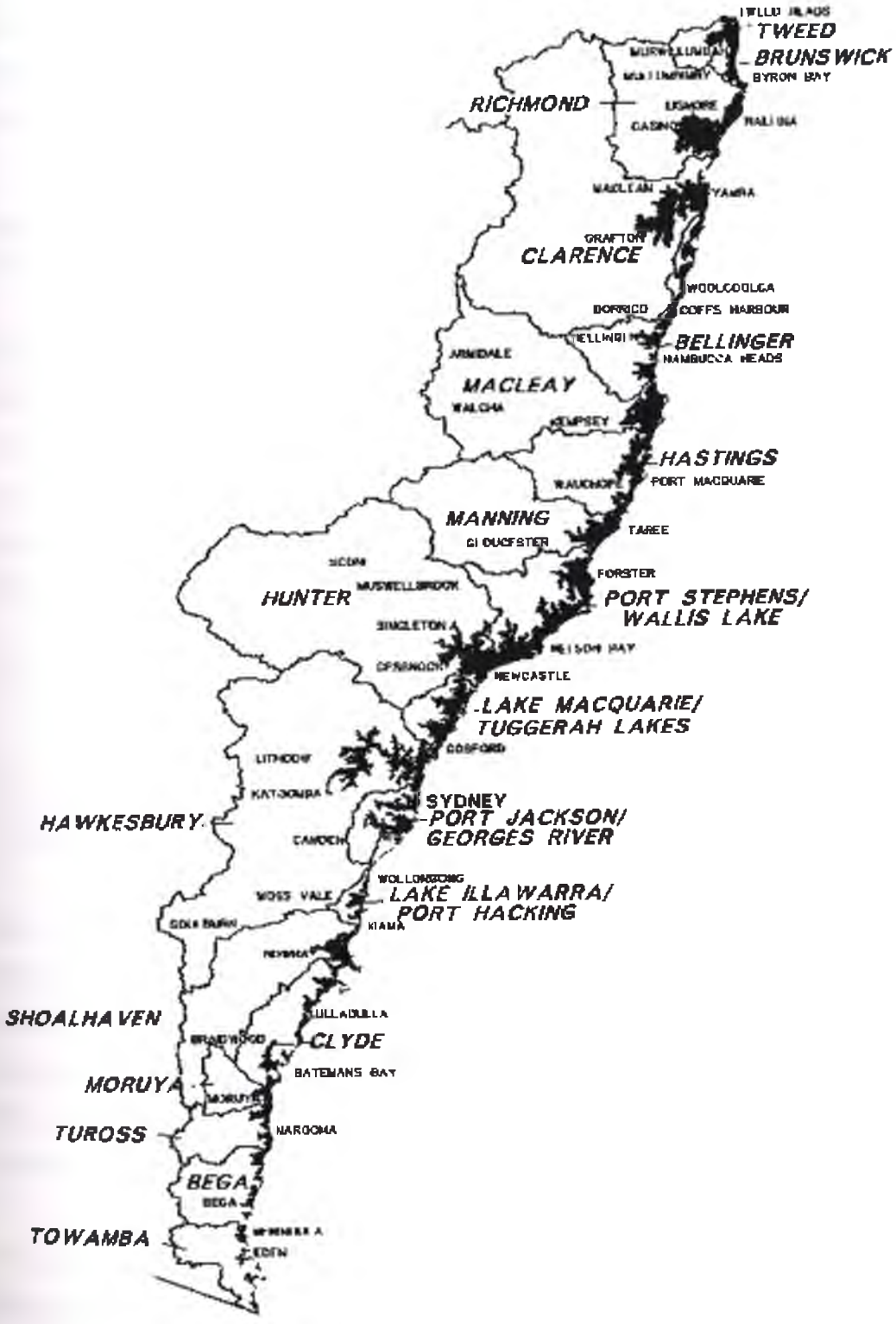

Figure 2.2: Risk map of acid sulphate soils within coastal NSW (Naylor et al., 1995)

Pyrite is stable under severely reducing conditions but oxidation, following drainage, generates sulphuric acid and mobile Fe^{2+}. The complex series of reactions may be simplified to:

$$\underset{\text{Pyrite}}{FeS_{2\,(s)}} + \underset{\text{Oxygen}}{7/2O_{2\,(aq)}} + H_2O \rightarrow \underset{\text{Iron}}{Fe^{2+}_{(aq)}} + \underset{\text{Sulphuric acid}}{2SO_4^{2-}_{(aq)}} + 2H^+_{(aq)} \qquad (2.4)$$

For every tonne of sulphidic material that completely oxidises, 1.6 tonnes of pure sulphuric acid is produced. The dissolved Fe^{2+}, SO_4^{2-} and H^+ produced in Equation 2.4 are readily transported in soil water, groundwater and drainage water. The second stage oxidation of Fe^{2+} (Equation 2.5) may occur at some distance from the original source of pyrite, either in other soils or in drainage and floodwater (Dent and Pons, 1995).

$$Fe^{2+}_{(aq)} + 1/4O_{2\,(aq)} + 3/2H_2O \rightarrow \underset{\text{Ochre}}{FeO{\cdot}OH_{(s)}} + \underset{\text{Acid}}{2H^+_{(aq)}} \qquad (2.5)$$

This oxidation can produce iron oxyhydroxide or hydroxide flocs that coat benthic communities and stream banks (Sammut *et al.*, 1996).

The presence of bacteria enhances the oxidation processes by orders of magnitude (Ritsema *et al.*, 2000). The microorganisms involved are Fe- or S-oxidising bacteria, chiefly, *Thiobacillus ferrooxidans*, which is an autotrophic microorganism. Bacteria present in the soil derive energy for growth from that released during the oxidation of FeS_2. Through this, they catalyse a series of chemical reactions and under certain conditions speed up the oxidation process considerably (Ritsema *et al.*, 2000).

The oxidation of FeS_2 depends on the supply of O_2, the availability of water, and the physical properties of FeS_2 for the reaction to proceed and generates acid and releases heat; consequently, the acidity and temperature of the surrounding solution would affect the overall reactions (Ritsema *et al.*, 2000). The supply of oxygen to cultures of bacteria is, in some respects, the most important factor determining their activity. Supplying oxygen, or air, to a bacterial oxidation system in which solid rock particles are present generally involves two factors: (i) aeration of a portion of the bacterial

solution, and (ii) circulation of aerated solutions to the site of bacterial activity. These two factors mutually determine the influence of aeration on bacterial activity, and both must be considered in evaluating the performance of a bacterial oxidation system (Malouf and Prater, 1961). *T. ferrooxidans* are facultative with respect to their oxygen requirements, requiring low or undetectable oxygen concentrations, as shown in Figure 2.3. Therefore, they do not require oxygen if a substitute electron acceptor is present, such as the ferric ion.

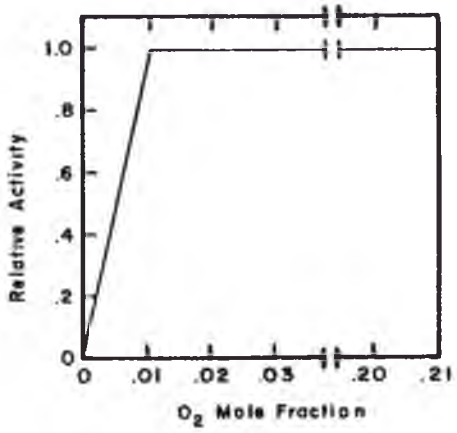

Figure 2.3: Influence of oxygen concentration on bacteria activity (Jaynes et al, 1984)

Temperature, which influences both chemical and microbial oxidation, is an important factor in determining the oxidation rate of pyritic materials. Biological oxidation only occurs between 0 to 55°C (optimum 24-45°C) but chemical oxidation can take place above this temperature (Ritsema *et al.*, 2000). Maximum bacterial activity has been found to occur at approximately 35°C (Malouf and Prater, 1961), as shown in Figure 2.4. Below 35°C, the rate of bacterial action decreases non-linearly as the temperature is reduced. The oxidising bacteria are also active only in acid media.

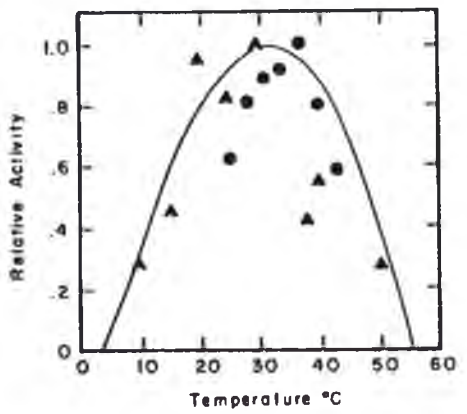

Figure 2.4: Influence of temperature on bacterial activity (Jaynes et al, 1984)

In general, bacterial action is most pronounced in a media having a pH of between 2.0 and 3.5. Both above and below this range the rate of bacterial oxidation decreases, and at pH values above 6.0 bacterial action is almost completely inhibited. In alkaline media (pH 9) the bacteria are destroyed (Malouf and Prater, 1961). The optimum pH for bacterial oxidation of pyrite is 3.2 (Jaynes *et al.*, 1984), as illustrated in Figure 2.5.

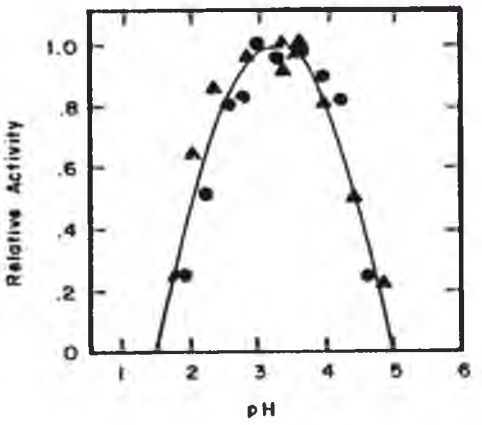

Figure 2.5: Influence of pH on bacteria activity (Jaynes et al, 1984)

The role of microorganisms in the oxidation of pyrite has been classified as either direct or indirect (Evangelou, 1995). The direct role (iron II formation) involves the attachment of microorganisms to the surface of FeS_2, which results in pitting of the mineral surfaces. This causes corrosion of insoluble minerals allowing metals otherwise locked inside mineral particles to dissolve. It is believed that the bacteria that has a direct role can oxidise elemental sulphur and metal sulphides, according to the following reaction:

$$S_2^{2-} + 4O_2 \rightarrow 2SO_4^{2-} \quad (2.6)$$

Disulphide (pyrite) + Oxygen + Bacteria → Sulphate

The indirect role (Iron III formation) involves the oxidation of pyritic minerals by the products of microbial metabolism. It is believed that this process enhances the oxidation process by orders of magnitude as previously mentioned (Ritsema *et al.*, 2000). Pantelis and Ritchie (1992) introduced a ceiling temperature (100°C) above which microorganisms cease to be effective as catalysts in FeS_2 oxidation.

The iron (II) that is produced from pyrite oxidation (Equation 2.2) can undergo further oxidation to form ferric iron (iron III) if the pH is at 3.5 or below. This reaction, however, is slow, with a half-life in the order of 100 days (Evangelou, 1995). Certain types of bacteria (*T. ferrooxidans*) can act as catalysts for this reaction. Nordstrom (1982) represented these chemical reactions that involve *T. ferrooxidans*, shown in Figure 2.6. This diagram identifies the iron minerals that are associated with the biological oxidation of pyrite within acid sulphate soils.

The bacteria can oxidise Iron (II) according to the following equation:

$$Fe^{2+} + 1/2O_2 + 2H^+ + \text{bacteria} \rightarrow Fe^{3+} + H_2O \quad (2.7)$$

Iron (II) Acid Iron (III)

The Iron (III) produced by this reaction is able to oxidise pyrite within the soil, even under anaerobic conditions (Moses *et al.*, 1987), as shown by the following equation.

$$FeS_2 + 14Fe^{3+} + 8H_2O \rightarrow 15Fe^{2+} + 2SO_4^{2-} + 16H^+ \quad (2.8)$$

Pyrite Iron (III) Iron (II) Sulphate Acid

A simplified equation of the overall process of complete pyrite oxidation is:

$$FeS_2 + 15/4O_2 + 7/2H_2O \rightarrow Fe(OH)_3 + 2SO_4^{2-} + 4H^+ \quad (2.9)$$

In this equation, for every one mole of pyrite consumed, 4 moles of acid are generated.

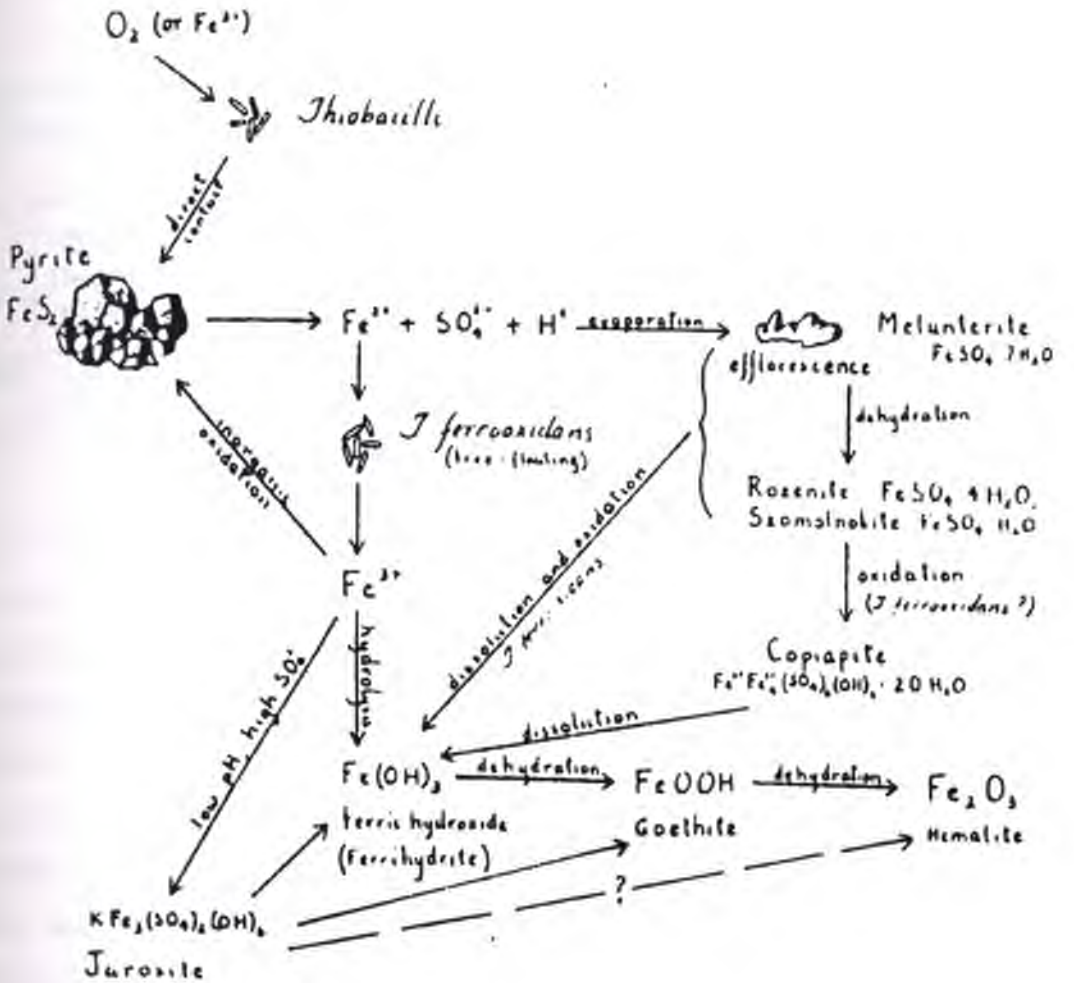

Figure 2.6: Sequence of mineral reactions for biological pyrite oxidation, showing relationships between oxidising agents, catalysts and mineral products (Nordstorm, 1982)

2.3.2 Physical Properties of Acid Sulphate Soils

The physical properties of acid sulphate soils determine the rate of acid generation and its discharge to the surrounding environment. Due to the depositional environment the soil structure of potential acid sulphate soils is texturally uniform with a fine, tortuous, heterogenous pore space and is usually saturated with moisture contents of over 80% (Blunden, 2000), giving the soil a texture similar to that of a gel (White and Melville, 1993). Chapman (1994) reported saturated hydraulic conductivities between 0.83-1.12 mm/h for potential acid sulphate located near Berry, NSW. These low hydraulic conductivities reduce both the influx of oxygen into the soil and the drainage of these soils. The lack of a lot of organic matter in acid sulphate soils causes the soil to compact and have relatively low permeabilities. Typical physical properties of acid sulphate soils are shown in the following table.

Table 2.2: Physical properties of potential acid sulphate soil layer (Blunden and Indraratna, 2000)

Soil Layer	Bulk Density (kg/m^3)	Hydraulic Conductivity vertical (m/day)	Hydraulic Conductivity horizontal (m/day)	Porosity (%)	Residual moisture content (volumetric)	Saturated moisture content (volumetric)
Potential ASS	1030	2.02	0.20	61	0.06	0.49

Cation exchange processes due to the development of acid sulphate soils enlarges pore size due to clay flocculation and the formation of aggregates (Mulvey, 1993). The combination of clay flocculation and plant and animal intrusion increases the soil macroporosity, permeability and diffusivity (Blunden, 2000). A change in the colloidal structure of the clay fraction of the soil due to the oxidation of pyrite is known as 'ripening' (van Breeman, 1973; Dent, 1986). In this process, potential acid sulphate soils undergo shrinkage due to the removal of water from the vadose zone. White and Melville (1993) reported that a potential acid sulphate soils with 80% volumetric moisture content had a shrinkage of 50% upon complete drying. This process can restrict plant growth through increased waterlogging and flooding.

2.3.3 Oxidation Products

Raw acid sulphate soils can be identified by straw yellow mottles of jarosite $KFe_3(SO_4)_2(OH)_6$ that develop around pores and on ped faces and by acid, red drainage water. Occasionally, organic-rich soils that remain wet do not develop yellow mottles, although they become severely acid, possibly because of formation of iron-organic complexes that pre-empt precipitation of jarosite (Andriesse, 1993). Acid sulphate peats do not have jarosite but often exhibit an inky black subsoil as some of the SO_4^{2-} generated by drainage is reduced to FeS deeper in the profile (Ritsema *et al.*, 2000).

Jarosite is formed as a by-product of the pyrite oxidation process and as a result is most often observed in old root channels (where the oxygen has reached the pyrite as the root decomposed), in soil cracks, and on banks or cuttings. These roots often

become jarositic and then over time become iron-coated as the jarosite is converted to a 'rust-red' iron coating. The formation of jarosite is described by:

$$3Fe(OH)_3 + 2H_2SO_4 + K^+ \rightarrow \underset{\text{Jarosite}}{KFe_3(SO_4)_2(OH)_6} + 3H_2O + H^+ \quad (2.10)$$

Jarosite is part of the rhombohedral alunite group of minerals and K may be substituted for Na, Pb, NH_4, H_3O, and Fe^{2+} for Fe^{3+} or Al^{3+} (Lin *et al.*, 1998). Jarosite hydrolyses slowly and represents a substantial store of acidity in the oxidised profile as shown in Equation (2.11).

$$\underset{\text{Jarosite}}{KFe_3(SO_4)_2(OH)_6} + 3H_2O \rightarrow 3Fe(OH)_3 + \underset{\text{Acid}}{SO_4^{2-}} + K^+ + 3H^+ \quad (2.11)$$

Acid sulphate peats do not have jarosite but often exhibit an inky black subsoil as some of the SO_4^{2-} generated by drainage is reduced to FeS deeper in the profile (Ritsema *et al.*, 2000). The formation of jarosite depends on a number of factors, including oxidising conditions (Eh), the pH of the pore water, and a sufficient supply of K, Fe and SO_4 (Lin *et al.*, 1998). Significant accumulation of jarosite in the upper layers of an acid sulphate soil profile indicates that the formation rate of jarosite is quicker than its dissolution rate. Eh-pH diagrams, such as Figure 2.7 show that jarosite is formed under strongly oxidising (Eh>400) and acidic conditions (pH<4). When the Fe oxidises at a higher Eh, the ferrous sulphate can be converted to ferric sulphate minerals, such as jarosite, depending on the pH (Fanning *et al.*, 2002). The figure shows mineral phases that might be expected to be stable under various conditions and colours likely to be associated with these minerals.

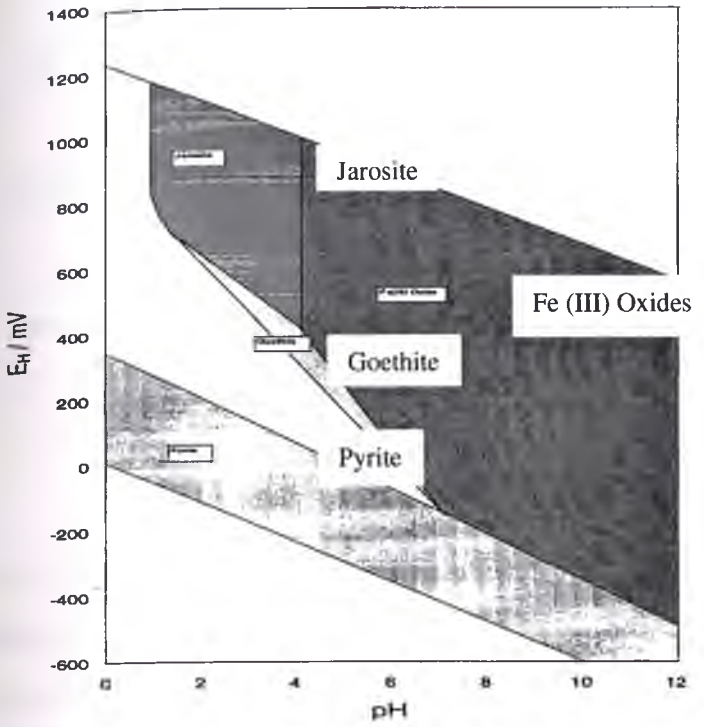

Figure 2.7: Idealised Eh-pH diagram for the Fe-S-O system (van Breeman, 1976)

2.3.4 Acid Drainage

Three factors determine the amount of acid sulphate oxidation products removed from soil systems to drainage systems (Lin *et al.*, 1995b):

(a) The intensity of sulphuric acid production in the soil;

(b) The starting depth of the oxidised pyritic layer relative to the drain base; and

(c) The effectiveness of the drainage system in exporting water from coastal flood plains.

The construction of deep flood mitigation drains in SE NSW during the 1960s has caused major problems. The deep drains create a steeper hydraulic gradient, which causes an increase in groundwater flows and a faster generation of acid. Figure 2.8 shows how acid drainage is generated from acid sulphate soil. The oxidation of the pyrite layer is due to dissolved oxygen in the water moving through the soil. The pyrite layer can also be directly exposed to oxygen when the base of the drain wall cuts into it.

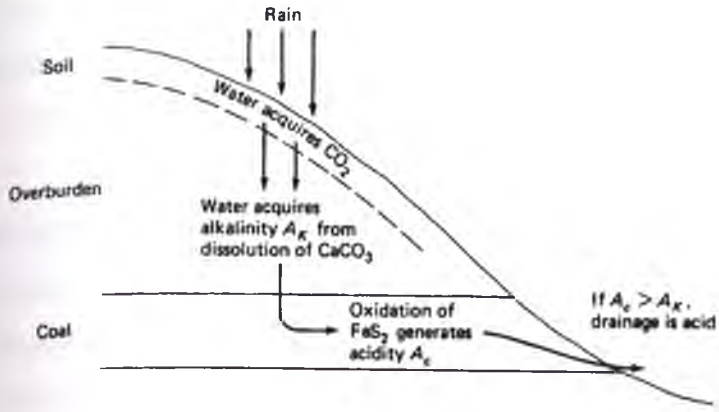

Figure 2.8: Generation of acidic water by drainage (Drever, 1997)

2.3.5 Release of Metals

The acid drainage water generated attacks clay minerals to release silica and metal ions principally liberating soluble aluminium. The formation of aluminium hydroxy ions blocks negatively charged sites in silicate clays, liberates other metals, and limits cation exchange (Nriagu, 1978).

$$(K_{0.5}Na_{0.36}Ca_{0.05})(Al_{1.5}\ Fe^{3+}_{0.25}\ Mg_{0.3})(Al_{0.45}Si_{3.46})(O_{10}OH)_2 + 7.41H^+ + 2.59H_2O \rightarrow 0.5K^+ + 0.36Na^+ + 0.05Ca^{2+} + 0.3Mg^{2+} + 0.25Fe(OH)_3 + 1.95Al^{3+} + 3.46H_4SiO_4 \quad (2.12)$$

Studies on aluminium states of buried mangrove soils in the Clarence River floodplain (Lin and Melville, 1992) show that both monomeric aluminium (0.01M $CaCl_2$ extract) and exchangeable aluminium (1M KCL extract) concentrations are closely correlated to pH (R=-0.75, n=22; and R=-0.67, n=22, respectively). Monomeric aluminium concentration values at 57.6mg/kg (mean value of the top 1 metre of soil profile) and the exchangeable aluminium concentration reaches a mean value of 1292 mg/kg (Lin and Melville, 1992).

The clarification of water by the flocculation of aluminium further acidifies the water and lead to increased UVB infiltration, enhanced acid tolerant plant growth in deeper water, and increased temperature (Brierley, 1995). The quantity of soluble Al released in the soil layers containing acid sulphates is of particular interest since aluminium toxicity in acid soils is considered to be a factor in poor growth of plants

(Calvert and Ford, 1973). Iron, potassium, sodium and magnesium, as in the acid hydrolysis of the common estuarine clay mineral illite (Nriagu in Sammut et al., 1996), can also be released.

Soluble ferrous iron is present at pH<4 in acidified drainage water, but when pH increases above 4, and oxygen is present, iron oxyhydroxides may be formed (Simpson and Pedini, 1985). Iron produced can range from insoluble Fe (III) oxides and hydroxides such as goethite ($Fe_2O_3 \cdot H_2O$) to haematite in severely oxidised soils. Soluble forms of iron include iron sulphate hydroxides (Nordstrom, 1982). The oxidation of ferrous iron (an initial product of pyrite oxidation) to iron hydroxide, consumes oxygen and releases hydronium ions (H_3O^+), thereby decreasing dissolved oxygen concentration and pH (Sammut *et al.*, 1995).

The oxidation of pyrite also produces large concentrations of sulphates. Hydrated ferrous sulphate minerals can concentrate and precipitate within macropores formed by old root channels. Wilson (1995) described sulphates that can form by this process. These included melanterite ($FeSO_4 \cdot 7H_2O$), rozenite ($FeSO_4 \cdot 4H_2O$) and szomolnokite ($FeSO_4 \cdot H_2O$). Sodium sulphate salts may also arise as a by-product of the oxidation of pyrite. The dissolved salt, Na_2SO_4, is brought to the surface through capillary action or by an increase in watertable height due to rainfall or a change in hydrological conditions (Fanning, 1993). Evaporation then results in salt formation at the surface and promotes flocculation and cracking of the soil, which in turn increases the transport of oxygen to the pyritic material.

Drainage water may also be enriched in heavy metals, which can be highly toxic to plants and gilled organisms (van Breeman, 1973; Nriagu, 1978; Willett *et al.*, 1982; Ritsema *et al.*, 2000) and can corrode engineering infrastructures (White and Melville, 1993; Sammut *et al.*, 1996). In acid sulphate soils, the most common heavy metals are Zn, Cd, Cu, Ni, Mn, Cr, Pb, Au and Co. Toxic drainage waters may be released only episodically, for example, at the onset of the wet season after a period of low watertable during which oxidation has taken place (Ritsema et al., 2000). Sammut *et al.*, (1996) and Indraratna and Blunden (1997) have reported dissolved aluminium concentrations up to three orders of magnitude in excess of these guideline

recommendations in surface and groundwater discharged from oxidising acid sulphate soils.

Metal toxicity is dependent on a number of characteristics including the concentration of metal ions, the concentration of suspended matter, pH, redox potential, salinity, alkalinity, temperature, and numerous physico-chemical factors. Blunden (1997) verified that both Al and Fe concentrations decreased logarithmically with a decrease in pH (Figure 2.9). The solubility of most of the common metal ions increases when the groundwater pH falls below 5.5. ANZECC (1992) recommended that aluminium concentrations in coastal waterways should be less than 5μg L^{-1} when the pH is less than 5.5 to ensure the protection of the ecosystem.

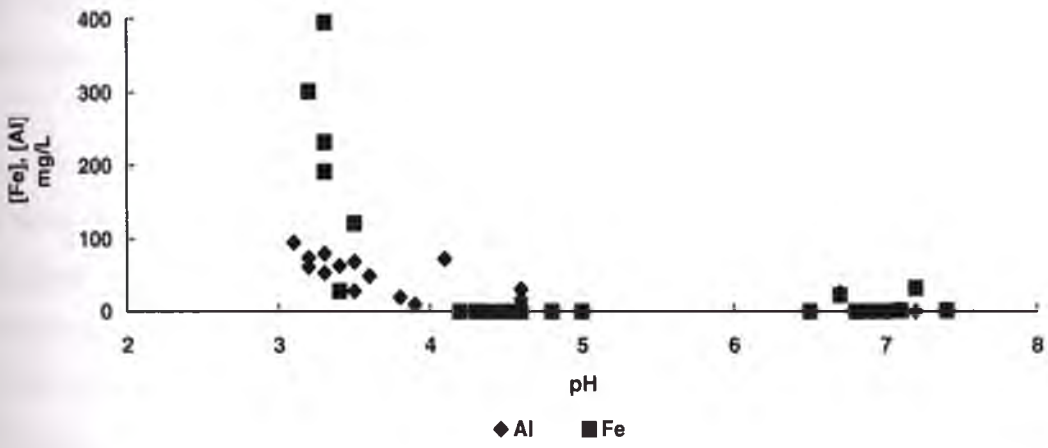

Figure 2.9: Relationship between pH and concentrations of $[Al^{3+}]$ and $[Fe^{3+}]$ (Indraratna, Sullivan and Nethery, 1995)

2.4 Problems associated with Acid Sulphate Soils

The development of acid sulphate soils in coastal floodplains can cause a number of environmental, agricultural and engineering problems. Acid drainage has deleterious impacts on aquatic environments and plant life.

2.4.1 Impacts on aquatic environment

Toxic drainage waters may be released from acid sulphate soils only intermittently, for example, at the onset of rainfall after a period of low watertable during which oxidation has taken place. Acid drainage can have disastrous effects on freshwater

and estuarine fisheries, especially on invertebrates that are unable to escape. Hydrogen ions and dissolved species of monomeric aluminium and iron play crucial roles in fish and crustacean deaths (Driscoll *et al*, 1980).

Massive fish kills and ulcerative diseases have often been reported in estuarine waters but these have only recently been linked to acid sulphate soils (Ritsema *et al.*, 2000). Massive fish kills associated with toxic aluminium laden water have been recorded in several Australian rivers (Brown *et al.*, 1983; Easton, 1989). When dissolved aluminium binds to negatively charged gill surfaces, this displaces calcium and gill permeability is increased (Playle and Wood, 1991). This results in a net efflux of sodium and chloride from the bloodstream under freshwater conditions causing an ionic imbalance and physiological stress (Freda and McDonald, 1988). Gill damage has been suggested as a cause of fish mortalities in Australia where acidified water and high concentrations of aluminium have been recorded (Brown *et al.*, 1983).

An ulcerative fish disease, epizootic ulcerative syndrome (EUS), has shown a pattern of seasonal recurrence in eastern Australia and this is now believed to be related to estuarine contamination by acid sulphate draining water with low pH and high concentrations of dissolved aluminium (Lin and Melville, 1992). Callinan *et al.*, (1989) showed that massive invasion of the skin by fungi plays a central role in the induction of ulcers. Acid-induced skin damage, like experimental abrasion, may allow the invasion of the skin by *Aphanomyces* sp. propagules, such as zoospores, leading to the development of EUS lesions (Sammut *et al.*, 1995). This is supported by Callinan *et al.* (1995) who found that EUS affected yellowfin bream (*A. australis*) collected in water with pH 5, had bronchitis and areas of epidermal degeneration and necrosis consistent with acid-induced damage.

The impact of acid sulphate soils on aquatic animal life is of particular economic interest because 70% of all commercial species spend some portion of their life cycle in estuarine environments (Sammut *et al.*, 1996). The EUS costs commercial estuarine fisheries on Australia's east coast approximately A$1 million in discarded fish annually (Callinan *et al.*, 1995). Mass mortalities of worms and crustaceans in an acidified tidal reach have also been reported (Sammut *et al.*, 1996).

Iron may also have deleterious effects on aquatic fauna. Simpson and Pedini (1985) reported that iron precipitated as iron hydroxide onto the gills of crustaceans and fish, limited gas exchange and caused suffocation. They also reported that iron precipitates and decreases in dissolved oxygen caused by the iron oxidation process might affect eggs and larvae.

Impacts on aquatic plants are due to direct toxicity of acid and dissolved species as well as to changes in the light climate (Sammut *et al.*, 1996). While the clarification of streams by aluminium flocculation has significant ecological impacts on the benthic communities (Sammut *et al.*, 1994), iron flocs also tend to smother and kill vegetation and lead to the destruction of fish eggs, loss of habitat, reduced recruitment and a decrease in the availability of nutrients (Sammut *et al.*, 1996). Decaying vegetation coupled with extensive iron flocs and sulphate in estuarine water may lead to the formation of large amounts of iron monosulphides that can oxidise rapidly when exposed to air. The effects on aquatic vegetation are more variable since many species rooting in the reduced mud are little affected. Species of reed (Phragmites australis), rush (Juncus spp.) and water lily (Nymphaea spp.) often become dominant in freshwater subject to acid flumes (Ritsema *et al.*, 2000).

2.4.2 Impacts on terrestrial plant life

Chemical problems are variable due to the wide range of tolerances of different plants. At pH of less than 3.5, Fe^{3+} and H^{+} are likely to be inhibitory (to plant metabolism), then up to pH 5.0 aluminium and ammonium ions may be the major inhibitors.

The quantity of soluble Al released in the soil layers containing acid sulphates is important since aluminium toxicity in acid soils is considered to be a factor in poor growth of plants. Al^{3+} accumulates in root tissues and prevents cell division and elongation resulting in stunted roots, where concentrations as low as 1 to 2ppm could be toxic (Dent, 1986). Fe^{2+} may be toxic in flooded soils, so too hydrogen sulphide ($1\text{-}2 \times 10^{6}$mol m^{-3} may impair root functioning) though usually only above pH of 5. CO_2 concentrations may also rise to 15kPa in flooded soils that is enough to retard

root development (Dent, 1986). Manganese ions are directly toxic to plants as they affect the metabolism of the plant, with toxicity symptoms including chlorosis (yellowing) of the leaves and necrosis (dead, brown tissue) of the leaves.

The occurrence of acid scalds also has an impact on plant growth. In general, the formation of acid scalds can be attributed to high acid levels and associated element toxicities and nutrient deficiencies (Lin *et al.*, 2001b). In the Shoalhaven Floodplain, a small scald has developed in an area that has been extensively drained to assist in draining water from the surrounding land for grazing. In areas where the acid sulphate soil layer is exposed to the surface, large scalds can occur in which few plants can survive and surface cracking enhances oxygen transport (Sammut *et al.*, 1996). Lin *et al.* (2001b) found that, in general, scaled acid sulphate soils have less organic matter and soluble phosphorus, and a greater salinity, soluble acidity, soluble Al, Mn and Zn concentrations, compared with adjacent non-scaled acid sulphate soils. The low phosphorus reserve in the scalded soils implies that the availability of phosphorus may be insufficient in the scaled soil to raise the pH. Greater soil acidity and EC values in scaled areas, relative to their adjacent non-scalded soils, may be attributed to inputs of acid runoff from surrounding areas, as well as the upward movement of soluble salts and acid sulphate products, through capillary action, from the underlying sulphidic sediments (Lin *et al.*, 2001b).

2.4.3 Engineering problems

Engineering problems include:

1. Corrosion of steel and concrete;
2. Uneven subsidence, low bearing strength and fissuring leading to excessive permeability of unripe soils;
3. Blockage of drains and filters by ochre; and
4. The difficulties of establishing vegetation cover on earthworks and restored land (Ritsema *et al.*, 2000).

In relation to concrete structures, unless these have low porosity, acid can react with calcium carbonate and calcium hydroxide to form gypsum.

$$\underset{\text{Calcium carbonate}}{CaCO_3} + \underset{\text{Acid}}{H_2SO_4} + H_2O \rightarrow \underset{\text{Gypsum}}{CaSO_4.2H_2O} + CO_2 \quad (2.13)$$

$$\underset{\text{Calcium Hydroxide}}{Ca(OH)_2} + \underset{\text{Acid}}{H_2SO_4} + H_2O \rightarrow \underset{\text{Gypsum}}{CaSO_4.2H_2O} \quad (2.14)$$

The gypsum further reacts with tricalcium aluminate $3CaO.Al_2O_3$ in the concrete, forming etteringite $3CaO.\ Al_2O_3.CaSO_4.32H_2O$. The formation of both gypsum and etteringite involves an increase in volume (van Host and Westerveld, 1973). Therefore, the concrete expands and becomes weak eventually resulting in failure. Due to their high volumetric moisture content, acid sulphate soils have a low bearing capacity and foundations often require extensive reinforcements to offset subsidence and localised failure (Dent, 1986).

Iron and sulphides released indirectly from oxidised pyrites may lead to the formation of sludges that clog the pores of drainpipes and ditch banks and thus make field drainage of agricultural lands difficult (Calvert and Ford, 1973).

2.5 Hydrological Dynamics of Acid Sulphate Soils

2.5.1 Subsurface Water Flow

Subsurface water flow in acid sulphate soils is a critical factor in the impacts of acidic groundwater drainage on surrounding waterways. Therefore, an understanding of groundwater hydrology is necessary for determining the characteristics of acid transport. The flow of groundwater in soil is controlled by differences in hydraulic gradients. The relationship between the flux of water, pressure gradients, and hydraulic conductivity, which is a function of soil porosity, is shown by Darcy's Law:

$$q = -K \frac{\Delta h}{\Delta s} = -ki \quad (2.15)$$

where, v = Darcy flux or specific discharge velocity, k = hydraulic conductivity, Δh = total head potential, Δs = length of soil elements, and i = hydraulic gradient

The flow velocity (v) is referred to as Darcy's Velocity. This is proportional to the hydraulic gradient of the water i.e. the hydraulic head difference over the distance of flow. Darcy's Law is only sufficient when the entire flow system is known.

2.5.2 Hydrological Interactions

In Acid Sulphate Soils floodplains, the production, transport and quality of acidic water sourced from the oxidation of pyrite is controlled by the water balance of the floodplain and its upland catchment. To develop appropriate acid sulphate soil management strategies it is essential to understand a number of properties. White *et al.* (1997) summarised these as:

(1) The depth of the acid sulphate soil layer from the surface;
(2) The dynamics of the groundwater table relative to the acid sulphate soil layer;
(3) The impact of climate, drain and land management on the floodplain water balance and its control of water table dynamics and export of oxidation products.

An expression of the water balance of a coastal floodplain is given by (White *et al.*, 1997):

$$P + I + L_i = E_t + R + L_o + D + \Delta S \qquad (2.16)$$

where, P is precipitation, I is irrigation, L_i is the lateral inflow of water, E_t is evapotranspiration, R is surface runoff, D is vertical drainage to the water table, ΔS is change in groundwater and soil-water storage (positive or negative) above the water table, and L_o is the lateral outflow (all units are measured in volume per unit area of the floodplain, generally in mm water). Acid sulphate soils occur where E_t and $P > E_t$ are the dominant factors. This results in the inundation of low-lying backswamps for prolonged periods of time. The high density drainage greatly increases the rate of L_o, but this does not alter P or E_t (assuming cropping density does not differ vastly from natural vegetation), thus a net increase in the water discharged from the system occurs (Indraratna et al., 2001). In dry summer periods when evapotranspiration rates increase production and export of acidity depends on temporal variability and its

impact on the change in soil water storage above the pyritic layer, ΔS (White *et al.*, 1997).

According to White *et al.* (1997) the change in shallow watertable height, ΔH, at any given time period is a function of the vertical drainage, D, lateral groundwater inflows, L_{gi}, and outflows, L_{go}, direct evaporation from the water table, E_g, and the available porosity of the soil expressed as specific yield, Y_g, which is the volume of groundwater per unit area per unit change in water table height. Therefore, the shallow groundwater dynamics in the vertical plane can be described by:

$$Y_g \ \Delta H = D + L_{gi} - (E_g + L_{go}) \qquad (2.17)$$

The groundwater recharge rate, $E_g \leq E_t$ and $D - E_g$, is determined by comparing Equations 2.16 and 2.17.

2.5.3 Effect of Prolonged Wet and Dry Periods on Floodplain Hydrology

White *et al.* (1997) states that upland inflow depends on the area of the upland catchment A_u, upland rainfall P_u, and the fraction of rainfall r_u, which becomes inflow to the total floodplain area A_f so that:

$$L_i = \frac{r_u P_u A_u}{A_f} \qquad (2.18)$$

In wet periods, $P_u \approx P$, $r_u \approx 1$, and the water table is at or above the surface. Due to this, drainage to the water table (D) is close to zero and water storage is from ponded surface water (ΔS_p). The water balance for the floodplain under very wet conditions can be described by (White *et al.*, 1997):

$$P\frac{A_f + A_u}{A_f} \approx E_t + L_O + \Delta S_p \qquad (2.19)$$

In eastern Australia most river catchments are relatively small (A_f/A_u of order 10) (White *et al.*, 1997). Therefore, Equation 2.19 shows that upstream inflow can have a major influence on the floodplain water balance during wet periods. During dry periods when inflow, drainage, and outflow are negligible, the water table is solely

determined by evaporation from the watertable. This is described as (White *et al.* 1997):

$$Y_g \cdot \Delta H = -E_g \qquad (2.20)$$

The rate of evaporation from the water table is influenced by surface vegetation, its leaf area and rooting depth, solar radiation, humidity, wind speed, air temperature and pressure, soil water availability, position of the water table and soil hydraulic properties (White *et al.*, 1997). The potential evaporation (E_p) at a well-watered site with short grass was calculated by White *et al.* (1997) using Brutsaert's (1982) equation:

$$E_p = E_q + E_a \qquad (2.21)$$

where, E_q is the equilibrium evaporation determined by the net radiation and air temperature, and E_a is the drying power of the air dependent on wind speed, vapour pressure deficit (dryness of air), air temperature and pressure.

Brutsaert's (1982) defines E_q, which is related to R_n (net radiation) as:

$$E_q = \frac{\Delta(R_n - G)}{(\Delta + \gamma)\lambda} \qquad (2.22)$$

where, G is the daytime heat flux into the ground (about 5% of R_n), Δ the slope of the saturation vapour pressure versus temperature curve at the air temperature of interest, γ the psychrometric constant and λ the latent heat of vaporisation.

Indraratna *et al.* (2001) and Blunden (2000) showed the effect of evapotranspiration on reducing watertable height during a drought (Figure 2.10). After 250 days, acid production is occurring in the soil as an effect of the drought period i.e. low rainfall-evapotranspiration.

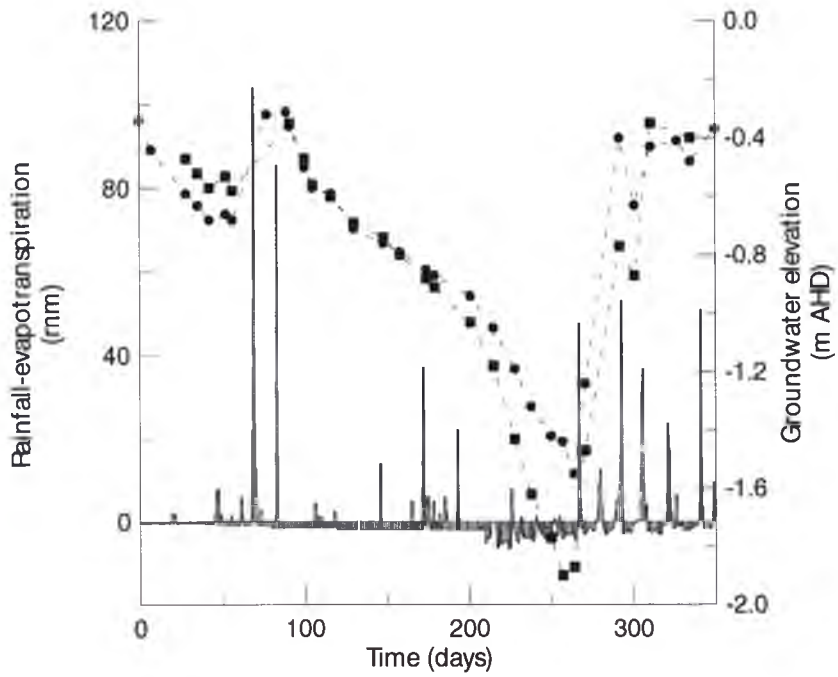

Figure 2.10: Groundwater elevation at 10 m (•) and 90 m (■) from the drain, with the rainfall and evapotranspiration per day for the 1997-1998 period (Indraratna et al., 2001)

2.5.4 Artificial Drainage

Artificial drainage has taken place throughout the world and in particular eastern Australia in order to increase agricultural productivity. The network of extensive floodplain drainage system in the coastal floodplains has had a large impact on the hydrology. Natural drainage across floodplains have been straightened, deepened and widened and floodgates have been installed to the detriment of the surroundings areas. Figure 2.11 is a schematic representation of a typical flood mitigation system.

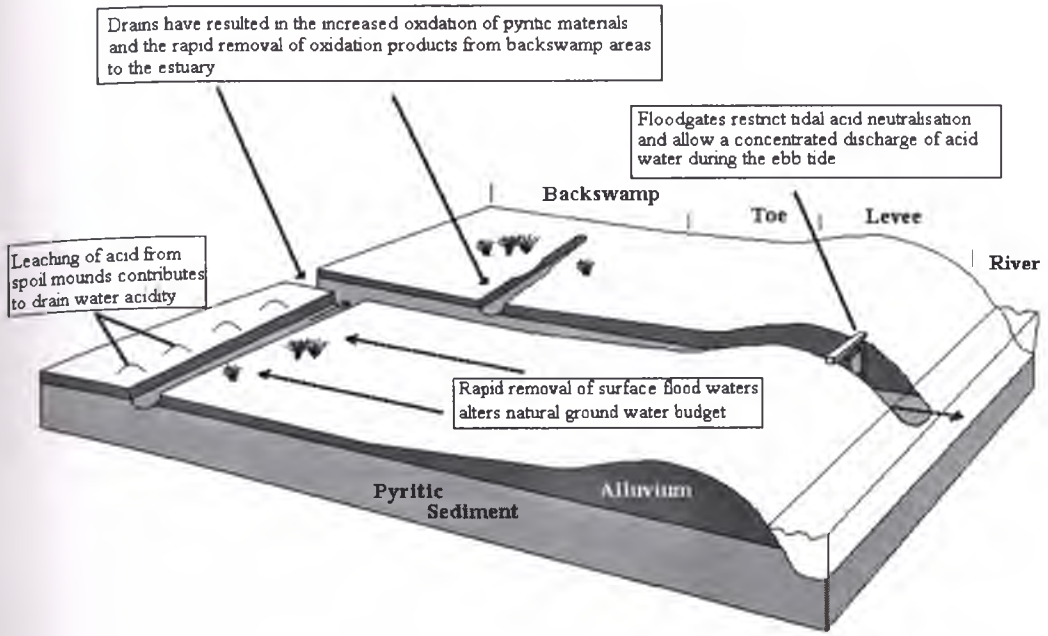

Figure 2.11: Artificial drainage scheme for an acid sulphate soil affected floodplain (Naylor et al., 1993)

2.5.5 One-way Floodgates

One-way floodgates prevent the neutralisation of acidic drain water by tidal inflows of estuarine water. Acid reservoirs can occur behind the floodgates and acts as a barrier to fish migration, impeding feeding, recruitment and breeding (Sammut *et al.*, 1996). The occurrence of flood events after long periods of drought can lead to a slug of acidic water into estuaries. Groundwater flushing following large rainfalls (>50mm) has been linked to fish kills and decreased pH levels (Sammut *et al.*, 1995). On the Tweed River, approximately 2600 tonnes of sulphuric acid can be released annually through floodgates (Wilson, 1995). A difference in hydraulic gradients, shown in Figure 2.12, promotes the transport of oxygen into sulphidic subsoil material and the leaching of acid products into the drain.

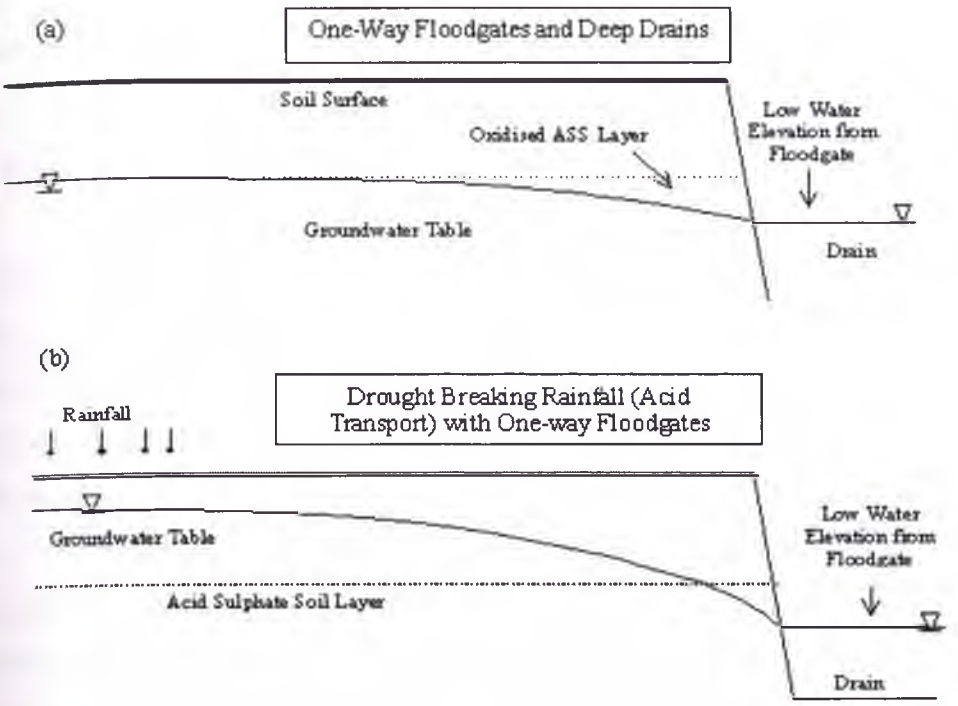

Figure 2.12: Impact of one-way floodgates on groundwater elevation under normal (a) and flood (b) conditions (Glamore, 2003 adapted from Indraratna et al., 2002)

Artificial drainage systems modify the habitat upstream of the control structures. With restricted tidal inflow, the upstream reaches become less saline therefore, less buffered than the tidal reaches downstream. Floodgates also dampen water level fluctuation in the upstream reaches. Freshwater habitat is expanded at the expense of important brackish water habitat, and the flood-gated reaches are more susceptible to acidification (Sammut *et al.*, 1995).

2.5.6 *Tidal Buffering*

Tidal buffering is known as the transportation of carbonate (CO_3^{2-}) and bicarbonate (HCO_3^-) anions, which are buffering agents, throughout an estuary. The effective concentrations of these anions, particularly bicarbonate are related to estuarine pH. Equation 2.23 shows the buffering reaction of sulphuric acid (pK_a = -3) with bicarbonate to form carbonic acid (pK_a = 3.8) (Stumm and Morgan, 1996).

$$\underset{}{Ca^{2+}} + \underbrace{HCO_3^-}_{\text{Saline water}} + \underbrace{H^+ + SO_4^{2-}}_{\text{ASS oxidation}} \rightarrow \underbrace{H_2CO_3}_{\text{Weak Carbonic Acid}} + Ca^{2+} + SO_4^{2-} \qquad (2.23)$$

For every mole of bicarbonate available, one mole of H^+ ions is consumed. The removal of $[H^+]$ from solution by the formation of H_2CO_3 raises pH levels (Indraratna *et al.*, 2002). The removal of hydrogen ions in solution by the formation of H_2CO_3 leads to an increase in pH as shown below (Indraratna *et al.*, 2002).

Strongly acidic, highly ionised:

$$H_2SO_4 \rightarrow 2H^+ + SO_4^{2-} \quad (2.24a)$$

Weak acid, less ionised:

$$H_2CO_3 \leftarrow HCO_3^- + H^+ \quad (2.24b)$$

$$H_2CO_3 \leftarrow CO_3^{2-} + 2H^+ \quad (2.24c)$$

It is possible to determine the resultant pH when tidal mixing occurs by attaining the neutralising capacity of the alkaline water. If brackish water with an alkalinity of 6.25 x 10^{-4} moles of proton per litre (1/4 of seawater) were mixed in equal proportions with acidic water (with a pH of 4.0), then the resulting pH would be 6.89 (Indraratna *et al.*, 2002).

2.6 Management and Rehabilitation of Acid Sulphate Soils

There are a number of practical management techniques to help manage acid sulphate soils and alternatives for reclaiming acid sulphate soils. The best acid sulphate soils management option (Dent, 1986; White and Melville, 1993) is to keep the soil in a natural, undisturbed state. Avoiding the disturbance of potential acid sulphate soils is both cost effective and environmentally efficient. In areas that have already been affected by acid sulphate soils, treatment may be needed to improve both the water and soil quality of the areas. In undrained areas where the pyrite layer is less than 0.5 metres below the ground surface, any development that involves drainage should be avoided (White *et al.*, 1996). In undrained areas where the pyrite layer is 0.5 to 2.0 metres below the soil surface, drainage should only be attempted with properly designed drains and control of the acid released (White *et al.*, 1996).

Bowman (1996) outlined a number of management techniques to prevent the oxidation of pyrite within acid sulphate soils profiles. These included:

1. Water table control

2. Capping
3. Excavation and removal
4. Reduced permeability
5. Biotreatment

Understanding groundwater is the key to better management of acid sulphate soils, especially in drained sub-catchments. Water table control returns the unoxidised sulphidic materials to anoxic conditions beneath the water table. This however, only prevents further oxidation but does not deal with existing acidity unless severely reducing conditions are also reinstated (Ritsema *et al.*, 2000). In order to minimise the amount of acid generated in acid sulphate soils in a drained catchment is necessary to limit the exposure of pyrite in the soil to oxygen. Also acid can still be generated even under anaerobic conditions due to the action of bacteria. As was mentioned earlier, microorganisms act as a catalyst in the first stages of oxidation of Fe^{2+}.

Capping involves the placement of a relatively impermeable material over the sulphidic material to lower the rate of oxygen and water entering the soil. This lowers the acid production rate and the rate at which the acid is drained from a site. The problems with capping of acid sulphate spoils have proved universally ineffective since this does not prevent continued oxidation of the sulphide (Ritsema *et al.*, 2000).

By using compaction, clay sealing layers and geotextiles the permeability of the potential acid sulphate soil layer can be decreased by interception, lateral diversion or reduced transmissivity. The influx of water is stripped of dissolved oxygen by microbial activity in the topsoil.

Biotreatment, which is a technique not commonly used in Australia, involves retarding the soils oxidising microorganisms' catalytic influence on pyrite oxidation by sterilising the soil. Anionic surfactants, organic acids and food preservatives have been used as bactericides, are commonly sprayed directly on the soil (Evangelou, 1995). There has been limited research into bactericide products that can eliminate the iron and sulfur oxidising bacteria.

2.6.1 Oxidation and Leaching

Leaching involves the excavation of actual or potential acid sulphate soils into raised stockpiles. To prevent contamination of groundwater and streams, the stockpiles should be located away from any freshwater. The time required to complete oxidation and leaching is unpredictable and is influenced by factors such as rainfall, temperature, wind speed, and the size and shape of the stockpile (White and Melville, 1993).

2.6.2 Removal of Pyritic Material

Excavation and removal of acid sulphate soils involves moving the affected soil and burying it beneath a permanent water table in a pit excavated in a non-acid sulphate soil area. It can also involve storage below a permanent water body with a protective cover of clean sediment; burial in thin compacted layers within an earthen mound that is capped with low permeability, non-acid sulphate soil material.

2.6.3 Acid Neutralisation

The application of chemical neutralisation materials can take various forms, including direct application through liming, active barrier systems, profile mixing and sub-surface lime injection.

2.6.4 Liming

The addition of calcium carbonate ($CaCO_3$) or agricultural lime to acid sulphate soils is the most common method of liming. Liming affected acidic areas can help to neutralise them. Lime can be applied to both soil and water bodies. Applying lime to soil requires thorough mixing of the soil and lime in order to neutralise the acid in the soil. Mechanical mixing with a rotary hoe device may be used to mix lime into the topsoil. A disadvantage of this method is that only the topsoil layer is directly mixed with the lime. It is also however not an economically viable technique (Shearer, 2001), as large amounts of lime would be needed and the application of lime needs to be repeated to keep the pH to the required levels. Drain liming may be effective when only a relatively small amount of acidity is contained within the drain water. Applying lime to open drains can be done by placing sandbags (with lime

incorporated in them) on the drain face. When leachate water flows through the bag it is neutralised. Water bodies can also be directly neutralised by adding lime by a concrete pump, as a slurry to be affective in water.

2.6.5 Permeable Reactive Barriers

Permeable Reactive Barriers (PRBs) are a relatively new, innovative and passive technique for groundwater remediation. A permeable reactive subsurface barrier can be defined as an emplacement of reactive materials in the subsurface designed to intercept a contaminant plume, provide a preferential flow path through the reactive media, and transform the contaminant(s) into environmentally acceptable forms to attain remediation concentration goals at the discharge of the barrier. The main advantages of permeable reactive barriers are the elimination of pumping, mass excavation, offsite disposal and significant cost reductions. Figure 2.13 shows a cross-sectional view of the permeable reactive barrier process respectively.

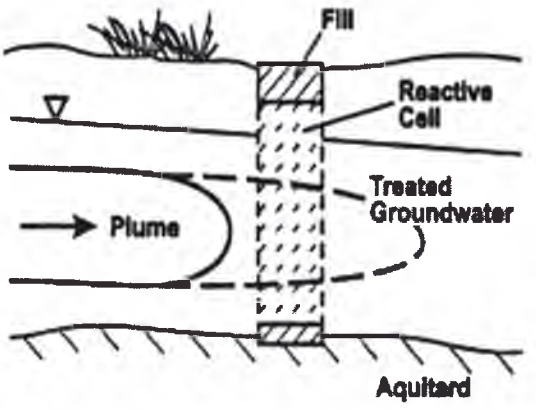

Figure 2.13: Cross-sectional view of the permeable reactive barrier process (Gavaskar, 1999)

The use of permeable reactive barriers filled with neutralising agents such as calcite appeared to have some potential as a treatment technology for assisting in the management of drainage from acid sulphate soils.

2.6.5.1 Calcareous Reactive Barriers

The most commonly used material within reactive barriers is limestone due to its low cost and high availability. There are four types of calcareous reactive barriers, as described below, that are of potential use in acid sulphate soils regions.

2.6.5.1.1 Open Limestone Channels

Open Limestone Channels (OLCs) are constructed by placing coarse limestone into a drainage channel. Problems occur when Fe (III) and Al are present in the water. These cations precipitate as metal hydroxides and coat the limestone surfaces (armoring) and can plug the limestone void space, thereby reducing limestone dissolution and acid neutralisation (Ziemkiewicz *et al.*, 1997). Ziemkiewicz *et al.* (1997) concluded that limestone channels could neutralise acid mine drainage if the channels were constructed on steep slopes so as to reduce plugging of the limestone void spaces, and if channels were built five times bigger to account for the armoring effect. Ziemkiewicz *et al.* (1997) also recommended that OLCs should have a slope of greater than 20% to keep the limestone active.

2.6.5.1.2 Anoxic Limestone Drains

Anoxic limestone drains (ALDs) are buried trenches or channels containing crushed limestone into which acidic drainage is channelled. As the acid mine drainage flows through, the limestone is dissolved, alkalinity is added and pH is increased. The channels are covered to reduce or eliminate the presence of oxygen; the elimination of oxygen prevents the development of an iron oxide coating (armor) on the limestone. At a pH of less than 6 and under anoxic conditions, the limestone within the ALD will not become armored with iron hydroxides because Fe^{2+} does not usually precipitate under such conditions (Skousen, 1997).

2.6.5.1.3 Oxic Limestone Drains

Oxic limestone drains (OLDs) are similar to ALDs, but they are more experimental. Iron or aluminium hydroxides form within them, and hopefully these solids are periodically flushed out by temporarily increasing the pressure or head and then releasing water from the drain rapidly. This system is designed to treat water that contains dissolved oxygen and ferric iron in one stage. The partial pressure of CO_2 is

concentrated due to the drain being covered. Subsequently, there is a higher limestone dissolution and alkalinity produced in this system compared to the ALD system (Waite *et al.* in Naftz *et al.* (2002)).

2.6.5.1.4 Alkalinity Producing Systems

Alkalinity Producing Systems (APSs) are vertical-flow systems where water flows from the surface of the APS through organic matter and limestone layers. They have been given a variety of names: successive alkalinity producing systems (SAPS) (Kepler and McCleary, 1994); (RAPS) reducing and alkalinity producing systems (Watzlaf *et al.*, 2000); alkalinity producing systems (APS).

In this system the incoming water is under reducing conditions before it enters the limestone, therefore minimising the possibility of clogging as a result of metal oxyhydroxide formation.

2.6.5.2 Other Materials

A variety of neutralising agents can be used, other than calcium carbonate. Other materials that have been used at mine sites includes: alkaline tailings liquor, fly ash (multiple metal oxides, carbonates), red mud from alumina operations, quicklime (CaO), hydrated lime ($Ca(OH)_2$), calcium peroxide (CaO_2), dolomite ($CaMg(CO_3)_2$), magnesite ($MgCO_3$), caustic magnesia (MgO), witherite ($BaCO_3$), hydroxyapatite ($Ca_5(PO_4)_3OH$), sodium orthosilicate (Na_4SiO_4) and alkaline paper-pulp residues (Taylor *et al.*, 1997).

2.7 Review previous research into the use of lime and/or fly ash for the improvement of soils

Various methods of applying lime have been reviewed and one particular injection technique on soft marine clay proved to be practical and successful in creating a zone of influence from the injection nucleus (Narasimha Rao and Rajasekaran, 1994). Indraratna (1983) has summarised the relevant concepts of sub-surface lime grout injection. Other areas of acid mine drainage and areas of injection grouting have been used to formulate appropriate technology for testing and appropriate rates of lime

(Kitsugi and Azakami, 1982). No one test has considered the type of clay that is represented in the site investigated in this study.

2.7.1 Lime Columns

Lime columns are widely used for the stabilisation of clay soils. The terms 'lime column' and 'lime piles' can be used interchangeably. Lime column is the process of mixing of dry unslaked lime in soft clays and silts to form a column of treated soil. Rogers and Glendinning (1997) summarised the stabilisation mechanisms of lime piles, which are lateral consolidation, water content reduction, clay-lime reaction, reduction in pore water pressure, and the consolidation of the shear zone and pile strength. The addition of quicklime to soil draws in water from surrounding areas and forms hydrated lime. Solidity of the soil will occur as a result of this. Kitsugi and Azakami (1982) attributed the improvements in the bearing capacity of soils to the strength of the piles. Yamanouchi *et al.* (1992) studied the use of lime in the construction of embankments.

2.7.2 Studies using Lime and/or Fly ash

Indraratna *et al.* (1991) investigated the stabilisation of a dispersive soil by the addition of fly ash. Numerous combinations of fly ash-soil mixtures were investigated and the engineering properties of these mixtures were studied. The addition of 5-8% fly ash caused a flocculation of clay particles within the soil and decreased its dispersivity. Increases in fly ash content led to an increase in unconfined compressive strength. The maximum dry density of the soil mix also increased as a result. Indraratna *et al.* (1995) also studied the effect of fly ash on the strength and deformation characteristics of a Bangkok clay. Lime and cement were also used as admixtures to allow for self-hardening of the blend. It was found that a 18% fly ash and 5% lime treated clay achieved a compressive strength that was 2-3 times greater than that of untreated clay. Fly ash and lime also caused an increase in the shear strength of the clay. Those clays treated with just lime showed larger excess pore water pressures and thus enhanced effective shear strengths than those treated with fly ash.

Indraratna (1996) investigated the use of hydrated lime, milled blast furnace slag and fly ash on a fine-grained colluvial soil. Their effectiveness was compared with that of hydrated lime. Soil treated with hydrated lime and milled slag showed an improvement in engineering behaviour. The addition of 2% lime increased the uniaxial compressive strength of blended clay soil samples by nearly 50%. It was also found that all additives increased the pH value of the soil, as shown in Figure 2.14.

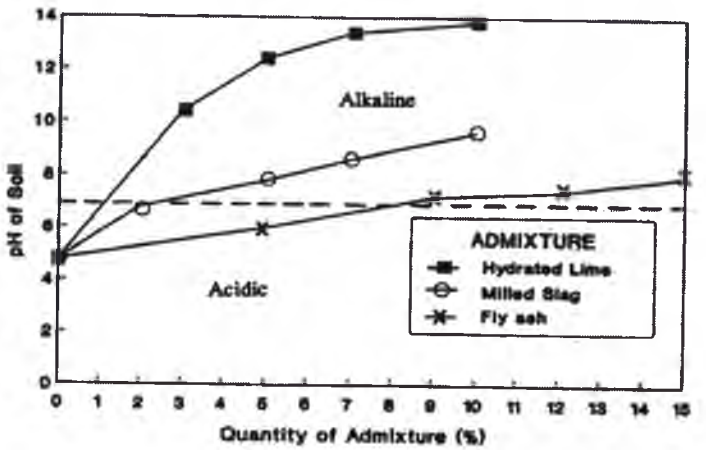

Figure 2.14: Effect of additives on pH levels of colluvium (Indraratna, 1996)

Pekrioglu *et al.* (2003) demonstrated the potential use of fly ash in grouting applications. Thirteen composite grouts (composed of mixture combinations of fly ash, cement, lime, silica fume, water educing admixture and water) were investigated in terms of engineering performance i.e. physiochemical (chemical compound analysis, unit weight, void ratio, linear shrinkage, hydraulic conductivity) and mechanical properties (unconfined compressive strength and flexural strength). It was found that the rate of strength gain for fly ash-cement groups is less than fly-ash/lime groups.

Akbulut and Saglamer (2003) studied the use of grout additives fly ash and clay in soil grouting and the effects that these admixtures had on soil strength. In this study a granular soil (sand and gravel) was grouted with fly ash and clay under grouting pressure of 100kPA. In a comparison between the treated and untreated granular soil, it was found that the fly ash and clay improved the compressive strength. Soil

grouted with 5% fly ash had a greater compressive strength than soil that was grouted with 10% fly ash.

Scheetz *et al.* (1993) describes the application of fly ash-based grouts for the abatement of acid mine drainage. It is proposed that by using fly ash in a mining situation the neutralisation capacity of the fly ash can insure a reduction in the environmental problems associated with acid mine drainage.

2.7.3 Sub-surface Chemical Injections using Lime and/or Fly ash

Narashimha Rao and Rajasekaran (1994) investigated the ability of lime treatment to improve the engineering qualities of soft marine clay, using an experimental injection implement. The experimental work in this study was carried out in a test tank filled with soft marine clay that had been mixed with seawater. A steel injection with 40 perforations in the bottom 300-400 mm section was used to carry out the injections. A lime slurry of 40% concentration (by weight) was injected into the test tank at a pressure range of 0-0.8 N/mm^2. It was found that adequate quantities of lime had penetrated the surrounding soil in the test tank, to increase the pH values from pH 7.3 to pH 9.4 at a distance of 75mm from the injection source. The liquid limit and plasticity index of the soil were reduced significantly and the penetration of the lime in the soil and the formation of calcium hydroxide brought about increased rigidity. These changes and improvements were due to the effective formation of cementation products.

A study into the penetrability of the lime slurry demonstrated that the lime effectively penetrated into the soil through the lime columns and the lime-injection points (Rajasekaran and Narasimha, 1996). The radial distance of lime seepage was 4-6 times in the case of lime columns and 8-10 times the diameter of the injection pipe in the injection system. Rajasekaran and Narasimha (2002) also investigated the lime induced permeability changes in the engineering behaviour of lime treated soil. Lime columns in treated marine clays were constructed and tests on these soils showed an increase in permeability up to a maximum of 15-18 times that of untreated soil. These studies illustrated that lime injection techniques and lime columns can be use to improve the engineering behaviour of marine clays.

Lime-fly ash injection has also been utilised in studies by Joshi and Wright (1978) and Blacklock *et al.* (1983). Joshi and Wright (1978) illustrated earth dike stabilisation to reduce seepage and increase the shear strength of soil, embankment stabilisation to increase slope stability and reduce settlement. Due to the fact that fly ash is a relatively inexpensive product its wide availability, fly ash has also been investigated for the stabilisation of landfills to support the construction of buildings (Joshi, 1983; Blacklock *et al.*, 1983).

Slurry injection stabilisation of rail track formations is another application of grouting. This involves the pumping of a cementitious slurry of both lime and fly ash, under pressure from a hi-rail mounted vehicle, through probes pushed into the subgrade (Kayes *et al.*, 2000). The aim of this is to create impervious barriers against moisture and in turn control the instability of the underlying clays. This slurry injection has been carried out along rail track formations from Gladstone to Moura Mine and from Rockhampton to Blackwater (Queensland, Australia). The slurry injection reduced the swelling of these clays and controlled shear failures. It was also effective in stabilising settlement of the rail track formations.

2.8 Review of previous Acid Sulphate Soil rehabilitation research and management strategies relevant to this current study

This review concentrates on the previous acid sulphate soils mitigation measures in place within the Shoalhaven Floodplain investigated in this current study in comparison with the installation of the lime-fly ash barrier. They include: v-notch weirs, a self-regulating tilting weir and two-way modified floodgates.

2.8.1 V-notch Weirs

Blunden (2000) undertook a study to maintain an elevated groundwater table above the pyritic layer via the installation of three v-notched weirs at the Berry field site (Plate 2.1). Blunden also carried out a high-density soil-sampling program including soil physical and chemical parameters over depth and distance, as summarised below.

- Physical properties: bulk density, porosity, saturated hydraulic conductivity, moisture characteristic curves, and particle and pyrite crystal size distribution and van genuchten parameters.
- Chemical properties: carbon, pH, salinity, sulphate, chloride, exchangeable cations, oxidisable sulphur, aluminium, calcium and base saturation, peroxide oxidisable sulphur concentrations.

A schematic of sampling sites and location of the three v-notch weirs at the Berry field site is shown in Figure 2.15.

Plate 2.1: High v-notch weir

The installed v-notch weirs were successful in maintaining the groundwater table at or above the pyritic layer. Figure 2.16 shows that before the installation of the weirs the groundwater table fluctuated in a considerable range and was often below the pyritic layer. Proceeding weir installation the groundwater table was maintained above the pyritic layer and fluctuated less. The lower hydraulic gradients established under the influence of the higher drain water level maintained by the v-notch weir reduced the rate of discharge of acidic oxidation products from the groundwater to the drain. Numerical simulations combining groundwater flow and pyrite oxidation models were used to predict the magnitude and distribution of pyrite oxidation for various boundary conditions that simulate potential groundwater management strategies.

They showed that maintaining a higher water level in the drains and/or applying regular irrigation can achieve substantial reductions in the volume of pyritic soils exposed to oxidising conditions.

Blunden and Indraratna (2001) also demonstrated that the weirs reduced the hydraulic gradient between the drain and the phreatic zone. The elevated groundwater levels did not improve the long-term groundwater quality. pH values remained at approximately 4 throughout the monitoring period following the installation. Al, Fe and Mg levels remained high after the installation of the weir. Sulphate levels were high with low chloride to sulphate ratios. The installation of weirs can prevent the production of 'new' acid, but cannot manage the leaching of 'stored' acid.

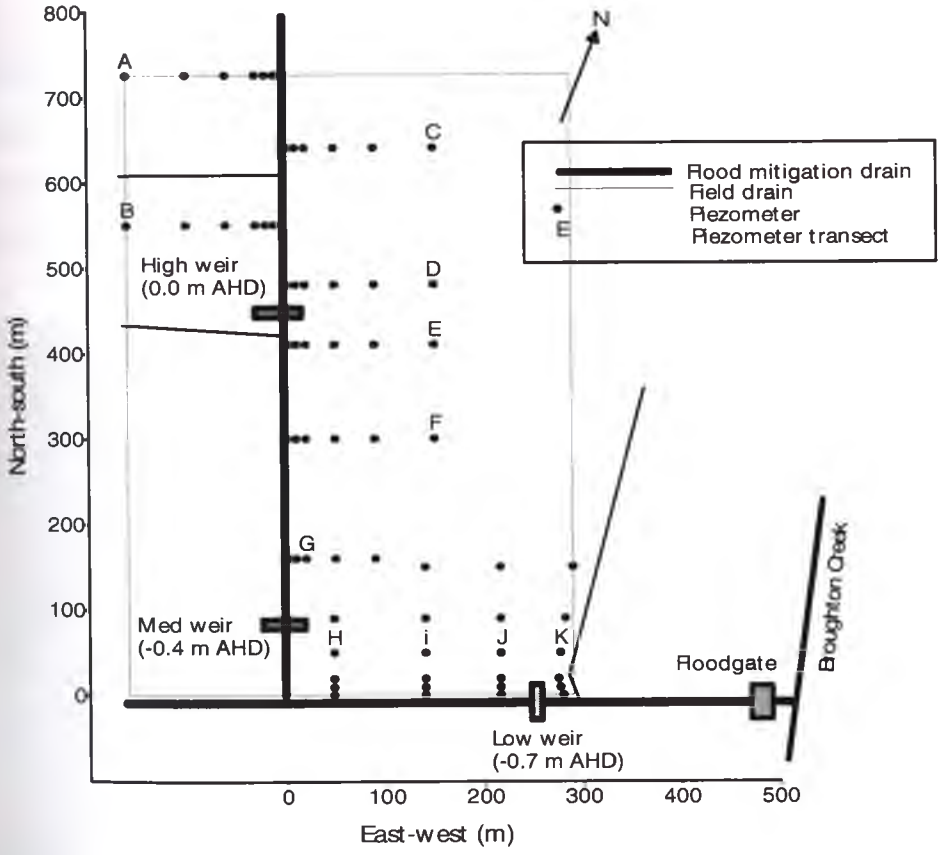

Figure 2.15: Location of weirs, floodgate and piezometers at the study site (Blunden, 2000)

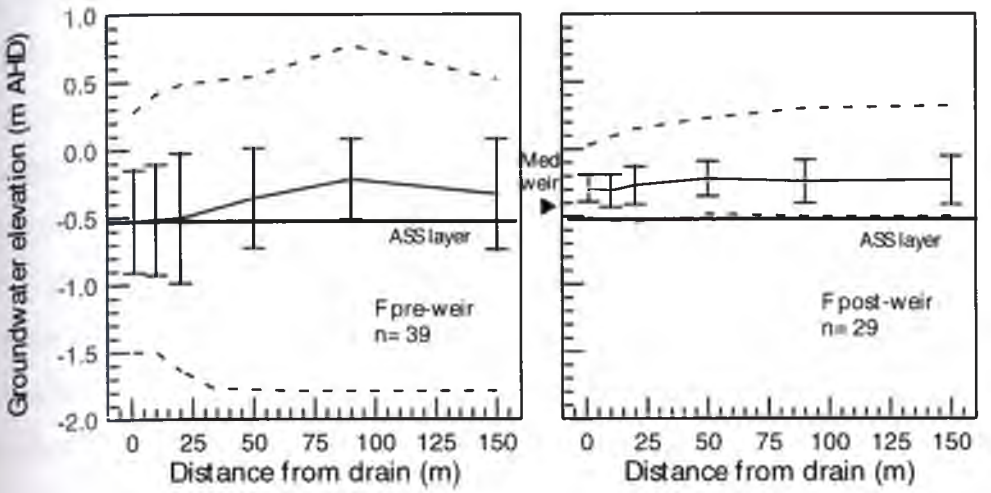

Figure 2.16: Comparison of the average groundwater elevation at a transect prior to and proceeding weir installation, also showing the maximum and minimum groundwater elevation and standard error bars (Indraratna et al., 2001)

2.8.2 Self-regulating tilting weir

The self-regulating tilting weir (Plate 2.2), which was installed in June 2001, was designed to maintain a high groundwater table, in order to decrease the oxidation of sulphidic sediments, through saturation of the soil.

Plate 2.2: Self-Regulating Tilting Weir (built in 200 by UOW Acid Sulphate Soils Research Team)

The weir maintains an elevated drain water level and compensates for flood and drought periods. Figure 2.17 shows that the tilting weir continued to maintain the same drain water level as the nearest v-notch weir, ensuring that the groundwater elevation did not fall significantly. The installation of the tilting weir also failed to improve the groundwater quality. pH values remained low (Figure 2.18) and high concentrations of dissolved metals were found (Figure 2.19). Total Fe and Total Al concentrations in the groundwater were observed to be high during sampling period. The lower levels of Total Fe towards the end of the sampling period as attributed to the dilution of freshwater caused by flood events.

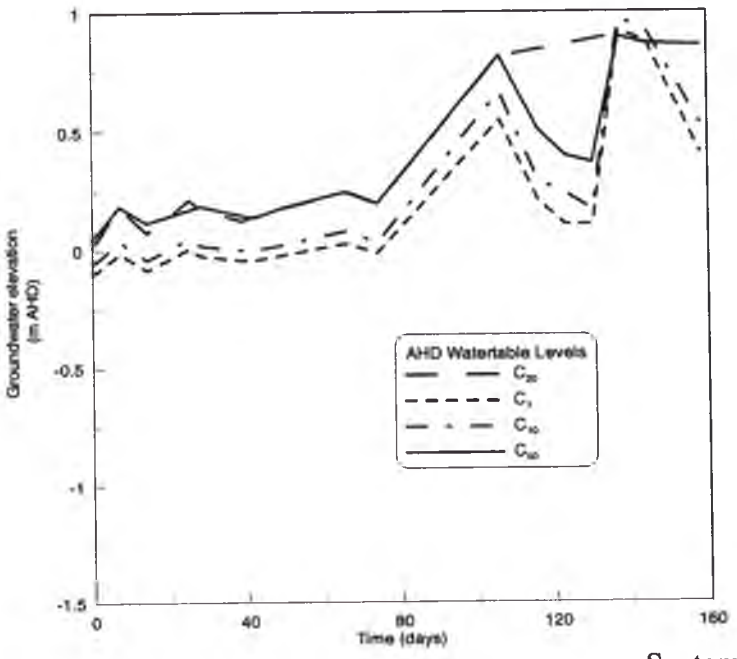

17th April 2001 September 2001

Figure 2.17: Post-weir groundwater elevations following the installation of the Self-Regulating Tilting Weir (Earnshaw, 2001)

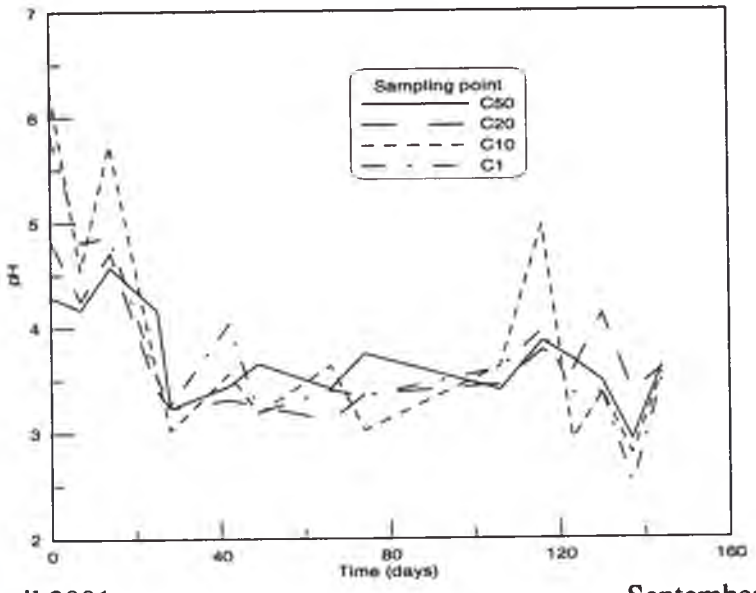

17th April 2001 September 2001

Figure 2.18: pH values for sampling points C1, C10, C20 and C50 during the sampling period (Earnshaw, 2001)

(a)

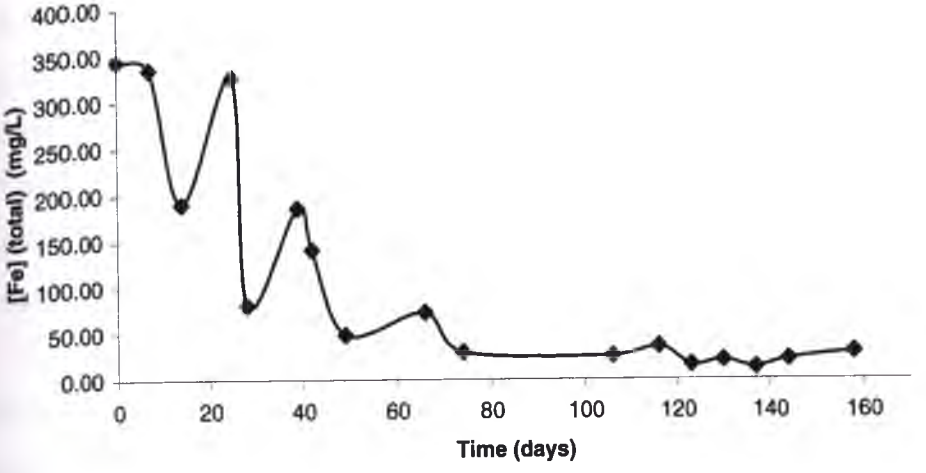

(b)

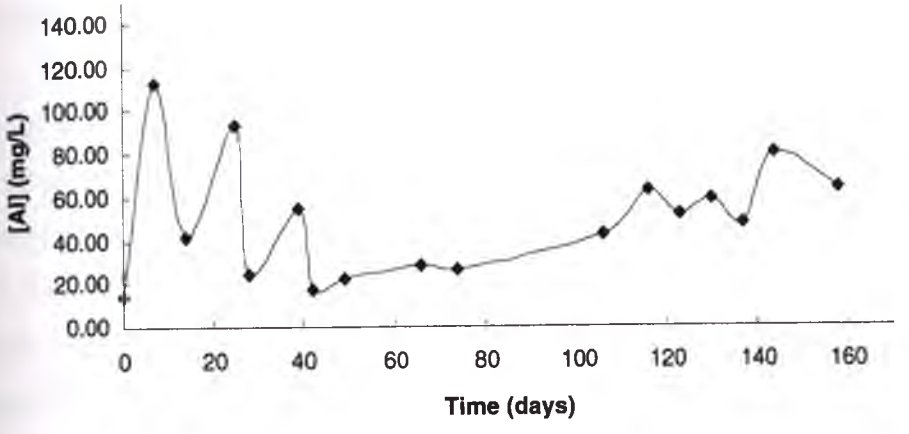

17th April 2001 September 2001

Figure 2.19: Total Fe (a) and Total Al (b) concentration at sampling point C1 during the sampling period (Earnshaw, 2001)

2.8.3 *Modification of Floodgates*

Glamore (2003) examined several criteria relating to floodgate management and the effectiveness of the installation of a modified two-way floodgate (Plate 2.3). The project examined: hydrology, environmental and geo-hydraulic concerns relating to floodgate manipulation using GIS techniques; the kinetics of tidal buffering including the development of an aqueous ion speciation model; floodgate design criteria and design techniques to optimise saline buffering and reduce risk; the influence of tidal restoration on drain water quality and the influence of altered drain hydraulics on the phreatic zone; and the extent and distribution of saline contaminants within the soil matrix through field analysis and a 3-D finite element analysis.

Glamore et al. (2001) and Indraratna et al. (2002) suggested that allowing tidal flushing into flood mitigation drains via modified floodgates may: (a) decrease the 'acid reservoir effect', (b) raise dissolved oxygen levels, (c) decrease the hydraulic gradient between the drain and groundwater, (d) diminish aluminium flocculation, (e) eliminate 'acid at a distance', (f) combat exotic freshwater weeds, (g) enhance runoff during wet periods; and (h) allow fish passage into important breeding grounds.

With the installation of a modified two-way floodgate, water quality within a flood mitigation drain was greatly improved. The buffering capacities of the seawater helped to bring the drain water to near neutral levels abruptly after the installation of the modified floodgate, as depicted in Figure 2.20.

The drain water pH was observed to increase by two orders of magnitude and dissolved aluminium and iron decreased more than 50%. Concentrations of dissolved monomeric aluminium ranged from 0.005 mmol/L (250m upstream, Days 763 and 857) to 3.16 mmol/L (45 upstream, Day 563) after the installation of the modified floodgate, while before the impact of tidal buffering aluminium concentrations averaged 0.62mmol/L (26% decrease).

Average total dissolved iron concentrations decreased by 33% from 0.62mmol/L to 0.163mmol/L (Glamore, 2003). The aluminium and total iron concentrations after floodgate modification are shown in Figure 2.21. Tidal flushing of the drain also (i) reduced the 'acid reservoir', (ii) increased drain water dissolved oxygen levels, (iii) enhanced fish passage, (iv) decreased exotic freshwater weeds and (v) recharged the phreatic zone during dry periods (Glamore, 2003).

Plate 2.3: Modified two-way Floodgate

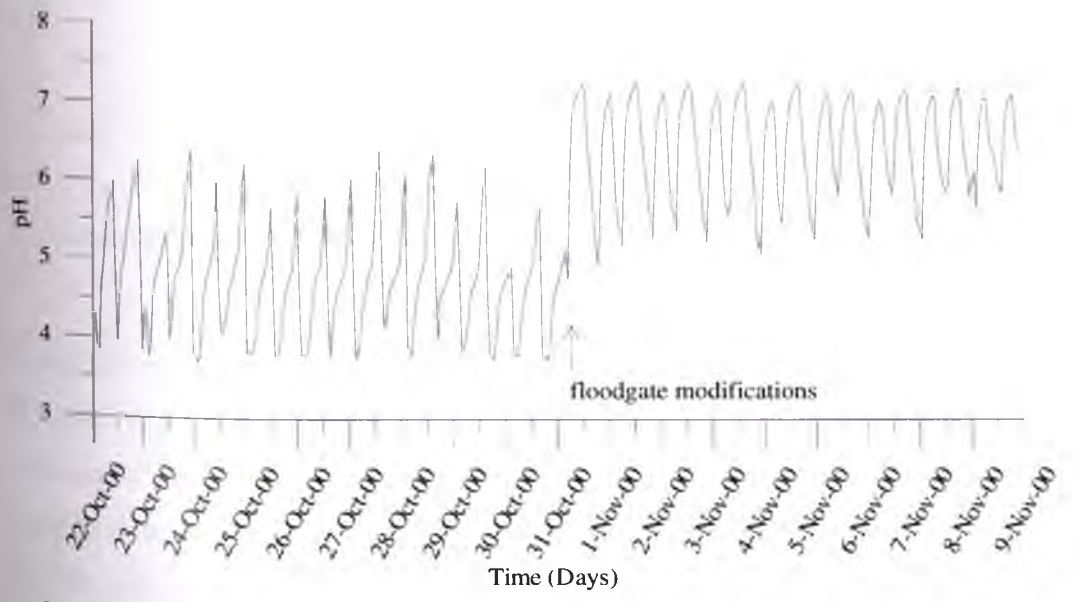

Figure 2.20: In situ drain water pH readings taken immediately before and after floodgate modifications (Days 296-314) (Glamore, 2003)

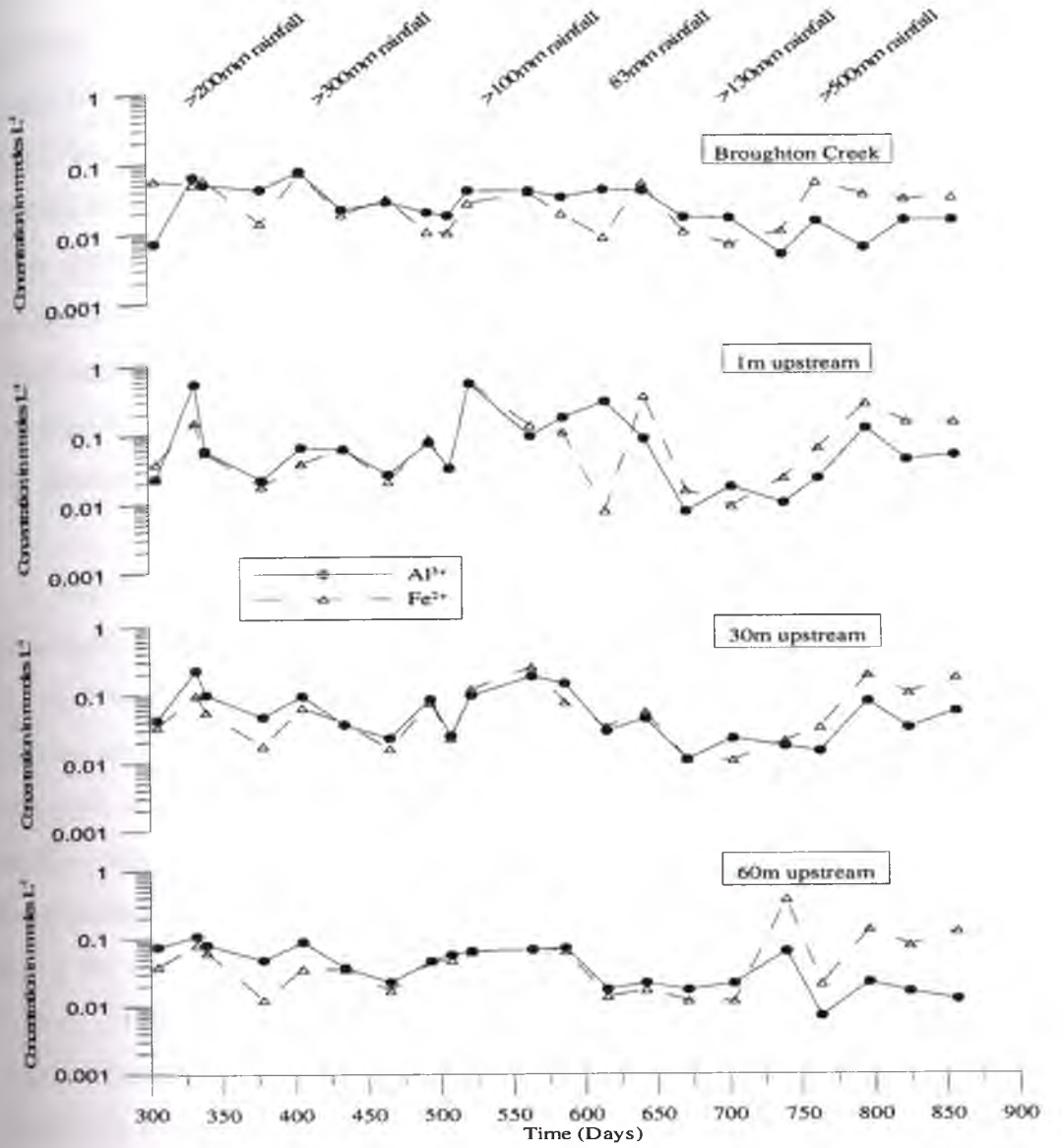

Figure 2.21: Soluble aluminium and iron concentrations following floodgate modifications with rainfall (Glamore, 2003)

Finite element analysis indicated that saline intrusion was not a concern as long as the hydraulic conductivity of the soil in the lateral plane was below critical levels. Simulations using the 3-D finite element model showed that even under extreme conditions, the intrusion of saline water at the study site was limited to 10m inland and that this saline water was flushed out of the soil with drought breaking rain (Glamore, 2003).

2.8.4 *The role of anaerobic oxidation*

Although the processes of biotic oxidation of pyrite that contributes to acid production has been studied in the acid mine drainage area, there has been little study of these

processes in the acid sulphate soils of the Shoalhaven floodplain, NSW. Thong's (1998) research entailed soil column experiments coupled with numerical modelling (SMASS). The model predicted that the presence of high organic matter content reduced the rate of pyrite oxidation, especially in the lower layers. It was found that under submerged and reducing conditions the model predicted that drainage of the soil would cause a much higher sulphate concentration and lower pH values. Thong (1998) attributed sulphate production in the anaerobic columns to ferric oxidation and hypothesised that, "the submergence of the pyritic layer will merely reduce the rate of acid production, but not prevent it".

It is hypothesised that bacteria can promote biotic oxidation of the pyrite in submerged conditions, beneath the groundwater table (Evangelou, 1995; Dent, 1986). The traditional management technique of ground water level manipulation would be rendered ineffective in arresting biotic oxidation where the pyrite layer is submerged. Therefore, a preliminary study of sub-surface lime injection was examined as a possible solution to arresting biotic oxidation. Rudens (2001) undertook field investigations on acid sulfate soil of the Low Shoalhaven Floodplain, involving testing the soil for organic content (Loss on ignition method), and acid sulfate pH analysis. Microbiological analysis was conducted to determine the type of pyrite oxidizing bacteria, and their Most Probable Number in the soil profile of the Lower Shoalhaven Floodplain. Column experiments were set up to examine the extent of biotic oxidation and the ability of a sub-surface lime layer to arrest his process in pyrite soils removed from the study area. The parameters manipulated in the column experiment were the water level; presence of bacteria; and the presence of a submerged lime layer in the soil columns. Soil water extracted from the columns was tested for the following parameters: pH, Fe^{2+} and Fe^{3+} concentrations. The column experiments revealed that soil that contained *Thiobacillus ferrooxidans* bacteria could possibly produce acid in totally submerged conditions, while soil that was sterilized did not. The *Thiobacillus ferrooxidans* bacteria present in the column sample possibly contributed to an increase in ferric iron concentration, enabling the pyrite contained in the soil to be oxidized in submerged conditions, thus producing sulfuric acid. The microbiological results did not indicate the presence of any other bacteria that could contribute to the biotic oxidation of the pyrite in the soil.

The addition of a lime chemical barrier in the column samples contributed to a rise in pH of the soil at a distance of less than 40mm. The rise in pH significantly reduces the population of *Thiobacillus ferrooxidans* bacteria at a distance of 30mm from the lime chemical barrier. Results of the MPN analysis and the pH values for the soil samples from columns 5 (anaerobic conditions) and 6 (aerobic conditions) are shown in Table 2.3.

Table 2.3: Most Probable Number of iron oxidising bacteria (Thiobacillus ferrooxidans) and pH analysis results for soil sample from columns containing the lime chemical barrier (Rudens, 2001)

Column	Distance from Lime barrier (mm)	MPN of iron oxidising bacteria cells per gram of soil sample	Soil pH
5	30	37	9.45
5	150	18400	4.48
6	30	16	6.45
6	150	-	4.43

A possible reason for the difference in surface pH between column 5 and 6 is the greater diffusion of hydroxide ions to surrounding soil in column 5 due to the watertable being maintained at the surface, submerging the lime layer (Rudens, 2001). The rise in pH within close proximity to the lime barrier is the key mechanism for the reduction in *T. ferrooxidans* bacteria numbers. The lime used in sub-surface injection would not only neutralise acid in the soil, but also inhibit the growth of *T. ferrooxidans* bacteria, therefore reducing the possibility of biotic oxidation of the pyrite in the soil.

2.9 Implications for Current Research

A detailed understanding of the processes involved in pyrite oxidation is imperative for the management of acid sulphate soils and the development of appropriate mitigation measures. As previously mentioned a thorough understanding of the processes fundamental to the field investigations of the lime-fly ash barrier is important. A review of previous research into grouting and the use of lime and fly ash slurry injection systems (See Chapter 2, Section 2.7) were necessary for

determining the appropriate injection methods and grout ratios to employ in this current study. This will be expanded upon in Chapter 5.

The hypothesis for this research is that the installation of a lime-fly ash barrier above the pyrite layer will control pyrite oxidation and its subsequent generation of acidic products. The objective of this research is to assess groundwater and drain water quality before and after the installation of the lime-fly ash barrier and to determine the effectiveness of the barrier as an effective acid sulphate soil remediation strategy. This study follows on from previous research undertaken within the Shoalhaven Floodplain and illustrates a link between groundwater and drain water quality and the role of an impermeable barrier in pyrite oxidation.

To assess the effectiveness of the lime-fly ash barrier, groundwater and drain water quality and climatic influences were studied comprehensively. This research investigates whether the installation of a lime-fly ash barrier is suitable for improving groundwater and drain water quality, where the installation of weirs is not appropriate, and reducing the further oxidation of pyrite. The use of a lime-fly ash barrier in pyritic soils has never been investigated before in Australia. This presents the innovative component of the current study.

Chapter 3 Properties of Grouts and Grouting Theory relevant to Sub-surface Lime-Fly ash Barrier Installation

3.1 Introduction

To comprehend the development of a sub-surface lime-fly ash barrier there needs to be a thorough understanding of the principles involved in the injection (grouting) process. The first section of this Chapter deals with the principles of grouting including the properties and requirements of grouts that need to be considered before undertaking grouting operations including viscosity and optimum injection pressures. The second section introduces the constituents that were used in this study, namely fly ash and lime. In the final section of this Chapter, the radial flow of grout in soil is analysed and the theory of this is introduced.

3.2 Grouting Principles

3.2.1 Introduction to Grouting

Grouting may be defined as the injection of appropriate materials (grouting fluid) under pressure into certain parts of the earth's crust through specially constructed holes in order to fill and therefore seal voids, cracks, seams, fissures or other cavities in soils or rock strata (Bowen, 1981). Grouting fluid will solidify over time by physico-chemical action and interaction with pores, thereby increasing the strength and/or reducing the permeability of the grouted mass (Shroff and Shah, 1993). A number of authors have demonstrated the importance and many specific applications of grouting (Bowen, 1981; Nonveiller, 1989; Broms, 1992; Fell et al., 1992; Munfakh and Wyllie, 2000).

3.3 Properties of Grouts

The properties of grouts that must be considered before a grout can be selected for a grouting project include:

- Penetrability (Sowers and Sowers, 1970; Anagnosti, 1985; Munfakh and Wyllie, 2000);

- Viscosity (Indraratna, 1983);
- Durability (Indraratna, 1983); and
- Groutability: expanded upon in Section 3.3.1.

3.3.1 Groutability

For grouting treatment of any kind of soil or rock, it is essential to specify, as well as possible, the conditions under which a particular grout material may be expected to satisfactorily penetrate the ground and to fill up the voids. The groutability is the ability of a grout to penetrate ground formations in order to seal its voids or fissures. Groutability depends on a number of factors including (i) the relative geometric dimensions of the voids and grout particles, (ii) surface action between the injected grout and the voids, and (ii) the penetration properties of the grout (Indraratna, 1983).

The groutability of a soil can be found from the grain-size distribution of any soil that can be improved effectively by a grout (Akbulut and Saglamer, 2002). In determining the groutability of a given formation with a particular grout, the maximum particle size in the grout and also the stability and set time of the grout (Lambe, 1962) must be considered. For the injection of soils, the groutability ratio is defined by:

$$\text{Groutability} = \frac{D_{15\,\text{formation}}}{D_{85\,\text{grout}}} \tag{3.1}$$

Where, D_{15} = the maximum grain size of the smallest 15% (by weight) of the soil sample and D_{85} = the maximum particle size of the smallest 85% (by weight) of the grout.

According to this equation, if the groutability is larger than 25, then grout can be successfully injected into the soil. If the groutability is smaller than 11, then grout cannot be sufficiently injected into the soil (Akbulut and Saglamer, 2002). Accurate prediction of the groutability of granular soils can be complicated due to the effects of the gran-size of the soil and cement-based grouts, the relative density and fine

contents of soil, the water/cement ratio of grout mixture and grouting pressure, which directly affects the groutability of soil media (Akbulut and Saglamer, 2002).

3.4 Requirements for Grouts

The factors influencing the above grout properties include:

- Fluidity (Shroff and Shar, 1993);
- Strength;
- Minimum Shrinkage;
- Optimum pressures (Ischy and Glossop, 1962; Craig, 1987); and
- Grout admixtures.

3.5 Constituents and Use of Grout Fluids

3.5.1 Lime

The composition of the grout fluid used during this study is a mixture of water, lime and fly ash. By using a strong admixture of cement or quicklime in the grouting process soil improvement can be intensified (van Impe, 1989). When lime is added to wet soil two chemical reactions occur:

1. Base-exchange phenomenon: the high pH of the lime alters the nature of the adsorbed water layers of the soil particles (Lambe, 1962; Singh, 1975).
2. Pozzolanic/cementing action: the lime reacts chemically with available silica and alumina to form 'natural cements' composed of calcium silicate hydrate and calcium aluminate hydrate gels (Rogers and Glendinning, 1997).

As can be seen in Figure 3.1, the calcium silicate forms an enveloping seam between the soil particles.

$$CaO + CO_2 \rightarrow CaCO_3 \downarrow$$

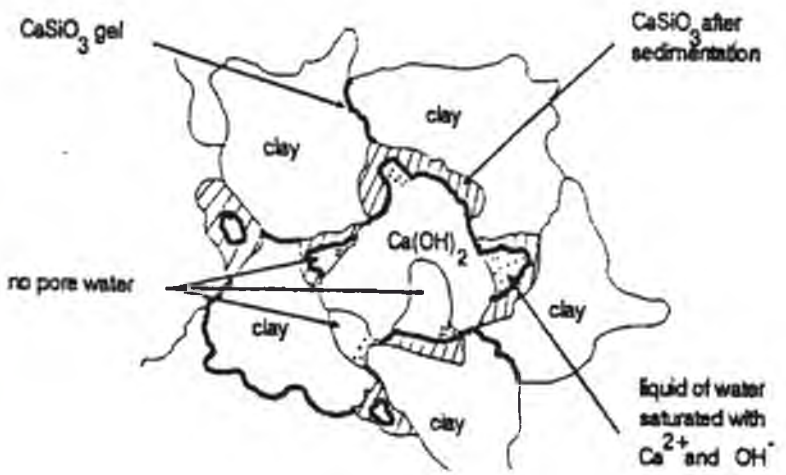

Figure 3.1: Formation of calcium silicate around soil particles (van Impe, 1989)

Several principal changes occur in the soil due to lime stabilisation. In general:

(i) Lime increases the strength of almost all types of soil (Lambe, 1962) and also increases the durability of the soil (Singh, 1975).

(ii) Changes in the plasticity of the soil also occur. Because clay particles flocculate into larger sizes, the plastic limit increases. The plasticity index of highly plastic soil decreases. The soil becomes more friable with clay clods disintegrating more readily.

(iii) The shrinkage limit increases and the shrinkage ratio decreases. Resistance to water absorption, capillary rise and volume change on wetting and drying increases (Singh, 1975).

(iv) There is an increase in the optimum water content and a reduction in the maximum compacted density.

One limiting factor in the formation of this silicate gel is that its formation is dependent on sufficient water to enable the transfer of Ca^{2+}- and OH^-ions to the surface of the clay material (van Impe, 1989). The pozzolanic reaction of lime with available reactive silica or alumina can often be improved with the addition of a material high in reactive silica or alumina such as fly ash.

3.5.2 Fly ash

Fly ash is an industrial waste product containing hydrated oxides of aluminium, zeolites, and silica constituents and trace elements of As, Sb, Se, V, Pb, Mo, Ni, B, Zn, Cd, Cr and Cu. The leachability of these elements when mixed with lime would be low due to the high alkalinity of the lime. The product of the pozzolanic reaction of fly ash and lime has a cementitious action (Hilton, 1975):

$$3Ca(OH)_2 + 2SiO_2 \rightarrow 3CaO.2SiO_2.3H_2O \qquad (3.2)$$

Various factors influence the fly ash reactions including temperature and the type of fly ash used. Before choosing the grouting materials or grouting technique to be applied to a problem, it is essential to perform preliminary test injections. From these tests a number of characteristics can be determined including the boring possibilities in the soil, the stratifications and heterogeneities present in the soil, the in-situ permeabilities and the grouting pressures that give the best results (van Impe, 1989).

3.6 Theoretical analysis of the radial flow of grout in a soil

3.6.1 Plane of Weakness Theory

Jaeger in 1959, used the linear law:

$$\tau = S_0 + \mu\sigma \qquad (3.2)$$

Where: τ = the magnitude of the tangential stress across the plane; S_0 = appropriate value of the shear stress; μ = appropriate value of the coefficient of internal friction ($\mu = \tan\theta$) and σ = normal stress across the plane.

In two dimensions suppose that the material has a plane of weakness whose normal makes an angle β with the greatest principal stress, σ_1. It is assumed that the criterion for slip in the plane is:

$$|\tau| = S_0 + \mu\sigma \qquad (2.16)$$

In reference to the theory of stress in two dimensions σ and τ are given by:

$$\sigma = \sigma_1\cos^2\theta + \sigma_2\sin^2\theta = \tfrac{1}{2}(\sigma_1 + \sigma_2) + \tfrac{1}{2}(\sigma_1 - \sigma_2)\cos 2\theta \quad (2.17)$$

$$\tau = -\tfrac{1}{2}(\sigma_1 - \sigma_2)\sin 2\theta \quad (2.18)$$

These may be put into an alternative form:

$$\sigma = \sigma_m + \tau_m\cos 2\beta \quad (2.19)$$

$$\tau = -\tau_m\sin 2\beta \quad (2.20)$$

Where, σ_m = mean stress and τ_m = maximum shear stress.

So that:

$$\sigma_m = \tfrac{1}{2}(\sigma_1 + \sigma_2),\ \tau_m = \tfrac{1}{2}(\sigma_1 - \sigma_2) \quad (2.21)$$

Writing: $\mu = \tan\phi$ (2.22)

Where: ϕ = angle of friction, and using (2.19) and (2.20) in (2.16) gives:

$$\tau_m\{\sin 2\beta - \tan\phi\cos 2\beta\} = S_0 + \sigma_m\tan\phi \quad (2.23)$$

or $\tau_m = (\sigma_m + S_0\cot\phi)\tan\delta$ (2.24)

Where: $\tan\delta = \sin\phi\,\mathrm{cosec}(2\beta - \phi)$ (2.25)

Alternatively, using the values (2.21) of σ_m and τ_m (2.23) may be written in the form:

$$\sigma_1[\sin(2\beta - \phi) - \sin\phi] - \sigma_2[\sin(2\beta - \phi) + \sin\phi] = 2S_0\cos\phi \quad (2.26)$$

Finally, (2.23) can be rewritten in the forms:

$$\sigma_1 - \sigma_2 = \frac{2S_0 + 2\mu\sigma_2}{(1 - \mu\cot\beta)\sin 2\beta} \quad (2.27)$$

and

$$\sigma_1 = \frac{2S_0 + 2\mu\sigma_2}{(1-k)\sin(2\beta - \phi)\,\mathrm{cosec}\,\phi - (1+k)} \quad (2.28)$$

Where: $k = \sigma_2 / \sigma_1$ (2.29)

3.6.2 Allowable injection pressures

Establishment of allowable injection pressures can be based on hydraulic fracture tests and theory. Hydraulic fracture tests involve the injection of water into the ground at increasing pressures (generally for rock and stiff clay), and at the fracture pressure the flow rate will rapidly accelerate. The optimum injection pressure must be that pressure which would maintain an acceptable grout flow at the same time without causing hydraulic fracture.

Theory

For isotropic homogeneous soils by assuming the Mohr-Coulomb failure criterion in terms of effective strength parameters, the excess injection pressure is given by:

$$P_e = \frac{(\gamma_h - \gamma_w h_w)(1+K)}{2} - \frac{(\gamma_h - \gamma_w h_w)(1-K)}{2\sin\phi} + c'\cot\phi' \quad (2.30)$$

(i.e. σ_1 being the vertical effective stress; $\kappa = \sigma_3 / \sigma_1 \leq 1$

for isotropic material.

Hence neglecting friction losses, the maximum injection pressure is given by:

$$P_{max} = P_e + \gamma_w h_w \quad (2.31)$$

Where, γ = bulk density of material considered; h = height of material above the level of consideration; h_w = piezometric level of the ground water above the level under consideration; K = principal stress ratio (less than or equal to one) and γ_w = bulk density of water.

If σ_1 is horizontal, then replace the term (1- K) by (K-1).

For anisotropic conditions, combining the Mohr-Coulomb criterion and Jaeger's single plane of weakness theory gives:

$$\frac{P_{max}}{\gamma h} = 1 + \frac{c'}{\gamma h}\cot\phi' \qquad (2.32)$$

$$P_{max} = \gamma h + c'\cot\phi \qquad (2.33)$$

Where: P_{max} = maximum allowable injection pressure

3.6.3 Radial (lateral) flow from an injection borehole

In 1938, Maag proposed the first theory of alluvial injection by taking into consideration pump pressure, density and viscosity of grout, rate of injection, permeability of the ground and the geometry of flow. Maag's expression for alluvium is based on the following assumptions:

1. Isotropic homogeneous soil (same permeability in all directions);
2. The grout is a Newtonian fluid;
3. A steady state of flow should exist; and
4. A spherical flow is assumed; if the injection is done with an open-ended pipe whose radius is very small compared to the depth of the injection pipe below the groundwater level and above the impermeable barrier.

Maag's formula can be written as:

$$t = \frac{\alpha n}{3khr_0}\left[R^3 - r_0^3\right] \qquad (2.34)$$

Where, R = the radius of the grout front after time, t; r_0 = the radius of the injection pipe (sphere of origin); n = the porosity of the soil; k = the permeability of the soil; α = the ratio of the viscosity of the grout to that of water and h = the piezometric head in

the grout pipe which can be related to the pumping pressure and to the density of the grout.

However, these simple conditions are never realised in practice because the flow hydraulics are complex and the viscosity and rheological consistency of grouts may alter with time. These formulae are also limited to a situation where the grout front is far from the injection point. Nonetheless, the study of Maag's simple expression is valuable since it gives a clear indication of the progress of an injected grout.

More complex expressions for spherically radiating displacement flow have been given by Raffle and Greenwood (1961) based on the 'two-fluid formula' of Muskat for infiltration of oil wells. The theorem is based on the following assumptions:

1. Soil is homogeneous and isotropic;
2. For the purpose of calculations, replace cylindrical injection source (borehole) by a spherical source (radius a) of identical surface area;
3. Darcy's Law is applicable; and
4. Neglect the effects of gravity.

If the grout has reached a radius R at time t, the volume flow rate Q is related to the hydraulic head h at the source of radius r by (Raffle and Greenwood, 1961):

$$h = \frac{Q}{4\pi k}\left[\alpha\left(\frac{1}{r} - \frac{1}{R}\right) + \frac{1}{R}\right] \tag{2.35}$$

Where, α = ratio of grout viscosity to that of surrounding groundwater; e = void ratio of the soil; k = permeability of the soil; h = hydraulic injection head at the source of radius a; Q = flow rate and R = the radius which the grout has reached after time t.

The rate of movement of the interface between the grout and the soil is given by:

$$\frac{dR}{dt} = \frac{Q}{4R^2 e} = \frac{Kh}{e}\left[n.R^2\left(\frac{1}{a} - \frac{1}{R}\right) + R\right] \tag{2.36}$$

If the void ratio of the soil is e, the time for grout to reach a radius R is given by:

$$t = \frac{er^2}{kh}\left[\frac{\alpha}{3}\left(\frac{R^3}{r^3}-1\right)-\frac{\alpha-1}{2}\left(\frac{R^2}{r^2}-1\right)\right] \qquad (2.37)$$

This time t has its upper limit at the binding time of the injection product. If it concerns an injection product with increasing shear strength over time (Bingham-type) then the grouting pressure h is, moreover, counteracted by a high variable α – value and increasing friction resistance between the liquid and the grains of the skeleton (van Impe, 1989). These equations can be used to estimate the required hydraulic head or the flow rate of the grout knowing the relationship between t and R for given soil and grout parameters.

Rearranging (by the author) (2.35) for R:

$$h = \frac{Q}{4\pi k}\left[\alpha\left(\frac{1}{r}-\frac{1}{R}\right)+\frac{1}{R}\right]$$

$$\text{Therefore, } R = \frac{1-\alpha}{\frac{4\pi kh}{Q}-\frac{\alpha}{r}} \qquad (2.38$$

Also rearranging (by the author) for Q:

$$h = \frac{Q}{4\pi k}\left[\alpha\left(\frac{1}{r}-\frac{1}{R}\right)+\frac{1}{R}\right]$$

$$\text{Therefore } Q = \frac{4\pi kh}{\left[\alpha\left(\frac{1}{r}-\frac{1}{R}\right)+\frac{1}{R}\right]} \qquad (2.39)$$

Considering the radius of the borehole, R_0, the following equations describe horizontal (radial) flow from a section of a borehole:

$$p_e = \frac{Q\gamma\mu}{2\pi mk\mu_w} \ln \frac{R}{R_0} \qquad (2.40)$$

Where: p_e = excess pressure necessary to maintain flow rate of grout (Q); R = radius grout has reached from the injection point; R_0 = radius of the borehole; m = thickness of grout layer; γ = bulk unit weight of grout; k = permeability of the soil to water; μ = viscosity of grout and μ_w = viscosity of water.

These equations are analogous to those relating to a single well fully penetrating a confined aquifer. This case represents recharge rather than draw down, which also has the added benefit of creating a perched water table above the lime barrier. During recharge the pressure p(R) of the grout diminishes with distance R from the borehole according to the equation:

$$p(R) = p_e - \frac{Q\gamma\mu}{2\pi mk\mu_w} \ln \frac{R}{R_0}$$

The above model is based on the premise that the grouting pressure at the base of the injection tube should just exceed the hydraulic fracturing pressure of the clay, in order to create a lateral tensile plane. The factors affecting the hydraulic fracture will be determined through large-scale laboratory simulations and further field trials.

Moreover, the following significant points of the model should be noted:

(i) The time required for grout to reach a given distance in the soil depends on the grouting rate Q;

(ii) The grouting rate can be increased by increasing the pressure of grouting or by using a lower viscosity grout (i.e. increasing water to lime ratio); and

(iii) The viscosity and setting time of the grout must be controlled such that sufficient time is available for the grout to permeate the required lateral extent within the soil stratum. This dictates the design of injection hole spacing.

3.7 Implications for the current research

As previously mentioned a thorough understanding of the background information regarding the processes fundamental to the field investigations of the lime-fly ash barrier is important. A review of previous research into grouting and the use of lime and fly ash in slurry injection systems were necessary for determining the appropriate injection methods and grout ratios to employ in this current study. This will be expanded upon on Chapter Five.

Chapter 4.0 Field Study Site Information and Monitoring Details

4.1 Introduction

The field study site and the monitoring equipment used to investigate the physical and chemical attributes of both the ground and drain water are described in detail in this chapter. A study site was selected to trial and assess the installation of a lime-fly ash barrier adjacent to an acid sulphate soil drain. The study site is suitable for this purpose due to four major attributes, namely:

1. The site is underlain by Acid Sulphate Soils;
2. Accessibility to the site is easy in regards to the transportation of grouting equipment;
3. The pyrite layer is relatively close to the ground surface (1.2m below ground surface); and
4. The site has a network of artificial drainage that has lowered the groundwater table below the elevation of the acid sulphate soil layer causing acidic soil, groundwater and drain water conditions.

The exact location of the study site within the Shoalhaven Catchment is described in the first section of this Chapter, along with the geomorphology of the catchment and the nature of the drainage scheme at the site. The second section of this Chapter describes the equipment installed at the site and the monitoring regime undertaken to test routine groundwater and drain water parameters. This includes the construction, location and installation of observation holes and piezometers; routine pH, electrical conductivity, temperature, groundwater table height; and the collection of water samples for laboratory analysis.

The baseline chemical, physical and morphological properties of the soil at the Lime-fly ash barrier site are described in the third section of this Chapter. The climatic conditions of the area obtained over the entire study period are described in the fourth and final section of this Chapter.

4.2 Study Site Location

The study site is a small sub-catchment of approximately 120ha that has been drained for agricultural and flood mitigation purposes. The site is adjacent to the township of Berry (34°S, 150°E) on the South Coast of New South Wales, Australia. A network of drains was constructed across the site in the late 1960s. The drains discharge into Broughton Creek, a left bank tributary of the Shoalhaven River. The location of the study site, known as the Lord drain area, is located east of Broughton Creek, in the northern end of the hotspot area near Berry. Land near the north drain ranges in elevation from 0.6m AHD up to 2m or more on the levee bank. The top of the sulphidic layer generally occurs below –0.5m AHD (top of the layer ranging from –0.1 to –0.65m AHD) i.e. about 120 to 150cm below the soil surface in the lowest areas. The study site is typical of coastal floodplains in New South Wales with the maximum elevation of 1.14 m Australian Height Datum (AHD) and the lowest elevation less than 0.82 m AHD.

A location map of the lime-fly ash barrier study site, along with the other sites investigated in this study is shown in Figure 4.1 and a photograph of the lime-fly ash barrier study site is shown in Plate 4.1.

Figure 4.1: Location of the study site

Plate 4.1: Photo of the study site.

4.2.1 Geology and Geomorphology

The Shoalhaven River is located 160km south of Sydney on the tectonically stable south coast of New South Wales. The river drains a catchment of 9260km^2 and in its lower reaches incises into Permo-Triassic sandstone and siltstones of the Sydney Basin (Umitsu *et al.*, 2001). Figure 4.2 illustrates the landforms of the Shoalhaven River floodplain. The lower Shoalhaven River catchment (Broughton Creek catchment) is comprised of low hill slopes, a coastal sand barrier and coastal floodplains. Mount Coolangatta, rising to over 300m, controls the route of Broughton Creek. To the east, a late Quaternary sand barrier separates the floodplain from the Pacific Ocean. Both the Shoalhaven River and Broughton Creek are highly channelised and are considered to have almost completely infilled the pre-existing estuarine embayment (Roy, 1984). The extensive estuarine alluvial floodplain extends on both the northern and southern sides of the Shoalhaven River. Berry Siltstone and Nowra Sandstone underlie the unconsolidated sediments of the floodplain. This floodplain currently supports pastureland for mainly dairy farming.

It has been suggested by Roy (1994) that the formation of sulphidic sediments in the northern Shoalhaven was typical of processes associated with infilling of a barrier estuary. The infilling of the Shoalhaven River valley commenced about 12000 years

Radiocarbon dating of unoxidised estuarine sediments and shell collected in these sediments (ages 4280±110 and 3800±110 years BP respectively) suggested that the elevated sea levels might have occurred up to 4000 years ago (Willett and Walker, 1982; Woodroffe *et* al., 2000). The formation of levees served to impound a series of low-lying flood basins with initial infilling occurring around the margins. As ocean heights receded and stabilised to current levels, pyrite formation ceased and freshwater alluvial processes dominated.

Roy (1984) described the evolution of the lower Shoalhaven River as belonging to the "barrier estuary" system. According to Roy (1984), in early stages of development, the shorelines of barrier estuaries are often rocky and highly irregular (Figure 4.3a). Estuary infilling creates sinuous channels with smooth level banks (Figure 4.3b), which promote the attenuation of tides and enhances mixing with the water column. Broughton Creek has a significant tidal range with Pease (1994) observing tidal fluctuations up to 0.75 m at a location 11.5 km's from the mouth of the Shoalhaven River. These shorelines develop into lobate deltas with bifurcating distributary channels, shoal grounds and embayments (Figure 4.3c). The final stages of infilling are characterised by sinuous channels with smooth levee banks (Figure 4.3d). These final stages are typical in the lower Shoalhaven floodplain.

It has been suggested that the sedimentation in the Shoalhaven barrier estuary occurred at approximately 5 mm/year to form an extensive 'mud basin' up to 30m thick (Roy, 1984). Inland, these muds interlayer with tidal sand deposits within the river mouth. However, since the Shoalhaven barrier estuary is at a mature stage of development infilling has ceased and river sand is being exported from the system and is accreting on Seven Mile Beach. A diagram of the stratigraphy of the Shoalhaven River catchment is shown in Figure 4.4.

The formation of acid sulphate soils within the Broughton Creek catchment is attributed to the geomorphologic evolution of the Shoalhaven estuary. ASS risk maps produced by the NSW Department of Land and Water Conservation (now the Department of Infrastructure, Planning and Natural Resources) and described by

Naylor *et al.* (1995) show that approximately 2500 ha of land with a high risk of occurrence of acid sulphate soils are found within the Broughton Creek floodplain. The distribution and location of ASS in the Broughton Creek Hotspot area are shown in Figure 4.5.

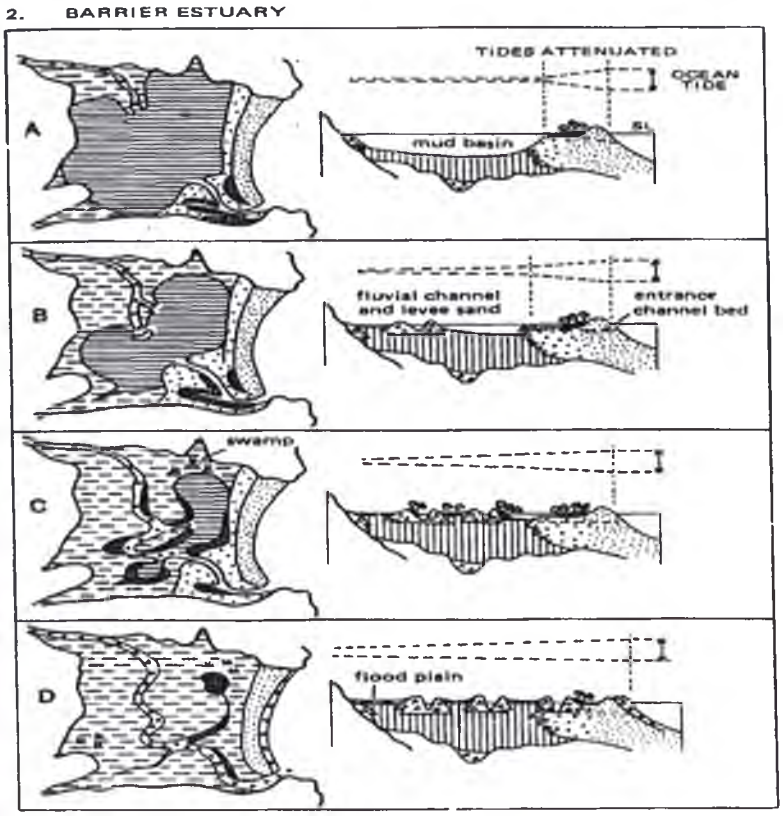

Figure 4.3: Evolution of the lower Shoalhaven floodplain (Roy, 1984)

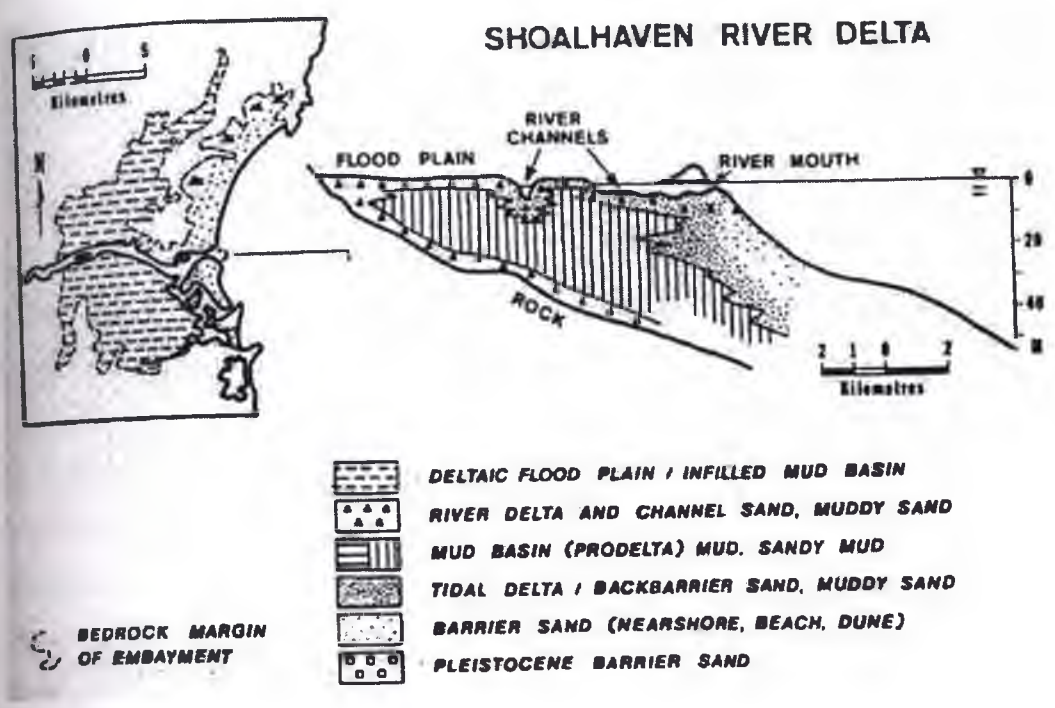

Figure 4.4: Geomorphology of the Shoalhaven River Catchment (Roy, 1984)

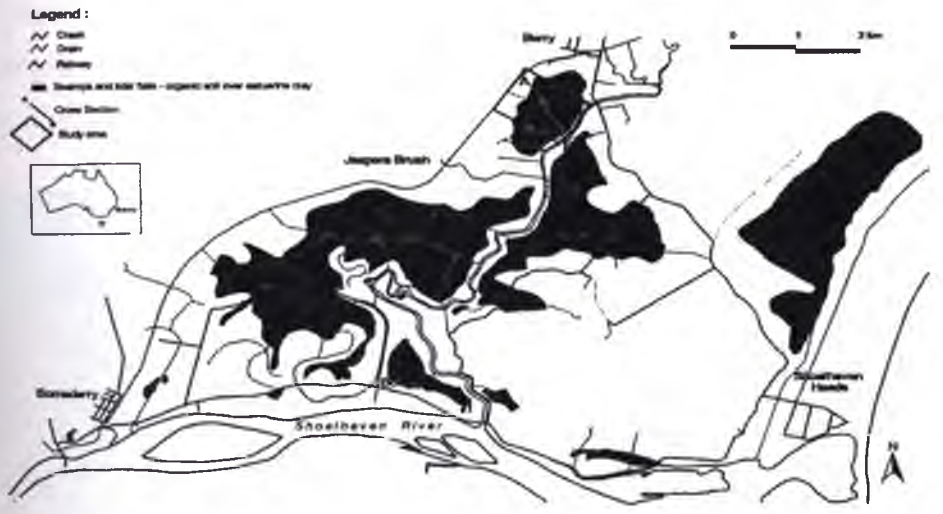

Figure 4.5: Location and distribution of Acid Sulphate Soils

4.2.2 *Shoalhaven Flood Mitigation System*

Artificial drainage started in the Shoalhaven floodplain in 1820 when a small number of shallow drains were excavated near Mt Coolangatta (Bayley, 1975). The first form of major artificial drainage in the lower Shoalhaven was the construction of Berry's canal in 1840, which allowed navigation between the Shoalhaven and Crookhaven Rivers. Floodwaters in 1860 and 1870 were observed to recede more rapidly than prior to construction of the canal (Bayley, 1975). This suggests that the construction

of Berry's canal was the first cause of the lowering of the watertable in the lower Shoalhaven, possibly inducing pyrite oxidation in nearby acid sulphate soils.

A 'tenant farming policy' allocated twenty acre plots rent free on the condition that they were cleared, fenced and drained by the end of the two to five year leave (Bayley, 1975). By 1850 dairy farming had become established as the primary industry of the Shoalhaven region. The introduction of *Paspalum* pasture for cattle feed during the 1890s was found to significantly increase milk and cream production therefore additional flat land was sought thereafter. By 1901, 32km^2 of floodplain surrounding Broughton Creek had been drained with 210 km of drains fitted with floodgates and walls (Blunden, 2000). Improved drainage had lowered the groundwater table, consequently promoting pyrite oxidation and acid production. The present drainage network on the Broughton Creek floodplain was in place by 1949. During 1965-72 all of the existing drains were deepened and widened in accordance with government flood mitigation policies and funding arrangements of the day. Drain inverts were set at –4 ft KAZI datum (20 cm below Australian Height datum). All floodgate structures were upgraded and expanded during 1965-72. The flood mitigation drain located at the study site is shown in Plates 4.2 and 4.3.

Plate 4.2: Flood mitigation drain at the lime-fly ash barrier study site looking downstream. Drain width is approximately 5m

Plate 4.3: Flood mitigation drain at the lime-fly ash barrier study site looking upstream. Note close proximity of study site to Coolangatta Road.

Floodgates installed across Broughton Creek range in size and capacity. However, most consist of a battery of 1-4 concrete culverts (2m x 2m) with vertically suspended steel plates operating to control the entrance of saltwater from the Creek into the drains. The floodgates are lined with a rubber seal between the steel plate and the concrete, so as to minimise leakage. However, floodgates often leak due to objects being stuck between the gate and the culvert wall holding the gate open, or poor sealing of the gate due to the rubber seal perishing or the steel gate warping (Blunden, 2000). Pease (1995) and Blunden (2000) noted minor leakage upstream of the floodgate when debris became jammed between the floodgate and the culvert wall and when the rubber seal deteriorated.

A number of other floodgate styles have been installed in the Broughton Creek catchment. These are however small structures built on mole drains (i.e. circular gates attached to underground pipes) and function on the same principle as the larger gates. A selection of floodgates monitored in this study including the floodgate found approximately 858 m downstream from the lime-fly ash barrier study site is shown in Plate 4.4. Generally, the artificial drainage system (approximately 230km of drains are found on 40km^2 (Pease, 1994)) across the Broughton Creek catchment contains deep (~3m) drains that remove surface and groundwater from the surrounding land

through straightened and cleared channels. Given the geometry of these drains and the operation of floodgates, it would be expected that the high drainage density would lead to significant and extensive groundwater drawdown (Blunden, 2000). The deep drains increase the hydraulic gradient between the groundwater and the drain, causing the groundwater elevation to decrease.

The current operation of flood-gated systems across the Broughton Creek catchment ensures that the elevation of water in the drains is at about the low tide level (approximately –1.0m AHD). At the study site, low tide level is well below the elevation of the acid sulphate soil layer. Such a low drain water level gives rise to a hydraulic gradient where the shallow groundwater flows into the drain. As groundwater drainage occurs, the acid sulphate soils become unsaturated giving rise to the entrainment of oxygen and subsequent generation of acid thereby causing environmental problems.

Plate 4.4: Tidal restricting floodgate installed on flood mitigation drain in the Broughton Creek Estuary. Floodgate (a - FG1), modified floodgate is located downstream from the Lime Injection Site. Floodgates (b - FG2), (c - FG3) and (d – FG4) are the other floodgates monitored during this study

The geomorphology, soil characteristics and drainage systems in the Shoalhaven Floodplain are typical of coastal floodplains in New South Wales affected by acid sulphate soils. The lime-fly ash barrier site investigated in this study contains a pyritic layer approximately 1.2 m below the ground surface and flood mitigation drain (5m wide x 2m deep x 600 m long (to Coolangatta Road)) adjacent to the site. This drain contains a tidal-restricting floodgate, which was converted from a one-way floodgate to a modified two-way floodgate in December 2003 and commissioned in March 2004.

4.3 Field equipment and monitoring

A comprehensive monitoring program was undertaken to investigate the relationship between groundwater, drain water and creek water quality before and after the installation of the lime-fly ash barrier. The monitoring program commenced on 1 August 2003 after the installation of observation wells and piezometers. Baseline data was collected until the lime-fly ash barrier was installed at the beginning of April 2004. Preliminary field lime-fly ash injections were undertaken in November 2003 and were completed in June 2004.

Four floodgate sites (FG1: Lords Drain P6D1; FG2: Forsyth Drain P6D2; FG3: Harris Drain P3D8; FG4: Stewart Drain P6D8), one weir site (Tilting weir, 25m downstream) and one proposed weir site (400 metres upstream from FG1) were also monitored for water quality parameters throughout the study for comparison with results from the lime-fly ash barrier site. The locations of the four floodgate sites and two weir sites in relation to the lime-fly ash barrier site are shown in Figure 4.6.

4.3.1 Lime-fly ash barrier Study Site Elevation Characteristics and Site Topographic Survey

A comprehensive survey of the Broughton Creek area was undertaken to assess the topography of the floodplain. High-resolution airborne laser surfacing (ALS) was used by Environmental Systems Research Institute Inc (ESRI) Australia, in conjunction with Shoalhaven City Council, to develop digital terrain maps and digital elevation maps (DEM) using ArcGIS. The topographical elevation data was related to Australian Height Datum (AHD). Ground-truthing was conducted on floodgates and weirs. A digital elevation map of the Broughton Creek topography is shown in Figure 4.7.

Allen, Price and Associates prepared a detail and level survey at 1:100 scale of the study site. The topographic elevation data was related to the Australian Height Datum (AHD). A temporary benchmark at the water trough was established. Figure 4.8 shows the survey of the study site.

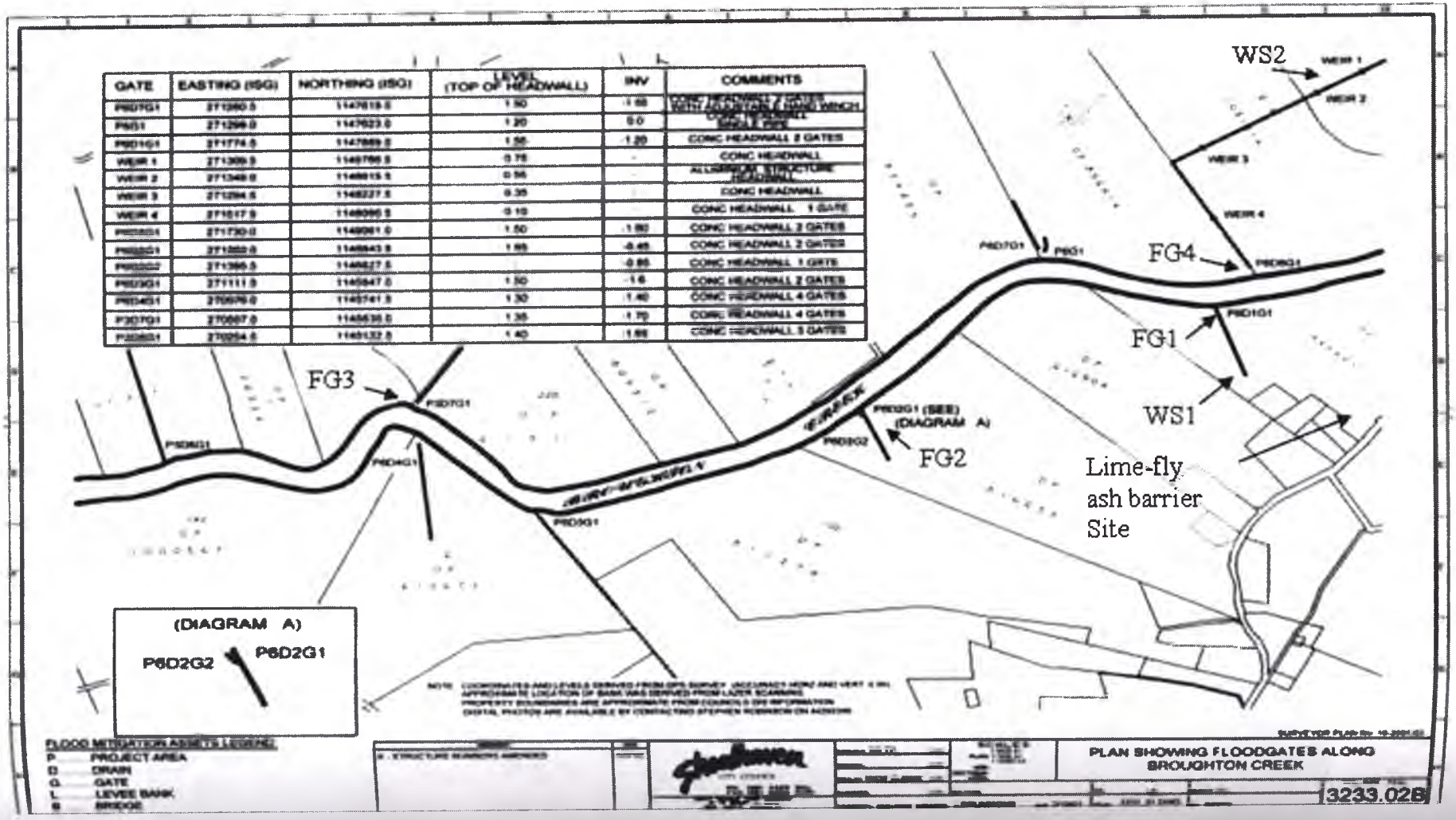

GATE	EASTING (ISG)	NORTHING (ISG)	LEVEL (TOP OF HEADWALL)	INV	COMMENTS
P6D7G1	271260.5	1147619.0	1.50	-1.68	CONC HEADWALL 2 GATES WITH FLOODGATE BANG WEIGH
P6D1	271296.0	1147623.0	1.20	0.0	CONC HEADWALL SINGLE PIPE
P6D1G1	271774.5	1147889.2	1.56	-1.20	CONC HEADWALL 2 GATES
WEIR 1	271309.5	1149786.5	0.76	-	CONC HEADWALL
WEIR 2	271349.0	1149815.5	0.56	-	ALLSPRIDGE STRUCTURE HEADWALL
WEIR 3	271284.5	1148227.5	0.35	-	CONC HEADWALL
WEIR 4	271517.5	1148090.5	0.10	-	CONC HEADWALL 1 GATE
P6D5G1	271730.0	1149081.0	1.50	-1.80	CONC HEADWALL 2 GATES
P6D5G1	271850.0	1148843.5	1.65	-0.45	CONC HEADWALL 2 GATES
P6D2G2	271366.5	1148627.5	-	-0.85	CONC HEADWALL 1 GATE
P6D3G1	271111.0	1148647.0	1.50	-1.6	CONC HEADWALL 2 GATES
P6D4G1	270979.0	1148741.5	1.50	-1.40	CONC HEADWALL 4 GATES
P3D7G1	270887.0	1148636.0	1.35	-1.70	CONC HEADWALL 4 GATES
P3D8G1	270254.0	1149132.5	1.40	-1.85	CONC HEADWALL 3 GATES

Figure 4.6: Location of Floodgate and Weir sites in relation to Lime-fly ash barrier study site

Figure 4.7: Digital Elevation Map (DEM) of Broughton Creek floodplain

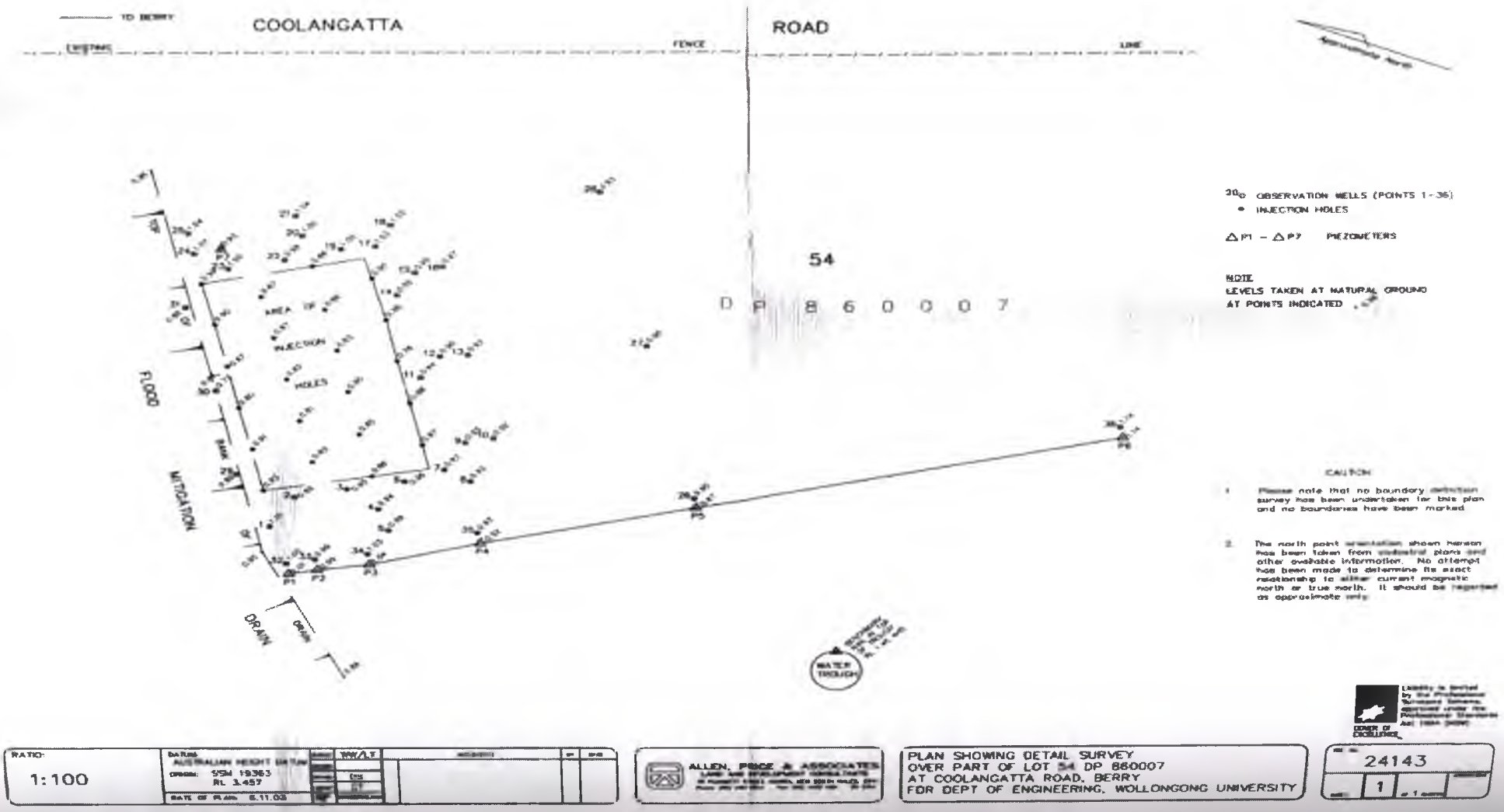

Figure 4.8: Topographic survey of Lime-fly ash barrier study site

Plate 4.6: Installation of Observation Holes by the author.

4.3.3 Water Quality Monitoring

The measurement of pH, electrical conductivity (mS), temperature (°C) and groundwater table elevation was conduction at each site, whereas water quality analyses for the determination of Al^{3+}, Ca^{2+}, Mg^{2+} and Fe^{2+} were carried out at the University of Wollongong's Environmental Engineering Laboratory. Water analyses for the determination of chloride and sulphate in filtered samples were undertaken at Southern Cross University's Environmental Analysis Laboratory. The methods are briefly described below.

4.3.3.1 pH, Electrical Conductivity, Temperature and groundwater table elevation

A TPS Aqua CP Meter was used to measure pH, as well as electrical conductivity and temperature of groundwater on site. It consists of two probes, which were placed into the groundwater sample and a hand-held display. It was calibrated before each day of sampling using standard pH and electrical conductivity buffer solutions, namely 4.0 and 6.88 and 2.65 mS/cm respectively.

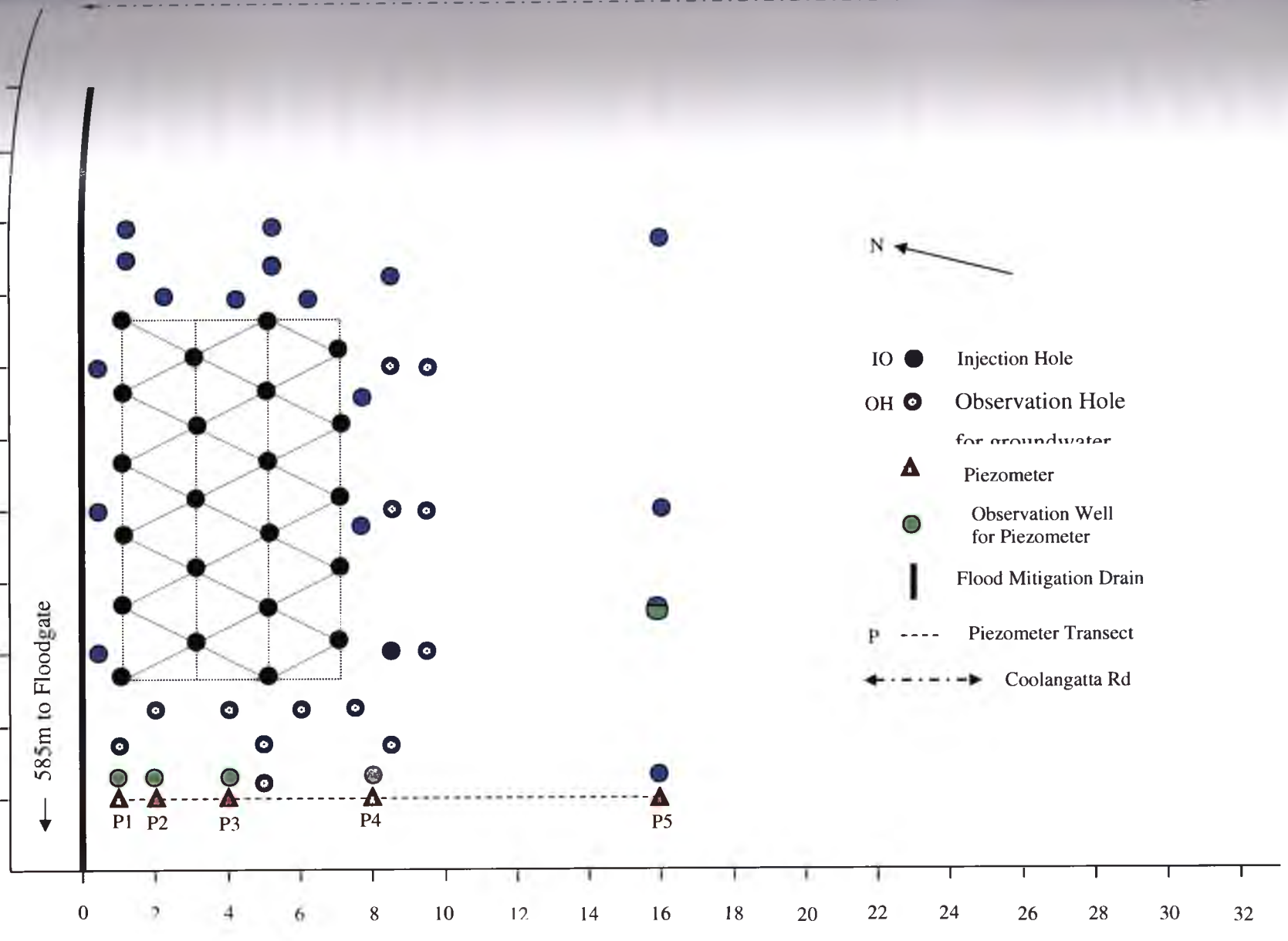

Figure 4.9: Layout of Study site showing location of observation holes and piezometers.

The pH, electrical conductivity, and temperature (along with groundwater table elevation) were recorded fortnightly, unless otherwise stated. By inserting a bailer (1.5m length of PV pipe with a stainless ball bearing inside) into each observation hole the groundwater table elevation was measured. When the bailer reached the groundwater table, a 'plopping' sound was heard signalling the level of the groundwater. The distance from the groundwater table to the top of the observation hole was read via a measuring tape attached to the bailer; the distance measured was converted to m AHD.

4.3.3.2 Chloride and Sulphate Concentration

Both chloride and sulphate concentration were unable to be determined using the ion chromatography facility at University of Wollongong's Environmental Engineering Laboratory due to technical problems. The samples were initially filtered through a 0.40-0.45 μm polycarbonate membrane to remove particulate matter and were then sent to Southern Cross University's Environmental Analyses Laboratory for analysis. Analysis for chloride and sulphate was performed according to APHA methods (1998). The filtered water samples were analysed by ICP-MS (Inductively Coupled Plasma-Mass Spectrometry) or ICP-OES (Inductively Coupled Plasma - Optical Emission Spectrometry). The results were reported in mg/L.

4.3.3.3 Determination of cations

The concentration of Al^{3+}, Ca^{2+}, Mg^{2+} and Fe^{2+} in each water sample was determined using a Varian SpectrAA 300 Atomic Absorption Spectrometer using methods described by Dharmappa and George (2000). Samples (100mL) were initially digested with concentrated nitric acid (HNO_3). The solution was boiled to the lowest possible volume (20 mL) while adding 5 mL HNO_3 to avoid boiling dry. Digestion was complete when the solution turned a light straw yellow colour. The solution was then filtered through a 0.40-0.45 μm polycarbonate membrane to remove particulate matter. The metals were then measured by placing the solution into an air-acetylene flame in the Varian SpectrAA 300 Atomic Absorption Spectrometer and the wavelength and ion specific hallow cathode lamp appropriate for each metal. The results were reported in mg/L.

4.3.4 Construction and Installation of Piezometers

Five piezometers were constructed and installed at the study site to monitor pore water pressures. The piezometers have been set at perpendicular intervals of 1 m, 2 m, 4 m, 8 m and 16 m from the drain. See Figure 4.9 for the location of the piezometer transect (Transect A) in relation to the observation holes.

The design of the piezometers used was based on the Penman Formula (1994).

$$t = 3.3e^{-6} \times \frac{d^2 \ln\left[L/D + \sqrt{1+(L/D)^2}\right]}{kL} \qquad (4.1)$$

Where:

t = time required for 90% response in days

d = inside diameter of standpipe in cm

D = diameter of intake filters (or sand zone) in cm

L = length of intake filter (or sand zone around the filter) in cm

k = permeability of soil in cm per second

The piezometers were designed so that the time lag was ideally less than 2 days so when measurements were taken from the piezometers the pressures calculated were close to the actual present pore water pressures in the ground. The time lag can be minimised by using a minimum diameter standpipe and a maximum sized sand zone (See Appendix A for Time lag calculations).

The diameter of the standpipe was designed to fit down a 100 mm diameter hole. Therefore, diameter of the intake filter was 100 mm. The height of the filter was generally 250 mm to allow for a time lag less than 2 days. The permeability of the soil was assumed to be 1 x 10^{-6} cm/s, which is typical of soil of this nature. The height of the piezometers was based on water table heights along the transect at the time of installation. Figure 4.10 shows the design layout of the piezometers and Table 4.1 shows the dimensions of each of the installed piezometers. Plate 4.7 is a photo of the constructed piezometers with a close up of the piezometer tip before they were placed in the ground.

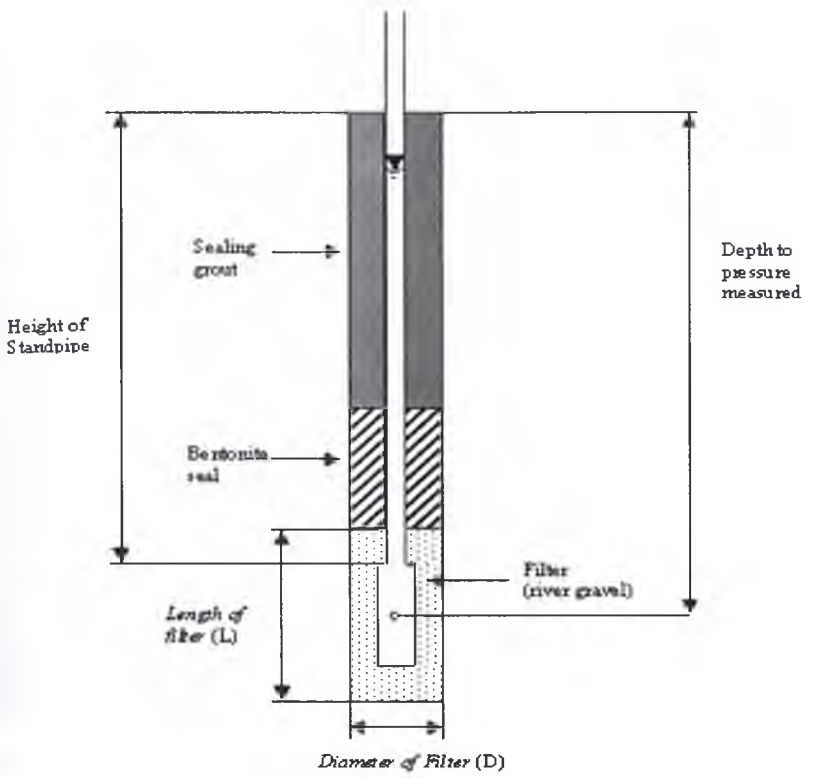

Figure 4.10: Design Layout of Piezometers

Table 4.1: Piezometer Dimensions

Piezometer Dimensions	Piezometer Number				
	1	**2**	**3**	**4**	**5**
Total length (m) including length of pipe above ground	2.20	1.70	1.50	1.30	1.10
Standpipe length (m)	1.90	1.40	1.20	1.0	0.80
Tip length (m)	0.2	0.2	0.2	0.2	0.2
Standpipe inside diameter (mm)	20	20	20	20	20
Standpipe outside diameter (mm)	23	23	23	23	23
Tip inner diameter (mm)	50	50	50	50	50
Tip outer diameter (mm)	56	56	56	56	56
Filter Dimensions					
Height (cm)	25	25	27.5	25	26.2
Width (cm)	10	10	10	10	10
Depth below tip (cm)	2.5	2.5	2.5	2.5	2.5
Depth above tip (cm)	2.5	2.5	5.0	2.5	3.7
Installation Dimensions					
Hole depth (m)	2.125	1.625	1.425	1.225	1.025
Hole diameter (m)	0.10	0.10	0.10	0.10	0.10
Standpipe height above ground (m)	0.1	0.1	0.1	0.1	0.1
Depth of pressure measured (m)	1.8	1.5	1.3	1.1	0.88
Time lag (assumed permeability) (days)	0.87	0.87	0.83	0.87	0.85

Plate 4.7: Piezometers and close up of piezometer tip (filter section)

The piezometers were installed at boreholes on the site. A drilling contractor drilled the 2m holes, shown in Plate 4.8.

Plate 4.8: Drilling of Piezometer Holes

4.4 Soil Investigations

A wide selection of soil chemical properties can be used to describe pyritic soils and the influence that pyritic oxidation products have on the chemical properties of a soil profile. A number of routine soil chemical properties such as soil pH and electrical conductivity, titratable acidity and sulphate concentration both before and after pyrite oxidation have been suggested by Stone *et al.* (1998).

4.4.1 Soil Sampling Methods

A soil core was acquired by pushing a 60 mm diameter steel tube into the soil to a depth of 1.6 m using the NSW Agriculture Proline drill rig. The core was sectioned at 0.1 m intervals with soil samples collected down the soil profile at depths of 0-0.1 m, 0.25-0.35 m, 0.60-0.70 m, 0.80-0.90 m, 1.20-1.30 m and 1.50-1.60 m. The soil samples were sealed in plastic bags, stored below 4°C until they were oven dried at 85°C (Stone et al., 1998). The soil was then ground and passed through a 2 mm sieve.

The routine soil chemical properties that were tested for included (See results in Appendix A: Soil Laboratory Data):

1. Soil *pH* (1:5 in 0.01M $CaCl_2$ solution) and *electrical conductivity* (1:5 soil/water).
2. *Total Actual Acidity (TAA)*: A 5-gram soil sample was suspended with 50mL of KCl and shaken overnight. A filtered 25ml aliquot was titrated with 0.25 M NaOH until pH 5.5. The volume of alkali required to reach pH 5.5 established the total actual acidity. The results are expressed as mol H^+/tonne of dry soil.
3. *Reduced Inorganic Sulphur Content*: The inorganic sulphur content is reduced to H_2S by digestion with an acidified chromous chloride solution under a nitrogen atmosphere. The H_2S is then collected in a zinc acetate buffer as ZnS and is acidified. Finally, the H_2S content is analysed by iodometric titration. The results are expressed as $\%S_{cr}$.
4. *Dissolved Chloride Concentration*: The soil samples were extracted with a 1:5 water extract for water-soluble chloride. Soluble chloride in the extracts was analysed by Ion Chromatography. The results are expressed as mg/kg.
5. *Dissolved Sulphate Concentration*: The soil samples were extracted with a 1:5 potassium phosphate (0.01M KH_2PO_4) solution for phosphate extractable

sulphate. The total sulphur in the extracts were analysed by ICP-AES with the results reported as mg/kg.

The depth of the lime-fly ash slurry injection was determined by the location of the top of the pyrite layer. An investigation of the soil acidity using pH (laboratory) and hydrogen peroxide (in the field) tests facilitated the identification of the actual and possible acid sulphate soil layers (See Table 4.2). Low pH values, between 3.04 and 4.33, were found in the soil. Hydrogen peroxide reacted within the soil at a depth of 1.2 – 1.6 m (below the ground surface). This indicated the presence of actual acid sulphate soils at profile depth of 1.2 – 1.6 m (below the ground surface). The depth of the preliminary lime-fly ash injections were determined to be most advantageous at 1.2 m, just above the pyrite layer.

Table 4.2: Preliminary Investigations Borehole 1 – Lime-fly ash barrier injection site

Sample Depth (cm below ground surface)	Description	pH	EC	Hydrogen Peroxide
0-10	Dark brown, Organic matter, roots and grasses	4.33	0.63	No reaction
10-25	Dark brown loam with iron mottles – reddish colour	-	-	-
25-35	Peat Loam Very dark grey/black	3.74	0.55	No reaction
35-60	Peat Loam Very dark grey/black	-	-	-
60-70	Very Dark grey, clayey loam	3.31	0.61	No reaction
70-80	Very Dark grey, clayey loam. Becoming silty.	-	-	-
80-90	Grey/Black. More clay, More silty	3.38	0.36	No reaction
90-120	Light grey black/Silty clay with good root penetration	-	-	-
120-130	Potential Dark Grey Silty clay	3.04	1.35	5. Very vigorous fizzing
130-135	Distinct gritty sand layer	-	-	-
135 - 150	Potential dark grey silty clay with partly decomposed vegetation, no mottling.	-	-	-
150-160	Potential dark grey silty clay with partly decomposed vegetation, no mottling.	3.55	1.5	5. Very vigorous fizzing
160-175	Potential dark grey silty clay with partly decomposed vegetation, no mottling.	-	-	-

4.4.2 Results and Discussion

4.4.2.1 Soil pH

The oxidation of pyrite produces H^+ ions and under acidic groundwater conditions, additional H^+ ions are produced through the biologically enhanced ferrous-ferric oxidation/reduction reaction. pH is calculated as:

$$pH = -\log [H^+] \quad (4.2)$$

Stone et al. (1998) indicated that soil pH < 4 is only likely to occur as a result of the oxidation of pyrite. The pH of the soil profile, measured before the installation of the lime-fly ash barrier, is shown in Figure 4.11.

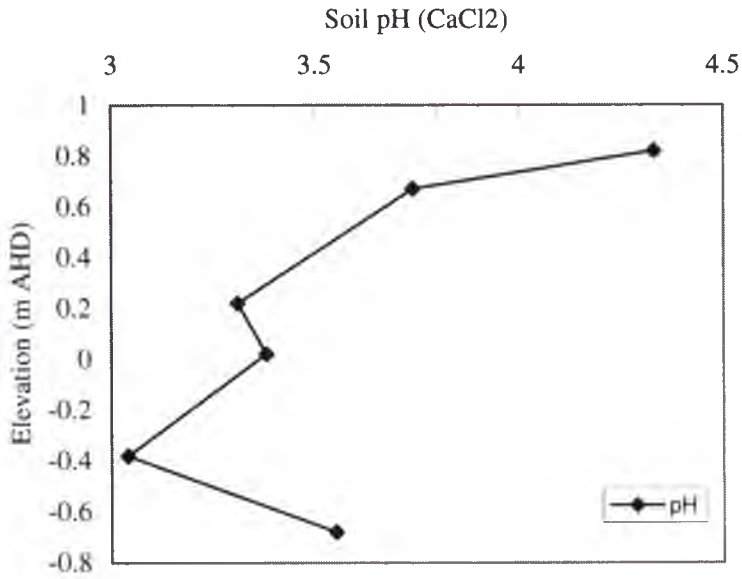

Figure 4.11: Change in soil pH with depth at Lime-fly ash Barrier Site

Acidic conditions exist at the surface of the soil profile, however with a pH value of 4.33 it is most likely that this acidity is a result of decomposed organic matter, as well as from the movement of pyritic oxidation products to the surface from depth. The acid stored within the zone directly above the pyritic layer may have a number of sources. One source of acidity is soluble sulphuric acid that has been transported from the pyrite oxidation zone to the higher elevation estuarine clay by rising

groundwater. Another source of acidity available in this soil layer is aluminium and hydrogen ions stored on cation exchange sites, which can be related to the salt content of the soil solution. The usual tendency of salts is to lower the pH of the soil as the salt content increases.

Underneath this upper layer the pH falls below 4.0 due to pyrite oxidation. The increase in pH in the lower section of the soil profile (below – 0.38 m AHD) indicates potential acid sulphate soils. Soil samples from this section however, reacted vigorously with hydrogen peroxide signifying the presence of sulphidic material.

4.4.2.2 Soil Electrical Conductivity

The electrical conductivity of the soil profile is shown in Figure 4.12. Electrical conductivity of the soil is low in the upper metre of the profile (< 0.63 dS/m), below which it increases to a maximum of 1.5 dS/m. This increase in electrical conductivity is a result of the generation of dissolved pyrite oxidation products.

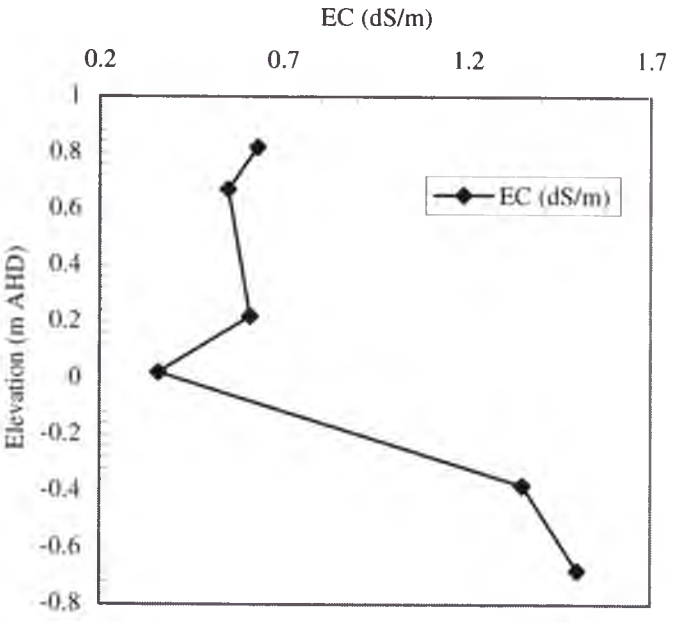

Figure 4.12: Change in soil Electrical Conductivity with depth at the Lime-fly ash Barrier site

The peak in electrical conductivity at 0.22 m AHD is most likely due to the formation of ferrous sulphate minerals, for example copiapite ($Fe_2(SO_4)_3$), which can precipitate

during dry conditions (Fanning, 1993). The oxidation of the iron in ferrous sulphate is described by the following equation:

$$FeSO_4 + \frac{1}{2}H_2SO_4 + \frac{1}{4}O_2 \rightarrow \frac{1}{2}Fe_2(SO_4)_3 + \frac{1}{2}H_2O \qquad (4.3)$$

The increase in electrical conductivity down the soil profile corresponds with increases in the concentration of dissolved sulphate (Figure 4.15). Iron sulphate minerals are also significant sources of acidity (Fanning, 1993). Equation 4.4 shows the oxidation and hydrolysis of ferrous sulphate to iron oxide.

$$FeSO_4 + \frac{1}{4}H_2O \rightarrow Fe(OH)_3 + H_2SO_4 \qquad (4.4)$$

4.2.2.3 Soil Total Actual Acidity

Total Actual Acidity is a measure of the amount of acidity stored in the soil excluding the potential sources acidity such as unoxidised pyrite (Dent and Bowman, 1996). The soil profile of total actual acidity (TAA) measured at the lime-fly ash barrier study site is shown in Figure 4.13. The increase in total actual acidity measured between 0 – 0.35 m below the ground surface can be attributed to organic material in the topsoil. The main features of this profile are the bimodal peaks in total actual acidity at 0.22 m AHD and – 0.38 m AHD. The total actual acidity was relatively low at the soils surface (80 mol H^+/tonne). The peak in acidity at 0.22 m AHD corresponds with the actual acid sulphate soil layer. The decrease in total actual acidity below this layer indicates the potential acid sulphate soil layer.

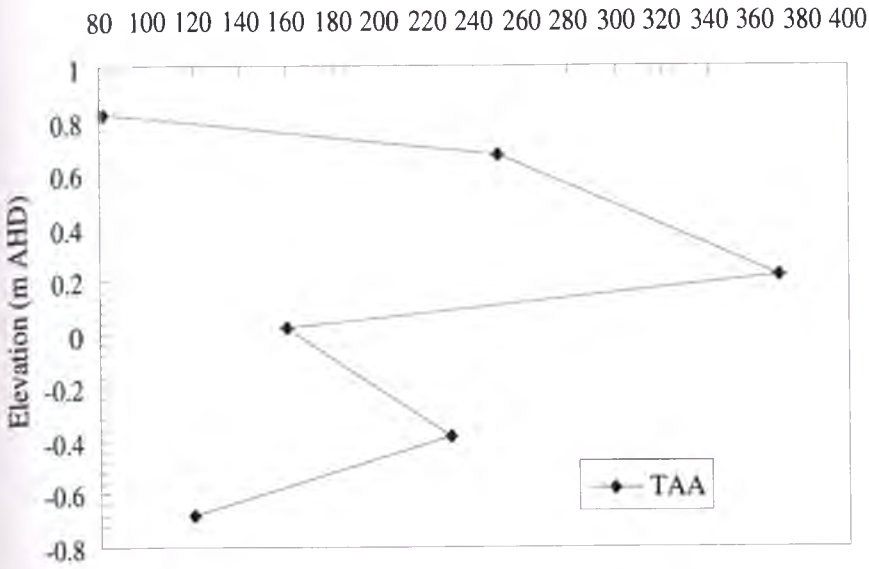

Figure 4.13: Change in Soil Total Actual Acidity (TAA) with depth at the Lime-fly ash barrier site

4.2.2.4 Soil Inorganic Reduced Sulphur (%S_{cr})

Inorganic reduced sulphur exists in natural environments in a solid phase as a number of compounds (pyrite, elemental sulphur, thiosulfate and sulphate), whereas its oxidation leads to sulphur solubilisation and further production of acidity. Microbes can enhance the rate of this oxidation by several orders of magnitude. Microbial growth is also enhanced by this sulphur oxidation. High concentrations of reduced sulphur species can occur in the pore water of sediments and in anoxic subregions of estuaries. Environmental concerns as a result of this oxidation include the mobilisation of toxic heavy metals. The S_{cr}% concentration down the soil profile is shown in Figure 4.14. S_{cr}% is low in the soil profile in the upper metre of the soil profile (<0.045 S_{cr}%), below which it increases to a maximum of 3S_{cr}%. The concentration of inorganic reduced sulphur in the lower section of the profile exceeds the management action criteria of 0.05S_{cr}% (Stone et al., 1998). The top 0.98 m of the soil profile is below the action criteria.

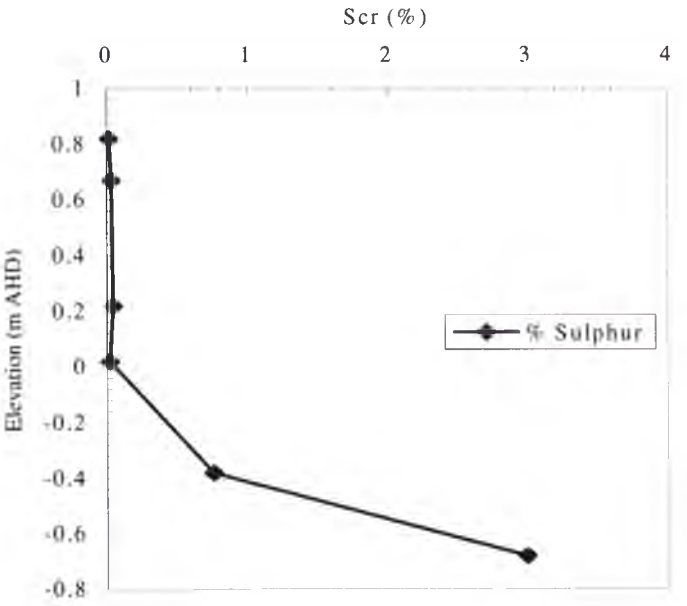

Figure 4.14: Change in Soil % Sulphur with depth at Lime-fly ash barrier site

4.2.2.5 Soil Sulphate and Chloride Concentrations

The concentration of dissolved sulphate and chloride down the soil profile is shown in Figure 4.15. The concentration of dissolved sulphate is typical of soils that have undergone pyritic oxidation. The concentration of the dissolved sulphate is highest at an elevation of 1.2-1.3 m, which corresponds to the upper surface of the pyrite layer. The decrease in sulphate concentration above the actual acid sulphate soil layer indicates the upward movement of sulphate ions and the abrupt decrease below the actual acid sulphate soil layer indicates the location of the potential acid sulphate soil layer.

Chloride concentrations in the soil profile are low compared to sulphate, however the greatest concentration of chloride in the soil profile also coincides with the upper layer of the pyritic soil layer. Low chloride concentrations in the top 1.0 m of the soil profile are possibly due to chloride leaching as a result of rainfall in the region.

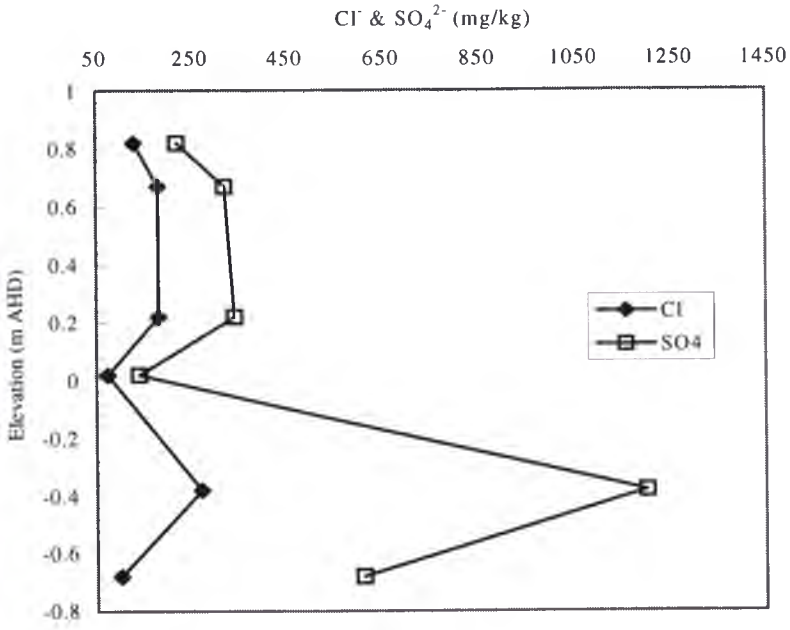

Figure 4.15: Change in Soil Cl- and S042- concentration with depth at the Lime-fly ash barrier site

Figure 4.16 shows the sulphate: chloride ratio down the soil profile. This is symptomatic of soil that has undergone previous pyrite oxidation. The highest chloride: sulphate ratio was found at 0.82 m AHD. The decrease in the chloride: sulphate ratio down the soil profile indicates the presence of oxidation products within the actual acid sulphate soil zone.

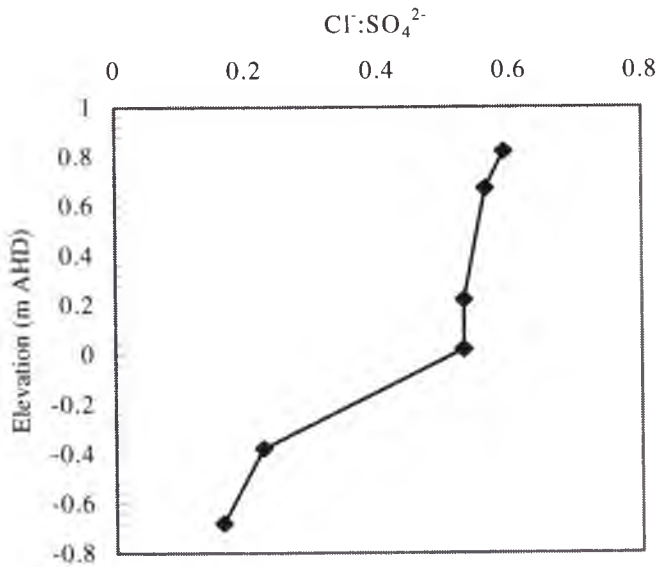

Figure 4.16: Change in Soil Cl-:SO42- ratio with depth at Lime-fly ash barrier site

4.5 Climatic Conditions

This section examines rainfall data before (Days 1-299) and after (Days 300-440) the installation of the lime-fly ash barrier. The relationship between rainfall and evapotranspiration is directly related on the concentration of buffering agents within a tidal reach. This relationship also has an impact on the elevation of the groundwater table in coastal floodplains and in turn on acid production in those areas affected by acid sulphate soils. During periods of high evapotranspiration, the groundwater table can fall below the pyritic layer leading to an increase in the production of acidic products. Following rainfall these acidic products are transported into nearby drains and creeks. Therefore, the management of acid sulphate soils requires a comprehensive understanding of rainfall and evapotranspiration rates at the study site. The Southern Oscillation Index measured over the study period is also presented and its relevance to acid generation and discharge is discussed.

4.6 Site Weather Conditions

Daily rainfall data was collected from a nearby weather station at the Berry Masonic Village (34.78°S, 150.69°E, 10 m above MSL) or from the Nowra Treatment Works (34.87°S, 150.62°E, 10 m above MSL) when data from the Barry Masonic Village was unavailable. The Bureau of Meteorology provided this data, which is presented in Appendix B.

4.6.1 Rainfall

The total rainfall received at the study site during the study period was 846.4mm. The daily rainfall at the study site before and after the installation of the lime-fly ash barrier is shown in Figures 4.17a and 4.17b respectively. Prior to the installation of the barrier, rainfall at the site was grouped into four events: Days 112-117, 166-195, 207-235 and 248-249. During Days 112-117, 161.6 mm of rainfall was recorded within 5 days. This event caused widespread flooding across the study sites. From Days 118-165, a prolonged dry period was followed by 66.8 mm of rain falling over a 47-day period. Rainfall of 107.8 mm occurred during Days 166-195, which was followed by a short drought period where no rainfall occurred between Days 196-206. During Days 207-235, precipitation led to 114 mm of rain falling within 28 days.

From 236-247, another dry period returned and 4.7 mm fell over the 12-day period. Rainfall of 111.8 mm during Days 248-249 caused minor creek and surface flooding. There was a prolonged dry spell after the installation of the lime-fly ash barrier bringing drought conditions.

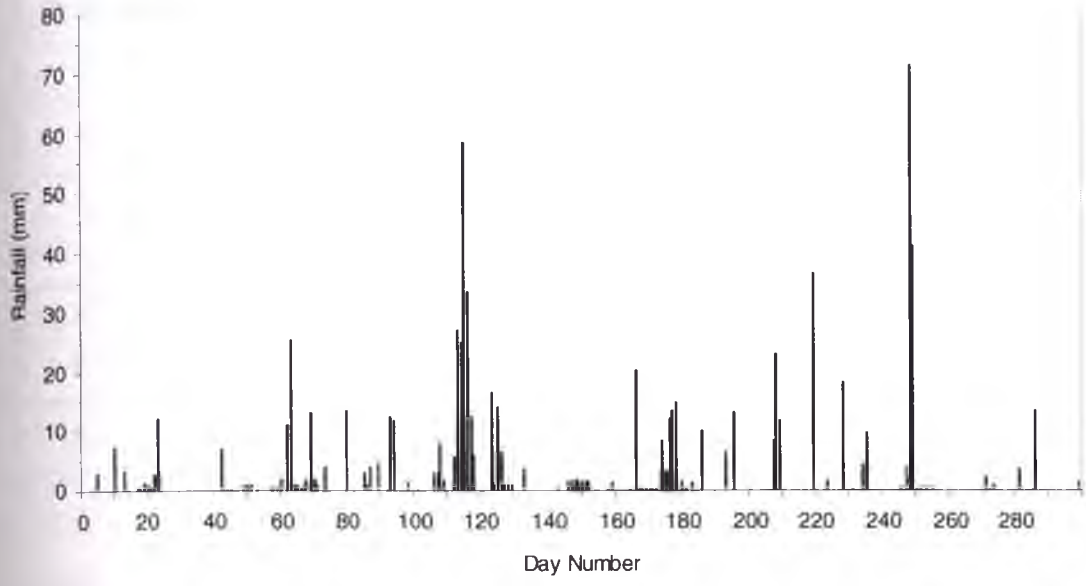

Figure 4.17a: Daily rainfall pre-barrier

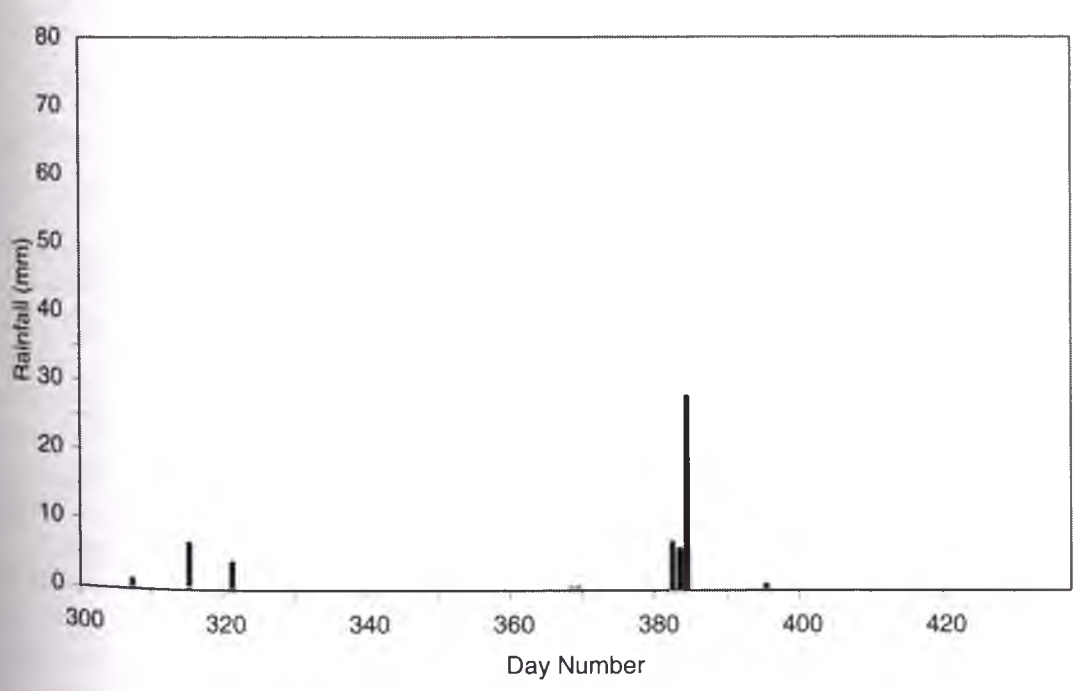

Figure 4.17b: Daily rainfall post-barrier

Table 4.3 identifies and describes the significant rainfall events that occurred during the study period.

Table 4.3: Summary of significant rainfall events during study period. # - Rainfall data was not available for Berry Masonic Village or Nowra Treatment Works

Date	Day number	Daily Rainfall (mm)	Description of weather conditions
24/8/03	23	12.2	Cold front and associated rain band brought widespread rain and gale force winds
2/10/03	63	11.2	Low-pressure system and extensive cloud mass brought widespread rain
3/10/03	80	25.2	Low-pressure trough brought further rain and showers, thunderstorms
1/11/03	92	12.4	SW to SE winds brought light showers; fog
2/11/03	93	11.7	SW to SE winds brought light showers; frost
21/11/03	112	5.8	Low-pressure trough developed and became complex with widespread rain with moderate to heavy falls
22/11/03	113	27	Low-pressure trough developed and became complex with widespread rain with moderate to heavy falls
23/11/03	114	25	Low-pressure trough developed and became complex with further widespread rain with moderate to heavy falls; fog
24/11/03	115	58	Low-pressure trough developed and became complex with further widespread rain with moderate to heavy falls
25/11/03	116	33.2	Low-pressure trough developed and became complex with further widespread rain with moderate to heavy falls
26//11/03	117	12.6	Low-pressure trough developed and became complex with further widespread rain with moderate to heavy falls; fog
2/12/03	123	16.6	Slow moving inland trough approaching from the west and associated upper disturbance triggered widespread thunderstorms; fog; hail
14/1/04	166	20.2	Thunderstorms; fog
24/1/04	176	12.2	Low-pressure trough developed bringing light showers and thunderstorms; fog
25/1/04	177	13.5	Low-pressure trough stalled bringing heavy rainfall; fog
26/1/04	178	14.8	Low-pressure trough stalled bringing heavy rainfall
3/2/04	186	10	Low-pressure trough accompanied by light showers, thunderstorms
12/2/04	195	13	Slow moving trough line with light showers, thunderstorms; fog
25/2/04	208	23	Surface low-pressure tough and upper air instability brought widespread rain
26/2/04	209	11.8	Surface low-pressure tough and upper air instability brought widespread rain
7/3/04	219	36.4	Weak low-pressure system and upper air disturbance developed causing moderate showers

16/3/04	228	18.2	Series of low-pressure troughs caused heavy showers
5/4/04	248	70.8	Surface trough developed over inland NSW and combined with moist easterly winds bringing rain to the coast with moderate to heavy fall, thunderstorms
6/4/04	249	41	Surface trough developed over inland NSW and combined with moist easterly winds bringing rain to the coast with moderate to heavy fall, thunderstorms
13/5/04	286	13.6	Weak low-pressure trough off NSW coast caused light showers
19/8/04	384	28	Low-pressure trough and upper level cold pool caused showers and rain with scattered thunderstorms

The monthly average rainfall at the study site is compared to the long-term average calculated for the rain gauge at the Berry Masonic Village or the Nowra Treatment Works in Figure 4.21. Below average rainfall was experienced throughout the entire study period with the exception of November 2003, largely as a result of the 161.6 mm rain that was recorded during Days 112-117 (See Table 4.3). Rainfall close to the long-term average occurred during April 2004.

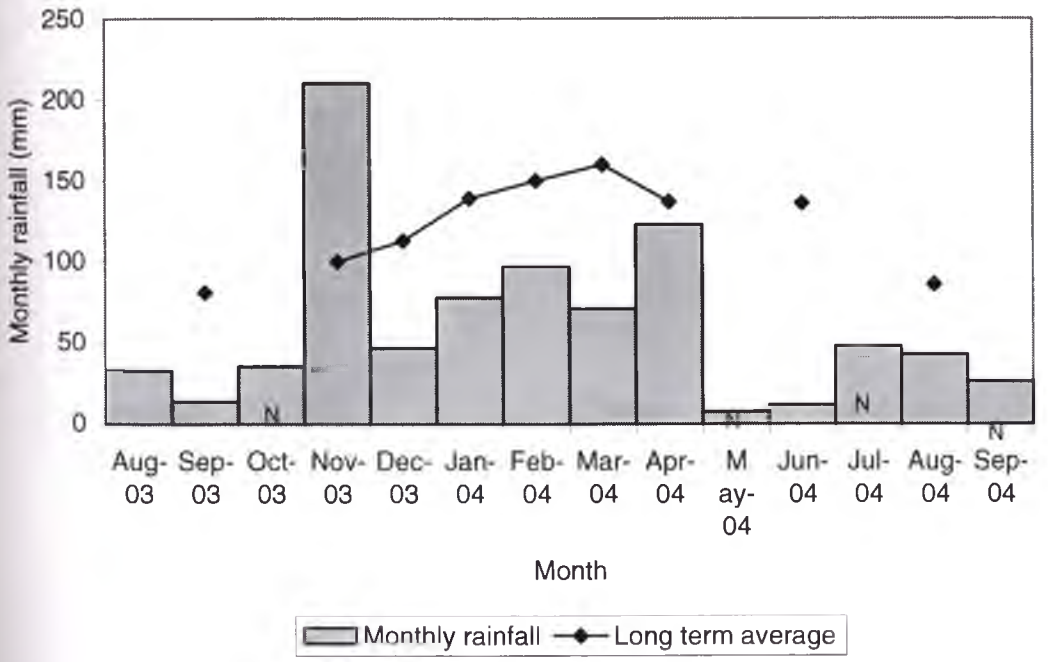

Figure 4.18: Monthly rainfall measured at the site compared to the long-term monthly average. Data labelled with an 'N' was recorded at the Nowra Treatment Works Station. Long-term average data was missing for some months during study period.

A total of 124 rainfall events were recorded during the study period, with 115 during the pre-barrier period and 9 events during the post-barrier period. The pre-barrier

period was significantly longer than the post-barrier period and drier than normal conditions were experienced during the post-barrier period. Rainfall events were those when the rainfall was greater than 0.2mm/day. The total number of rainfall events that occurred is less than those in other studies (i.e. 233 rainfall events in 813 days for Blunden, 2000 and 255 rainfall events in 908 days for Glamore, 2003). However, the study period in those studies was of a longer duration.

The distribution of daily rainfall intensities is shown in Figure 4.19 (a and b). The majority of daily rainfall events, during the pre-barrier stage, were between low rainfall intensities with 1-5mm/day comprising 43% of the total rainfall events, followed closely by <1mm/day with 28% of the total rainfall events. During the pre-barrier period, 6.45% of rainfall events were greater than 20mm/day, whereas during the post-barrier period only 0.8% of rainfall events were greater than 20mm/day. In the pre-barrier period there were 8 rainfall events between 20-50 mm and 2 rainfall events between 50-100 mm, whereas during the post-barrier period there were no rainfall events of these intensities.

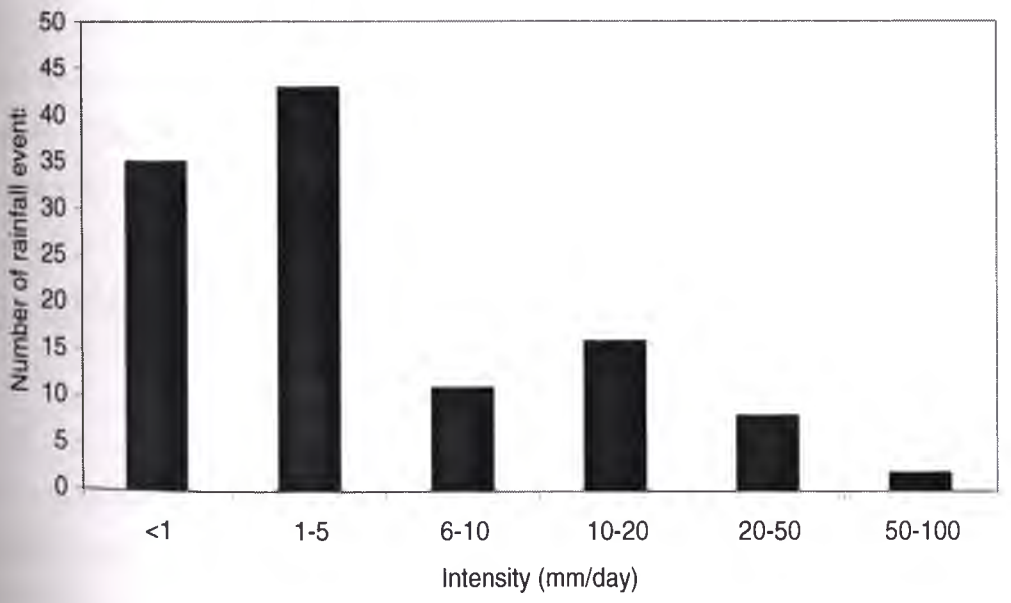

Figure 4.19a: Distribution of rainfall intensities for the pre-barrier period

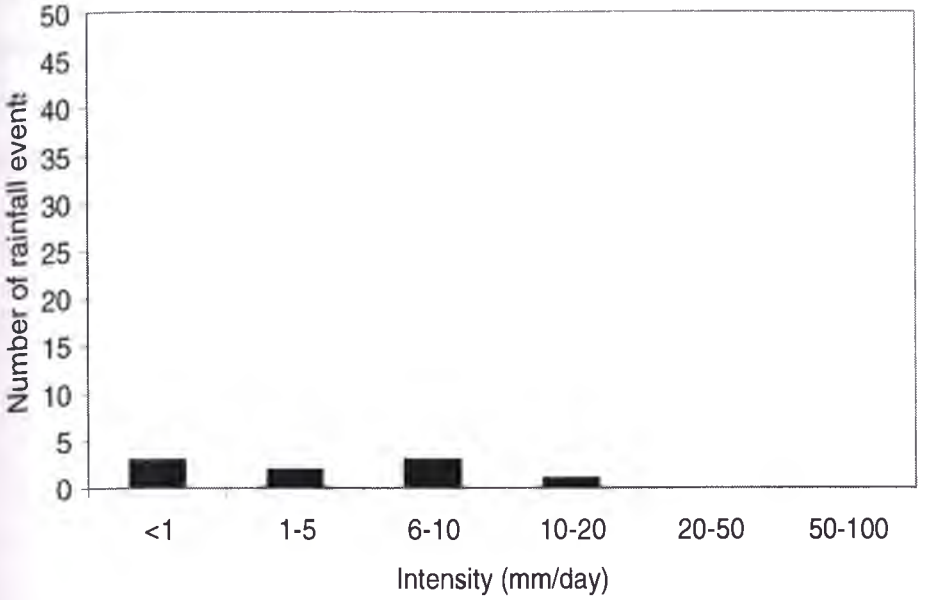

Figure 4.19b: Distribution of rainfall intensities for the post-barrier period

4.6.2 Southern Oscillation Index (SOI)

The Southern Oscillation Index (SOI) is based on the mean sea level pressure difference between Tahiti, French Polynesia and Darwin, Australia (Tahiti - Darwin). There are a number of different methods used to calculate the SOI. The method used by the Australian Bureau of Meteorology is the Troup SOI, which is the standardised anomaly of the Mean Sea Level Pressure difference between Tahiti and Darwin. It is calculated by using the following equation

$$SOI = 10\frac{(Pdiff - Pdiffav)}{SD(Pdiff)} \tag{4.6}$$

Where:

Pdiff = (average Tahiti MSLP for the month) - (average Darwin MSLP for the month)

Pdiffav = long term average of Pdiff for the month in question

SD (Pdiff) = long term standard deviation of Pdiff for the month in question.

When the SOI is positive, the trade winds typically blow strongly across the warm western Pacific Ocean and pick up plenty of moisture; this can then lead to rain over eastern Australia (La Niña event). In years with a positive SOI the rainfall is commonly above average. When the SOI is negative the trade winds are usually

weakened, and the rainfall in eastern Australia will often be below average (El-Niño even) and drought conditions can be expected in eastern Australia. The more negative the number, the further south does the drought extend. The SOI for the study period is shown in Figure 4.20.

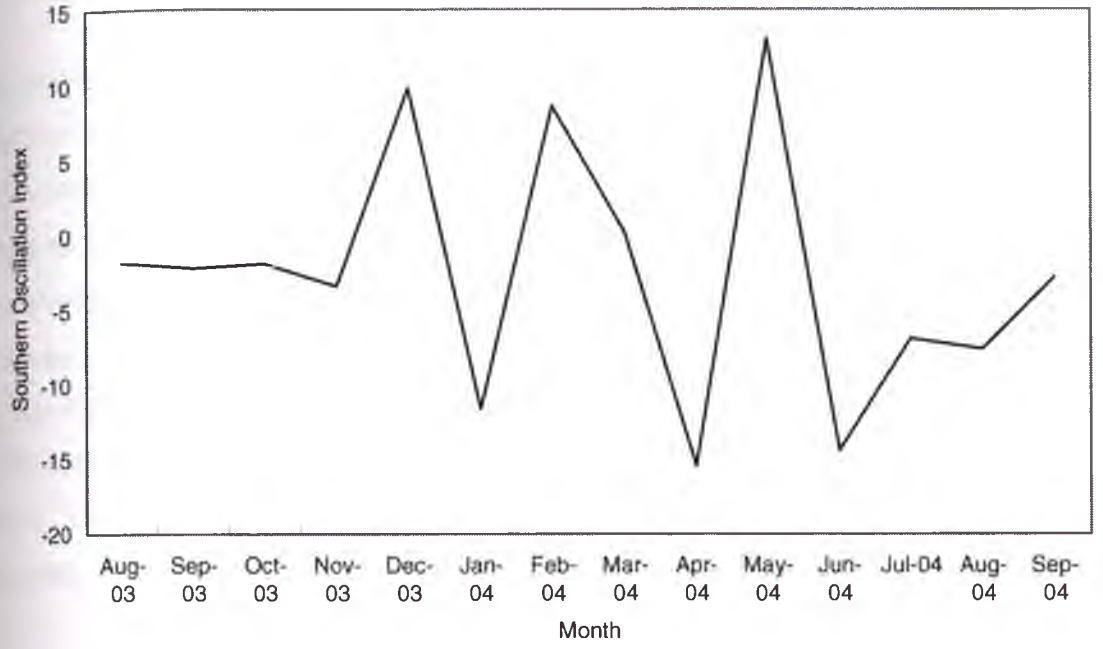

Figure 4.20: SOI for the study period

The SOI fluctuated greatly over the study period, with a period of negative SOI values up to November 2003 then subsequent periods of fluctuation between positive SOI and negative SOI values. Although the SOI was positive during December of 2003 and February and May of 2004, the monthly rainfall was below the long term average during these months (Figure 4.18). Rainfall was also greater than long-term average during November 2003, while the SOI value was negative (-3.4). According to the SOI value of 13.1 during May 2004 greater than average rainfall conditions were expected to occur. However, no values for the long-term average were available for this month. The positive SOI values during February and March 2004 (8.6 and 0.2 respectively) coincided with the rainfall events that occurred between Days 166-195 and 207-235. However, the rainfall during the event that occurred during March 2004 was less than rainfall that fell during the event in February 2004 (Figure 4.18).

There is an association between the SOI (SOI < -10) and climatic conditions necessary for lowering the groundwater table and in turn leading to the generation of pyritic oxidation products and the export of these products after heavy rainfall (SOI > 10). Therefore, SOI values may be used to predict periods of acid generation and discharge.

4.7 Implications for Acid Sulphate Soils

The initial soil chemical properties described in this Chapter indicate past pyritic oxidation. The pre-barrier period was distinguished by several large rainfall events, while the post-barrier period was characterised by extended dry periods. The climatic conditions experienced during the post-barrier period gave rise to conditions necessary for the generation of pyritic oxidation products. These conditions are ideal to test the effectiveness of the barrier in minimising the generation of acid pyrite oxidation products. The climatic interactions with the groundwater dynamics, creek water, drain water and groundwater chemistry for the study sites are discussed in Chapters 6, 7 and 8.

Chapter 5.0 Lime-fly ash Barrier Field Trials

5.1 Introduction

The installation of the lime-fly ash barrier and the equipment used in the preliminary test injections are described in detail in this Chapter. The selection of grout slurry constituents is described in the first section of this Chapter along with the ratios of these constituents used. The second section of this Chapter describes the preliminary injections and the completion of the lime-fly ash barrier. The establishment of a sub-surface barrier involves the injection and lateral grout permeation method. This technique involves the injection of the lime-fly ash/water slurry through boreholes via pressure pumping. The procedure does not require the development of new engineering concepts but relies on the innovative application of the existing theory and practice. The final section of this Chapter describes the post-installation investigation of the barrier.

5.2 Grout Selection and Injection Pressure

Lime and fly ash were chosen as grout components due to their neutralising and pozzolanic characteristics respectively. As previously mentioned the fly ash has a high content of active silica, which is able to undergo a pozzolanic reaction with lime.

There are a number of properties and requirements of lime-fly ash slurries that have an impact on the injection process. These include: fluidity; strength, which is dependent on the proportion of water in the slurry; minimum shrinkage, viscosity and the optimum injection pressure. The lower is the viscosity of the grout fluid, the easier the penetration into the ground. Varying lime-fly ash slurry ratios were tested to decide on most appropriate viscosity and ratio of constituents were to be used in the preliminary injection trials. The final decided mixture ratio of water: lime: fly ash was 40:40:20. Each injection hole was to be injected with approximately 314L of lime-fly ash/water slurry.

The depth of the injection was determined by the location of the top of the pyrite layer. The lime-fly ash barrier was to be constructed 0.1m above the pyrite layer, however following preliminary injections it was found that soil at this level was too

soft to create an adequate seal between the injection pipe and the surrounding soil. This is further discussed in Section 5.4.

As a general rule of thumb, grouting pressures were kept as low as possible but so as to allow optimum success of the grouting. The injection pressure was also kept below the pressure of the soil overburden otherwise heaving of the ground surface may have occurred and fissures may open within the soil. The optimum pressure was found to be between 60-80kPa.

5.3 Injection Equipment

The equipment used in the injection process consisted of a M100 grout pump and a 150 litre mixing tank with an Eagle Mk2 air powered mixer motor, as shown in Plate 5.1. Specifications and operator instructions related to the M100 grout pump and Air powered mixer motor can be found in Appendix C.

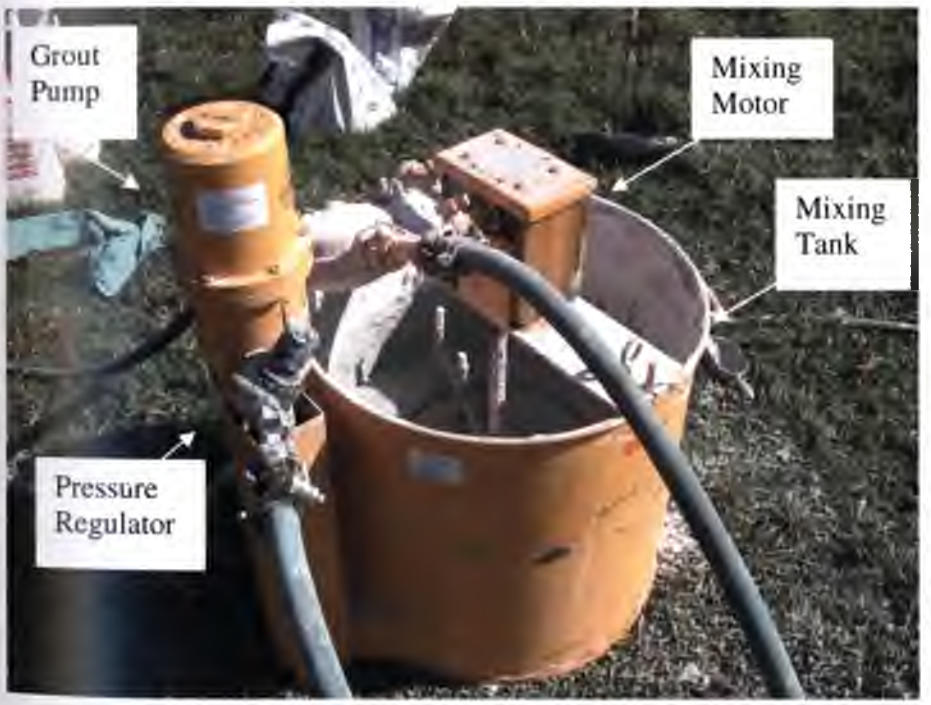

Plate 5.1: Injection equipment including Mixing tank, grout pump, mixing motor and pressure regulator.

The original design of the injection pipe consisted of two hollow pipes (one within the other) with slits at the base where the grout slurry is pumped out of and one set of grout packers to seal the injection hole during injection (See Plate 5.2). The handle at

the top of the injection pipe was used to expand the packers and seal the injection hole.

Plate 5.2: Original design of Injection Pipe. Note one set of packers.

5.4 Preliminary Test Injections

Two test holes were injected with the lime-fly ash/water slurry on Day 98 based on the original specifications (injection depth of 1.1 m). The lime: fly ash: water ratio of 40:40:20 (by mass) was found to be viscous enough to great a layer thick enough and to be pumped by the injection equipment. From the tests in the field it was found that the viscosity of the slurry was suitable for the soil conditions. However, during the placement of the injection pipe in the hole and the expansion of the packers to seal the holes, the soil expanded with the packers and the packers jumped the washers holding them in place. This reduced the seal of the injection hole and caused some slurry to come back up the hole during injection. Modification of the injection pipe in the field stopped this from occurring. Blockages in the slits on the end of the injection pipe caused some problems during the preliminary injection process. These slits were widened to prevent/reduce this problem, as shown in Plate 5.3.

Plate 5.3: Modified tip of injection pipe.

After the injection was completed boreholes were drilled to locate slurry underground. Results from the preliminary injections were considered before performing the final injections. The test injections led to modifications in the depth of injection. While the slurry was found 1m from the point of injection it was found deeper, which indicated that although the slurry did move in a lateral direction it also moved vertically, due to pressure and the soil conditions. Injection depth was raised to 0.7m due to the elevation of the groundwater table and the resulting soft soils. The injection pipe was further modified to add a second set of packers to reduce to further reduce the possibility of slurry escaping back up the injection hole. The modified injection pipe is shown in Plate 5.4. A pressure regulator was also added to allow the injection pressure to be reduced and to allow increased accuracy in controlling the pressure.

Plate 5.4: Modified design of injection pipe. Note the two sets of packers.

A further three holes were injected with the slurry to determine whether these changes made to the injection equipment and injection regime allowed the successful completion of a horizontal barrier. Trenches were dug to investigate the coverage of the barrier. It was expected that some of the slurry could offshoot through macropores in the soil, however the radius of influence of the slurry was found to be approximately 1m, which would give a continuous lime-fly ash layer and maximise interaction between the injection holes. Plate 5.5 shows a section of the lime-fly ash barrier. Plate 5.6 also shows an excavated section of the barrier.

Plate 5.5: Trench showing section of lime-fly ash barrier at 1m below ground surface. Grout at upper right hand corner from an adjacent injection hole.

Plate 5.6: Excavated section of barrier (from preliminary injections)

5.5 Installation of the Lime-fly ash Barrier

The lime-fly ash barrier was completely installed by 9th June 2004 (Day 313. The installation of the barrier was divided into two stages, with half the barrier (section furthest from flood mitigation drain) being completed on Day 299. This was due to restrictions on the amount of grout constituents that could be transported to the study site and the inability to store the lime/fly ash onsite.

5.5.1 Drilling of injection holes

Twenty-two injection holes were drilled adjacent to the flood mitigation drain (See Figure 4.9). PVC pipes were placed in these holes until the time of injection. Holes were also drilled 0.4m from the injection holes to inspect the lime slurry coverage in the spacings between the injection holes. Groundwater samples were not collected from these holes; however pH and conductivity were tested on a number of occasions.

5.5.2 Mixing of lime-fly ash/water slurry

Generally, for each injection hole three mixes of the lime-fly ash/water slurry were injected (some holes reached saturation point and only 2-2.5 mixes were injected). Calculations for the amount of lime/fly ash and water are outlined in Appendix C. Each slurry mix (104.7 litres) consisted of water (36.36 litres), lime (51.8 litres (36.27

kg)) and fly ash (16.54 litres (18.2 kg)). These volumes were based on the projected optimum thickness of the barrier (0.1m) and radius of influence (1m).

For each mix half of the lime and water was mixed first before the fly ash was added. The remaining lime and water was then added to reduce the possibility of the mixture clogging. The slurry was also mixed for several minutes to allow the constituents to mix completely.

Plate 5.7: Mixing of lime-fly ash/water slurry.

5.5.3 Injection of lime-fly ash/water slurry

Before the injection pipe was placed into the injection holes and the slurry was injected into the soil, the injection pipe was tested for possible blockages as shown in Plate 5.8. The injection was placed in the ground and the handle at the top of the injection pipe was tightened to expand the packers and seal the injection hole above the point of injection. While the injection pipe was still in the ground subsequent mixes were created so as not to allow the slurry to harden at the point of injection. Between the injections undertaken in each hole, the slits at the base of the injection pipe were cleaned to prevent blockages.

Plate 5.8: Testing of injection pipe.

5.6 Evaluation of the lime-fly ash barrier in the field

As was previously mentioned, observation holes were drilled to inspect the lime slurry coverage in the spacings between the injection pipes. Watertable elevation and pH levels were monitored continuously through piezometers and observation holes and chemical species were also analysed on a continuous basis. Groundwater table elevation measured before and after the installation is discussed in Chapter 6, while groundwater and surface water quality results from the Lime-fly ash barrier field site are outline in Chapter 7.

Chapter 6.0 Groundwater Dynamics Before and After the Installation of the Lime-fly ash Barrier

6.1 Introduction

The oxidation of pyrite and the subsequent generation of acidic products are influenced by the elevation of the groundwater table in respect to the potential acid sulphate soil layer. When the groundwater table is above the pyritic soil layer it is under reducing conditions and therefore oxidation of the soil does not occur. However in some cases, as previously mentioned in Chapter 2 Section 2.3.1, the presence of bacteria also enhances the oxidation process and can occur even while the pyritic soil in inundated. If the groundwater table falls below the top of the potential acid sulphate soil layer, atmospheric oxygen is able to pass through the macropores in the soil causing the oxidation of the pyritic soil and the discharge of acidic oxidation products to nearby drains and creeks.

An understanding of the groundwater table characteristics of a particular site is important in determining the processes controlling the oxidation of the acid sulphate soil layer. The groundwater elevation data measured at the lime-fly ash barrier study site are presented in this Chapter. The elevation of the groundwater table in relation to the location of the acid sulphate soil layer is addressed. To determine if the lime-fly ash barrier had an influence on the groundwater table elevation a comparison between the pre- and post-barrier groundwater table elevation characteristics are also presented. Groundwater table elevation data are presented in Appendix C.

6.2 Groundwater elevation characteristics during the study period

Groundwater elevations were measured at all thirty-one observation holes during the study period (1st August 2003 – 9th October 2004). The average groundwater elevation at the Lime-fly ash Barrier site is presented in Figure 6.1. The groundwater table fluctuated greatly during the study period. The groundwater table at the lime-fly ash barrier study site is significantly influenced by the climatic conditions. The average groundwater elevation measured at the study site, as shown in Figures 6.1 and Figures 6.2a and b, increased after significant rainfall events i.e. Day 125 and Day 251. The maximum average groundwater table elevation also occurred on Day 125

(Days 123-125 – Rainfall 32 mm). This significant increase in the groundwater table on this day is not only attributed to rainfall but also to a burst water main that flooded the site with freshwater. This also had an impact on the pH and electrical conductivity of the groundwater (See Chapter 7).

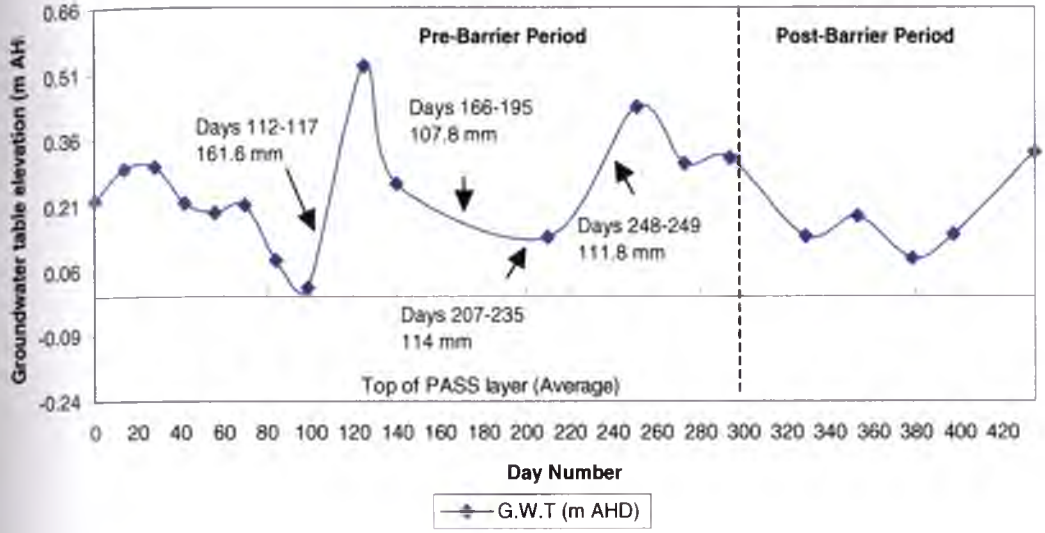

Figure 6.1: Average groundwater elevation at the Lime-fly ash Barrier Site during the study period

The groundwater table differed between observation holes within each transect and also between transects, indicating groundwater flow conditions at the lime-fly ash barrier study site. Figure's 6.2a and 6.2b show the groundwater table elevations measured for transects B, C, D, E and F, G, H, I respectively.

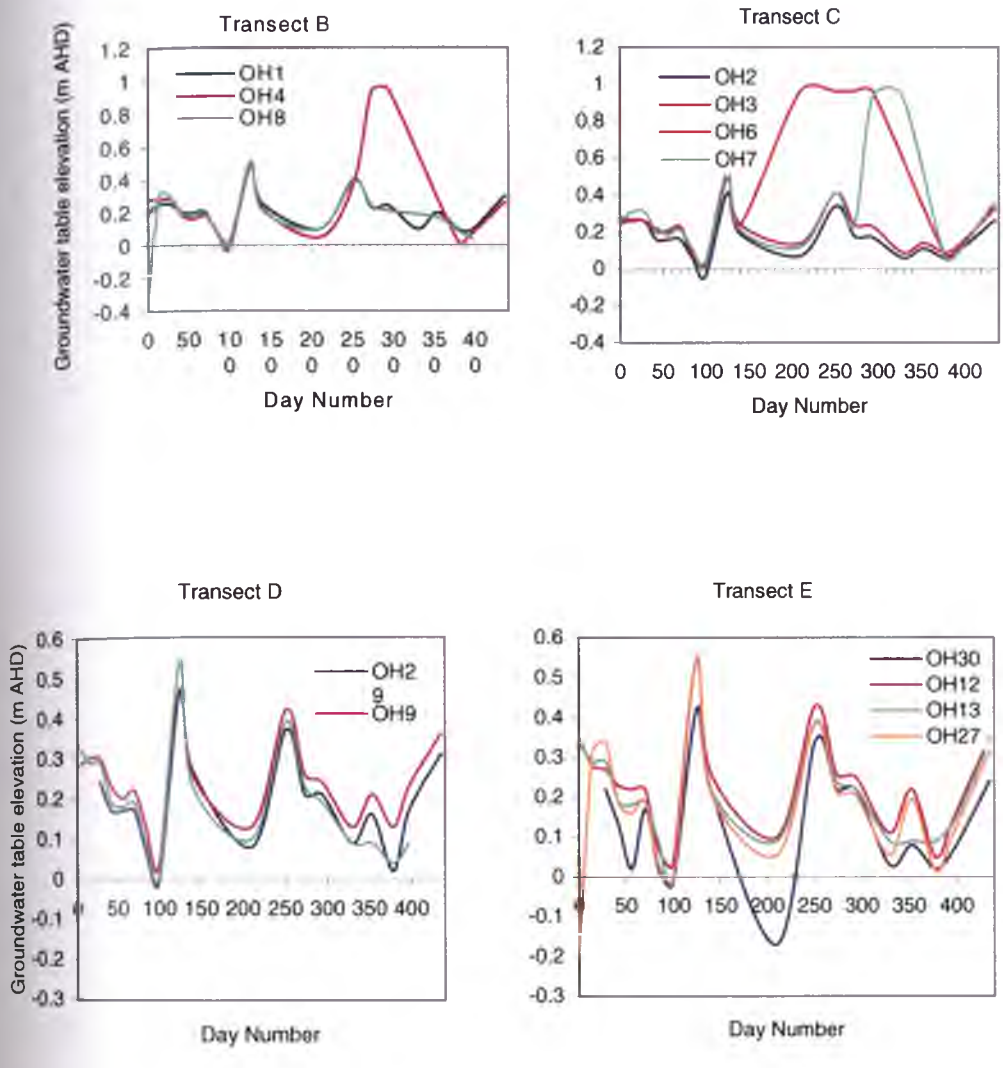

Figure 6.2a: Groundwater table elevations at transect B, C, D and E during the study period

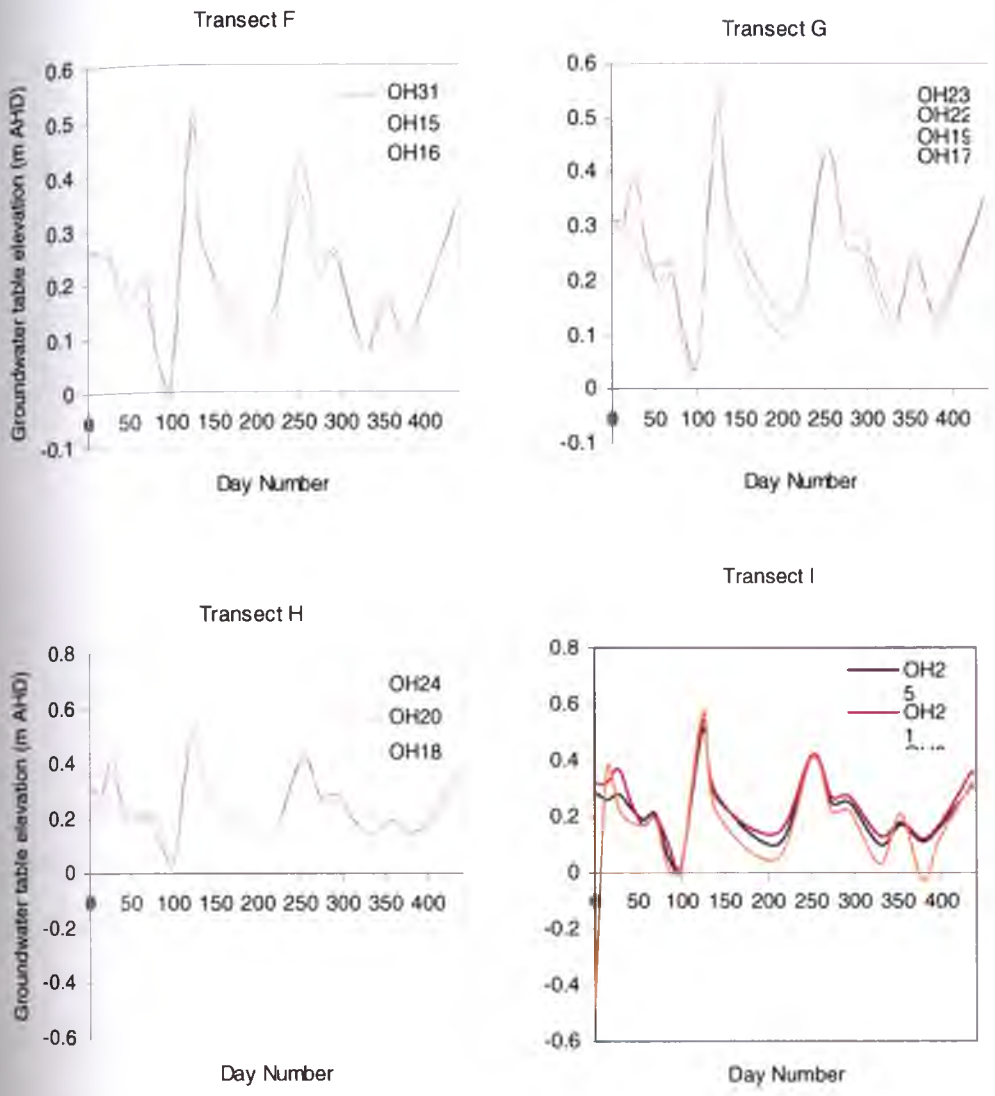

Figure 6.2b: Groundwater table elevations at transect F, G, H and I during the study period

The groundwater profile fluctuated between positive and negative gradients along the transects. After rainfall events the groundwater flow was positive towards the drain. Figure 6.3 illustrates changes to negative groundwater flow gradients after significant rainfall events.

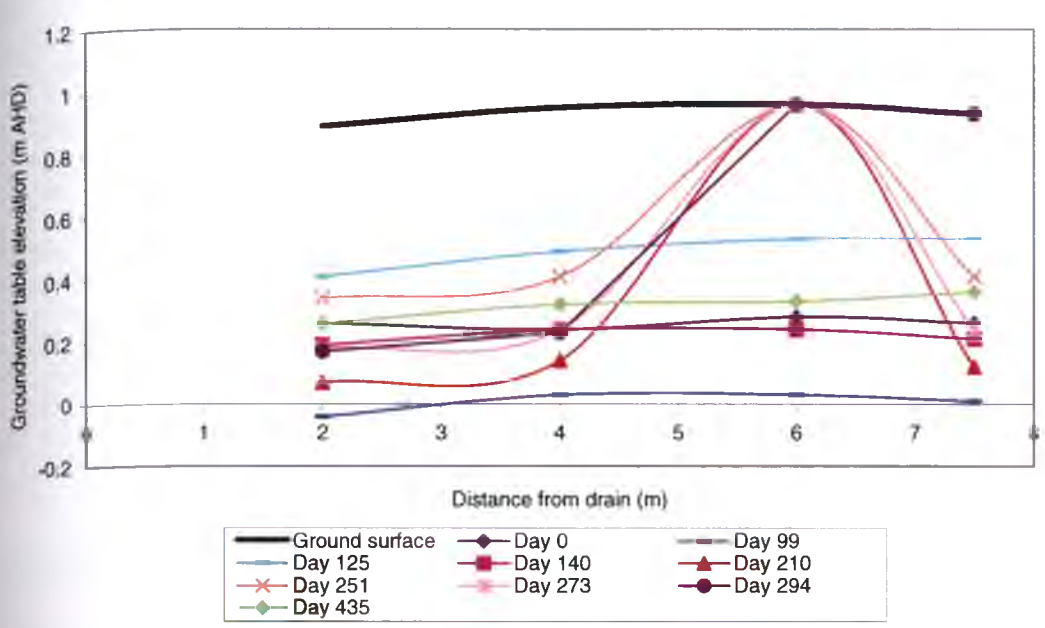

Figure 6.3: Groundwater elevation profile at Transect C showing positive and negative gradients

The groundwater table along Transect B frequently dipped showing a negative gradient towards the middle of the study site area. The groundwater table along transects F, G and H was relatively stable with little variation across the study site.

6.2.1 Relationship between groundwater table elevation and pyritic soil oxidation

The groundwater table fell below the upper surface of the potential acid sulphate soil layer on only one occasion at the study site (1st August 2003) during the study period. This was however, only measured at Observation Hole 8 and Observation Hole 28 (Figure 6.4 and Table 6.1). The groundwater table elevations measured at Observation Holes 8 and 28, at the beginning of the study period, were 0.03 m AHD and 0.21 m AHD below the upper surface of the PASS layer respectively. This demonstrates that the oxidation of pyrite at this study site is influenced by factors other than the elevation of the groundwater table, namely biotic oxidation.

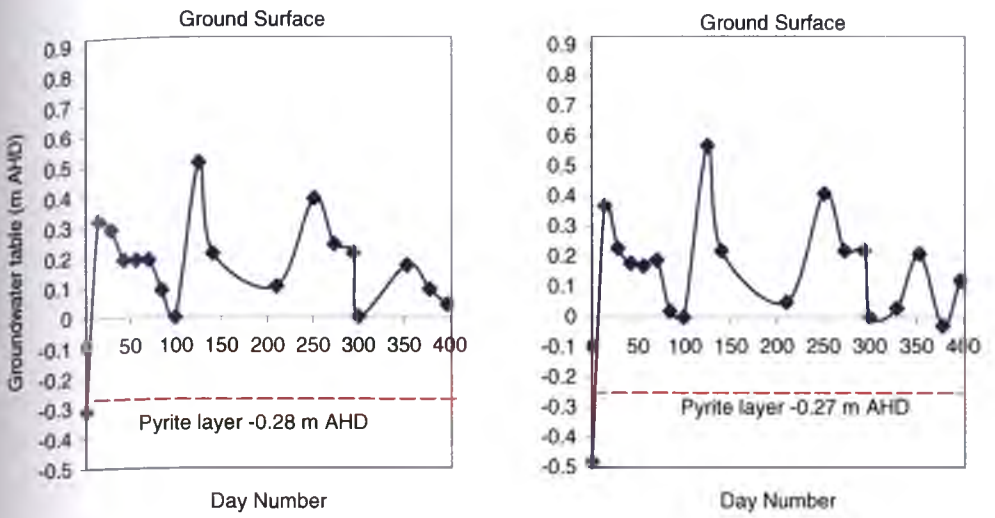

Figure 6.4: Groundwater table elevations at OH8 and OH28 during the study period

6.3 Pre-barrier groundwater dynamics

Pre-barrier maximum, minimum and the average groundwater elevations at each observation hole are summarised in Table 6.1, in respect to the height location of the potential acid sulphate soil layer.

Table 6.1: Pre-barrier groundwater table elevations measured at the Lime-fly ash Barrier Study Site during the study period

Observation Hole	PASS layer (m AHD)	Ground Surface (m AHD)	Max G.W.T (m AHD)	Min G.W.T (m AHD)	Average G.W.T (m AHD)
1	-0.19	1.01	0.48	0.02	0.21
2	-0.31	0.89	0.41	-0.04	0.17
3	-0.25	0.95	0.49	0.03	0.21
4	-0.26	0.94	0.94	-0.02	0.28
5	-0.21	0.99	0.48	0.02	0.20
6	-0.24	0.96	0.96	0.03	0.40
7	-0.27	0.93	0.93	0.01	0.31
8	-0.28	0.92	0.51	-0.31	0.17
9	-0.27	0.93	0.54	0.03	0.24
10	-0.28	0.92	0.54	0.00	0.20
11	-0.26	0.94	0.56	0.04	0.24
12	-0.24	0.96	0.55	0.03	0.23
13	-0.27	0.93	0.54	-0.01	0.21
14	-0.25	0.95	0.53	0.01	0.22
15	-0.25	0.95	0.51	0.01	0.21

16	-0.23	0.97	0.54	0.02	0.21
17	-0.17	1.03	0.54	0.04	0.25
18	-0.17	1.03	0.52	0.03	0.22
19	-0.2	1.00	0.55	0.05	0.26
20	-0.2	1.00	0.55	0.06	0.25
21	-0.16	1.04	0.54	0.02	0.24
22	-0.22	0.98	0.54	0.04	0.26
23	-0.2	1.00	0.51	0.04	0.23
24	-0.13	1.07	0.55	0.04	0.26
25	-0.16	1.04	0.51	0.01	0.22
26	-0.3	0.90	0.53	0.03	0.22
27	-0.3	0.90	0.55	-0.19	0.18
28	-0.27	0.93	0.57	-0.48	0.16
29	-0.31	0.89	0.47	-0.01	0.19
30	-0.47	0.73	0.42	-0.17	0.13
31	-0.34	0.86	0.49	-0.01	0.20

During the pre-barrier period, on average, groundwater table elevation varied between each observation hole indicating groundwater flow within the study site. During the pre-barrier period, the groundwater table elevation was level with the ground surface at Observation Holes 4, 6 and 7. This occurred on two occasions in Observation Hole 4 (Day 273 and Day 294), four occasions in Observation Hole 6 (Day 210, Day 251, Day 273 and Day 294) and one occasion in Observation Hole 7 (Day 294). The significant rise in the groundwater table in these observation holes coincides with high intensity and short duration rainfall events that occurred in days preceding the measurements i.e. Day 286 - 13.6 mm, Day 210 - 43.2 mm and Day 251 - 112.8 mm. Even though the groundwater table did not rise significantly in any other observation hole on Day 210, rain may have inadvertently entered Observation Hole 6 through a possible leak in the cap on the top of the hole.

Plate 6.1: Lime-fly ash Barrier Study Site after a high intensity rainfall event (Day 125)

6.4 Post-barrier groundwater dynamics

Post-barrier maximum, minimum and the average groundwater elevations at each observation hole are summarised in Table 6.2, in respect to the height location of the potential acid sulphate soil layer. During the post-barrier period, on average, groundwater table elevation varied between each observation hole indicating groundwater flow within the study site. During the post-barrier period, the maximum groundwater table elevation was level with the ground surface at Observation Hole 7 on one occasion (Day 329).

Table 6.2: Post-barrier groundwater table elevations measured at the Lime-fly ash Barrier Study Site during the study period

Observation Hole	PASS layer (m AHD)	Ground Surface (m AHD)	Max G.W.T (m AHD)	Min G.W.T (m AHD)	Average G.W.T (m AHD)
1	-0.19	1.01	0.30	0.10	0.16
2	-0.31	0.89	0.26	0.06	0.12
3	-0.25	0.95	0.32	0.09	0.16
4	-0.26	0.94	0.26	0.03	0.12
5	-0.21	0.99	0.30	0.05	0.13
6	-0.24	0.96	0.33	0.08	0.18
7	-0.27	0.93	0.93	0.06	0.37

8	-0.28	0.92	0.17	0.04	0.10
9	-0.27	0.93	0.36	0.13	0.21
10	-0.28	0.92	0.09	0.04	0.08
11	-0.26	0.94	0.36	0.10	0.19
12	-0.24	0.96	0.35	0.05	0.18
13	-0.27	0.93	0.34	0.09	0.15
14	-0.25	0.95	0.335	0.035	0.18
15	-0.25	0.95	0.33	0.06	0.16
16	-0.23	0.97	0.34	0.07	0.15
17	-0.17	1.03	0.36	0.13	0.21
18	-0.17	1.03	0.19	0.10	0.14
19	-0.20	1.00	0.35	0.15	0.22
20	-0.20	1.00	0.35	0.14	0.20
21	-0.16	1.04	0.36	0.12	0.19
22	-0.22	0.98	0.355	0.135	0.21
23	-0.20	1.00	0.35	0.11	0.20
24	-0.13	1.07	0.38	0.14	0.21
25	-0.16	1.04	0.31	0.1	0.17
26	-0.30	0.90	0.29	0.08	0.15
27	-0.30	0.90	0.315	0.015	0.14
28	-0.27	0.93	0.32	-0.03	0.13
29	-0.31	0.89	0.31	0.02	0.15
30	-0.47	0.73	0.24	0.02	0.09
31	-0.34	0.86	0.34	0.08	0.17

6.5 Comparison between pre- and post-barrier groundwater dynamics

The maximum groundwater table elevation during the pre-barrier period was measured in Observation Hole 6, whereas during the post-barrier period the maximum groundwater table elevation occurred in Observation Hole 7. During both the pre- and post-barrier period the maximum and minimum groundwater table elevation was measured in Observation Hole 28.

There was greater variance between the maximum and minimum groundwater table elevations measured in the observation holes during the pre-barrier period (Var. (max) = 0.0171; Var. (min) = 0.0129) than in the post-barrier period (Var. (max) = 0.0159; Var. (min) = 0.00188). There was however greater variance between the average groundwater table elevations measured in the observation holes during the post-barrier period (VAR = 0.00264) than in the pre-barrier period (VAR = 0.00257).

During the pre-barrier period, in each Observation Hole (except for OH7), the average groundwater table elevation (m AHD) was higher than during the post-barrier period (Figure 6.5). This can be attributed to the majority of rainfall events occurring during the pre-barrier period (See Chapter 4, Section 4.5.1 and Figure 4.14a). These rainfall events were also of a higher intensity during the pre-barrier period (Figure 4.16a).

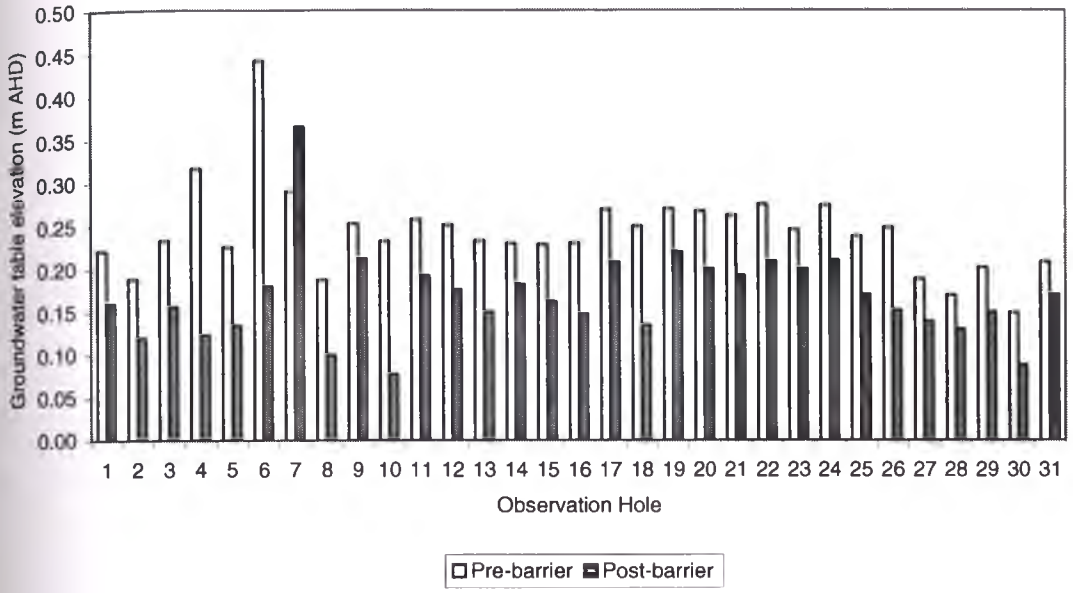

Figure 6.5: Pre- and Post-barrier average groundwater table elevations at the Lime-fly ash Barrier Site

6.6 Conclusions

There were minimal changes in the groundwater regime as a result of the installation of the lime-fly ash barrier at the study site. However, a comparison between the average groundwater table elevations before and after the installation of the barrier indicates a perched water table, as was expected to occur. This perched water table would reduce the exposure of pyritic soil to oxygen, reduce pyritic oxidation and hence the generation of acidic products. The groundwater table is also influenced by climatic factors. High rainfall events during the pre-barrier period led to high groundwater tables.

It is, however not just the perched water table that has resulted from the installation of the Lime-fly ash barrier. The alkaline barrier has reacted with acidic groundwater and

influenced the concentration of pyrite oxidation products in the groundwater and drain water. This is outlined in Chapter 7.

Chapter 7.0 Drain Water and Groundwater Quality at the Site of the Lime-fly ash Barrier

7.1 Introduction

The aim of this Chapter is to examine the influence of the lime-fly ash barrier on drain water and groundwater quality at the study site. The changes that occur in drain water and groundwater quality parameters before and after the installation of the lime-fly ash barrier are described. This Chapter is divided into two sections. In the first section, the spatial and temporal variance in drain water acidity is described.

The second section examines the spatial and temporal variance in groundwater quality. The collected data show that the installation of the subsurface barrier reduced problems associated with acid sulphate soils, namely low pH and the generation of acidic oxidation products such as dissolved inorganic monomeric aluminium and total dissolved iron.

In both these sections, the results are related to groundwater dynamics and climatic influences, and the possible sources of each chemical species are described. Data measured at the study site are presented in Appendix C.

7.2 Spatial variance in drain water quality

7.2.1 Drain water pH

Drain water pH and conductivity were tested along the drain adjacent to the Lime-fly ash barrier site, from the floodgate to just beyond the piezometer transect. This was conducted on two occasions, before and after the installation of the modified floodgate. It also coincides with before and after the installation of the sub-surface lime-fly ash barrier. Figure 7.1 shows the pH of the drain water within the flood mitigation drain before and after the installation of the modified floodgate and lime-fly ash barrier. As can be seen, the drain water pH decreased upstream, as a result of the brackish water neutralising the drain water pH. ANZECC guidelines (2000) require that marine waters to have a pH between 8-8.4, however, drain water immediately upstream of the floodgate was below this criterion. The modified

floodgate would have been closed for about 12 hours at the time of sampling on Day 300 so this explains the 'normal' rather than improved conditions. The trigger value for pH in estuaries is between 7 and 8.5. The drain water pH also falls below this guideline.

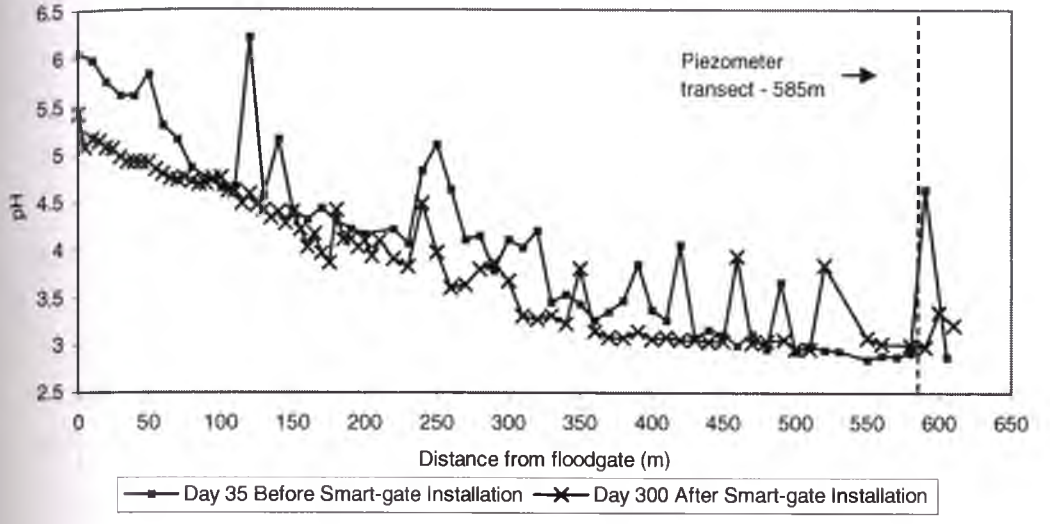

Figure 7.1: Drain water pH readings along the flood mitigation drain near the lime-fly ash barrier site

Figure 7.2 depicts the drain water pH upstream, downstream and also directly adjacent (middle) to the lime-fly ash barrier site during the study period. The sharp increase in pH to 5.2 upstream of the site is due to the rainfall event on this day (Day 125) and the burst freshwater main. The drain water pH directly adjacent to the site fluctuated greatly during the study period, due to climatic influences. Peaks in pH values at Day 125 (pH 5.18) and Day 251 (pH 5.73) both coincide with significant rainfall events. The minimum pH of 2.1 occurred on Day 99. In days preceding this sampling day, 24.1mm of rain fell on the study site, leaching acid into the drain that was formed during drought conditions. On Day 4, shallow lime injection took place on the bank opposite the study site. No discernible changes in drain pH were noticed adjacent to or downstream from the study site, as a result of this shallow lime injection. The drain water pH also significantly increased downstream of the study site on Day 125 (pH 5.13). After Day 125 the drain water pH dramatically decreased to 3.29. This is due to acidic oxidation products discharging to the drain. There was

also no significant change in drain water pH adjacent to (pH change of 0.06) and downstream (pH change of 0.02) from the site after the installation of the barrier. The average drain water pH also increased by just 0.16 after the installation of the barrier. This is because the drain water is influenced from upstream areas. Acid sulphate soils affected areas upstream of the Lime-fly ash barrier study site discharge acidic water downstream.

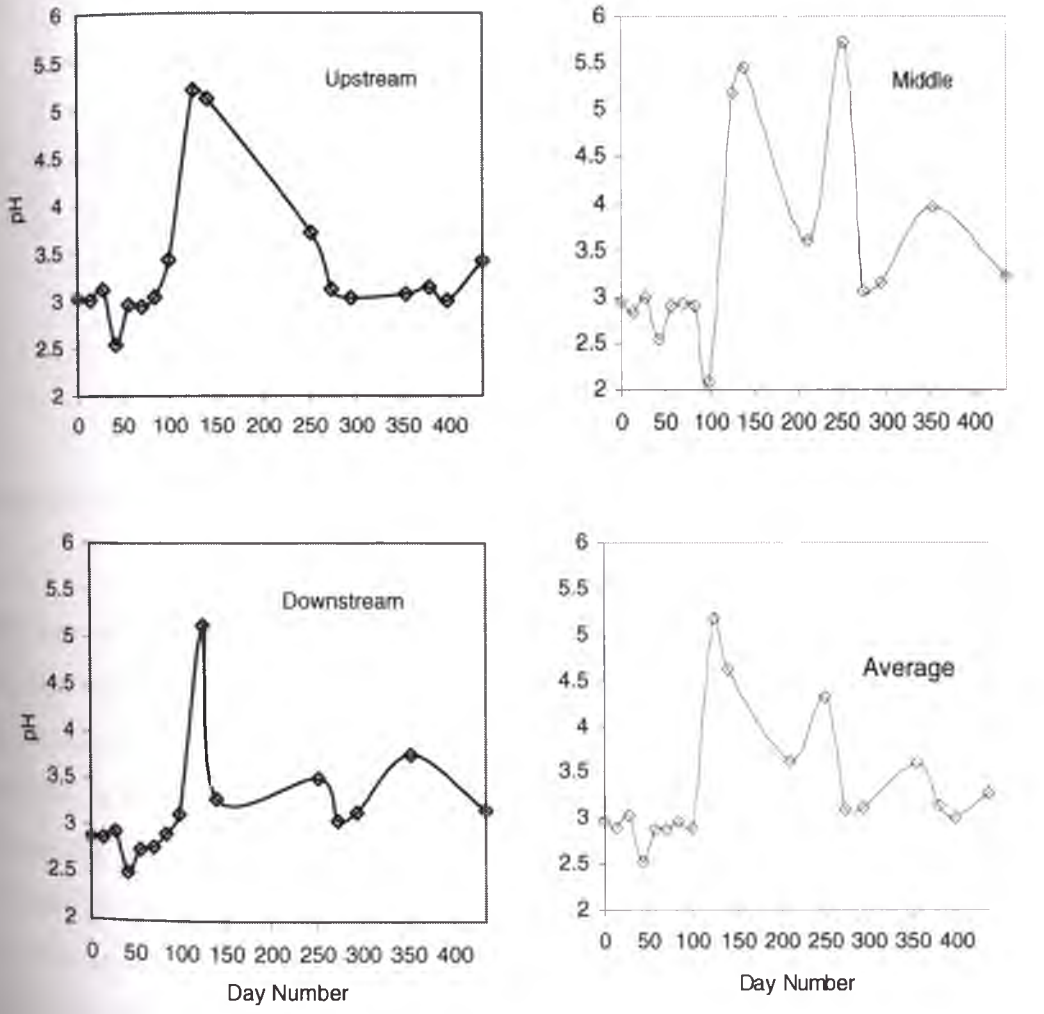

Figure 7.2: Drain water pH readings upstream, middle and downstream of lime-fly ash barrier site

7.2.2 *Electrical Conductivity*

Figure 7.3 depicts the drain water electrical conductivity (EC) before and after the installation of the modified floodgate and lime-fly ash barrier. The measured EC

shows the extent of the tidal front up the flood mitigation drain. It can be seen that the modified floodgate has an influence up to approximately 310m upstream. The electrical conductivity up to this point is significantly greater than that measured before the commission of the modified floodgate, indicating saline intrusion.

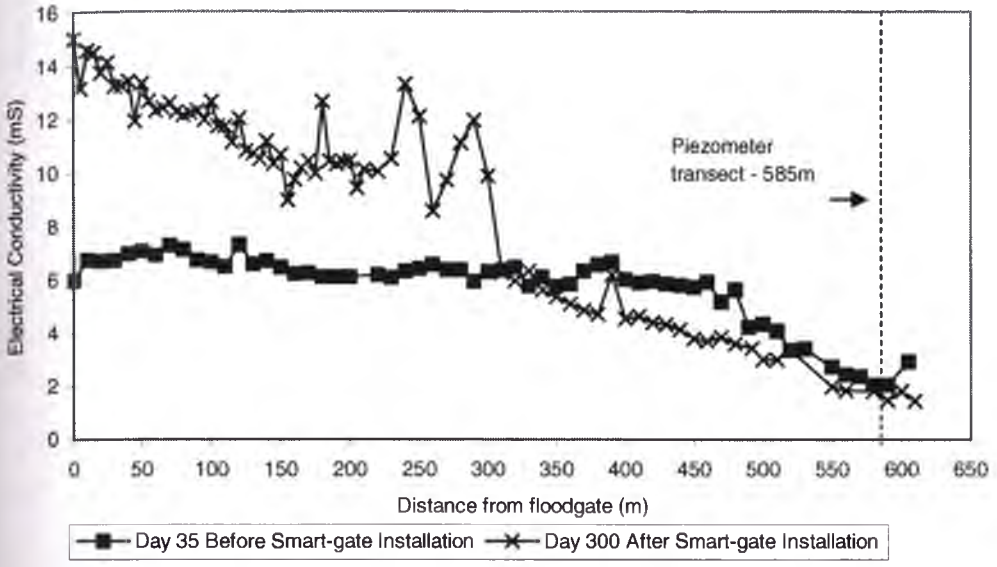

Figure 7.3: Drain water conductivity readings along the flood mitigation drain near the lime-fly ash barrier site

Drain water EC also correlated with rainfall events and pH. In Figure 7.4, drain water EC decreased significantly during rainfall events, specifically Day 125, which can be attributed to near neutral pH waters being discharged into the drain. The large increase in EC before Day 56 is due to the generation of pyrite oxidation products during the period of decreasing groundwater tables (Figure 6.1). The increase in groundwater tables after this period diluted the concentration of pyrite oxidation products in the drain water, therefore lowering the EC. The slight increase in drain water EC after Day 125 can also be attributed to the leaching of these oxidation products from the groundwater to the drain.

The EC of the drain water after the installation of the barrier has been relatively stable. There was no increase in EC after Day 384, when 28 mm of rain fell on the study site, indicating the influence of the barrier on reducing pyritic oxidation.

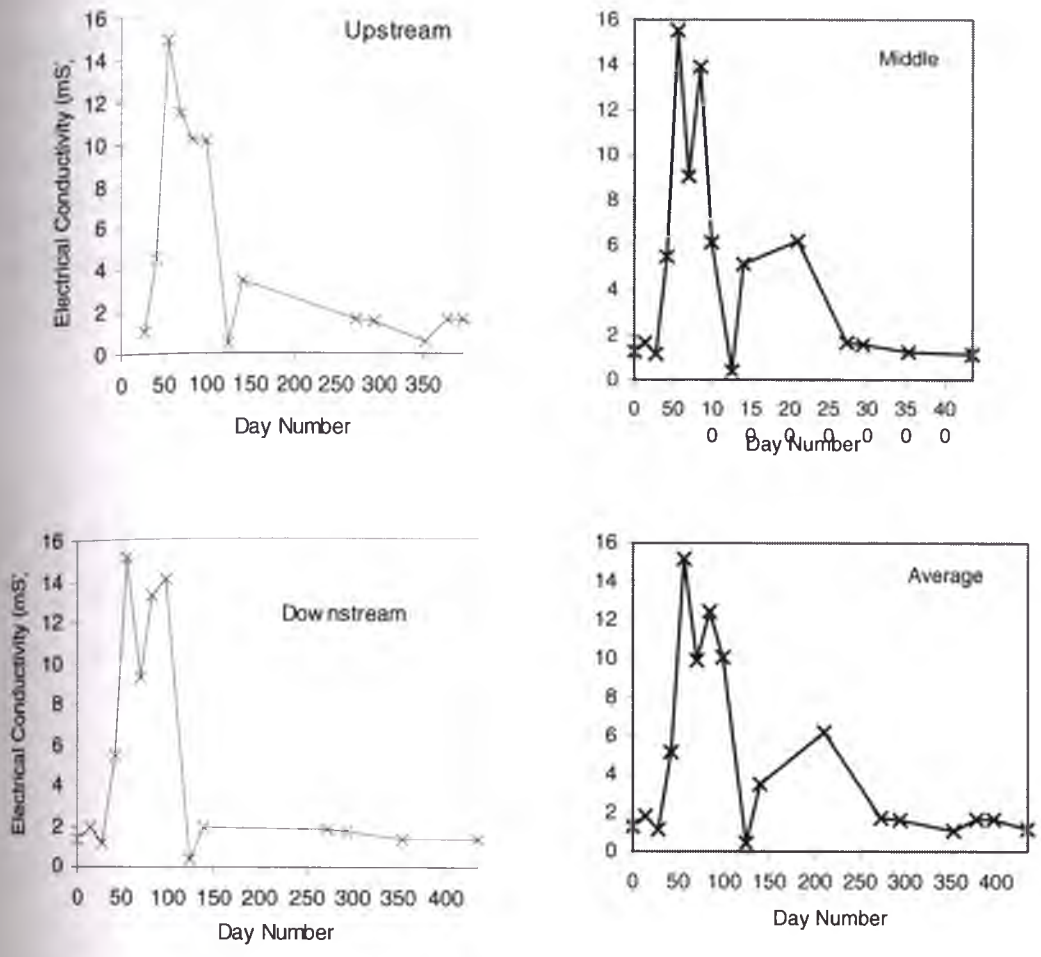

Figure 7.4: Drain water conductivity readings upstream, middle and downstream of lime-fly ash barrier site

7.2.3 Acidic cation concentrations

High concentrations of acidic cations, dissolved monomeric aluminium and dissolved iron, experienced in the drain water at the study site, are due the release of these cations from the soil as a result of pyritic oxidation. A detailed description of the concentrations of these cations in the drain water during the study period is described in the following sections.

7.2.3.1 Aluminium concentrations

The concentration of aluminium in the drain water is shown in Figure 7.5. The ANZECC guidelines (1992) state that when the pH is less than 6.5, aluminium

concentration levels must not exceed 0.005 mmol/L (0.1349mg/L). During the study period, drain water aluminium concentrations at all locations exceeded this level significantly. Concentrations upstream of the study site ranged from 4 mg/L (Day 353) to 56.8 mg/L (Day 70) with an average aluminium concentration of 31.6 mg/L. The maximum concentration of 56.8 mg/L is less than maximum Al^{3+} concentrations reported by Glamore (2003) and Blunden (2000), 117.36 mg/L (4.35 mmol/L) and 140.29 mg/L (5.2 mmol/L) respectively.

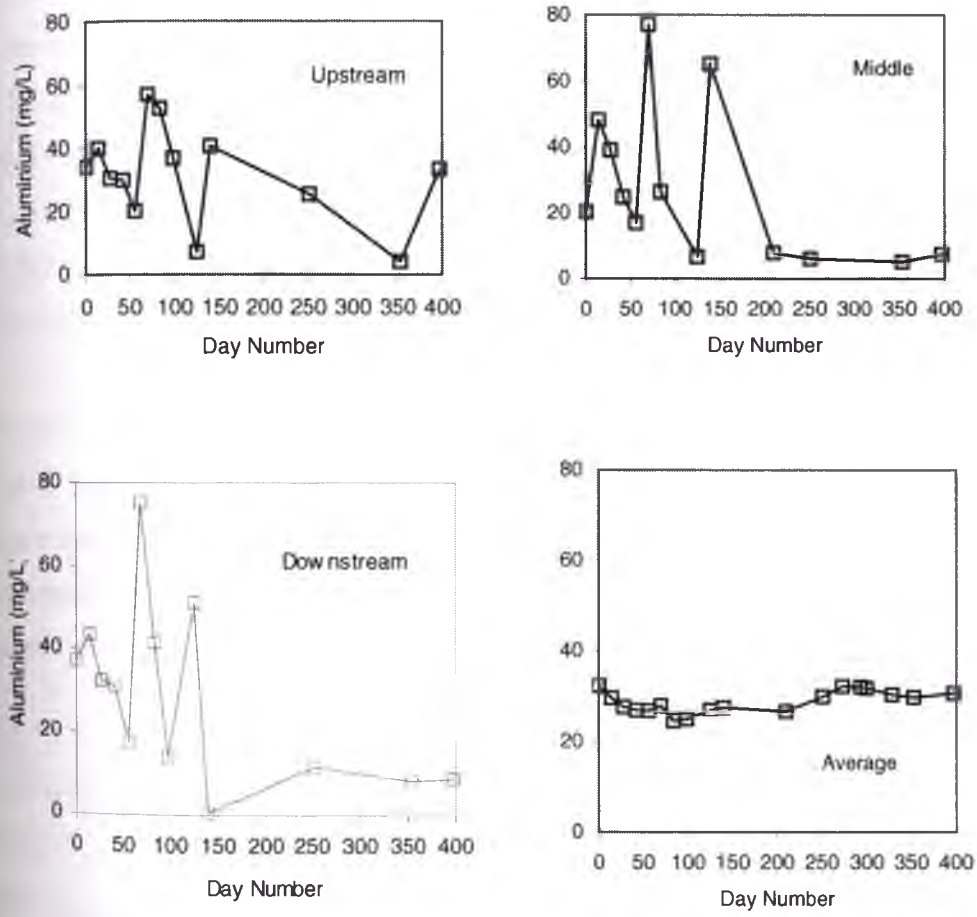

Figure 7.5: Dissolved inorganic monomeric Al^{3+} concentrations in drain water upstream, middle and downstream of the lime-fly ash barrier site. Average concentrations are also shown.

Figure 7.5 shows that aluminium concentrations in the drain water fluctuate with climatic conditions. After Day 125, aluminium concentrations increased upstream and adjacent to the study site. These elevated levels are largely due to the dissolution of silicate clays and aluminium minerals under acidic groundwater conditions. These silicate clays and aluminium minerals are transported to the drain during the 'first

flush' after pyritic oxidation. Aluminium concentrations receded after this period, although the concentrations were still several orders of magnitude above the ANZECC (1992) trigger guideline value. Although a rainfall event occurred on Day 384, aluminium concentrations in the drain water downstream of the study site only increased by 0.4 mg/L.

Average aluminium concentrations in the drain water at the study site did not vary significantly during the study period. The average concentrations before and after the installation of the barrier were 27.29 mg/L and 29.32 mg/L. The average concentration of aluminium downstream of the study site decreased from 32.23 mg/L to 8.50 mg/L after the installation of the barrier. Average drain water concentrations adjacent to the study site increased slightly after the completion of the barrier (27.29 mg/L to 29.15 mg/L). As was mentioned before, the lime-fly ash barrier study site does not only influence the section of drain sampled but by acid sulphate soil affected land upstream also.

There was little correlation between drain water pH and aluminium levels as has been reported previously (Glamore, 2003, Blunden and Indraratna, 1997). A possible explanation for the lack of correlation could be the numerous influences on the concentration of aluminium in the drain water, for example floodgate leakage and the influence of saline intrusion or the fluctuating climatic factors.

7.2.3.2 Iron concentrations

ANZECC Guidelines (1992) state that dissolved iron concentrations need to be below 0.0009 mmol/L (0.502 mg/L) for the protection of aquatic ecosystems. Total dissolved iron concentrations were above these guidelines on all occasions with the maximum concentration occurring on Day 140 at all sampling points in the drain (upstream – 611 mg/L; middle – 1405 mg/L; downstream – 778 mg/L). Between Days 118-165 there was a prolonged dry period in which iron oxides formed in the drain (See Plate 7.1).

The average drain water total dissolved iron concentration decreased from 141.8 mg/L before the installation of the barrier to 109.63 mg/L after the installation of the barrier,

showing that the barrier decreases the generation of pyrite oxidation products. The average iron concentrations also decreased adjacent to and downstream from the study site after the barrier was installed, although the elevated concentration on Day 140 (pre-barrier) influenced this average. Removing this value from average calculations, the average dissolved iron concentration in the drain water downstream and adjacent to the site still shows a decrease between pre- and post-barrier conditions.

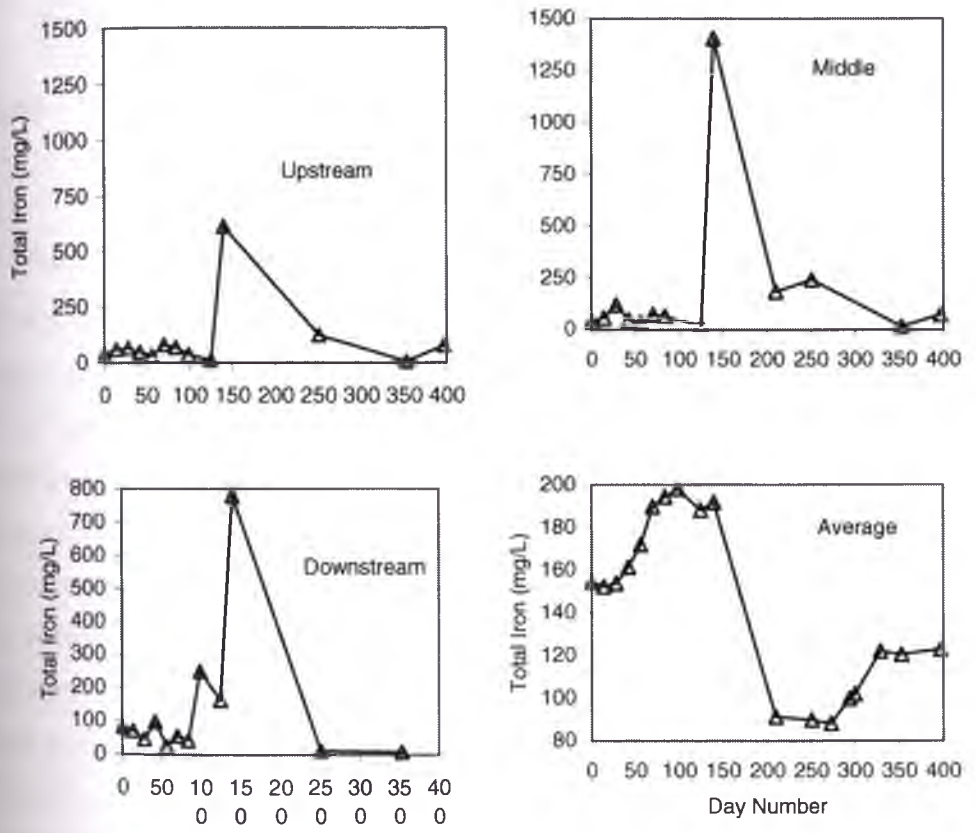

Figure 7.5: Total dissolved iron concentrations in drain water upstream, middle and downstream of the lime-fly ash barrier site. Average concentrations are also shown.

Plate 7.1: Iron oxide flocculation in flood mitigation drain adjacent to lime-fly ash barrier study site.

7.2.4 Basic cation concentrations

The concentration of basic cations (Ca^{2+} and Mg^{2+}) within the drain water is shown in Figure 7.6. Mg^{2+} was the dominant cation within the drain water. The concentrations of Mg^{2+} and Ca^{2+} were relatively similar at all points sampled in the drain. Mg^{2+} concentrations also followed Ca^{2+} concentrations. After Day 56, concentrations increased but then fell to relatively stable levels. Upstream and adjacent to the study site, the maximum Mg^{2+} concentration occurred on Day 56 (613 mg/L and 572 mg/L). The highest drain water Mg^{2+} concentration downstream from the study site was measured on Day 99 (743 mg/L). These elevated concentration levels would not be linked to saline ingress, as the influence of the floodgate on the drain does not reach the study site (See Figure 7.2). Another source of Mg^{2+} is from the dissolution of estuarine clays. A decrease in groundwater table elevations during this period (Figure 6.1) may have influenced this increase in Mg^{2+} in the drain water.

The maximum drain water Ca^{2+} concentration upstream and adjacent to the study site also occurred on Day 56 (upstream – 201 mg/L; middle – 178 mg/L). It has been suggested that high concentrations of Al^{3+} released during the hydrolysis of estuarine clays may exchange with Ca^{2+} from the cation exchange complex and release Ca^{2+} into solution (Blunden, 2000).

The sharp decrease in Ca^{2+} and Mg^{2+} on Day 125 is due to dilution from the rainfall event that occurred. A decrease also occurred after Day 251 (Day 249 – rainfall 41 mm).

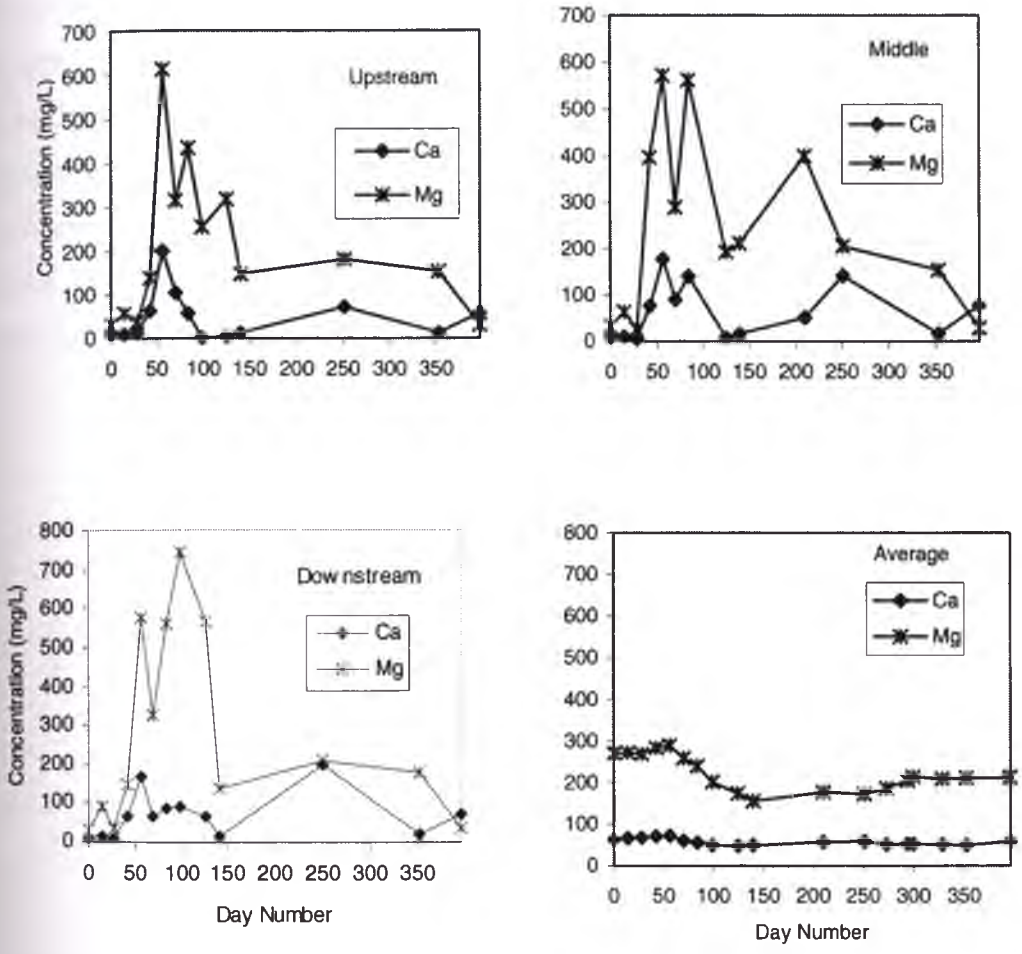

Figure 7.6: Soluble cation concentrations upstream, middle and downstream of lime-fly ash barrier site. Average drain water concentrations are also shown.

7.2.5 *Anion concentrations*

Soluble chloride and sulphate concentrations are shown in Figure 7.7 and Figure 7.8 respectively. Chloride is an indictor of saline intrusion while elevated sulphate levels in drain waters imply the leaching of pyritic oxidation products.

7.2.5.1 Chloride concentrations

There was a period of high soluble chloride concentrations in the drain water (between Days 42 and 125). Upstream and adjacent to the study site, the maximum chloride concentrations in the drain water occurred on Day 99 (upstream - 8966.1 mg/L; middle – 9439.2 mg/L). An explanation for these high concentrations could be drought conditions between Days 42 and 112 and the accumulation of chloride anions in the drain. Downstream of the study site, the maximum chloride concentration was measured on Day 56 (8563.9 mg/L). The minimum soluble chloride concentration upstream and adjacent to the study site occurred on Day 125 (upstream – 61.4 mg/L; middle – 65.4 mg/L). This is due to circum-neutral water from the rainfall event diluting the concentration of chloride in the drain.

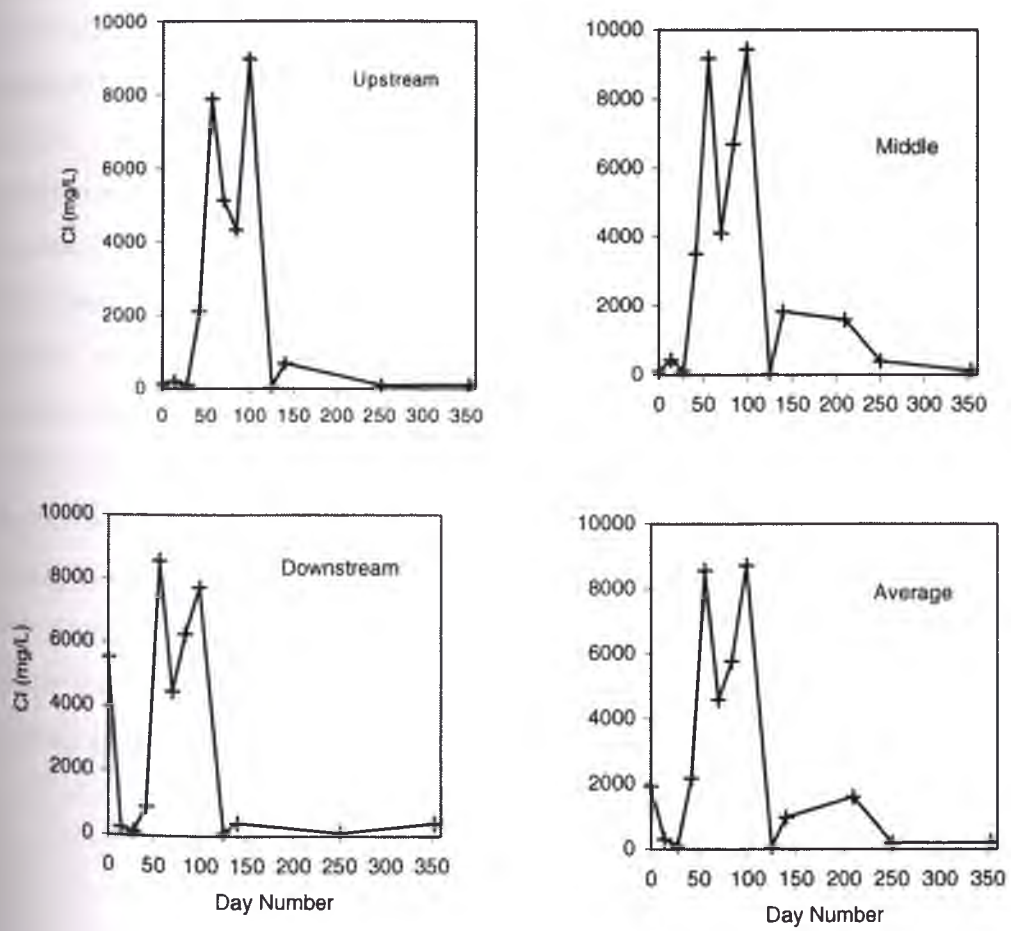

Figure 7.7: Dissolved chloride concentrations upstream, middle and downstream of lime-fly ash barrier site. Average concentrations are also shown.

After the installation of the lime-fly ash barrier, the average chloride concentration in the drain water adjacent to and downstream of the study site significantly decreased (middle: pre-barrier – 3120.2 mg/L, post-barrier – 121.16 mg/L; downstream: pre-barrier – 3139.11 mg/L, post-barrier – 399.7 mg/L).

7.2.5.2 Sulphate concentrations

High sulphate concentrations during the study period are a result of the oxidation of pyrite and the leaching of sulphate into the flood mitigation drain. Average sulphate concentrations upstream were 567 mg/L, while average sulphate concentrations were 693 mg/L and 668 mg/L adjacent to and downstream of the study site, respectively. Similar to chloride, the minimum sulphate concentration adjacent to the study site occurred on Day 125, showing the influence of climatic factors. Sulphate concentrations in the drain water at all sites increased after Day 125. Sulphate generated during preceding drought conditions were discharged into the drain after rainfall. Average sulphate concentrations in the drain water decreased after the installation of the lime-fly ash barrier. This indicates that the barrier decreases pyrite oxidation and the generation of pyrite oxidation products. The groundwater, once discharged into the drain, would therefore have a less detrimental impact on the aquatic environment in the drain. Adjacent to the site, the average sulphate concentration before the installation of the barrier was 739 mg/L, whereas after the barrier was installed the average sulphate concentration was 134 mg/L. This decrease in sulphate concentration was also measured downstream of the study site, with average sulphate concentrations of 695 mg/L pre-barrier and 367 mg/L post-barrier. This decrease illustrates the effectiveness of the barrier in reducing pyritic oxidation and hence the generation of sulphate, which is characteristic of acid sulphate soils affected areas.

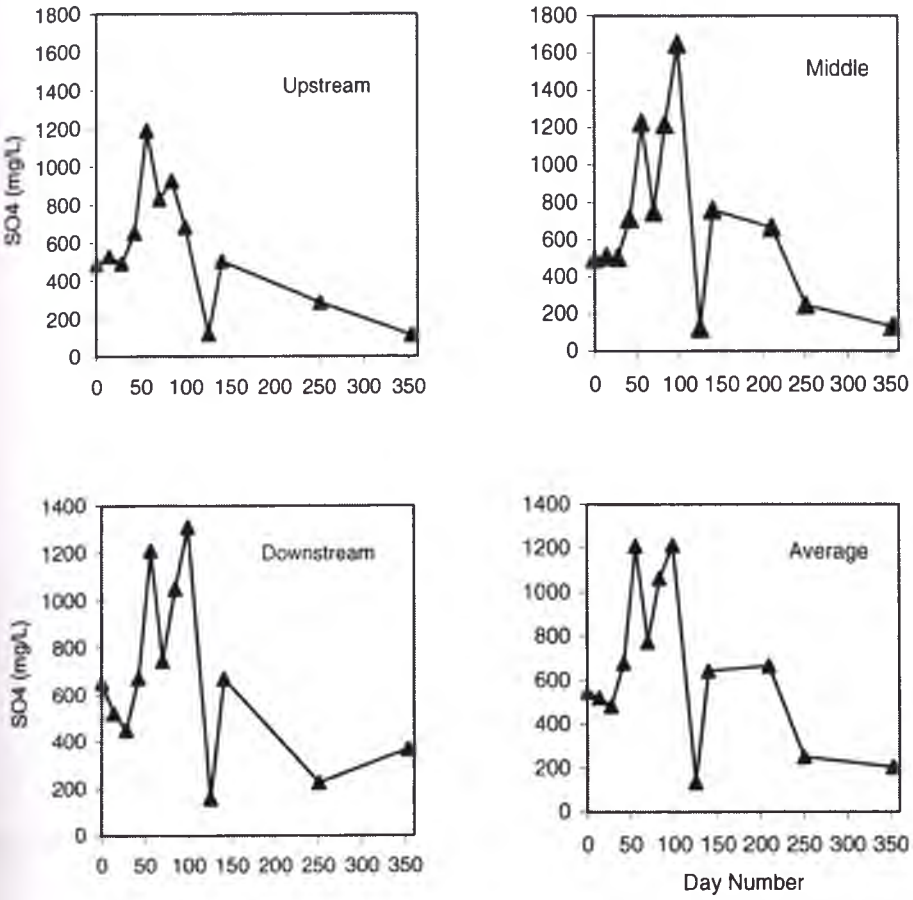

Figure 7.8: Dissolved sulphate concentrations upstream, middle and downstream of lime-fly ash barrier site. Average concentrations are also shown.

7.2.5.3 Cl:SO_4

The Cl:SO_4 ratio measured in drain water at the study site, which is an indication of pyrite oxidation conditions, is shown in Figure 7.9. The elevated chloride/sulphate ratios between Days 42 and 125 correspond with elevated chloride concentrations in the drain water during this period. On average, the Cl:SO_4 ratio in the drain water increased slightly after the installation of the lime-fly ash barrier. Downstream of the study site the Cl:SO_4 ratio increased from 0.43 (Day 251) to 1.09 (Day 353). This ratio is expected to continue to increase, indicating a reduction in pyrite oxidation since the installation of the lime-fly ash barrier.

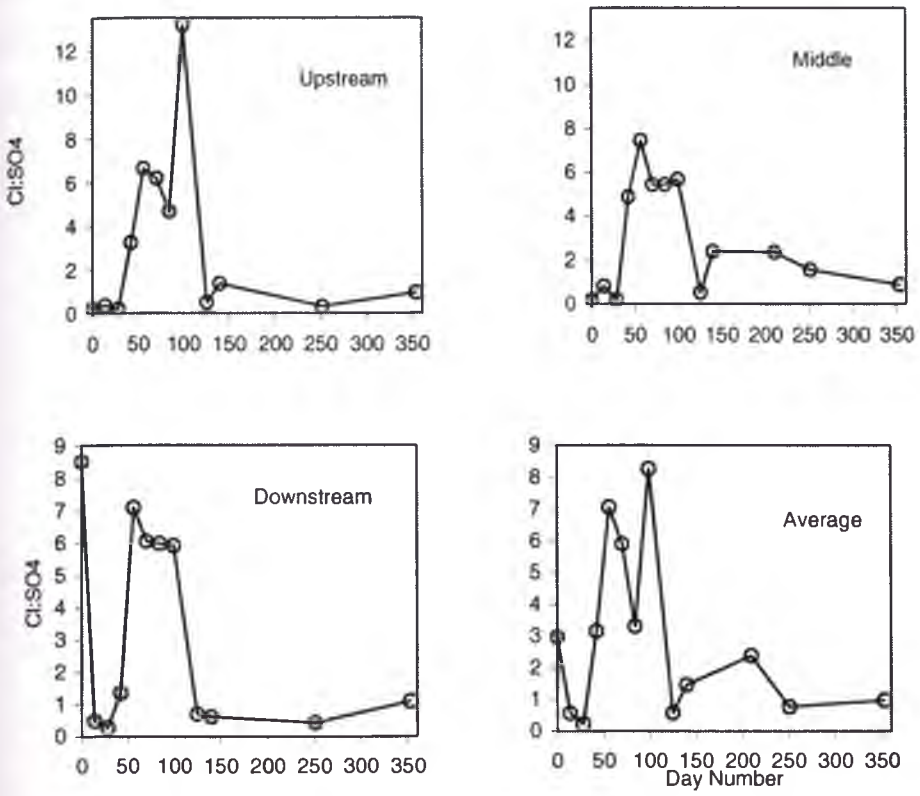

Figure 7.9: Chloride:sulphate ratio upstream, middle and downstream of lime-fly ash barrier site. Average concentrations are also shown.

7.3 Spatial and temporal variation in Groundwater Quality

An analysis of the groundwater quality at the lime-fly ash barrier study site is necessary to determine the influence of the barrier on acid sulphate soils and pyritic oxidation. The section below describes the chemical water quality parameters measured in the groundwater observation holes in the grid surrounding the installed barrier.

7.3.1 Groundwater pH

At the beginning of the study period the average groundwater pH was less than 4.9, with the minimum occurring on Day 14, even though the pyrite layer was submerged. The maximum average groundwater pH before the lime-fly ash barrier was installed was 4.9, measured on Day 125. This coincides with heavy rainfall and a burst freshwater main on the study site. After this event, acidic groundwater was transported into the drain causing an increase in the pH of the drain water. The average pH also peaked to 4.43 on Day 251 after a significant rainfall event. The

localised flooding transported acid to the drain. After this heavy rainfall, the groundwater table lowered. A prolonged dry spell saw the pH in the drain water decrease to 3.25. After the installation of the barrier, the groundwater pH has since increased to a pH value of 4.61 and it is expected to increase even further to approximately 5.5.

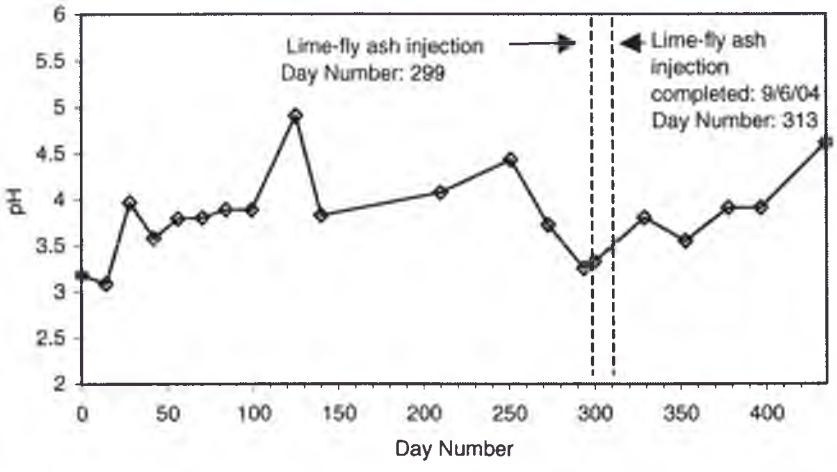

Figure 7.10: Average groundwater pH measured during the study period at the lime-fly ash barrier study site

The lime-fly ash barrier was expected to have a greater influence on those observation holes closer to the barrier. The influence of the barrier on the measured groundwater pH in these observation holes was greater than those further away. The average groundwater pH increased by 1.58 in those observation holes closer to the barrier, while the average groundwater pH increased by 1.38 in those observation holes further from the barrier. Figure 7.11 shows the groundwater pH measured in OH 2 (1m from the barrier), OH 1 (2 m from the barrier) and OH26 (9m).

Observation Holes 29, 30 and 31 monitor groundwater directly before it reaches the flood mitigation drain. The pH of the groundwater in these observations increased during the post-barrier period, showing that groundwater leaching from the study site into the drain is less acidic. On Day 294, the pH in OH29 was 3.80, which increased to 5.18 on Day 435. In OH30, pH increased 3.78 to 4.88, and in OH31 the groundwater pH increased from 3.17 to 4.74.

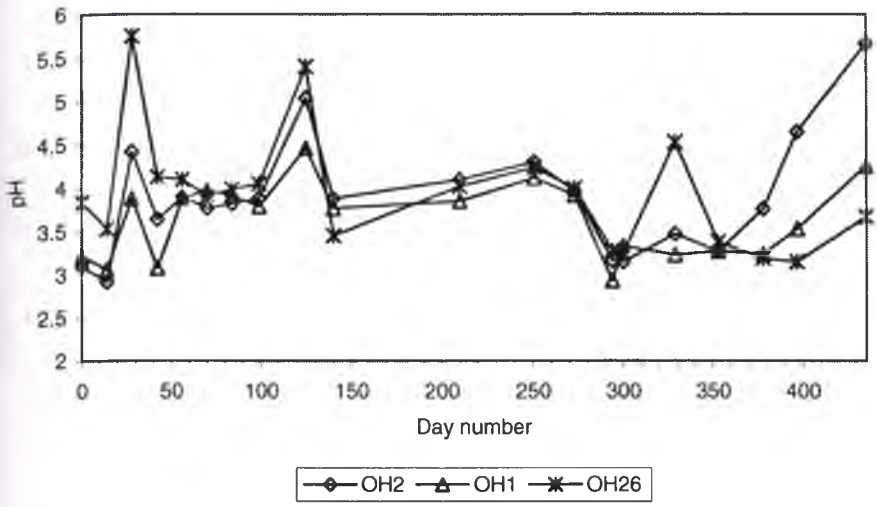

Figure 7.11: Average groundwater pH in OH1 and OH2 measured at the lime-fly ash barrier study site

7.3.2 Electrical Conductivity

The average groundwater electrical conductivity measured during the study period at the lime-fly ash barrier site is shown in Figure 7.12. The ANZECC (1992) trigger value for EC is 2800 µS/cm (2.8 mS) for long-term agricultural irrigation practices. The EC in the groundwater was relatively stable both during the pre- and post-barrier period and below this trigger value, except during heavy rainfall events when the EC levels rose significantly. These elevated EC levels, however, decreased rapidly indicating the rapid flushing of the study site and the movement of groundwater to the flood mitigation drain. The average groundwater EC during the pre-barrier period was 2.34 (3.64 discounting significant rainfall events on Day 125 and 251) compared with 1.46 during the post-barrier period, showing decreased pyrite oxidation as a result of the barrier. Although a significant rainfall event occurred during the post-barrier period (Day 384 – 28 mm), the average EC of the groundwater did not rise. Blunden (2000) showed that the EC of groundwater increased in relation with the concentration of dissolved ions such as SO_4^{2-}, Al^{3+} and Fe^{2+}, therefore, showing that EC can be used to estimate the concentration of pyritic oxidation products in the groundwater. Figure 7.12 shows that in the post-barrier period, the EC of the groundwater was relatively stable, therefore, indicating that the lime-fly ash barrier was effective in reducing pyritic oxidation.

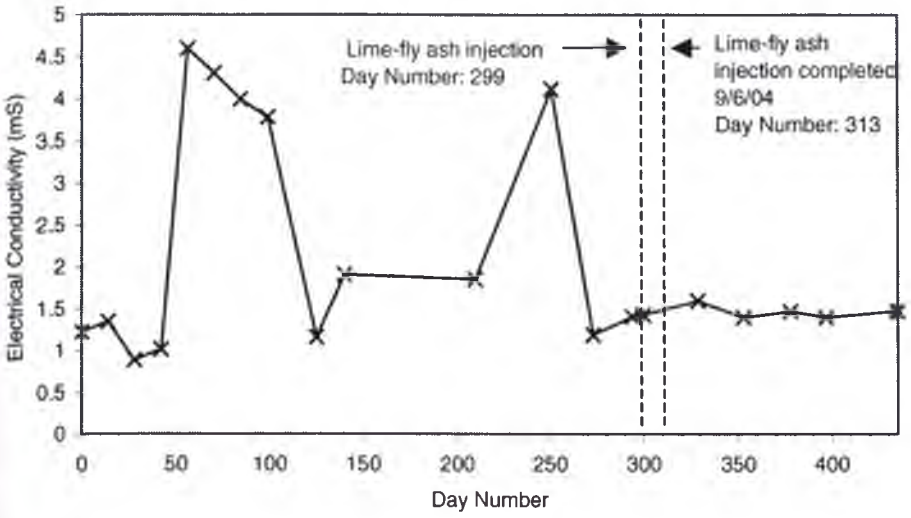

Figure 7.12: Average groundwater electrical conductivity measured during the study period at the lime-fly ash barrier study site

7.3.3Acidic cation concentrations

The influence of the barrier on pyrite oxidation can be assessed by analysing the concentration of pyrite oxidation products in the groundwater before and after the installation of the barrier. The oxidation of pyrite generates acidic products, such as Fe^{2+} and SO_4^{2-} (Equation 2.4), and Al^{3+} (Equation 2.12). The concentration of Al^{3+} and Fe^{2+} measured in the groundwater at the study site is analysed in the following section.

7.3.3.1 Aluminium concentrations

The concentration of Al^{3+} in groundwater at the study site is shown in Figure 7.13. The average total aluminium concentration in the groundwater (20.05 mg/L) is lower than in the drain water (29.15 mg/L). On all occasions the Al^{3+} concentration of the groundwater exceeded the ANZECC (1992) guideline of 0.005 mmol/L (0.1349 mg/L) where pH < 6.5. Concentrations also exceeded the guidelines for marine waters (0.02 mmol/L, 0.5396 mg/L). Al^{3+} fluctuated greatly during the pre-barrier period. The total Al^{3+} concentration in the majority of observation holes dropped significantly on Days 125 and 251 due to the heavy rainfall and localised flooding flushing the oxidation products into the drain. Total Al^{3+} in the groundwater subsequently increased after these rainfall events.

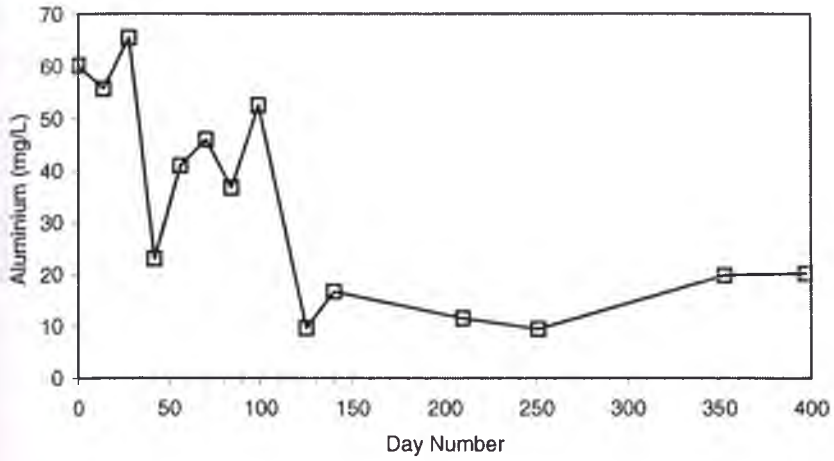

Figure 7.13: Average concentration of dissolved inorganic aluminium in the groundwater at the lime-fly ash barrier study site

Although Figure 7.13 shows that the average aluminium concentration in the groundwater seems to have increased since the installation of the barrier, the concentration of Al^{3+} may have been caused by the dissolution of aluminium minerals previously precipitated that become increasingly soluble as the pH increases from about 3.3 (Nordstrom, 1982). The groundwater measured in observation holes 29 and 30 showed a slight decrease in the total dissolved inorganic aluminium during the post-barrier period (Figure 7.14). As mentioned previously, OH29 and OH30 monitor groundwater flowing through the study site and barrier. Total Al^{3+} decreased from 19.8 mg/L to 18.6 mg/L in OH29 and from 13.8 mg/L to 11 mg/L in OH30.

In the pre-barrier period, the average total Al concentration in the groundwater was 35.68 mg/L compared with 20.05 mg/L in the post-barrier, showing a 44% reduction. By only considering those observation holes expected to be influenced significantly by the barrier, the pre-barrier average total Al concentration in the groundwater was 35.66 mg/L compared with 18.97 mg/L, showing a 47% reduction. This indicates that the lime-fly ash barrier was successful in reducing the generation of pyrite oxidation products.

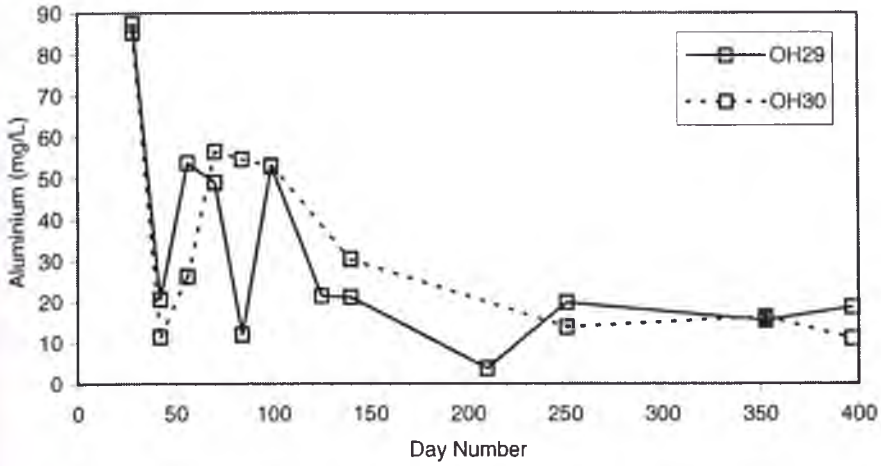

Figure 7.14: Concentration of dissolved inorganic aluminium in the groundwater in OH29 and OH30 at the lime-fly ash barrier study site

As was mentioned in the section on drain water, there is little correlation between groundwater aluminium and pH levels, as shown in Figure 7.15. This shows that there are a number of other influences on the concentration of inorganic monomeric aluminium in the groundwater at this study site, as was mentioned in the section on aluminium concentrations in the drain water at the lime-fly ash barrier site.

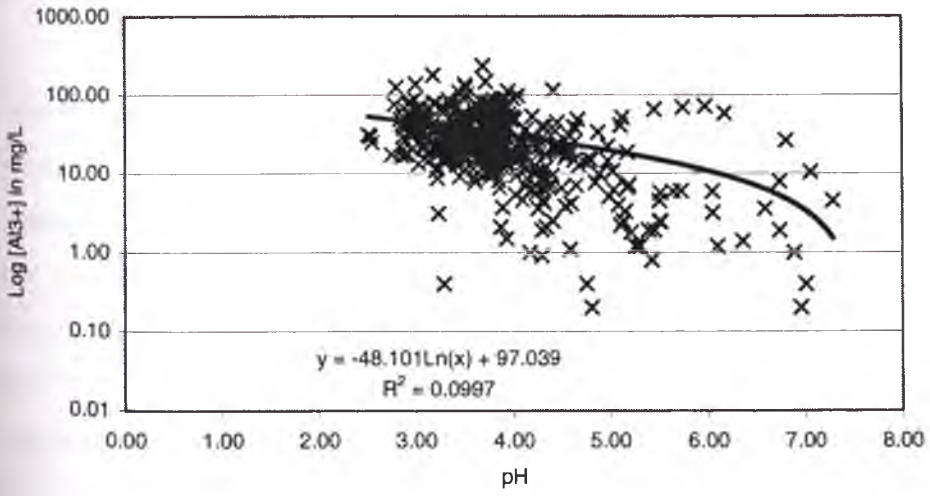

Figure 7.15: Poor correlation between groundwater pH and dissolved monomeric aluminium concentrations

7.3.3.2 Iron concentrations

While Figure 7.16 shows that the average total dissolved iron in the groundwater at the lime-fly ash barrier study site has slightly increased since the installation of the barrier, 83.9% of observation holes experienced a decrease in total dissolved iron (16.1% increase). The low Fe^{2+} concentration on Day 251 can be attributed to heavy rainfall. The average total dissolved iron concentration in the groundwater (37.03 mg/L) is lower than in the drain water (109.63 mg/L).

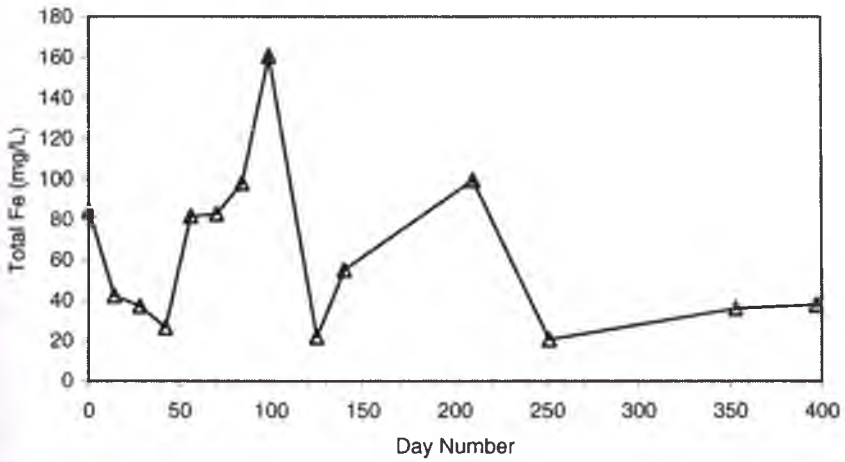

Figure 7.16: Average total dissolved iron in groundwater at the lime-fly ash barrier study site

In the pre-barrier period the average total dissolved iron concentration in the groundwater was 67.59 mg/L compared with 37.03 mg/L in the post-barrier, showing a 55% reduction. By only considering those observation holes expected to be influenced significantly by the barrier, the pre-barrier average total dissolved iron concentration in the groundwater was 71.68 mg/L compared with 41.49 mg/L, showing a 43% reduction. This decrease also indicates a reduction in pyrite oxidation and the generation of acidic oxidation products.

Figure 7.17 shows the decrease in total dissolved iron in selected observation holes from the study site. It can be seen that since the installation of the barrier, total dissolved iron in the groundwater has decreased slightly.

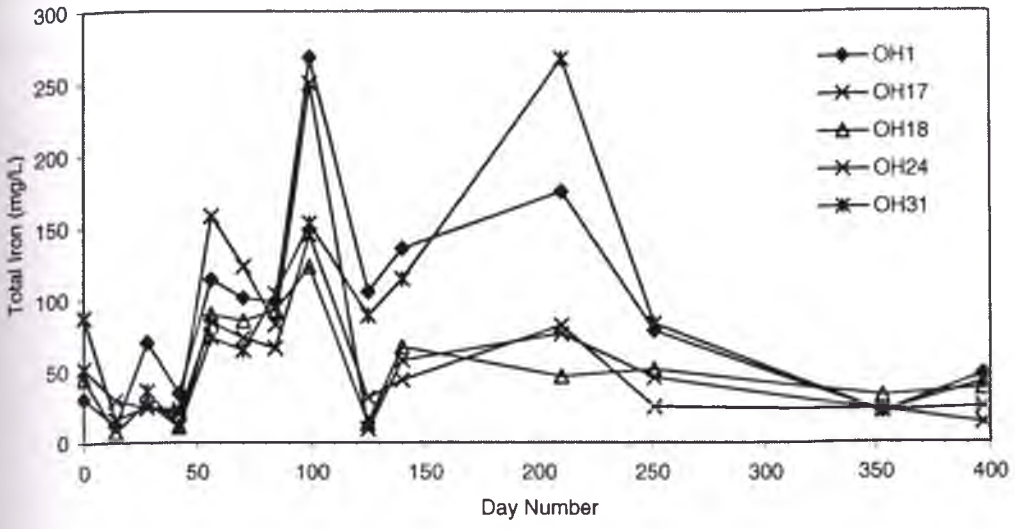

Figure 7.17: Total dissolved iron in OH1, OH17, OH18, OH24, and OH31

7.3.4 Basic cation concentrations

As was mentioned in Chapter 2 (Equation 2.12), Nriagu (1978) showed that acid hydrolysis of the mineral illite liberating basic cations, including Ca^{2+} and Mg^{2+}. The average concentration of Ca^{2+} and Mg^{2+} in the groundwater is shown in Figures 7.18 and 7.19 respectively. The concentration of Mg^{2+} in the groundwater was generally greater than the concentration of Ca^{2+}. A significant increase in the Ca^{2+} concentration occurred in all observation holes at the study site on Day 251. This high concentration (148.47 mg/L) may be derived from the dissolution of clay, however, the concentration of Al^{3+} (which is released during the dissolution of clay minerals) in the groundwater on this day was lower than measured on other days during the study period. Between Days 248-249, 111.8 mm of rain fell on the study site. Localised flooding raised the groundwater table, which may have brought Ca^{2+} to the surface.

The average Ca^{2+} concentration in the groundwater (40.70 mg/L) is lower than in the drain water (52.17 mg/L). Since the barrier was installed the Ca^{2+} in groundwater has decreased in 51.6% of the observation holes monitored. In the pre-barrier period the average Ca^{2+} concentration in the groundwater was 41.15 mg/L compared with 40.70 mg/L in the post-barrier, showing only a 2% reduction. By only considering those observation holes expected to be influenced significantly by the barrier, the pre-

barrier average Ca^{2+} concentration in the groundwater was 42.77 mg/L compared with 45.43 mg/L, showing a slight increase of 6%.

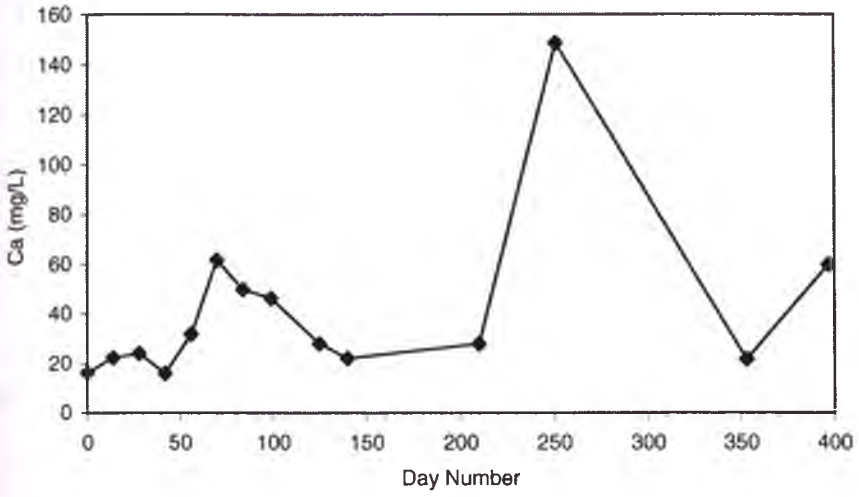

Figure 7.18: Average concentration of Ca^{2+} in groundwater at the lime-fly ash barrier study site

The average Mg^{2+} concentration in the groundwater (80.66 mg/L) is lower than in the drain water (210.92 mg/L). Since the installation of the barrier, the concentration of magnesium in the groundwater decreased in all observation holes at the study site. The average concentration of Mg^{2+} in groundwater, shown in Figure 7.19, in the pre-barrier period was 158.49 mg/L whereas in the post-barrier period the average concentration was 80.66 mg/L, showing a 49% reduction. By only considering those observation holes expected to be influenced significantly by the barrier, the pre-barrier average Mg^{2+} concentration in the groundwater was 181.23 mg/L compared with 80.47 mg/L, showing a concentration reduction of 56%.

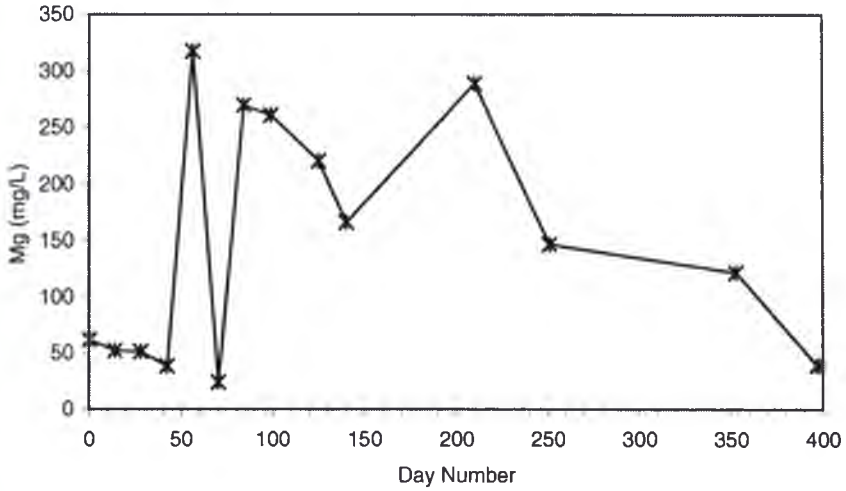

Figure 7.19: Average concentration of Mg^{2+} in groundwater at the lime-fly ash barrier study site

7.3.5 Anion concentrations

Analysing the concentration of chloride and sulphate in the groundwater will indicate the effectiveness of the lime-fly ash barrier in reducing pyritic oxidation, and hence, reducing the production of pyrite oxidation products.

7.3.5.1 Chloride concentrations

The average concentration of dissolved chloride in the groundwater during the study period is shown in Figure 7.20. Chloride is a conservative anion species in groundwater. There was generally no change in the average concentration of chloride in the groundwater, except for between Days 46 to 99. The maximum chloride concentration was measured in observation hole 29 on Day 99 (6488 mg/L). The rapid decrease after Day 99 shows that the chloride is rapidly flushed from the groundwater system. The low chloride concentrations in the groundwater reiterate the fact that there is no salt water intrusion from Broughton Creek up the flood mitigation drain to the study site.

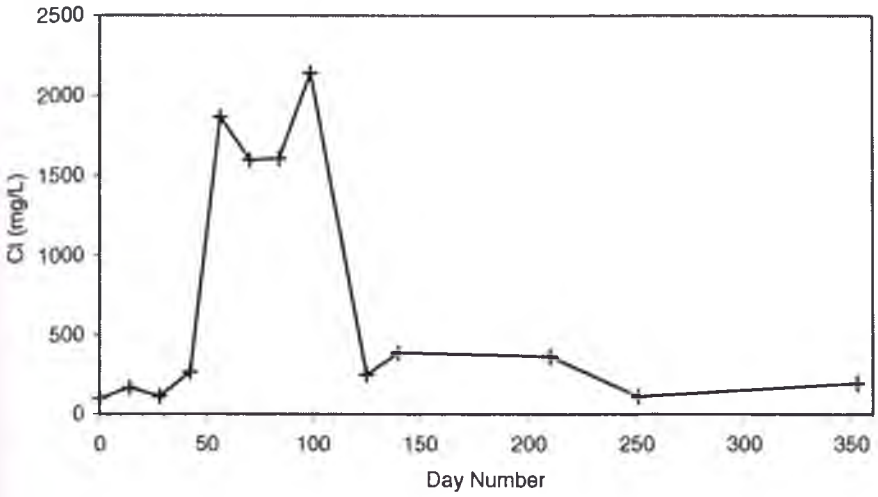

Figure 7.20: Dissolved chloride concentrations in groundwater at the lime-fly ash barrier study site

The average concentration of Cl^- in groundwater in the pre-barrier period was 747.24 mg/L whereas in the post-barrier period the average concentration was 195.47 mg/L, showing a 74% reduction. However, ignoring the high Cl^- concentrations between Days 42 to 99, the average concentration in the pre-barrier period was 219.04 mg/L, showing a 11% reduction in Cl^-.

7.3.5.2 Sulphate concentrations

The average concentration of dissolved sulphate in the groundwater is shown in Figure 7.21. The maximum sulphate concentration of 953 mg/L was measured in OH4. The ANZECC (1992) guideline recommends a sulphate concentration no more than 10 mmol/L (640.6 mg/L). Although the average concentration of sulphate remained below this criterion, the concentration of sulphate in most observation holes was above this level between Days 42 to 99. The rapid increase in sulphate during Days 42 to 99 is due to a decrease in the groundwater table at the study site and hence an increase in pyritic oxidation. It can be seen that since the completion of the barrier, the average concentration of dissolved sulphate in the groundwater has decreased.

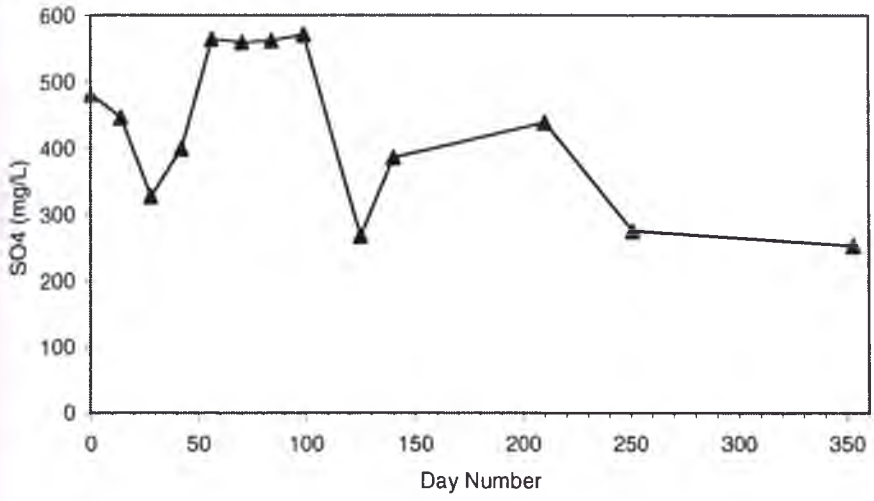

Figure 7.21: Dissolved sulphate concentrations in groundwater at the lime-fly ash barrier study site

Figure 7.22 shows the average $Cl^-:SO_4^{2-}$ ratio of the groundwater at the study site. The ratio was less than 1 on all but four occasions. As previously mentioned, a $Cl^-:SO_4^{2-}$ ratio below 2 is indicative of acid sulphate soil affected areas (Mulvey, 1983). From Day 46 to Day 99, the $Cl^-:SO_4^{2-}$ ratio increased above 2. The maximum average $Cl^-:SO_4^{2-}$ ratio was measured on Day 99 ($Cl:SO_4$ 3.65). Before the installation of the barrier (not including Day 251) the average $Cl^-:SO_4^{2-}$ ratio was 0.38, whereas after the barrier had been installed the ratio had increased to 0.80. The greatest increase in the average $Cl^-:SO_4^{2-}$ ratio after the installation of the barrier was measured in OH23 (pre-barrier 0.35; post-barrier 1.55). In observation holes just before the drain (OH29, OH30 and OH31) the $Cl^-:SO_4^{2-}$ ratio was also seen to increase in the post-barrier period. This shows that groundwater moving from the study site into the drain will have an increased $Cl^-:SO_4^{2-}$ ratio.

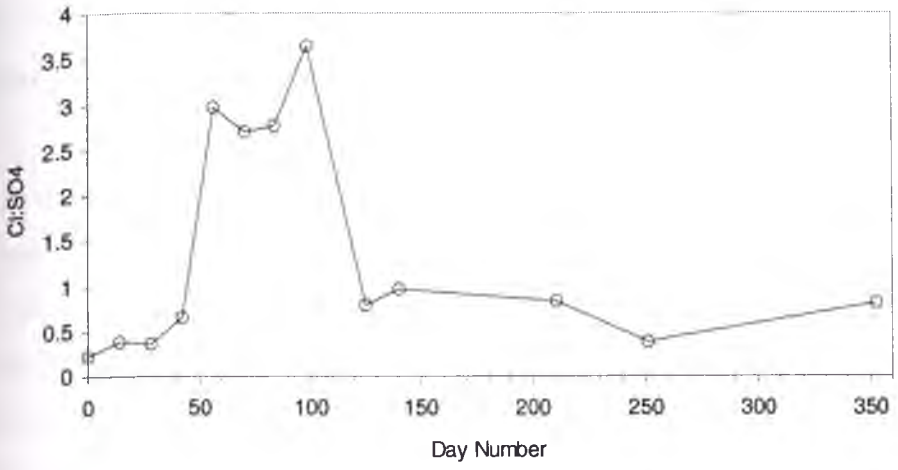

Figure 7.22: Average Chloride:sulphate ratio in the groundwater at the lime-fly ash barrier study site

7.4 Conclusions

The completion of the sub-surface Lime-fly ash barrier at the study site was successful in relation to improving groundwater quality. The groundwater quality data showed that pyrite oxidation products were generated in the pre-barrier period as a result of falling groundwater tables and biotic oxidation. Climatic conditions also had a strong influence on the concentration of these pyritic oxidation products in the groundwater. After the installation of the barrier, substantial improvements in groundwater quality occurred. pH increased to values between 4.5-5.5. Electrical conductivity in the groundwater was seen to be relatively stable after the completion of the barrier, indicating a reduction in pyrite oxidation. The concentration of the pyrite oxidation products, acidic cations Al^{3+} and Fe^{2+}, basic cations Ca^{2+} and Mg^{2+} and anions Cl^- and SO_4^{2-} on average decreased in the groundwater. Increases in the $Cl^-:SO_4^{2-}$ in the groundwater varied at the study site, however, on average the $Cl^-:SO_4^{2-}$ increased slightly as a result of the alkaline barrier.

Monitoring of the flood mitigation drain adjacent to the study site showed an acidic environment during the pre- and post-barrier period. The flood mitigation drain adjacent to the Lime-fly ash barrier study site is not only influenced by the barrier, but also by acid sulphate soils areas upstream. The influence of the barrier on drain water was inferred by the positive results in those observation holes directly before the drain.

Chapter 8.0 Surface Water and Groundwater Quality Results for the Floodgate and Weir Sites

8.1 Introduction

This Chapter deals with the surface and groundwater quality parameters that indicate pyrite oxidation. Water quality monitoring was undertaken at four Floodgate sites and Two Weir Sites so as to allow comparison between the different acid sulphate soils remediation measures on the Shoalhaven Floodplain. This Chapter is divided into two sections. The creek water and drain water chemical properties that were measured at the floodgate and weir sites are described and related to climatic and geochemical characteristics of the acid sulphate soils are discussed in the first section. The spatial and temporal distributions of these properties are also analysed. The second section of this Chapter describes the changes in groundwater quality at the floodgate and weir sites. Data measured at the study site are presented in Appendix D.

8.2 Spatial and temporal variance in creek and drain water quality

In this section, creek and drain water quality is described at the floodgate and weir sites. This data will be used as a comparison with data collected at the Lime-fly ash barrier study site.

8.2.1 pH

Figure 8.1 shows the pH of creek water taken from the floodgate sites. The ANZECC (2000) guideline recommends that pH should be 7-8.5 for estuaries and 8-8.4 for marine waters. pH values were generally the highest at FG2. The maximum creek water pH at FG2 was 7.55 (Day 329), which fell within this guideline. The pH in creek water at FG2 fell below this guideline on all occasions except between Days 56 and 99 and on Day 329. The pH of the creek water at FG4 was consistently below this guideline. The lowest pH recorded at FG4 was 4.43. The floodgate at this site leaked and a drain pipe leading from the drain allowed acidic water to flow into the creek.

The maximum pH values at FG1, FG3 and FG4 were 7.29 (beginning of study period), 7.29 (Day 378) and 6.96 (Day 28). The decrease in creek water pH (4.81) at FG2 on Day 125, which coincided with the minimum pH measured during the study period, could be due to the leaky floodgate allowing acidic water generated during pyritic oxidation from the flood mitigation to drain into the creek. Groundwater table elevations before this period were lowering which would have enhanced pyrite oxidation. The pH in creek water at FG3 was relatively stable throughout the entire study period.

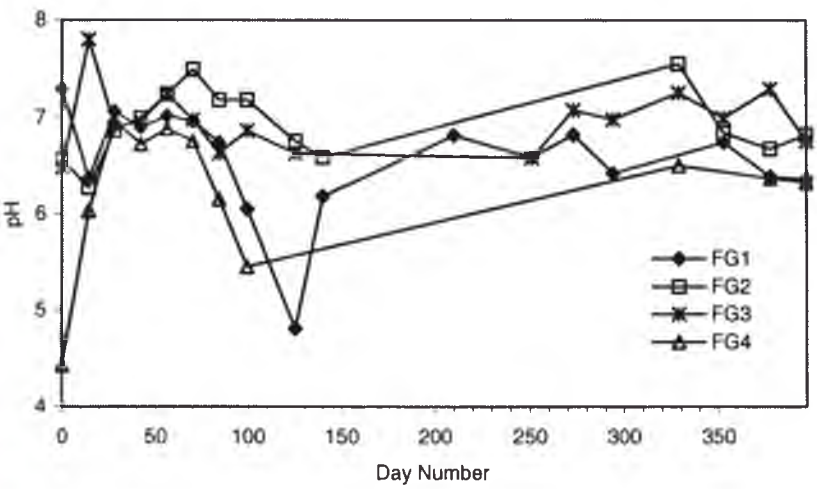

Figure 8.1: Creek water pH readings taken from Floodgate Sites

Drain water pH measured at the floodgate sites is shown in Figure 8.2. pH values were generally below the ANZECC (2000) guidelines up to Day 300, where pH rose above 7 at FG3 and FG2. This shows that up to Day 300, drain water discharging from the flood mitigation drains at these sites would have a detrimental impact on the aquatic environment in Broughton Creek. The rise in pH after Day 300 can be attributed to the installation of the modified floodgates and the intrusion of salt water into the flood mitigation drains. The rapid fluctuation in drain water pH at FG3 was due to operational problems with the floodgate allowing saline intrusion up the drain. The decrease in drain water pH from 6.46 (Day 99) to 4.11 (Day 140) at FG1 illustrates the influence of pyritic oxidation on drain water quality. Drain water pH also decreased in this period at FG3 and FG2.

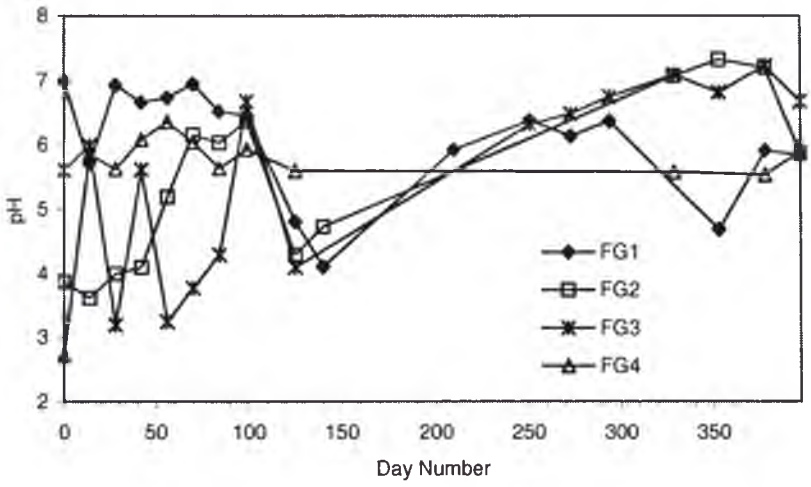

Figure 8.2: Drain water pH readings taken from Floodgate Sites

Figure 8.3 shows that drain water pH was generally higher at WS2. Groundwater tables at WS1 were elevated compared to the groundwater table at WS1. The elevated groundwater table submerges the pyrite layer, and hence, reduces pyrite oxidation and the generation of acidic groundwater. The reduced hydraulic gradient also reduces the transport of any previously generated pyritic oxidation products into the drain, therefore reducing the drain water pH. The rapid decrease in drain water pH from 5.99 (Day 70) to 3.58 (Day 84) can be attributed to a groundwater table rise due to rainfall before this period. This rising groundwater table entrained acidity generated by pyrite oxidation and transported this acidic water into the drain. The drain water pH at WS1 rose above the pH measured at WS2 on one occasion (Day 125). This may have been due to the heavy rainfall and localised flooding diluting the pH in this flood mitigation drain.

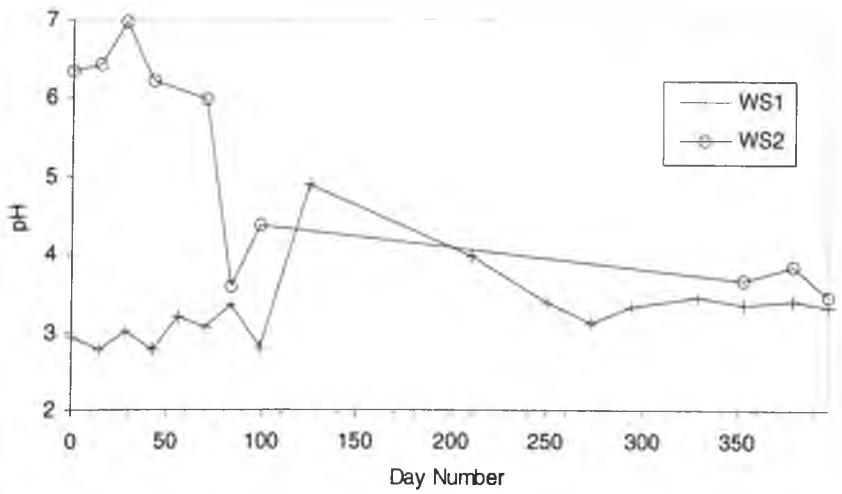

Figure 8.3: Drain water pH readings taken from Weir Sites

8.2.2 Electrical Conductivity

Electrical conductivity (EC) measurements taken from the floodgate sites (Broughton Creek) are presented in Figure 8.4. EC in creek water samples showed a pattern of rapid declines due to rainfall. The lowest recorded creek water EC was from FG1 (1.41 mS) on Day 125. EC measurements are able to indicate the extent of a tidal front within an estuary as shown by the maximum creek water EC recorded at FG3 (23.84 mS). This study site is located further downstream of Broughton Creek than the other floodgate sites.

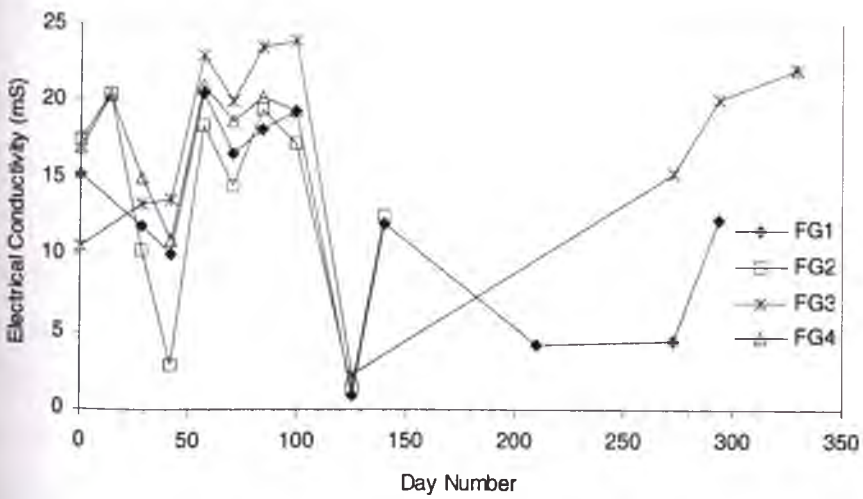

Figure 8.4: Creek water electrical conductivity readings taken from Floodgate Sites

Figure 8.5 shows the drain water EC measurements taken at the floodgate sites. All EC measurements, except on Days 42 and 125 at FG2 and Day 125 at FG1, were below the ANZECC (1992) guideline of 2800μS/cm (2.8 mS) for long term agricultural irrigation practices. EC in the drain water also fluctuated with rainfall. The maximum drain water EC was recorded at FG3 (23.44 mS), indicating saline intrusion. During the first 99 days, the drain water EC fluctuated at all sites indicating periods of pyrite oxidation and leaching of acidic water from the ground into the drain. The decline in EC on Day 125 at FG1, FG2 and FG3 can be attributed to the heavy rainfall event that occurred between Days 123-125 (32 mm). EC in the drain water sharply increased after Day 125. Rainfall on Day 251 also led to a decrease in EC at FG1.

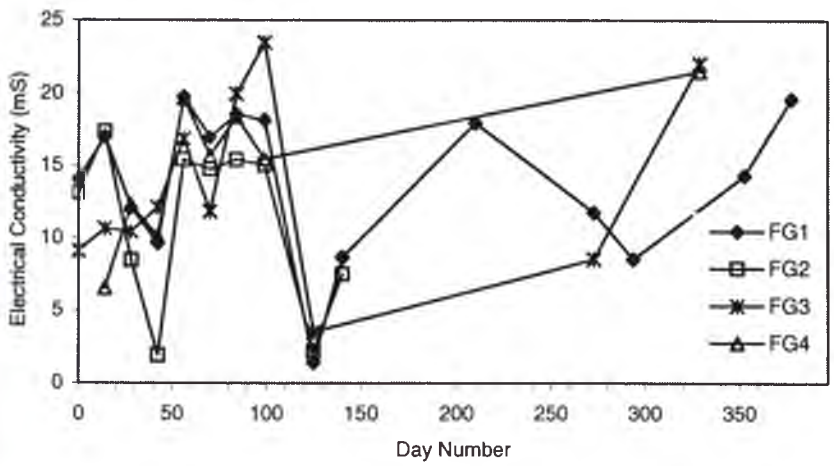

Figure 8.5: Drain water electrical conductivity readings taken from Floodgate Sites

EC in the drain water at WS1 was significantly greater than at WS2, as shown in Figure 8.6. The maximum EC recorded at WS1 was 15.75 mS (Day 56), whereas the maximum EC recorded in drain water at WS2 was 1.25 (Day 378). This is due to increased pyrite oxidation and the generation of pyrite oxidation products in the groundwater, which in turn leaches into the drain, at WS1. All EC measurements, except for EC recorded on Day 397, at WS1 were above the ANZECC (1992) criterion of 2800μS/cm (2.8 mS) for long-term agricultural irrigation practices, whereas all EC measurements at WS2 were below this criterion.

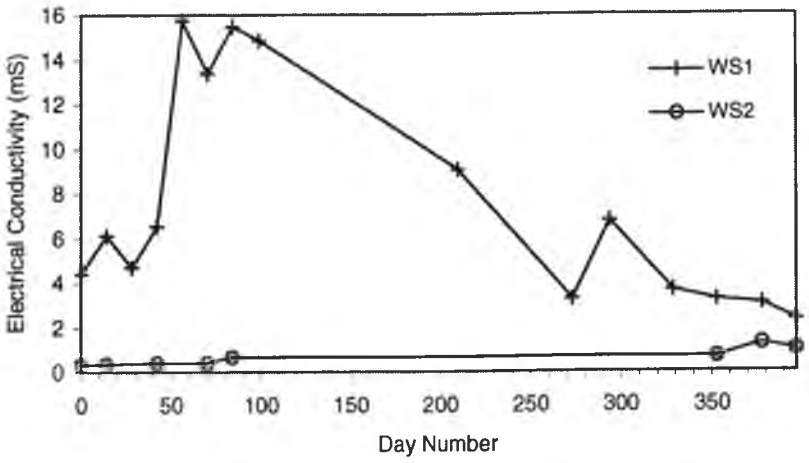

Figure 8.6: Drain water electrical conductivity readings taken from Weir Sites

8.2.3 Acidic cation concentrations

The high concentrations of dissolved inorganic monomeric aluminium and total dissolved iron in the creek/drain waters at the floodgate and weir sites is a result of the pyrite oxidation and the leaching of the generated acidic groundwater into the flood mitigation drains. The concentrations measured at these sites are described in the following sections.

8.2.3.1 Aluminium concentrations

The ANZECC (1992) guidelines state that when the pH is less than 6.5, aluminium concentrations must not exceed 0.005 mmol/L (0.5396 mg/L). Figure 8.7 presents the dissolved inorganic monomeric aluminium concentrations in creek water at the floodgate sites. In the first 99 days, when the pH was below 6.5, aluminium concentrations at FG2, FG3 and FG4 were above this guideline. Aluminium levels in creek water at FG1 were also all above this guideline. However, on Days 56 and 70, the aluminium concentration was close to this guideline, 0.4mg/L and 0.2 mg/L respectively. The high concentrations of aluminium in the creek water on Day 140 at FG1 (58.2 mg/L) and FG2 (40.4 mg/L) and Day 153 at FG3 (86 mg/L) indicate the flush of acidic drain water into Broughton Creek. These high aluminium concentrations could have severe environmental impacts on the estuarine environment.

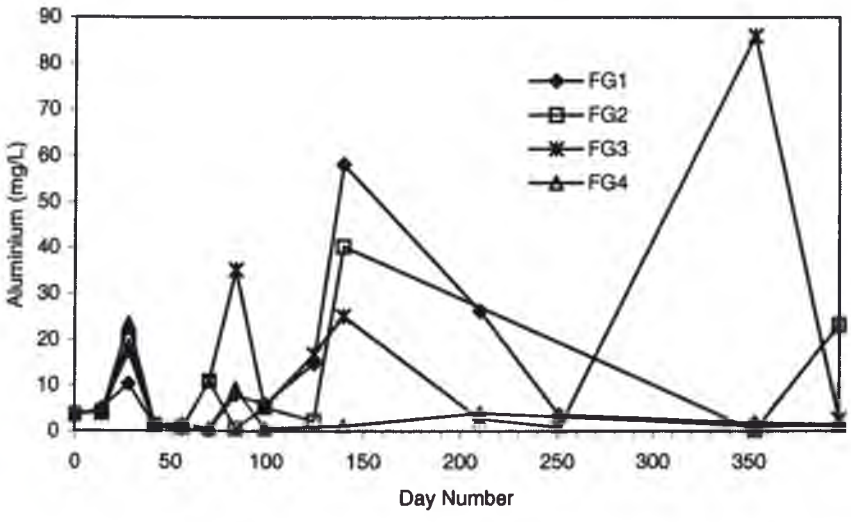

Figure 8.7: Dissolved inorganic monomeric Al^{3+} concentrations in creek water measured at the Floodgate Sites

Aluminium concentrations in drain water at all floodgate sites were also below the ANZECC (1992) criterion, as presented in Figure 8.8. The lowest dissolved aluminium concentration was measured at FG4 on Day 84 (0.6 mg/L). Aluminium concentrations fluctuated greatly in the first 140 days of the study period, indicating open/closed floodgate periods. Rainfall on Day125 decreased the concentration of Al^{3+} in the drain water. After this rainfall, the concentration of Al^{3+} in the drain water sharply increased due to aluminium previously entrained in the groundwater being flushed into the drain. After Day 210, the concentration of Al^{3+} in the drain water was relatively stable due to drought conditions. After Day 384 the concentration of Al^{3+} at FG1 increased, possibly due to the influence of a rainfall event coupled with pyrite oxidation.

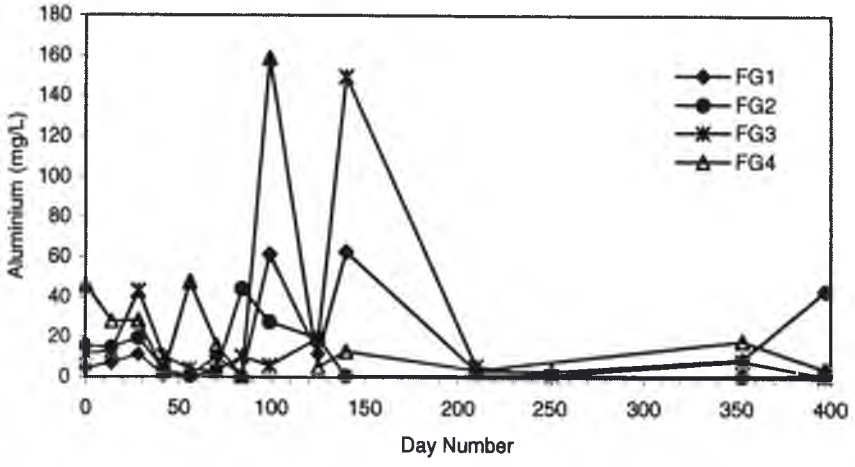

Figure 8.8: Dissolved inorganic monomeric Al^{3+} concentrations in drain water measured at the Floodgate Sites

The concentration of dissolved Al^{3+} in the drain water at WS1 was greater than the concentration in drain water at WS2 up to Day 84, as shown in Figure 8.9. This was expected because the elevated groundwater levels at WS2 decrease the generation of pyritic oxidation products. On Days 84, 99 and 125, the concentration of Al^{3+} in the drain water at WS2 was greater than that measured at WS1. It is possible the groundwater table may have been below the pyrite layer, hence enhancing pyrite oxidation and the dissolution of silicate clays and aluminium minerals under acidic groundwater conditions. The concentration of Al^{3+} in the drain water at both weir sites were above the ANZECC (1992) guideline on all sampling days during the study period.

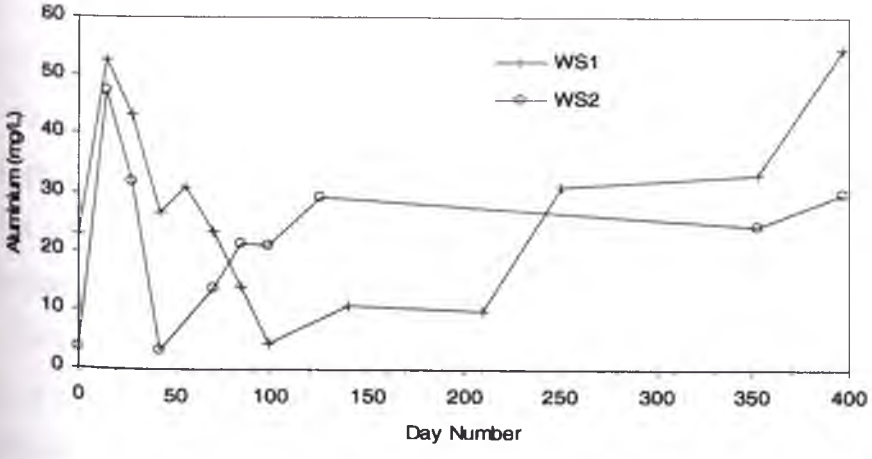

Figure 8.9: Dissolved inorganic monomeric Al^{3+} concentrations in drain water measured at the Weir Sites

8.2.3.2 Iron concentrations

The total dissolved iron concentrations in creek water measured at the floodgate sites are shown in Figure 8.10. In the first 140 days, the concentration of Fe was generally below 10 mg/L. On Day 140, total dissolved Fe concentrations in creek water reached a maximum of 139.9 mg/L at FG3. This maximum concentration of Fe in the creek water corresponded low drain water pH values caused by the discharge of groundwater containing pyritic oxidation products. This acidic drain water was flushed into the Broughton Creek. Total dissolved Fe in the creek water peaked again on Day 353 at FG3 with a concentration of 48.1 mg/L.

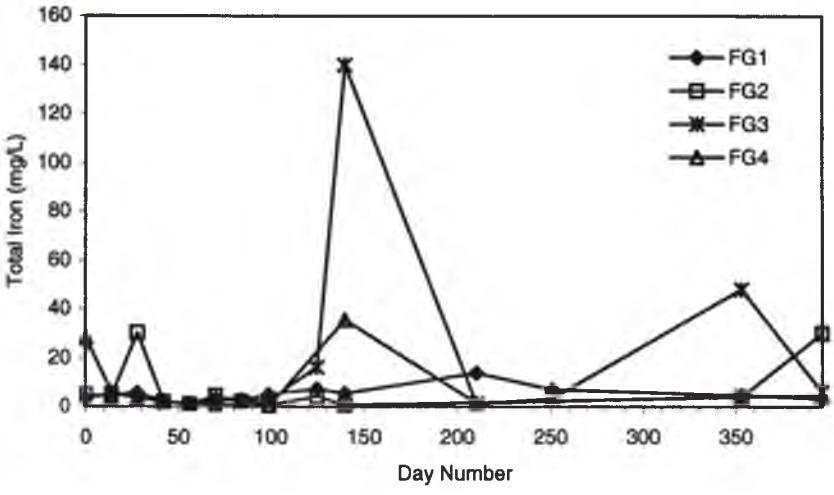

Figure 8.10: Total dissolved iron concentrations in creek water measured at the Floodgate Sites

ANZECC (1992) guidelines suggest that the concentration of dissolved iron should not exceed 0.009 mmol/L (0.502 mg/L) for the protection of aquatic ecosystems. In all cases, total dissolved iron concentrations in drain water at the floodgate sites were above this ANZECC (1992) criterion, as can be seen in Figure 8.11. The maximum concentration of dissolved iron in drain water was measured at FG2 on Day 99 (542 mg/L). Total dissolved Fe concentrations at FG4 and FG1 also increased on this day, possibly as a result of recent rainfall flushing dissolved iron from the groundwater into the drain. The rapid decrease in total Fe after Day 99 coincides with the increase in total dissolved Fe in the creek water at these sites.

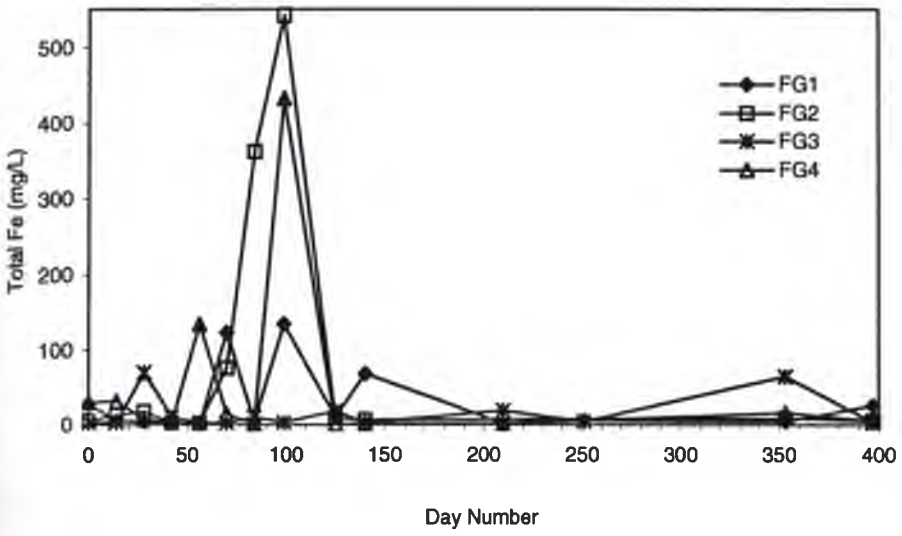

Figure 8.11: Total dissolved iron concentrations in drain water – Floodgate Sites

The high concentrations in the drain water at these sites have severe environmental consequences for the estuarine environment. Pyrite oxidation and the generation of ferrous iron and also the oxidation of dissolved Fe^{2+} to Fe^{3+} generates additional acidity, and is termed 'acid at a distance' (White *et al.*, 1997) due to the generation of acid away from the source. High concentrations of Fe^{2+} can also lead to the formation of iron monosulphides, as was noted in the flood mitigation drains at the floodgate sites.

The concentration of dissolved iron in the drain water at both WS1 and WS2 was high throughout the study period, as shown in Figure 8.12. Total dissolved Fe in the drain water exceeded the ANZECC (1992) guidelines on all sampling occasions during the study period. The high total Fe concentration of 274 mg/L at WS1 (Day 42) is preceded by a drought period. Fe^{2+} generated during pyrite oxidation in this period was discharged to the drain during the 'first flush' after rainfall on Day 42. The maximum total dissolved Fe concentration of 156.6 mg/L in drain water at WS2 also followed this trend.

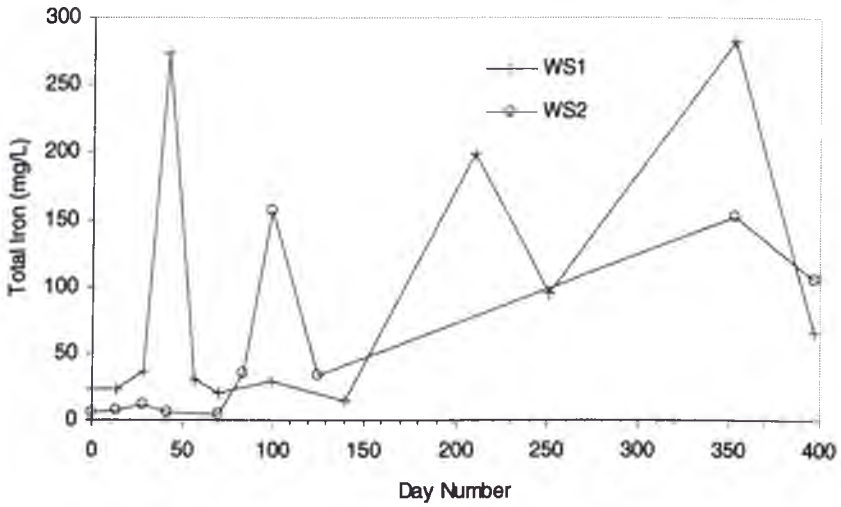

Figure 8.12: Total dissolved iron concentrations in drain water measured at the Weir Sites

The decrease in total dissolved Fe on Days 125, 251 and 384 at WS1 coincided with heavy rainfall. Total dissolved Fe then increased rapidly, due to pyrite oxidation products in the groundwater discharging to the flood mitigation drains.

8.2.4 Basic cation concentrations

The concentration of soluble calcium in creek water at the floodgate sites is presented in Figure 8.13. In the first 140 days, the concentration of Ca fluctuated at all the sites. The maximum soluble Ca^{2+} was measured at FG1 (284 mg/L on Day 84). Although the concentration of Ca^{2+} in the creek water was greater at FG1 on most sampling days, the average concentration of Ca^{2+} was 150.2 mg/L compared to 170.7 mg/L, 166.4 mg/L and 167 mg/L at FG2, FG3 and FG4 respectively. Ca^{2+} in the creek water decreased to a minimum of 15 mg/L at FG1 on Day 28. However, the rapid increase afterwards to 282 mg/L was due to the lowering of the groundwater table and dissolution of clays. This coupled with floodgate operation problems such as leaking led to the flushing of Ca^{2+} into the creek.

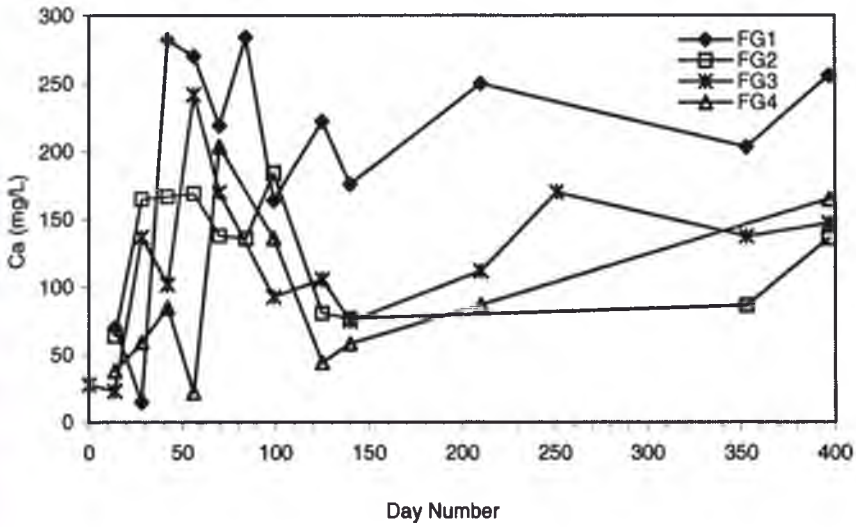

Figure 8.13: Soluble calcium concentrations in creek water measured at the Floodgate Sites

Figure 8.14 shows the concentration of soluble calcium in drain water at the floodgate sites. A wide range of Ca^{2+} concentrations were recorded during the study period. The maximum Ca^{2+} concentration in the drain water was recorded at FG3 on Day 353 (325.2 mg/L). The minimum Ca^{2+} concentration of 1 mg/L was recorded at both FG3 and FG4. FG1 had the greatest average Ca^{2+} concentration of 163.27 mg/L. This indicates that the leaky floodgate allows the ingress of brackish water into the flood mitigation drain. Rainfall on Day 125 enhanced drain water flushing and decreased Ca^{2+} concentrations at all the floodgate sites.

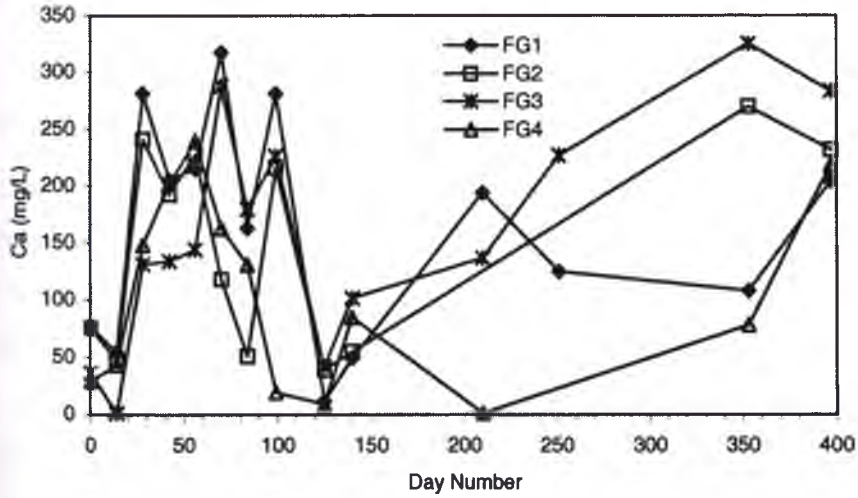

Figure 8.14: Soluble calcium concentrations in drain water measured at the Floodgate Sites

The concentration of Ca^{2+} in drain waters was greater at WS1 than WS2, as presented in Figure 8.15. The average Ca^{2+} concentration in drain water at WS1 was 83.3 mg/L, whereas the average Ca^{2+} at WS2 was 21.4 mg/L. The minimum Ca^{2+} concentration of 2.8 mg/L was recorded at WS1 at the beginning of the study period. After Day 28, the concentration of soluble Ca in the drain water at WS1 was greater than the concentration in drain water at WS2. The sharp decline in Ca concentration at WS1 after Day 99 is due to climatic influences, namely the heavy rainfall event on Day 125. After Day 125, Ca in the groundwater increased due to the dissolution of clay minerals, as saline intrusion does not influence the WS1 study site.

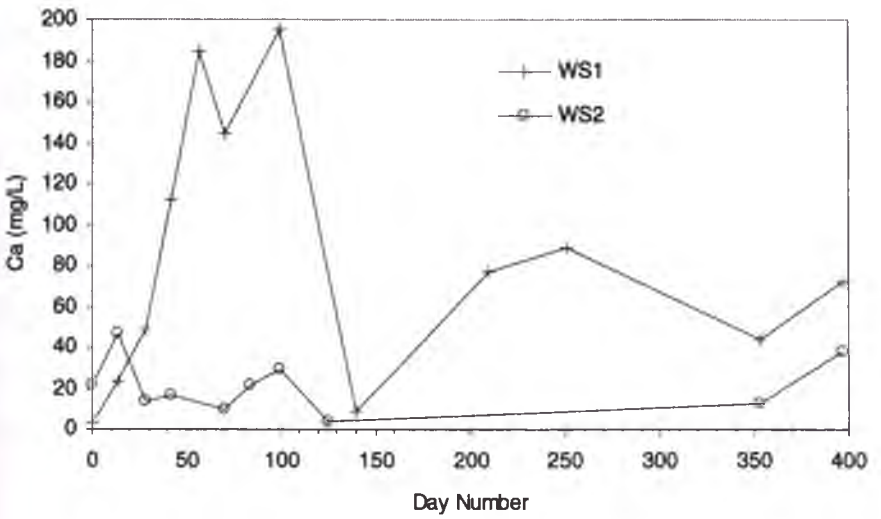

Figure 8.15: Soluble calcium concentrations in drain water measured at the Weir Sites

Generally, the concentration of Mg^{2+} is greater in creek water at FG1, as shown in Figure 8.16. High concentrations of Mg^{2+} concentrations are typical of saline water as the typical concentration of Mg^{2+} in seawater is 1300 mg/L. The tidal front in Broughton Creek has more of an influence on FG1 due to its position in Broughton Creek. The maximum Mg^{2+} concentration at all floodgate sites occurred on Day 14. Drought conditions preceding this period induced pyrite oxidation conditions. The generation of pyrite oxidation products and the subsequent dissolution of clays after rainfall led to the discharge of acidic groundwater to the drain and creek.

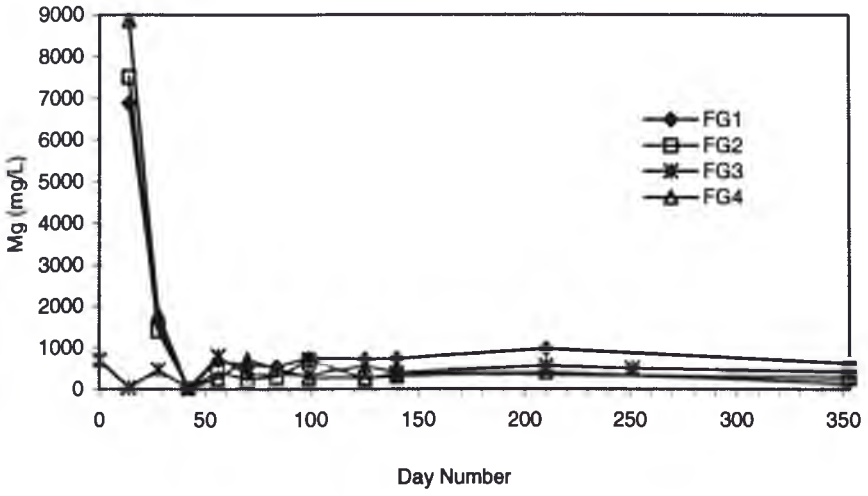

Figure 8.16: Soluble magnesium concentration in creek water measured at the Floodgate Sites

The concentration of soluble Mg^{2+} in drain water at the weir sites is shown in Figure 8.17. The high concentrations of Mg^{2+} in the drain water on Day 14 at FG1 (7320 mg/L) and FG4 (9410 mg/L) are due to the floodgates allowing saline water into the drain. Minor increases in Mg^{2+} during the study period would be due to the dissolution of estuarine clays. The minimum Mg^{2+} concentrations in drain water at all the floodgate sites occurred on Day 42 (FG1 – 68.6 mg/L, FG2 – 67.9 mg/L, FG3 – 55.6 mg/L, FG4 – 21.7 mg/L), indicating 'closed' floodgate conditions. Drought conditions preceding Day 42 entrained pyrite oxidation products in the groundwater.

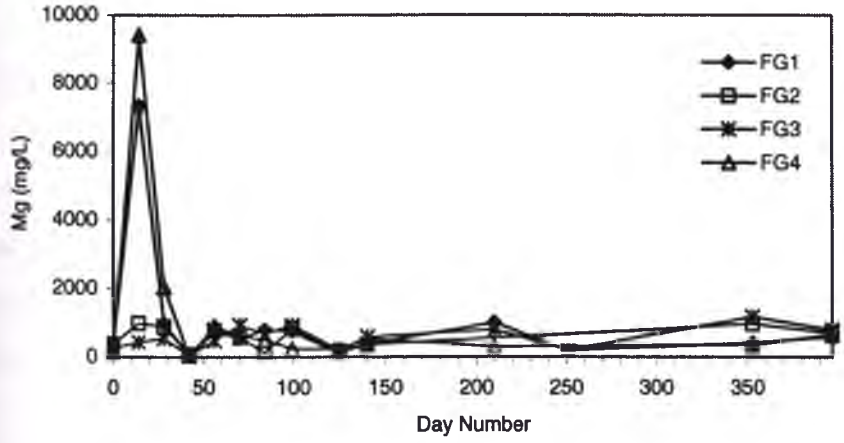

Figure 8.17: Soluble magnesium concentrations in drain water measured at the Floodgate Sites

Figure 8.18 presents the concentration of soluble magnesium in drain water at the weir sites. The average Mg^{2+} concentration at WS1 was 325.7 mg/L compared with 1173 mg/L at WS2. The high Mg^{2+} concentration on Day 14 at WS2 (8390 mg/L) would have been due to the dissolution of clay minerals, as there is little saline influence at this site. Removing this high concentration from average calculations gives an average drain water Mg^{2+} concentration at WS2 of 311.2 mg/L, showing that the self-regulating tilting weir is able to reduce the generation of pyrite oxidation products.

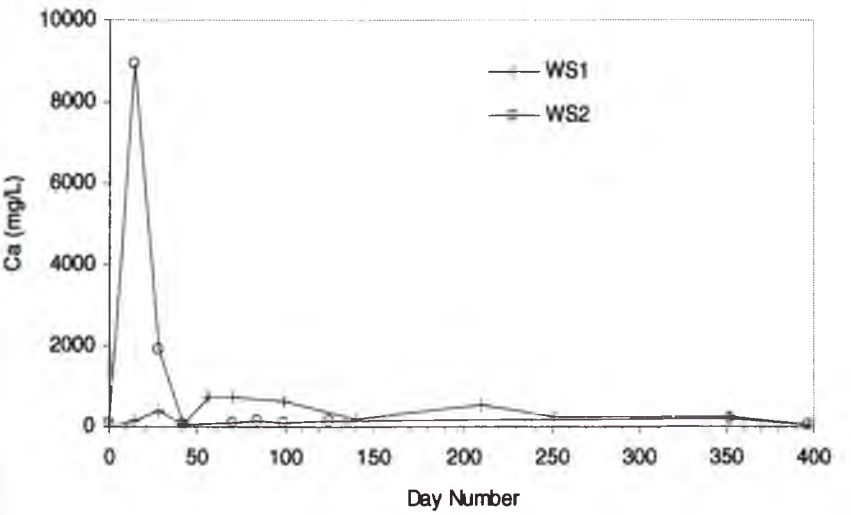

Figure 8.18: Soluble magnesium concentrations in drain water measured at the Weir Sites

8.2.5 Anion concentrations

Chloride is an indicator of saline ingress within an estuary and high concentrations of sulphate in drain water is a characteristic of acid sulphate soils and the leaching of pyrite oxidation products from groundwater. The following section analyses the concentration of chloride and sulphate in creek water and drain water at the floodgate and weir sites.

8.2.5.1 Chloride concentrations

The first 99 days were characterised by periods of high soluble Cl^- concentrations, as presented in Figure 8.19. The maximum concentrations at FG1 (11350 mg/L), FG3

(12459.6 mg/L) and FG4 (12103 mg/L) occurred on Day 99 saline ingress up Broughton Creek. Rainfall on Day 125 and 251 diluted the concentration of chloride salts in the creek water at FG1, FG2 and FG3. The sharp increase of Cl^- in the creek water samples after Days 125 and 251 indicate low resident periods.

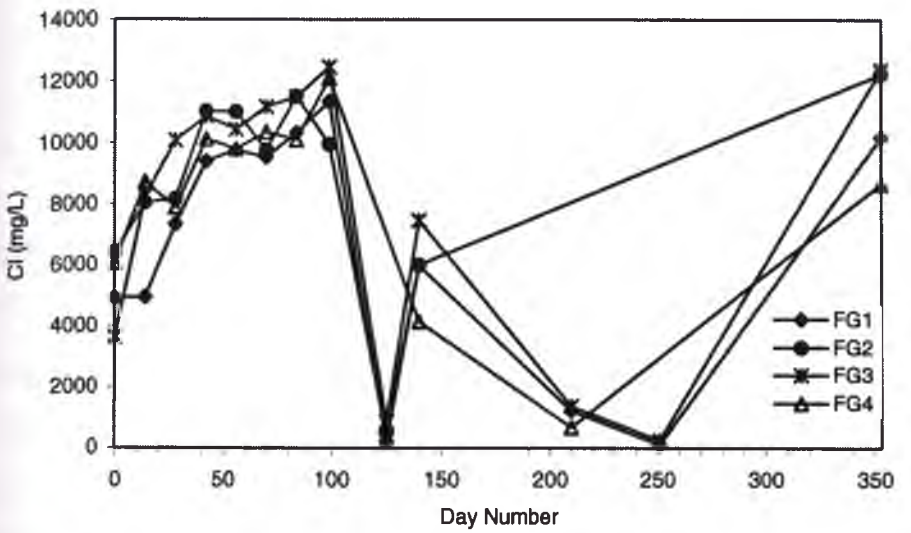

Figure 8.19: Dissolved chloride concentrations measured in creek water at the Floodgate Sites

The high Cl^- concentrations in drain water at the floodgates sites in the first 99 days, as shown in Figure 8.20, is evidence that the one-way floodgates do not restrict saline intrusion in flood mitigation drains as noted by previous researchers (Pease, 1997; Wilson *et al.*, 1999; Glamore, 2003). FG1 and FG3 were leaky on a number of occasions during the first 99 Days of the study period. The average Cl^- concentrations in drain water were 6707.9 mg/L and 5899 mg/L at FG1 and FG3 respectively. The high average Cl^- concentration at FG2 (7445 mg/L) was also caused by saline intrusion via a drainpipe leading from the creek to the drain just downstream of the floodgate. High Cl^- conditions were experienced at FG1 (12438 mg/L) and FG2 (10335 mg/L) on Day 42. High Cl^- concentrations were measured at FG3 (12299 mg/L) and FG4 (11619 mg/L) on Day 99. Significant rainfall events on Days 125 and 251 flushed chloride anions from the drain water at FG1, FG2 and FG4.

	Mg2+ (mg/L)	236	263	~	~
	Cl (mg/L)	794.7	249	~	~
	SO4 (mg/L)	509	295	~	~
	Cl:SO4	1.561	0.846	~	~
	pH	3.38	3.73	~	~
	Conductivity (mS)	~	~	~	~
	Groundwater table elevation (m below ground surface)	n/a	-0.78	n/a	~
	Temperature (C)	~	~	~	~
353	Total Fe (mg/L)	282	149.3	151.9	45
	Al3+ (mg/L)	33.2	8	24.2	74.3
	Ca2+ (mg/L)	43.8	66.3	13	20.7
	Mg2+ (mg/L)	258	279	213	241
	Cl (mg/L)	685	699	60	106
	SO4 (mg/L)	502	498	186	968
	Cl:SO4	1.364	1.404	0.322	0.110
	pH	3.35	4.29	3.67	3.11
	Conductivity (mS)	3.25	3.69	0.66	2.38
	Groundwater table elevation (m below ground surface)	~	-1.02	~	-1.28
	Temperature (C)	7.7	12.5	6.8	11

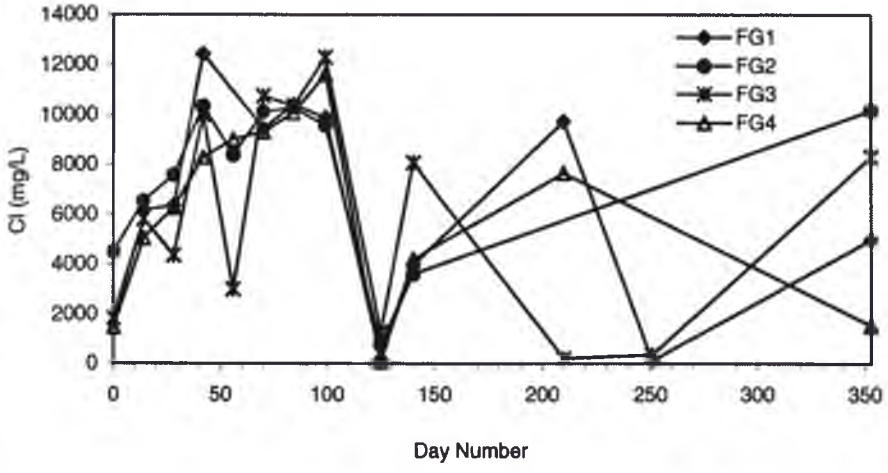

Figure 8.20: Dissolved chloride concentrations measured in drain water at the Floodgate Sites

Dissolved chloride concentrations in drain water at the weir sites are shown in Figure 8.21. Chloride in drain water at WS1 was consistently of a greater concentration than that measured at WS2, as presented in Figure 8.21. This was due to saline intrusion via the floodgate (FG1). Cl^- in drain water at WS2 was stable during the entire study period, ranging from 43.8 mg/L to 240.87 mg/L with an average concentration of 96.8 mg/L. The concentration of Cl^- in the drain water at WS1 was on average 3252.5 mg/L, but had expansive range of concentrations from 98 mg/L to 8320.8 mg/L. The decrease in Cl^- concentrations in the drain water on Days 125 and 251 corresponded with rainfall.

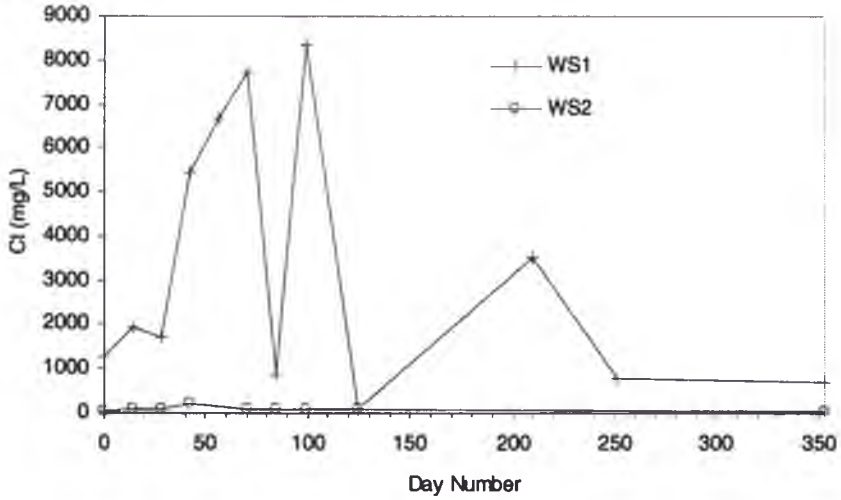

Figure 8.21: Dissolved chloride concentrations measured in drain water at the Weir Sites

8.2.5.2 Sulphate concentrations

The study period is characterised by high sulphate concentrations in creek water at all the floodgate sites, as shown in Figure 8.22. The high average SO_4^{2-} concentration (1221 mg/L) in creek water at FG3 is due to the leaky floodgate allowing pyrite oxidation products to be removed from the drain into Broughton Creek. SO_4^{2-} concentrations in the creek water samples were also influenced by rainfall, as can be seen by the rapid decrease in concentration at FG1, FG2 and FG3 on Days 125 and 251.

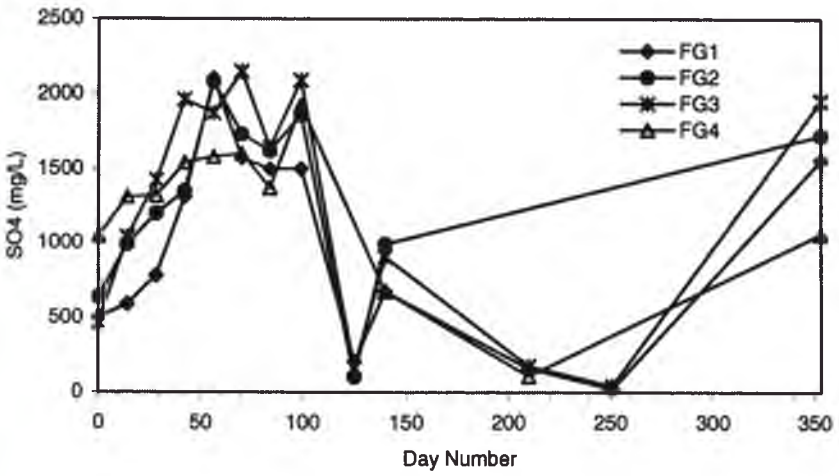

Figure 8.22: Creek water dissolved sulphate concentrations from Floodgate Sites

Sulphate concentrations in the drain water at the floodgate sites were also very high during the study period, as shown in Figure 8.23, indicating pyrite oxidation and the leaching of groundwater acidity into the drain. There was little variation in average SO_4^{2-} concentrations between the floodgate sites. FG2 had the highest drain water average SO_4^{2-} concentration (1311 mg/L) followed by FG3 (1102 mg/L). SO_4^{2-} concentrations exceeded the ANZECC (1992) guideline of 0.005 mmol/L (0.5396 mg/L) throughout the entire study period. SO_4^{2-} and Cl^- concentrations in the drain water at FG3 (71.2 mg/L) were influenced by heavy rainfall preceding Day 210 (43.2 mm). The low SO_4^{2-} concentration at FG1 (26 mg/L) is also due to rainfall.

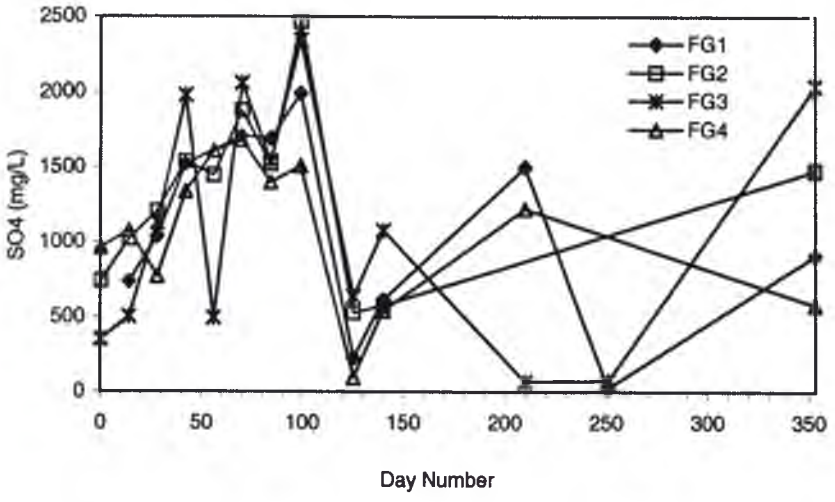

Figure 8.23: Dissolved sulphate concentrations in drain water at the Floodgate Sites

The average concentration of SO_4^{2-} in drain water was lower at WS2 than at the floodgate sites, showing that the weir is successful in raising the groundwater table and reducing the generation of pyritic oxidation products (See Figure 8.24). The average SO_4^{2-} concentration at WS2 was 20.6 mg/L compared with 163 mg/L at WS1. This shows that placing a weir at WS1 could possibly be successful in reducing the concentration of pyrite oxidation products in the drain water. The high SO_4^{2-} concentrations in the drain water at WS1 (1700 mg/L) and WS2 (469 mg/L) on Day 99 were caused by previously generated pyrite oxidation products being discharged into the drain as a result of rainfall. The low SO_4^{2-} concentration in drain water at WS2 at the beginning of the study period is also due to SO_4^{2-} being entrained in the groundwater.

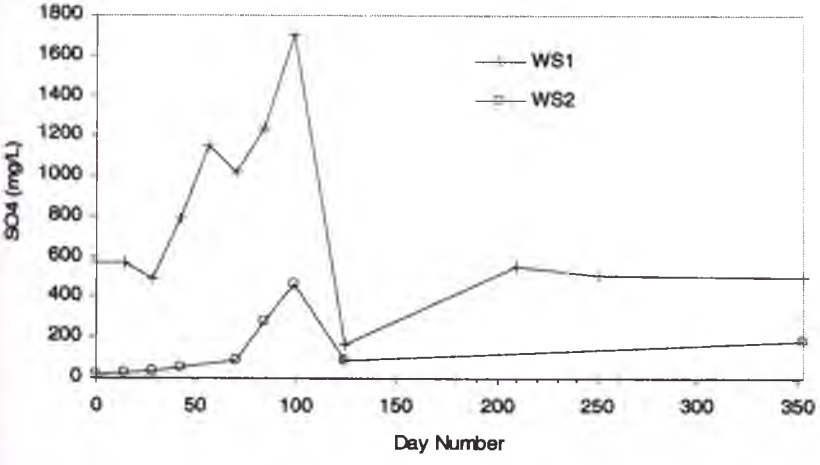

Figure 8.24: Dissolved sulphate concentrations in drain water at the Weir Sites

8.2.5.3 $Cl:SO_4$

As mentioned in Chapter 7, the chloride:suphate ratio can be used as an indicator of pyrite oxidation. As with the concentration of SO_4^{2-} there was also little variation in the average $Cl:SO_4$ in creek water between the floodgate sites, ranging from 6.5 at FG4 to 6.8 at FG1. The $Cl:SO_4$ in creek water at FG4 is less than the $Cl:SO_4$ at the other floodgate sites due to low Cl^- concentrations. The floodgate at FG4 did not have leakage problems; therefore, saline intrusion in the first half of the study period was reduced. The $Cl:SO_4$ in creek water at all the floodgate sites was consistently above 4, except for at FG2 on Day 125 when it decreased to 1. Localised flooding in the drain would have flushed acidic drain water into the creek at this site causing the $Cl:SO_4$ to decrease.

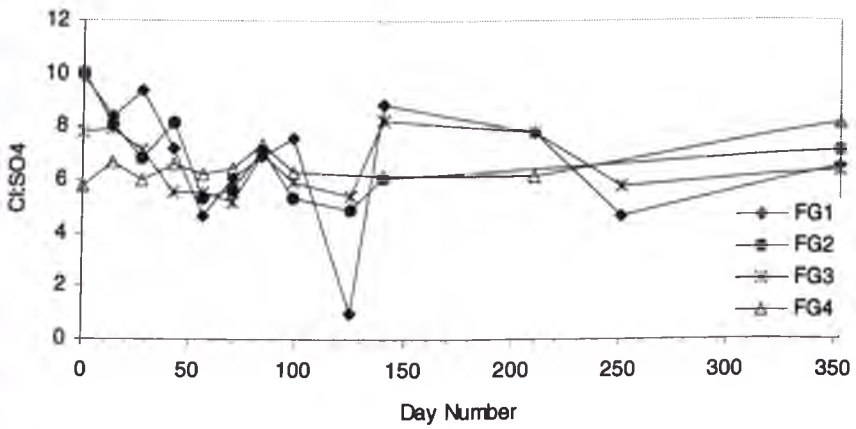

Figure 8.25: Chloride:sulphate ratios from creek water at the Floodgate Sites

The $Cl:SO_4$ in drain water at all the floodgate sites were also similar, as shown in Figure 8.26.

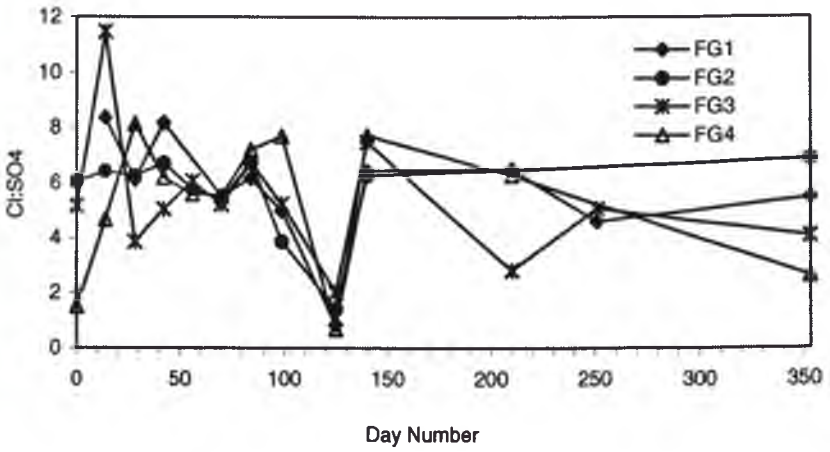

Figure 8.26: Chloride:sulphate ratios in drain water at the Floodgate Sites

The $Cl:SO_4$ ranged from 5.3 at FG4 to 5.7 at FG1. The lowest $Cl:SO_4$ in drain water was measured at FG4 on Day 125. The heavy rainfall would have diliuted the Cl^- concentration in the drain water and in turn lowered the $Cl:SO_4$. The maximum $Cl:SO_4$ was reported at FG3 (11.47) on Day 14. Saline intrusion caused by the leaky floodgate as well as the entrainment of SO_4^{2-} in groundwater is a possible cause of this high $Cl:SO_4$ in the drain water.

Figure 8.27 shows the $Cl:SO_4$ in the drain water at the weir sites. The average $Cl:SO_4$ in the drain water at WS1 was 3.73, whereas the average $Cl:SO_4$ at WS2 was 1.61. This is evidence of past pyrite oxidation at the self-regulating tilting weir site. The $Cl:SO_4$ lowered on Days 125 and 251 due to rainfall.

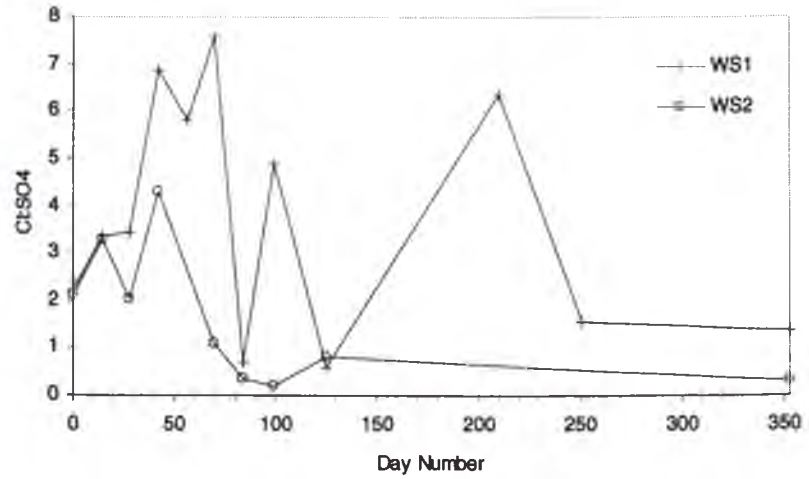

Figure 8.27: Chloride:sulphate ratios in drain water at the Weir Sites

8.4 Spatial and temporal variation in Groundwater Quality

The following section describes the groundwater chemical water quality properties investigated at the floodgate and weir sites. These are related to climatic influences and the generation of acidic groundwater as a result of pyrite oxidation.

8.4.1 Groundwater pH

Figure 8.28 compares the groundwater pH between the floodgates. Groundwater pH varied from 4.19 at FG4 to 5.13 at FG2. The high groundwater pH at FG2 was caused by the inflow of saline water from the creek via the leaky floodgate. This could also explain the high conductivity at FG1 (See Figure 8.30). The ANZECC (2000) guidelines recommend pH should be 7.0-8.5 in estuaries. The groundwater pH was within this guideline at FG3 on a number of occasions. On Day 125, the groundwater pH at FG3 was 7.38, possibly due to rainfall diluting the acidic groundwater.

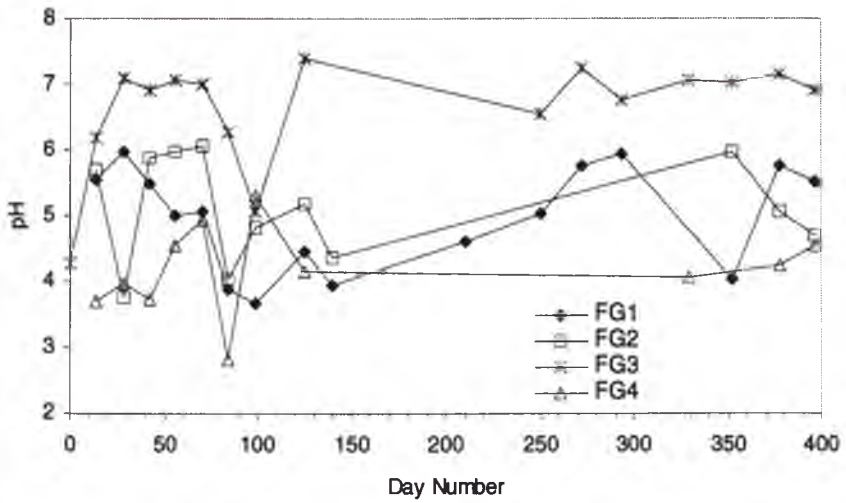

Figure 8.28: pH readings in groundwater taken from the Floodgate Sites

Figure 8.29 shows the groundwater pH at the weir sites. The average groundwater pH was similar between the sites, with WS1 having an average pH of 3.54 and WS2 an average groundwater pH of 3.51.

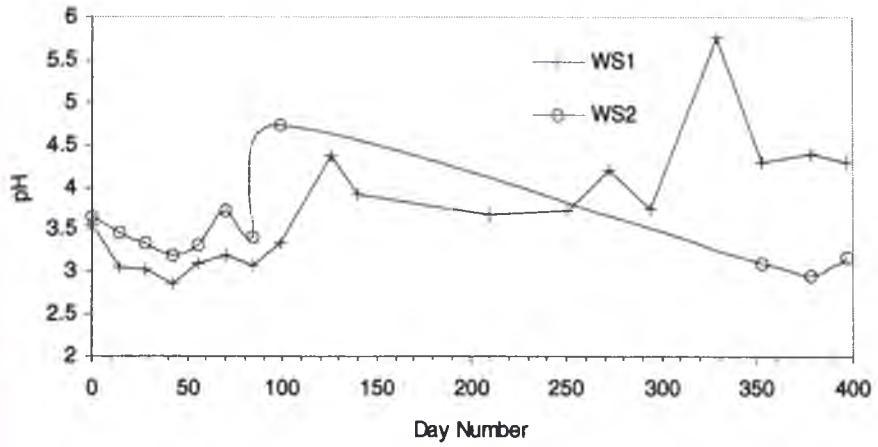

Figure 8.29: pH readings in groundwater taken from the Weir Sites

It was expected that WS2 would have a much greater groundwater pH than WS2, although as also reported by Blunden (2000) groundwater pH values after the installation of the weir were below 4. The low groundwater pH on Day 353 (3.11) is due to drought conditions entraining the acidity generated as a result of pyrite oxidation in the groundwater.

8.4.2 Electrical Conductivity

FG1 was found to have the highest groundwater conductivity (21.67 mS), while FG2 recorded the lowest groundwater conductivity (0.71 mS). This EC at FG2 was below the ANZECC (1992) criterion of 2800µS/cm (2.8 mS) for long-term agricultural irrigation practices. The high EC values recorded at FG1 is a result of the close proximity to the floodgate and the leakage of saline water from Broughton Creek into the drain and soil. Groundwater at FG3 also experienced high EC values, also as a result of saline intrusion via leaky floodgates. The heavy rainfall on Day 125 influenced the EC in the groundwater at all the floodgate sites.

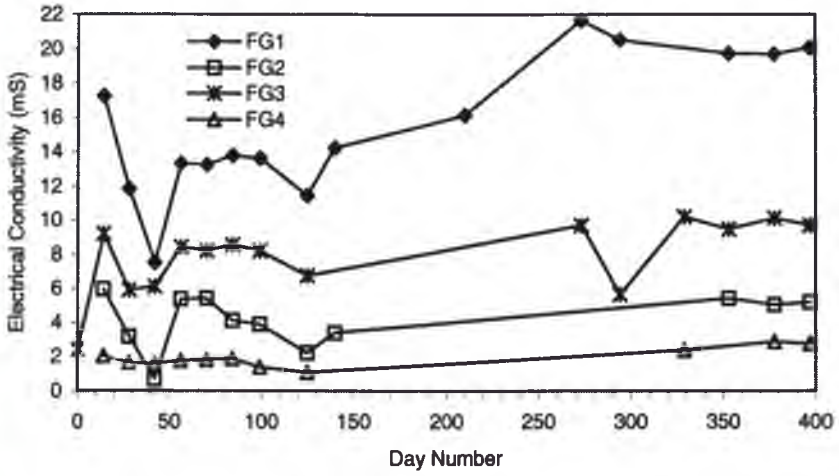

Figure 8.30: Electrical conductivity in groundwater taken from the Floodgate Sites

The EC of groundwater at the weir sites is presented in Figure 8.31. The EC in groundwater at WS1 is significantly greater than the EC measured in groundwater at WS2, due to increased pyrite oxidation and the generation of pyrite oxidation products at this site. The self-regulating tilting weir at WS2 raises the groundwater table, which in turn reduces pyrite oxidation and decreases the EC of the groundwater.

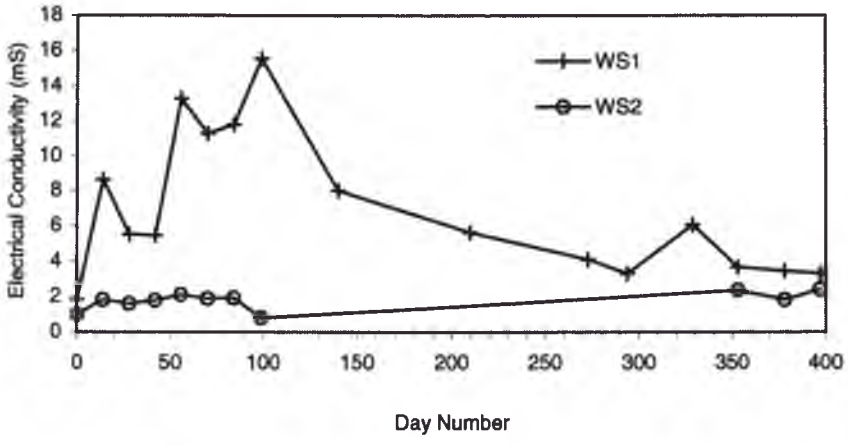

Figure 8.31: Electrical conductivity in groundwater taken from the Weir Sites

8.4.3 Acidic cation concentrations

The evaluation of the concentrations of dissolved inorganic monomeric aluminium and total dissolved iron can be used to assess the effectiveness of acid sulphate soils management techniques in reducing pyrite oxidation.

8.4.3.1 Aluminium concentrations

The concentration of dissolved aluminium in groundwater at the floodgate sites is shown in Figure 8.32. The average concentration of Al^{3+} in the groundwater ranged from 11.1 mg/L at FG2 to 55.3 mg/L at FG3. The maximum dissolved inorganic monomeric aluminium concentration in groundwater at the floodgate sites was measured at FG3 (639 mg/L). This was due to dissolved Al^{3+} entrained in the groundwater as a result of drought conditions before the study period. The concentration of Al^{3+} on Day 251 (0.3 mg/L) at FG3 was below the ANZECC (1992) criterion of 0.005 mmol/L (0.5396 mg/L). At the other floodgate sites, the Al^{3+} in the groundwater was significantly greater than this criterion during the study period, as a result of pyrite oxidation.

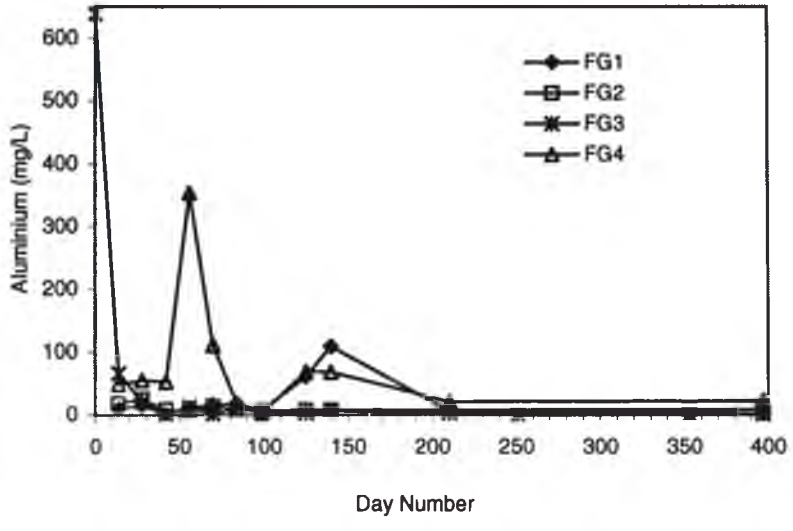

Figure 8.32: Dissolved inorganic monomeric Al^{3+} concentrations in groundwater at the Floodgate Sites

As can be seen in Figure 8.33, the dissolved Al^{3+} concentration in groundwater at WS2 is greater than the concentration measured in groundwater at WS1. The average Al^{3+} concentration at WS1 was 72.1 mg/L compared to 162.3 mg/L at WS2. The maximum dissolved Al^{3+} concentrations in groundwater was measured at WS1 (299) and WS2 (1222 mg/L) at the beginning of the study period. This is due to the generation of pyrite oxidation products in the groundwater during drought periods, as a result of lowered groundwater tables and the exposure of pyrite to atmospheric oxygen.

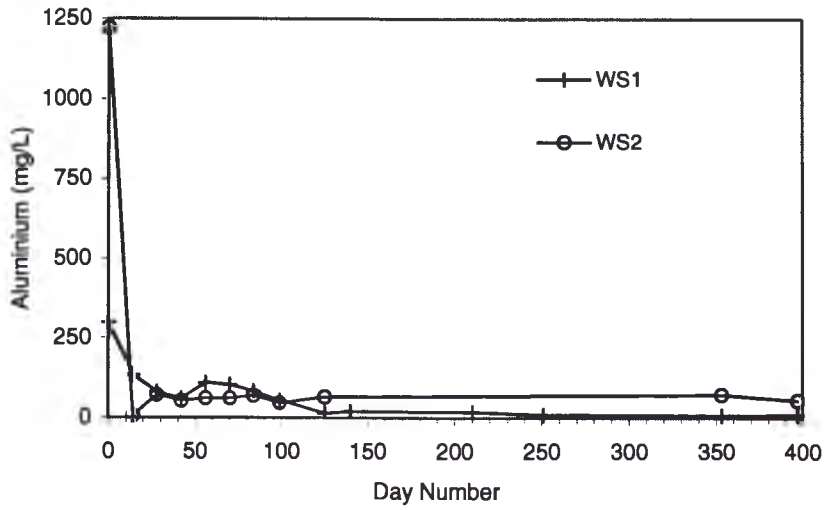

Figure 8.33: Dissolved inorganic monomeric Al^{3+} concentrations in groundwater at the Weir Sites

8.4.3.2 Iron concentrations

Total dissolved iron concentrations in groundwater at the floodgate sites are presented in Figure 8.34. Total Fe concentrations in the groundwater were similar between FG1 (87.5 mg/L) and FG2 (87.3 mg/L). The average total Fe concentrations in groundwater at FG3 and FG4 were 71.8 mg/L and 162.28 mg/L respectively. The total Fe concentration in groundwater at the floodgate sites was measured at FG3 (821 mg/L), due also to the entrainment of pyrite oxidation products in the groundwater as a result of drought conditions before and at the beginning of the study period.

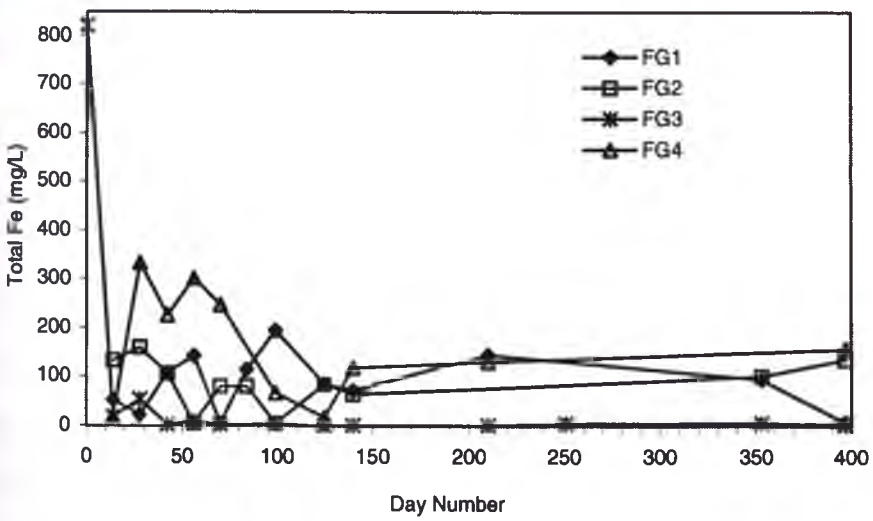

Figure 8.34: Total dissolved iron concentrations in groundwater at the Floodgate Sites

Total Fe concentrations in groundwater at the weir sites were greater than in the groundwater at the floodgate sites, shown in Figure 8.35, as a result of lowered groundwater tables and pyrite oxidation. The maximum total Fe concentration in groundwater at WS1 (365 mg/L) and at WS2 (435 mg/L) was measured at the beginning of the study period. In this respect, the concentration of total Fe in the groundwater at the weir sites follows the same trend as the dissolved Al^{3+} concentration in the groundwater.

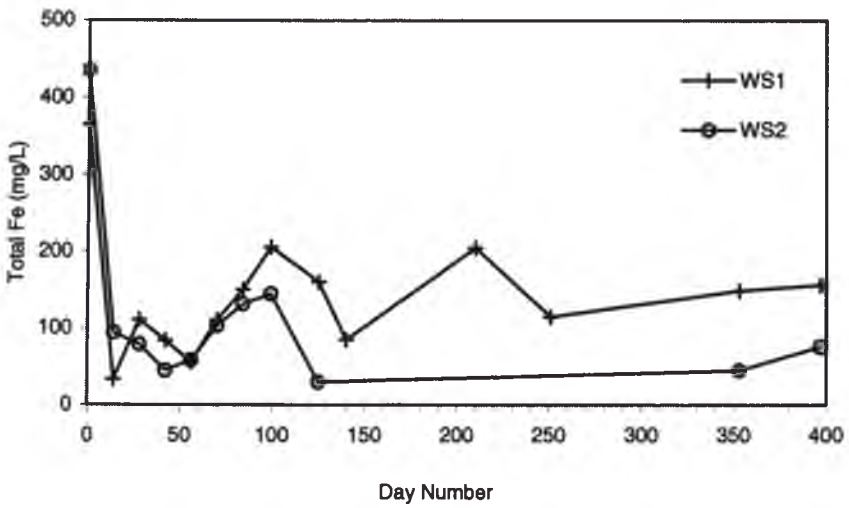

Figure 8.35: Total dissolved iron concentrations in groundwater at the Weir Sites

8.4.4 Basic cation concentrations

The dissolution of marine clays can liberate basic cations such as calcium and magnesium. The temporal and spatial variability in the concentration of these basic cations in groundwater at the floodgate and weir sites is described in the following section.

8.4.4.1 Calcium concentrations

Figure 8.36 shows the concentration of soluble calcium in the groundwater at the floodgate sites. It can be seen that the concentration of Ca^{2+} in groundwater at FG1 was greater than measured at the other floodgate sites. The average Ca^{2+} in groundwater at FG1 was 200.9 mg/L compared with 127.6 mg/L, 118.7 mg/L and 89.8 mg/L at FG2, FG3 and FG4 respectively. The maximum soluble calcium

concentration in groundwater at the floodgate sites was measured at FG1 (284 mg/L), whereas the lowest Ca^{2+} concentration in groundwater was measured at FG4 (22 mg/L). Soluble Ca^{2+} in groundwater at FG2 and FG4 decreased on Day 125 as a result of flushing of the groundwater due to rainfall.

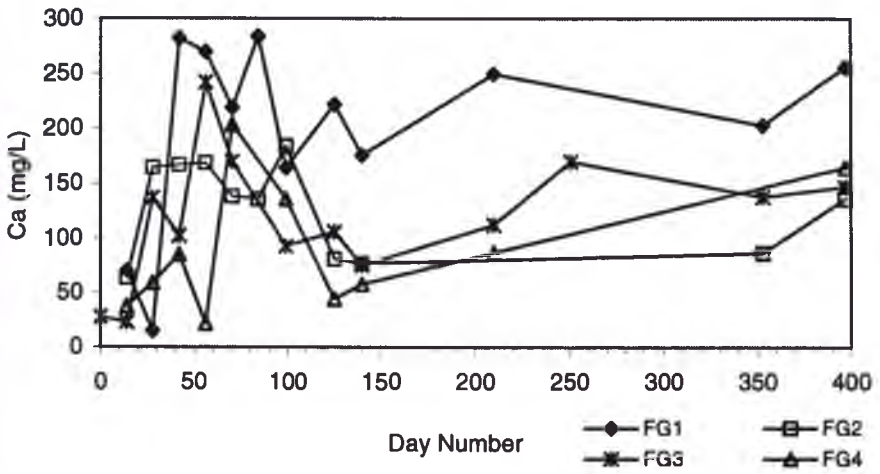

Figure 8.36: Soluble calcium concentrations in groundwater at the Floodgate Sites

The concentration of Ca^{2+} in groundwater was greater at WS1 than at WS2, as shown in Figure 8.37. The average Ca^{2+} concentration in groundwater at WS1 was 76.5 mg/L compared with 30.5 mg/L at WS2. The maximum soluble calcium concentration in groundwater was measured at WS1 (200 mg/L), as a result of saline intrusion.

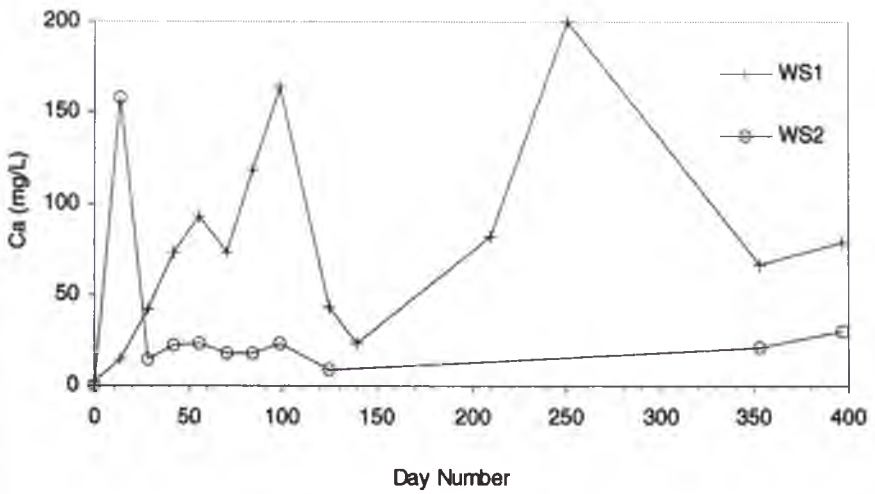

Figure 8.37: Soluble calcium concentrations in groundwater at the Weir Sites

8.4.4.2 Magnesium concentrations

Figure 8.38 shows the soluble magnesium concentration in groundwater at the floodgate sites. The average soluble Mg^{2+} concentration in groundwater ranged from 423.6 mg/L at FG3 to 1298.6 mg/L at FG4. The maximum soluble magnesium concentration in groundwater at the floodgate sites was measured at FG4 (8870 mg/L). The concentration of Mg^{2+} significantly declined in the groundwater on Day 42 at all floodgate sites. During the first 142 days of the study period, Mg^{2+} concentrations in the groundwater at all the floodgate sites fluctuated, however for the remainder of the study period Mg^{2+} concentrations were relatively stable. Fluctuations in the Mg^{2+} in the groundwater correspond to fluctuations in the electrical conductivity of the groundwater, showing that saline ingress has an influence on the concentration of Mg^{2+}.

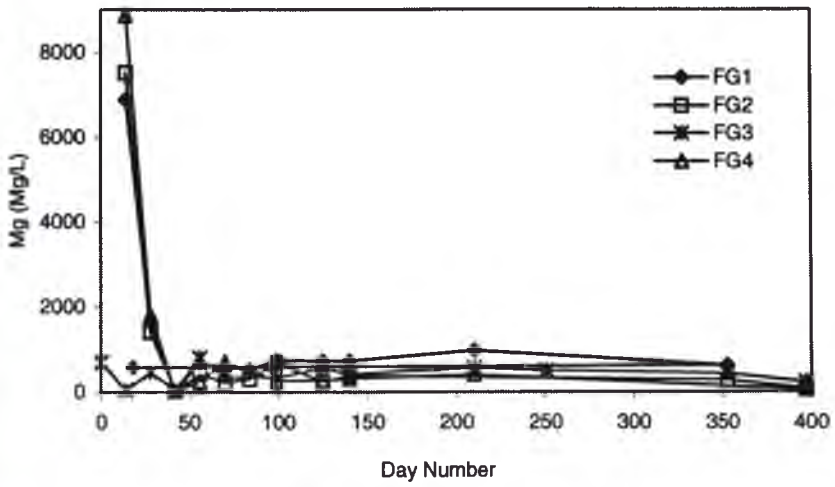

Figure 8.38: Soluble magnesium concentrations in groundwater at the Floodgate Sites

Generally, the soluble magnesium concentration in groundwater was greater at WS1, as shown in Figure 8.39. The maximum soluble magnesium concentration in groundwater was measured at WS1 (5820 mg/L). The average Mg^{2+} concentration in groundwater at WS1 was 861.3 mg/L compared with 118.9 mg/L at WS2. This high concentration is a result of the dissolution of clay minerals. The Mg^{2+} concentration in groundwater at both weir sites also declined on Day 42. A rainfall event on Day 42 may have flushed acidic runoff into the drain, discharging soluble Mg^{2+}.

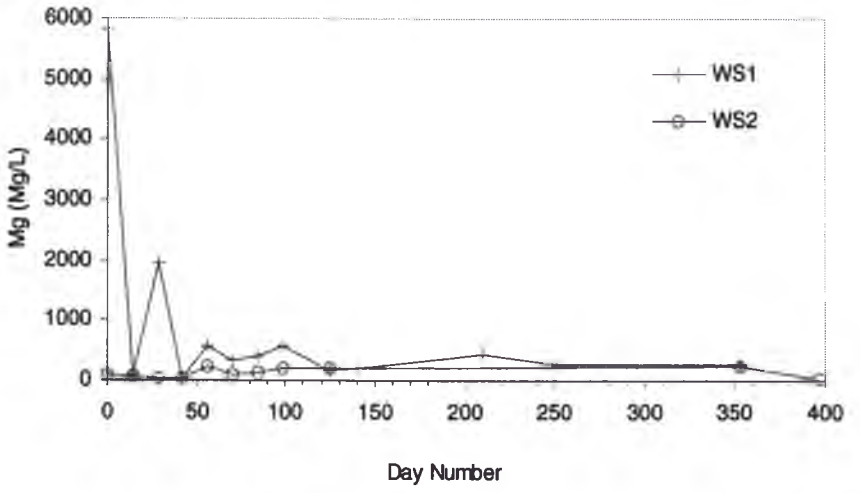

Figure 8.39: Soluble magnesium concentrations in groundwater at the Weir Sites

8.4.5 Anion concentrations

As previously mentioned, low concentrations of chloride in the groundwater at the floodgate and weir sites indicate the chloride that was present at the time of deposition of the pyrite and other estuarine clays has been removed from the soil as a result of freshwater flushing. High chloride concentrations can occur as a result of saline intrusion. Sulphate in groundwater is directly linked to pyrite oxidation.

8.4.5.1 Chloride concentrations

Dissolved chloride concentrations in groundwater at the floodgate sites are presented in Figure 8.40. The average soluble Cl^- concentration in groundwater ranged from 616.5 mg/L at FG4 to 7693 mg/L at FG1. High chloride concentrations were found in the groundwater at FG1 (8993 mg/L), due to its close proximity to the floodgate and salt water intrusion. The lowest soluble Cl^- concentration in groundwater was measured at FG4 (73.69 mg/L). Soluble Cl^- in the soil would have been leached into the drain as a result of freshwater flushing and the lack of saline intrusion into this flood mitigation drain would explain this low soluble Cl^- concentration.

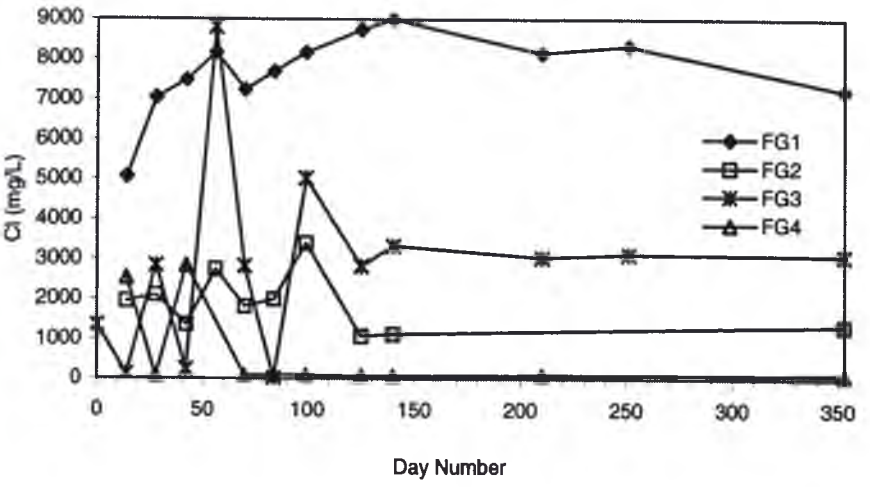

Figure 8.40: Dissolved chloride concentrations in groundwater at the– Floodgate Sites

Soluble Cl^- concentrations in groundwater at WS1 were significantly greater than concentrations measured in groundwater at WS2, as shown in Figure 8.41, indicating the influence of saline intrusion on the site. The average soluble Cl^- concentration in groundwater at WS1 was 3032 mg/L compared with 148.2 mg/L at WS2. The low Cl^- in the groundwater measured in this study was similar to that reported by Blunden (2000). The soluble Cl^- concentration in groundwater at WS2 was the lowest on Day 125 (45.6 mg/L) as a result of leaching of the Cl^- into the drain due to a rainfall event.

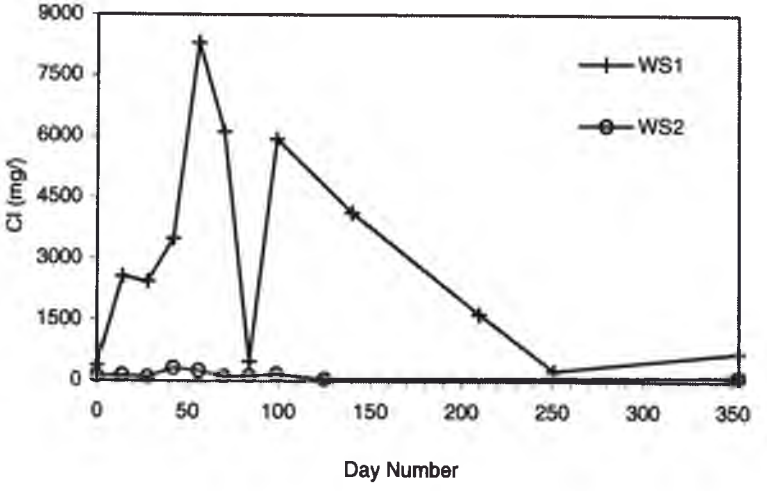

Figure 8.41: Dissolved chloride concentrations in groundwater at the Weir Sites

8.4.5.2 Sulphate concentrations

The concentration of dissolved sulphate was very high throughout the study period, as shown in Figure 8.42, with SO_4^{2-} concentrations between approximately 500 mg/L to 2350 mg/L. In the first 70 days, SO_4^{2-} concentrations in the groundwater at FG3 fluctuated between 490 mg/L and 1510 mg/L 470mg/L and between 1800 mg/L at FG4. After Day 70, SO_4^{2-} concentrations in groundwater at FG3 were stable at approximately 500 mg/L. Generally, dissolved sulphate concentrations were greater in the groundwater at FG1 than at the other floodgate sites. This is surprising since the groundwater was sampled close to the floodgate and would therefore be influenced by saline intrusion. The groundwater table at this site was however very low and below the pyrite layer on numerous occasions leading to pyrite oxidation. The maximum dissolved sulphate concentration in groundwater was measured at FG1 (2330 mg/L).

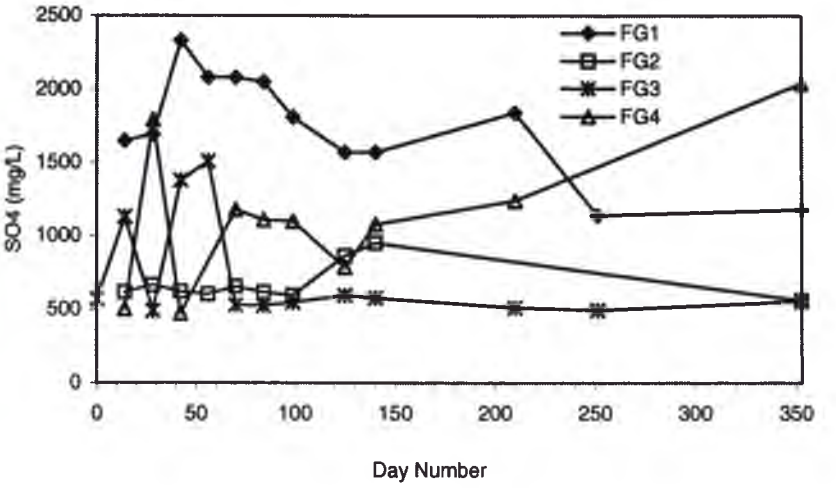

Figure 8.42: Dissolved sulphate concentrations in groundwater at the Floodgate Sites

Figure 8.43 shows the concentration of dissolved sulphate in the groundwater at the weir sites. The average SO_4^{2-} concentrations were 811 mg/L and 824 mg/L at WS1 and WS2 respectively. The maximum dissolved sulphate concentration in groundwater was measured at WS1 (1320 mg/L), as presented in Figure 8.43. The maximum SO_4^{2-} concentration in groundwater at WS2 was 1190 mg/L. These maximum SO_4^{2-} concentrations occurred at the beginning of the study period, when pyrite oxidation products were entrained in the groundwater as a result of drought conditions.

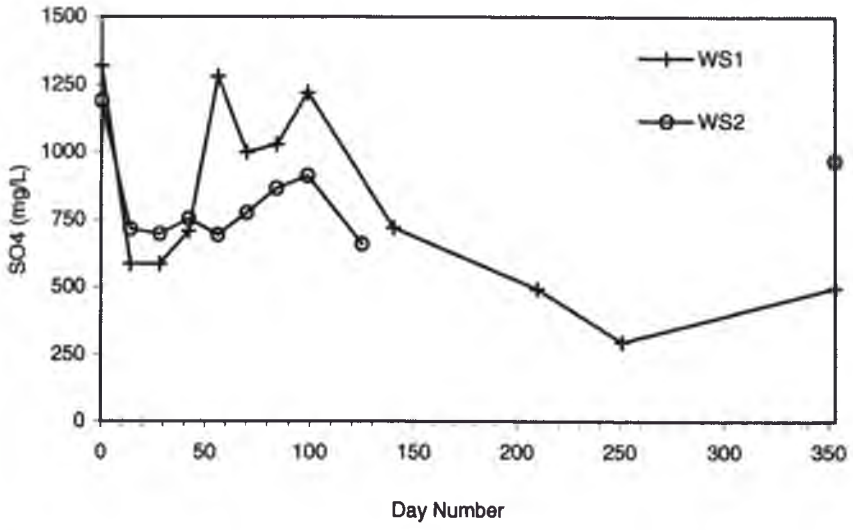

Figure 8.43: Dissolved sulphate concentrations in groundwater at the Weir Sites

8.4.5.3 Cl:SO_4

The chloride:sulphate (Cl:SO_4) ratio in the groundwater at the floodgate sites is shown in Figure 8.44. The low Cl:SO_4 ratio in the groundwater at FG4 compared to the other floodgate sites is due to the fact that this observation hole that was sampled at FG4 was further upstream from the floodgate and therefore less influenced by saline intrusion than the other groundwater samples. This also indicates pyritic oxidation. The Cl:SO_4 ratio in groundwater at FG1 and FG2 was above the suggested value of 2 (Mulvey, 1983) during the first 84 Days. The Cl:SO_4 ratio in groundwater at FG3 fluctuated above the below 2. It can be seen that climatic conditions also influenced the Cl:SO_4 ratio in groundwater, as the Cl:SO_4 ratio decreased during heavy rainfall.

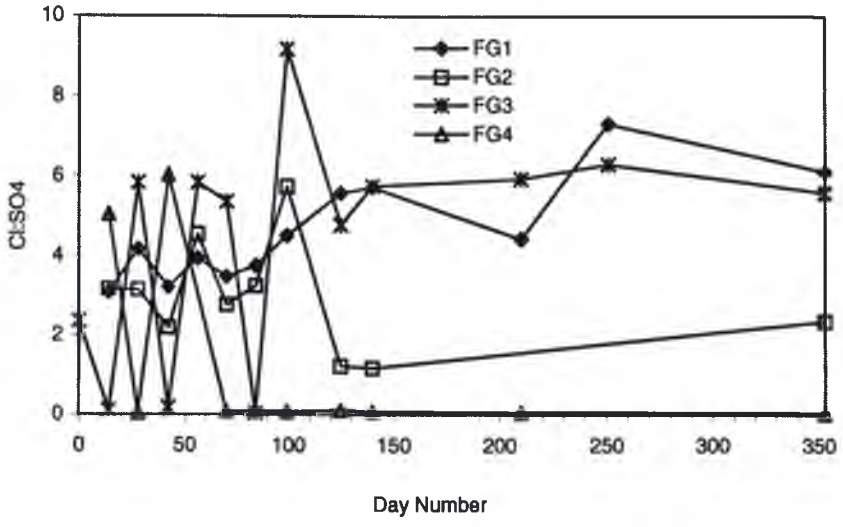

Figure 8.44: Chloride:sulphate ratio in groundwater at the Floodgate Sites

Figure 8.45 shows that the $Cl:SO_4$ ratio of the groundwater measured at the WS2 was always less than 1 during the study period. This is indicative of pyrite oxidation. The maximum and minimum $Cl:SO_4$ ratio in groundwater at WS2 was 0.42 on Day 42 and 0.07 on Day 125 respectively. The $Cl:SO_4$ ratio in the groundwater at WS1, which fluctuated throughout the study period, is significantly greater than the $Cl:SO_4$ ratio measured in the groundwater at WS2. This would be due to the influence of saline intrusion from the floodgate (FG1).

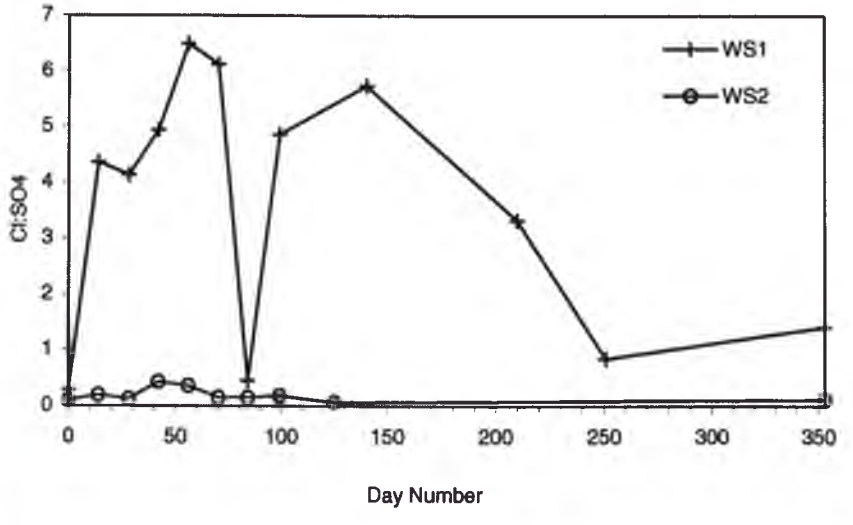

Figure 8.45: Chloride:sulphate ratio in groundwater at the Weir Sites

8.5 Conclusions

The groundwater quality data from the floodgate and weir sites showed that pyritic oxidation products were still being generated even though these acid sulphate soils management measures were in place. This indicates that acid and pyrite oxidation products, namely Al^{3+}, Fe^{2+} and SO_4^{2-}, generated before the floodgates and self-regulating tilting weir were installed are still entrained in the groundwater. Floodgates and weirs are aimed at treating the environmental effects of acid sulphate soils (high pH, iron and aluminium precipitation etc.) after they have occurred. Creek water, drain water and groundwater chemistry also showed that acidic conditions and that the water samples were in excess of the corresponding ANZECC (1992, 2000) criteria on most occasions throughout the study period. Water quality and the concentration of pyritic oxidation products fluctuated in response to climatic conditions, floodgate leakage and the dissolution of clay minerals.

A comparison between the Lime-fly ash barrier site and the floodgate and weir sites is presented in Chapter 9.

Chapter 9 Discussion and Comparison of results from the site of the Lime-fly ash Barrier and the Floodgate and Weir Study Sites

9.1 Introduction

The water quality results from the Lime-fly ash barrier study sites presented in Chapter 7 have shown the effectiveness of the alkaline barrier in reducing pyrite oxidation, and hence, the generation of pyritic oxidation products. However, the effectiveness of the Lime-fly ash barrier in the remediation of acid sulphate soils is not only assessed by monitoring water quality parameters at the barrier study site, but also by comparing these results with data collected from the other acid sulphate soils management measures in place in the Shoalhaven Floodplain, namely, floodgates and the self-regulating tilting weir. The Lime-fly ash barrier aims to prevent pyrite oxidation occurring and the generation of acidic water, whereas, floodgates and weirs are designed to treat the acidic water after it has been generated.

This Chapter outlines the results from all the study sites and compares the chemical water parameters measured at the Lime-fly ash barrier study site with the results from the floodgate and weir study sites.

9.2 Comparison between Lime-fly ash Barrier study Site and Floodgate/Weir Sites

Table 9.1 presents the results of the water quality-monitoring regime at the study sites. Averages for pH, Electrical conductivity (EC), acidic cations (Al^{3+} and Fe^{total}), basic cations (Ca^{2+} and Mg^{2+}) and anions (Cl^- and SO_4^{2-}) are outlined.

Table 9.1: *Comparison between water quality parameters measured at the Lime-fly ash Barrier Study Site and those measured at the Floodgate and Weir Study Sites*

Study Site	pH	EC (mS)	Al^{3+} (mg/L)	Total Fe (mg/L)	Ca^{2+} (mg/L)	Mg^{2+} (mg/L)	Cl^- (mg/L)	SO_4^{2-} (mg/L)	$Cl:SO_4$
Lime-fly ash Barrier Study Site									
Average groundwater (all observation holes)									
Pre-barrier:	3.28	2.34	35.68	67.59	41.15	158.49	747.24	440.13	1.39 (0.38*)
Post-barrier:	3.86	1.46	20.05	37.03	40.70	80.66	195.47	253.31	0.80
Average groundwater (barrier influenced)									
Pre-barrier:	3.74	2.62	35.66	71.68	42.77	181.23	718.8	534.88	1.10 (0.55*)
Post-barrier:	3.84	1.53	18.97	41.49	45.43	80.47	191.96	240.21	0.79
Lords drain upstream									
Pre-barrier:	3.40	5.92	33.96	107.28	50.05	230.30	2700.01	608.182	3.35
Post-barrier:	3.16	1.22	18.60	41.30	35.80	92.15	107.552	114	0.94
Lords drain middle									
Pre-barrier:	3.46	5.32	30.75	208.08	66.36	268.68	3120.2	739.67	3.09
Post-barrier:	3.59	1.20	6.25	44.60	47.10	92.20	121.16	134	0.90
Lords drain downstream									
Pre-barrier:	3.15	5.63	32.23	147.81	72.52	312.02	3139.11	695.909	3.39
Post-barrier:	3.47	1.40	8.50	7.70	47.95	106.34	399.76	367	1.08
Lords drain average									
Pre-barrier:	3.35	5.42	27.29	141.80	58.38	224.91	2912.63	682.03	3.06
Post-barrier:	3.25	1.39	29.15	109.63	52.17	210.92	209.49	205.00	0.98
FG1									
Creek water	6.56	12.10	10.02	5.01	150.2	1004.4	6561.9	960	6.8
Drain water	6.05	13.88	16.57	30.2	163.3	1015.2	6707.9	1088	5.7
Groundwater	4.78	15.60	21.9	87.5	200.9	1230.4	7693	1749	4.6

FG2									
Creek water	6.9	13.433	9.36	7.48	170.76	1292.8	8600.5	1299	6.7
Drain water	5.13	11.126	12.7	87.7	147.05	566.9	7445	1311	5.6
Groundwater	5.13	4.18	11.13	87.3	127.59	1053.4	1072.9	676	2.95
FG3									
Creek water	6.90	17	16.038	19.45	166.4	1338.8	7746.6	1221	6.58
Drain water	5.19	13.49	20.514	15.75	161.2	571.7	5899	1102	5.4
Groundwater	6.48	7.93	55.3	71.8	118.7	423.7	2827.2	725	4.4
FG4									
Creek water	6.19	18.2	4.4	8.07	167.01	2080.1	8057	1231	6.52
Drain water	5.58	14.96	28.738	52.5108	105.08	1222	6217	1066	5.32
Groundwater	4.19	1.95	74.9	162.28	89.8	1298.6	616.5	1131	1.17
WS1									
Drain water	3.30	7.51	27.5	91.18	83.4	325.8	3252.5	773	3.73
Groundwater	3.54	6.93	72.1	142.16	76.5	861.25	3032	811	3.57
WS2									
Drain water	5.23	0.63	22.6	51.8	21.5	1173	96.89	140	1.61
Groundwater	3.51	1.77	162.31	112.9	30.5	118.89	148.2	824	0.186

* Average calculation does not include concentration measured on sampling days heavily influenced by rainfall/flooding.

9.2.1 pH

The average groundwater pH (measured in all the observation holes) at the site of the lime-fly ash barrier during the pre-barrier period (3.86) is greater than the average groundwater pH measured at WS1 (3.54) and WS2 (3.51). This shows that the lime-fly ash barrier is more effective in reducing groundwater acidity than the self-regulating tilting weir. The groundwater pH at WS1 was expected to be lower than the average groundwater pH at the site of the lime-fly ash barrier; due to the fact that WS1 does not have an acid sulphate soils management measure installed on the site (a weir is being installed at this site). The average groundwater pH, measured in those observation holes closer to the barrier (3.84), is also greater than the groundwater pH at WS1 and WS2. The average groundwater pH measured at all the floodgates sites is greater than observed in the groundwater at the lime-fly ash barrier site. These floodgate sites are subjected to saline intrusion, which would lead to an increase in the pH of the groundwater, particularly in groundwater close the floodgate (pH 6.48 – FG3).

The average drain water pH measured adjacent to the site of the lime-fly ash barrier (3.59) is greater than the drain water pH measured at WS1 (3.30) indicating that the barrier was successful in reducing drain water pH compared to a site with no acid sulphate soils remediation measure installed. The post-barrier average drain water pH downstream of the lime-fly ash barrier site (3.47) is less than the average drain water pH measured at the floodgate (FG1 – 6.05, FG2 – 6.9, FG3 – 6.9, FG4 – 6.19) and weir sites (WS1 – 3.3, WS2 – 5.23). The average drain water pH values at the floodgate sites show the role of the floodgates in increasing the pH of drain water by allowing brackish water into the drains. As mentioned in Chapter 7, acid sulphate soils affected areas upstream of the lime-fly ash barrier study site discharge acidic water downstream. The low average drain water pH at WS1 and WS2 is due to acidic groundwater leaching into the drain.

Even though the data shows that the floodgates are successful in increasing groundwater and drain water pH, the installation of floodgates are restrictive in low-lying areas, as further increases in groundwater table elevation would create

accessibility and farming problems due to the inundation of surrounding land. The lime-fly ash barrier can be installed in these low-lying areas.

9.2.2 Electrical Conductivity

Table 9.1 shows that the average post-barrier groundwater electrical conductivity (EC) (measured in all the observation holes) at the site of the lime-fly ash barrier (1.46 mS) was less than the average EC in groundwater at the floodgate and weir sites. The average pre-barrier groundwater EC was, however, low compared to the EC measured at the FG1, FG2, FG3 and WS1. The low EC in groundwater during the pre-barrier period at the lime-fly ash barrier study site is a result of freshwater flushing of the groundwater and the lack of saline intrusion. The average post-barrier groundwater EC at FG1 (15.60 mS) was significantly greater than the average groundwater EC at the lime-fly ash barrier site, due to its close proximity to the floodgate and the influence of saline intrusion as a result of floodgate leakage.

High EC values in groundwater are not only due to saline intrusion but also by the generation of pyrite oxidation products in groundwater. WS2 was dominated by freshwater flushing, like the site of the lime-fly ash barrier. The average groundwater EC at WS2 was (1.77 mS) compared to 1.46 mS at the lime-fly ash barrier study site. This shows that the alkaline barrier has been effective in reducing pyrite oxidation and the generation of pyrite oxidation products. The average groundwater EC at FG4 (1.95) is only slightly greater than the groundwater EC at the lime-fly ash barrier site. Water quality parameters were measured in an observation hole further upstream from the floodgate, compared to monitoring at the other floodgate sites. This may explain the lower average EC in the groundwater.

The average post-barrier EC in drain water downstream of the lime-fly ash barrier (1.40 mS) was also less than the average EC in drain water at the floodgate and weir sites. The average drain water EC downstream during the pre-barrier period was 5.63 mS. This shows that the concentration of pyrite oxidation products in the drain water has decreased as a result of the lime-fly ash barrier and in turn led to a decrease in EC.

9.2.3 Acidic cation concentrations

A comparison of the concentration of acidic cations, such as Al^{3+} and Total Fe, in surface and groundwater at the site of the lime-fly ash barrier and the floodgate and weir sites is necessary to determine the effectiveness of the barrier in reducing pyrite oxidation and the production of these acidic cations.

9.2.3.1 Aluminium concentrations

The average groundwater aluminium concentration (measured in all the observation holes) at the lime-fly ash barrier site (20.05 mg/L) was significantly less than the average aluminium concentration measured at FG3 (55.3 mg/L), FG4 (74.9 mg/L), WS1 (72.1 mg/L) and WS2 (162.31 mg/L). This shows that the lime-fly ash barrier is more effective in hindering pyrite oxidation and reducing the concentration of dissolved aluminium in the groundwater than the floodgates and the self-regulating tilting weir. The barrier treats acid sulphate soils and their related environmental problems before they occur, whereas, the floodgates treat the aluminium after it has been generated and the weir entrains the pyrite oxidation products in the groundwater.

The average aluminium concentration in the groundwater at the lime-fly ash barrier site was only slightly less than the average groundwater concentration at FG1 (21.9 mg/L). Again, this relatively low (compared to the other floodgate sites) aluminium concentration may be due to saline intrusion in the groundwater at FG1 as a result of its close proximity to the leaky floodgate. The average aluminium concentration in groundwater at FG2 (11.13 mg/L) was significantly less than the average at the lime-fly ash barrier site. As mentioned in Chapter 8, salt water was allowed to flow into the flood mitigation drain at FG2 during the study period because of a drainpipe leading from the drain to Broughton Creek. The average EC of the creek water, which leached into the drain, at FG2 (13.43 mS) was greater than the average creek water EC at FG1 (12.10 mS). While saline intrusion also influenced the concentration of aluminium in the groundwater at FG1, EC concentrations in the drain at FG1 fluctuated, indicating open/closed floodgate periods.

The average aluminium concentration in drain water downstream of the lime-fly ash barrier site during the post-barrier period (8.50 mg/L) is less than the average

concentrations of aluminium in drain water at the floodgate and weir sites. This also shows the effectiveness of the barrier in reducing the generation of pyrite oxidation products.

9.2.3.2 Iron concentrations

The average post-barrier total Fe concentration in groundwater (average of all the observation holes sampled) at the lime-fly ash barrier site (37.03 mg/L) was less than at the other sites. The average groundwater total iron concentrations at FG1, FG2, FG3, FG4, WS1, and WS2 were 87.5 mg/L, 87.3 mg/L, 71.8 mg/L, 162.28 mg/L, 142.16 mg/L and 112.9 mg/L) respectively. Pre-barrier total Fe concentrations were also below the total iron concentrations in groundwater at the floodgate and weir site, showing that high groundwater total iron concentrations at these sites persist. Since the barrier was installed this concentration in the groundwater at the lime-fly ash barrier study site has decreased by almost 50%, indicating that the lime-fly ash barrier, unlike the floodgates and weir, reduces pyrite oxidation and hence the concentration of iron in the groundwater. This decrease in total iron in the groundwater would in turn reduce the effect of acidic water leaching into the drain and have a detrimental effect on aquatic fauna.

The average total iron concentration in drain water downstream of the lime-fly ash barrier site (7.70 mg/L) is significantly lower than the average drain water total iron concentrations at the floodgate and weir sites, particularly WS1 (142.16 mg/L). Again, this shows that the concentration of pyrite oxidation products in groundwater leaching into the flood mitigations drain were reduced as a result of the barrier hindering pyrite oxidation. The average total iron concentrations in drain water at FG1 (30.2 mg/L) and FG3 (15.75 mg/L), which were lower than the concentrations at FG2 and FG4, are a result of frequent periods of saline intrusion during the study period because of floodgate leakage. This shows that the modified floodgates are effectual in reducing the concentration of pyrite oxidation products in flood mitigation drains in acid sulphate soils areas.

9.2.4 Basic cation concentrations

The concentration of calcium and magnesium in surface waters and groundwater is an indication of the relative influence of saline intrusion. A comparison of the concentrations of Ca^{2+} and Mg^{2+} in the groundwater and drain water at the lime-fly ash barrier site and the floodgate/weir sites is described in the following section.

9.2.4.1 Calcium

Average dissolved Ca^{2+} concentrations in the groundwater (average of all the observation holes sampled) at the lime-fly ash barrier sites during both the pre- and post-barrier period, 41.15 mg/L and 40.70 mg/L respectively, were less than the average Ca^{2+} concentrations measured in the groundwater at FG1 (200.0 mg/L), FG2 (127.59 mg/L), FG4 (118.7 mg/L), FG4 (89.8 mg/L) and WS1 (76.5 mg/L). The high concentration of dissolved Ca^{2+} in groundwater at the floodgate sites and WS1 may be derived from the dissolution of clay minerals coupled with saline intrusion. The slight decrease in Ca^{2+} concentrations in the groundwater in the post-barrier may be a result of the barrier reducing the dissolution of these clay minerals. However, as mentioned by Blunden (2000), high concentrations of Al^{3+} may exchange with Ca^{2+} from the cation exchange site and release Ca^{2+} into solution. The average concentration of Al^{3+} in groundwater at the lime-fly ash barrier site had lowered during the post-barrier period, lending to this trend.

The average dissolved Ca^{2+} concentration in the groundwater at the lime-fly ash barrier site was, however, greater than the average Ca^{2+} concentration in the groundwater at WS2 (30.5 mg/L). Due to the self-regulating tilting weir the groundwater at WS2 may be subjected to greater rates of freshwater flushing, compared to the site of the lime-fly ash barrier.

The average post-barrier Ca^{2+} concentration in drain water downstream of the lime-fly ash barrier site (47.95 mg/L) is significantly less than the average Ca^{2+} concentrations in drain water at the floodgate (FG1 – 163.3 mg/L, FG2 – 147.05 mg/L, FG3 – 161.2 mg/L, FG4 – 105.08 mg/L) and WS1 (83.4 mg/L). These high Ca^{2+} concentrations in the drain water at the floodgate sites are due to brackish water flowing into the drains via the floodgates. The average Ca^{2+} concentration in drain water at WS1 is slightly

less than the concentrations at the floodgate sites, as the sampling point is located further upstream from FG1. The average Ca^{2+} concentration in drain water at WS2 (21.5 mg/L) is less than the average post-barrier Ca^{2+} concentration in drain water downstream of the lime-fly ash barrier site. The self-regulating tilting weir raises the groundwater table, and hence, entrains the cations generated as a result of pyrite oxidation within the groundwater. This illustrates that the weir is effective in reducing the concentration of pyrite oxidation products in the drain water.

9.2.4.2 Magnesium

Average Mg^{2+} concentrations were significantly less in the groundwater at the lime-fly ash barrier study site during the pre- and post-barrier period, 158.49 mg/L and 80.66 mg/L respectively, compared to average Mg^{2+} concentrations in the groundwater at the floodgate (FG1 – 1230.4 mg/L, FG2 – 1053.4 mg/L, FG3 – 423.7 mg/L, FG4 – 1298.6 mg/L) and weir sites (WS1 – 861.25 mg/L, WS2 – 118.89 mg/L) during both the pre- and post-barrier period. High concentrations at the floodgate sites are due to saline intrusion via the floodgates.

The average concentration of Mg^{2+} in the drain water downstream of the lime-fly ash barrier site (106.34 mg/L) is significantly less than the average concentrations in the drain water at the floodgate (FG1 – 1015.2 mg/L, FG2 – 566.9 mg/L, FG3 – 571.7 mg/L, FG4 – 1222 mg/L) and weir sites (WS1 – 325.8 mg/L, WS2 – 1173 mg/L). The lower average concentrations of Mg^{2+} in the drain water downstream of the lime-fly ash barrier site is an indication of freshwater flushing, compared to saline intrusion at the floodgate sites. The lime-fly ash barrier also reduces the dissolution of clays and hence the release of Mg^{2+} into solution. The self-regulating tilting weir (WS2 – 1173 mg/L) also entrains Mg^{2+} cations in the groundwater.

9.2.5 Anion concentrations

9.2.5.1 Chloride concentrations

Average chloride concentration in the groundwater (average of all the observation holes sampled) at the lime-fly ash barrier site during the post-barrier period (195.47 mg/L) was significantly lower than chloride concentrations in the groundwater at the

floodgate (FG1 – 7693 mg/L, FG2 – 1072.9 mg/L, FG3 – 2827.2 mg/L, FG4 – 616.5 mg/L) and WS1 (3032 mg/L). The low average Cl^- concentration in the groundwater indicates that Cl^- has been and is continually being removed by freshwater flushing. This low average concentration also shows that there was little saline intrusion from Broughton Creek via the floodgate at the end of the drain (FG1). This in turn indicates that the high average Cl^- concentration in groundwater at the floodgates results from saline intrusion. The average chloride concentration of the groundwater at WS2 (148.2 mg/L) was less than the average concentration in the groundwater at the lime-fly ash barrier site. This may also be a result of freshwater flushing.

The average post-barrier Cl^- concentration downstream of the lime-fly ash barrier site (399.76 mg/L) was less than the average drain water Cl^- concentration at the floodgate sites (FG1 – 6707.9 mg/L, FG2 – 7445 mg/L, FG3 – 5899 mg/L, FG4 – 6217 mg/L) and WS1 (3252.5 mg/L), indicating the role of the floodgates in allowing salt water into the flood mitigation drains. Again, the average Cl^- concentration in the drain water at WS2 (96.89 mg/L) was less than the average concentration in the drain water downstream of the lime-fly ash barrier site, also possibly as a result of freshwater flushing.

9.2.5.2 Sulphate Concentrations

Dissolved sulphate concentrations in the groundwater at the lime-fly ash barrier site were consistently less than those average sulphate concentrations measured in the groundwater at the floodgate and weir study sites. The average groundwater sulphate concentration, during the post-barrier period, at the site of the lime-fly ash barrier was 253.31 mg/L compared to 1749 mg/L, 676 mg/L, 725 mg/L and 1131 mg/L at FG1, FG2, FG3 and FG4 respectively. The lime-fly ash barrier reduces pyrite oxidation and the generation of pyrite oxidation products, whereas the floodgates treat the acidic groundwater after it has been generated.

The average post-barrier SO_4^{2-} concentration in drain water downstream of the lime-fly ash barrier site (367 mg/L) is also considerably less than the average SO_4^{2-} concentration in drain water at the floodgate sites (FG1 – 1088 mg/L, FG2 – 1311 mg/L, FG3 – 1102 mg/L, FG4 – 1066 mg/L). These high average SO_4^{2-}

concentrations indicate that pyrite oxidation continues to occur at the floodgate sites and acidic groundwater produced leaches into the flood mitigation drains. Saline water from Broughton Creek also contributes to this due to the high concentration of dissolved sulphate in seawater.

The average SO_4^{2-} concentration in the drain water at WS2 (140 mg/L) is less than the post-barrier concentration in drain water downstream of the site of the lime-fly ash barrier, indicating that SO_4^{2-} anions are entrained in the groundwater as a result of the high groundwater table caused by the self-regulating tilting weir.

9.2.5.3 Cl:SO_4

The average Cl:SO_4 in the groundwater at the lime-fly ash barrier site, during the post-barrier period, is less than the average Cl:SO_4 at the floodgate sites (FG1 – 4.6, FG2 – 2.95, FG3 – 4.4, FG4 – 1.17) and WS1 (3.57). This is expected though due the high chloride concentrations in the groundwater at the floodgate sites, as a result of saline intrusion. The post-barrier average Cl:SO_4 in the groundwater at the lime-fly ash barrier site is, however, greater than the average Cl:SO4 at WS2 (0.186). This again shows that the lime-fly ash barrier is more effective in reducing pyrite oxidation than the self-regulating tilting weir. The weir regulates the groundwater table and submerges the pyrite layer. However, acid is still formed due to biotic oxidation of pyrite. The lime-fly ash barrier has two roles. The first role is to reduce oxygen from reaching the pyrite layer, and hence, reducing pyrite oxidation. The second role is to neutralise the acidity in the groundwater and halt biotic oxidation.

The average post-barrier drain water Cl:SO_4 downstream of the lime-fly ash barrier site (1.08) is greater than the drain water Cl:SO_4 at WS2, indicating again that the barrier reduces pyritic oxidation and in turn the leaching of acidic groundwater into the drainage system. The role of the floodgates in increasing the drain water Cl:SO_4 is shown at WS1. The average drain water Cl:SO_4 at WS1 was 1.61 due to saline intrusion and an increase in the concentration of Cl^- in the drain water.

9.3 Conclusions

The Lime-fly ash barrier is effective in remediating acid sulphate soils in areas in which floodgates and weirs cannot be installed. A comparison of the result shows that the lime-fly ash barrier had greater success in increasing the groundwater pH than the self-regulating tilting weir. At this weir site, a significant amount of acid groundwater is still being produced due to biotic oxidation of the pyrite layer. Saline intrusion at the floodgate sites increases the groundwater and drain water pH, electrical conductivity (EC) and chloride concentration, illustrating the role of the modified floodgates in treating acidic water generated by the acid sulphate soils through saline intrusion. The EC of the groundwater at the lime-fly ash barrier study was signicantly reduced as a result of decreased production of pyrite oxidation products during the post-barrier period.

As mentioned, the lime-fly ash barrier treats acid sulphate soils and the related environmental problems before they occur, whereas, the floodgates treat the pyrite oxidation products generated after they have been discharged into the flood mitigation drains. Significantly greater concentrations of Al^{3+}, Fe^{total} and SO_4^{2-} were found in the groundwater at the floodgate sites. The self-regulating titling weir also entrains these pyrite oxidation products in the groundwater.

Chapter 10 Conclusions and Recommendations

10.1 Summary and Conclusions

This study was undertaken to introduce a novel alternative practical solution to the remediation of acid sulphate soils in low-lying areas. Prior to this research, the use of subsurface lime-fly ash barriers in the mitigation of acid sulphate soils and biotic oxidation of pyrite had not been thoroughly investigated. The effectiveness of the use of a lime-fly ash barrier for the management of acid sulphate soils was validated by this research study, which incorporated:

- The installation and the analysis of the effectiveness of a lime-fly ash barrier adjacent to a flood mitigation drain at a study site near Berry on the southeastern coast of NSW.

- Groundwater and surface water quality monitoring of lime-fly ash barrier site was undertaken with comparisons with water quality from sites mitigated through the use of modified floodgates and a self-regulating tilting weir. The effect of the lime-fly ash barrier on the groundwater and surface water quality was determined by testing for the following water quality parameters:
    - pH
    - Cl^- and SO_4^{2-} concentrations
    - The presence of Fe^{2+}, Al^{3+}, Ca^{2+} and Mg^{2+} ions.

- Laboratory and field-testing of the lime-fly ash slurry was undertaken. Varying lime-fly ash slurry ratios were tested to decide on the most appropriate viscosity and ratio of constituents to be used in the preliminary injection trials.

- Preliminary injections at the study site were undertaken and the Lime-Fly Ash Barrier was installed. Practical limitations of the in-situ injection process were determined and the results of the preliminary injections at the study site were used to make alterations to the proposed methods involved in the final installation of the barrier.

- Continued post-barrier water quality monitoring of the groundwater and surface waters at the lime-fly ash barrier site, floodgate sites and the site of the self-regulating tilting weir.

This research has demonstrated the effectiveness of the installation of a lime-fly ash barrier in remediating acid sulphate soils. The creation of a temporary perched water table at the site of the lime-fly ash barrier site reduced the exposure of the pyritic soil layer to atmospheric oxygen, and hence, reduced pyrite oxidation and the generation of acidic oxidation products.

The decrease in the concentration of pyritic oxidation products in the groundwater and surface waters at the lime-fly ash site is not only due to the temporary perched water table, but also as a result of the alkaline barrier neutralising groundwater acidity. During the pre-barrier period, groundwater and drain water quality indicated a highly acidic environment with average pH values of 3.28 in the groundwater and 3.35 in the drain water. The concentration of dissolved inorganic monomeric aluminium, total dissolved iron and dissolved sulphate in the groundwater at the lime-fly ash barrier site were consistently above the appropriate ANZECC (1992, 2000) guidelines. These high concentrations of acidic cations and anions are a result of falling groundwater tables and biotic oxidation.

After the installation of the lime-fly ash barrier, a substantial improvement in groundwater and surface water quality was observed. Groundwater pH increased from the average of 3.28 to average values between 4.5 and 5.5. Some variation in the groundwater pH and concentration of pyrite oxidation products is expected in the observation holes at the site of the lime-fly ash barrier site as a result of the fluctuating groundwater table. However, this variation would be of a temporary nature.

The concentration of the pyritic oxidation products, acidic cations Al^{3+} and Fe^{total}, basic cations Ca^{2+} and Mg^{2+} and anions Cl^- and SO_4^{2-}, also, on average decreased in the groundwater after the installation of the lime-fly ash barrier. The $Cl^-:SO_4^{2-}$ in the groundwater varied at the study site, however, on average the $Cl^-:SO_4^{2-}$ increased

slightly as a result of the alkaline barrier. This shows the effectiveness of the lime-fly ash barrier in reducing pyrite oxidation. Average drain water Al^{3+} and Fe^{total} concentrations also decreased downstream of the lime-fly ash barrier study site. This would reduce the effect of this drain water on the estuarine environment when flushed into Broughton Creek. Groundwater and surface water quality results during the pre- and post-barrier period varied at the site of the lime-fly ash barrier in conjunction with climatic factors.

The total area of acid sulphate soils to be remediated as a result of the installation of the lime-fly ash barrier is expected to be greater than 200sqm, with improvements to the flood mitigation drain adjacent to the site of the lime-fly ash barrier (Lords drain) (in regards to pH, Fe^{total} and Al^{3+}) also expected downstream of the site. Other improvements that would be expected include:

- A reduction in the intensity of acid discharge events;
- A reduction in the formation of iron oxides in the drain; and
- A possible reduction in weed infestation in the drain.

The role of the lime-fly ash barrier in managing acid sulphate soils is very different to the roles of the modified floodgates and the self-regulating tilting weir. The aims of the alkaline barrier are to reduce pyrite oxidation by providing a cut off and reduced permeability of the soil directly above the pyrite layer, and to neutralise groundwater acidity previously generated. The aim of the modified floodgates is to demonstrate the effectiveness of tidal buffering in reducing drain water acidity and the concentration of pyrite oxidation products. The self-regulating tilting weir aims to maintain the groundwater table at or above the pyrite layer, therefore, reducing the hydraulic gradient between the drain and the phreatic zone.

These varying roles show that the lime-fly ash barrier is designed to regulate the generation of acidic groundwater before it occurs in acid sulphate soils, whereas the modified floodgates and self-regulating tilting weir treat the acidity after it has been generated. Due to this, groundwater and surface water quality differs between these acid sulphate soils remediation measures. The lime-fly ash barrier had greater success in increasing the groundwater pH and decreasing the concentration of pyrite oxidation

products in the groundwater than the self-regulating tilting weir. The lime-fly ash barrier reduces pyrite oxidation and the generation of dissolved aluminium and total iron, whereas the weir entrains these products within the groundwater. Also, despite the elevated groundwater table at the self-regulating tilting weir, a significant amount of acid is still being formed and the concentration of dissolve aluminium and total iron remain high as a result of the dissolution of clays and the aluminium cation exchange reaction. The modified floodgates reduce the concentration of these oxidation products within the drain as a result of tidal buffering. Groundwater and surface water quality results varied at all the floodgate sites as a result of climatic factors and the efficiency of the floodgate seal.

This research has enabled the novel installation of a lime-fly ash barrier in areas where the use of floodgates and weirs is impractical, and demonstrated this technique as a novel effective ground improvement method. The lime-fly ash barrier has reduced the resulting acid and high concentrations of metals that enter the waterways and affect the fisheries industries.

Knowledge gained as a result of this research includes:

- An understanding of the theory (grouting theory) behind the installation of the lime-fly ash barrier and the role of injection pressures and viscosity.

- Knowledge of the techniques involved in grouting and the practical limitations of the in-situ injection process.

- An understanding of role of lateral permeability and hydraulic fracturing during the injection process.

- A thorough understanding of the surface and groundwater quality implications as a result of the installation of the lime-fly ash barrier.

10.2 Recommendations for further research

10.2.1 Numerical modelling

This research has shown the effectiveness of a lime-fly ash barrier in remediating acid sulphate soils affected areas and reducing the environmental effects on the estuarine environment. The results obtained from this research can be used for further study in the management of acid sulphate soils. To simulate the impact of lateral alkaline barriers in subsurface conditions, a finite element model could be constructed incorporating the lime injection process, the rate of lateral diffusion of lime, assessment of possible hydraulic fracturing of clay and the optimum thickness of the barrier to name a few.

The study of acid sulphate soils and the use of sub-surface lime-fly ash barriers could incorporate numerical analysis coupled with laboratory and field-testing in order to:

- Simulate the installation of a lime-fly ash barrier in acid sulphate soils areas and the resultant impacts on groundwater and surface water quality.

- The best possible 'fracture plane-fluid flow' relationships for the site soil conditions.

- Determine the role of lateral soil during the slurry injection process.

- Simulate the longevity of the alkaline barrier based on geo-chemical reactions and flow rates.

- Test the reaction of the groundwater with the barrier, life of barrier, reaction of groundwater with the barrier, varying thickness of the barrier

10.2.2 Field Investigations

Coupled application: The application of lime-fly ash barriers in conjunction with permeable reactive barriers is also another potential acid sulphate soil management option that could be investigated.

This research and previous research into the use of permeable reactive barriers have varying degrees of effectiveness in remediating acid sulphate soils. While the lime-fly ash barrier does reduce pyrite oxidation and the generation of pyrite oxidation products, drain water quality results still showed an acidic environment. The installation of both a lime-fly ash barrier and a permeable reactive barrier on the same site may further enhance the surface water quality. Finite element analysis of the flow of groundwater through this system may provide increased understanding in regards to the role of these measures in reducing acidity, as well as providing a better insight to the functioning of such alkaline barriers.

References

Akbulut, S. and Saglamer, A. (2002) Estimating the groutability of granular soils: a new approach. *Tunnelling and Underground Space Technology*, **17**(4):371-380.

Akbulut, S. and Saglamer, A. (2003) Evaluation of Fly Ash and Clay in Soil Grouting, pp.1192-1199. In L.F. Johnson, D.A. Bruce and M.J. Byle (Eds.) 'Grouting and Ground Treatment: Proceedings of the Third International Conference, February 10-12, 2003, New Orleans, Louisiana.

Anagnosti, P. (1985) Grouting of Soils, Soil Improvement Methods, Proceedings of the Third International Geotechnical Seminar, Singapore 27-29 November 1985.

Andriesse, W. (1993) Acid sulphate soils: Diagnosing the illness, pp. 11-29. In D.L Dent and van Mensvoort (Eds.) 'Selected Papers of the Ho Chi Minh City Symposium on Acid Sulphate Soils. ILRI Publication No. 53. Wageningen, The Netherlands.

ANZECC (1992) Australian Water Quality Guidelines for Fresh and Marine Waters. Australian and New Zealand Environment Conservation Council. Canberra.

ANZECC (2000) Australian Water Quality Guidelines for Fresh and Marine Waters. Australian and New Zealand Environment Conservation Council. Canberra.

APHA (1985) *Standard methods for the examination of water and wastewater*, 16th Edition. American Public Health Association, Washington DC.

Bayley, B. (1975) Shoalhaven – History of the Shire of the Shoalhaven (2nd Edition). South Coast Printers. Port Kembla, Australia.

Berner, R.A. (1984) Sedimentary pyrite formation: An update, *Geochimica et Cosmochimica Acta*, **48**, 605-615.

Blacklock, J.R., Joshi, R.C. and Wright, P.J. (1984) Pressure injection grouting of landfills. *Public Works.* May, p. 4.

Bloomfield, C. (1972) The oxidation of iron sulphides in soils in relation to the formation of acid sulphate soils, and of ochre deposits in field drains, *Journal of Soil Science*, **23** (1): 3-16.

Blunden, B. (2000) Management of acid sulfate soils by groundwater manipulation. PhD thesis. University of Wollongong.

Blunden, B. and Indraratna, B. (2000) Evaluation of surface and groundwater management strategies for drained sulphidic soil using numerical simulation models. *Australian Journal of Soil Research*, **38**, 569-590.

Bohn, H.L., Fu-Young and Huang-Chenge (1989) Hydrogen sulphide sorption by soils. Soil Society of America, **53**, pp. 1914-1917.

Bowen, R. (1981) Grouting in Engineering Practice, 2nd Edition, Applied Science Publishers Ltd., London.

Bowman,G.M. (1996). An overview of acid sulfate soil treatment. "Proceedings 2nd National Conference of Acid Sulfate Soils" Robert J Smith and Associates and ASSMAC, Australia, 200-206.

Brierley, G.S. (1995) Ground Improvement - Salvation or Snake Oil, *Civil Engineering*, **65**(12): 6.

Brinkman, R. (1982) Directions of further research on acid sulfate soils. In 'Proceedings of the Bangkok Symposium on Acid Sulfate Soils'. (Eds. Dost and van Breeman). IRRI Publication 31. Wageningen, The Netherlands.

Brown, J.A.H., R.D. Harrison and G. Jackson, 1983. Water demand and availability with references to particular regions. Water 2000: Consultants Report No. 12. Canberra, Australian Government Publishing Service.

Bush, R.T. and Sullivan, L.A. (1996) Some things standard soil analyses don't reveal about potential acid sulphate soils oxidation. Proceedings 2nd National Conference on Acid Sulphate Soils. (Eds. Smith and Smith). Pp. 72-75. Coffs Harbour.

Callinan, R. B., Fraser, G. C., and Virgona, J. L. (1989) Pathology of red spot disease in sea mullet, *Mugil cephalus* L., from eastern Australia. *Journal of Fish Diseases*, 12:467–479.

Callinan. R.B., Paclibre, J.O., Reantaso, M.B., Lumanlan-mayo, S.C., Fraser, G.C., and Sammut, J. (1995) EUS outbreaks in estuarine fish in Australia and the Philippines: associations with acid sulphate soils, and rainfall, and *Aphanomyces*. In *Diseases in Asian Aquaculture II*. Shariff, M., Arthur, J. R., & Subasinghe, R.P. (eds.), pp.291-298. Fish Health Section, Asian Fisheries Society, Manila.

Calvert, D.V. and Ford, H.W. (1973) Chemical Properties of Acid-Sulfate Soils Recently Reclaimed from Florida Marshlands, *Proceedings of the Soil Science Society of America*, **37**, pp. 367-371.

Craig, R.F. (1987) Soil Mechanics, 4th Edition, Chapman and Hall, London.

Davison, W., Lishman, J. P and Hilton, J. (1985) Formation of pyrite in freshwater sediments: implications for C/S ratios. *Geochimica et Cosmochimica Acta*, **49**, 1615-1620.

Dent, D. (1986) Acid Sulphate Soils: a baseline for research and development. IRRI Publication No. 39. Wageningen. The Netherlands.

Dent, D.L. (1992) Reclamation of Acid Sulphate Soils. Springer-Verlag Publishing, New York, USA, 117p.

Dent, D.L. and Pons, L.J. (1995) A world perspective on acid sulphate soils, *Geoderma*, **67**, p263-276.

Dent, D.L. and Bowman, G. (1996) Quick, quantitative assessment of the acid sulfate hazard. Proceedings 2nd National Conference on Acid Sulphate Soils. (Eds. Smith and Smith). pp. 96-98. Coffs Harbour.

Dharmappa, H.D. and George, J. (2000) Laboratory Manual: Industrial Waste Characterisation and Feasibility Studies, University of Wollongong, Australia.

Drever, J. (1997) The Geochemistry of Natural Waters: Surface and Groundwater Environments. Prentice Hall Inc, USA.

Earnshaw, K. (2001) The Remediation and Management of Acid Sulphate Soils using a Self Regulating Tilting Weir, Unpublished B.Env. E, University of Wollongong

Easton, C. (1989) The trouble with the tweed. *Fishing World* (March), 58.

Evangelou, V.P. (1995) Pyrite oxidation and its control, CRC Press, Boca Raton.

Fanning, D. (1993) Salinity problems in acid sulfate coastal soils. In 'Towards the Rational use of High Salinity Tolerant Plants'. (Eds., Lieth, H. and Masoom, A). Kluwer Academic Publishers. The Netherlands.

Fanning, D.S. Rabenhorst, M.C., Burch, S.N., Islam, K.R. and Tangren, S.A. (2002) Sulfides and Sulfates, *Soil Mineralogy with Environmental Applications, SSSA Book Series no.7.*

Fell, R., MacGregor, P. and Stapledon, D. (1992) Geotechnical engineering of embankment dams, A.A. Balkema, Rotterdam.

Freda, J. and McDonald, D.G. (1988) Physiological Correlates of Interspecific Variation in Acid Tolerance in Fish, *Journal of Experimental Biology*, **136**, 243-258.

Gavaskar, A.R. (1999) Design and construction techniques for permeable reactive barrier. *Journal of Hazardous Materials*, **68**: 41-71.

Glamore, W. and Indraratna, B. (2001) The impact of floodgate modifications on water quality in acid sulphate soil terrains. In '*15th Australasian Coastal and Ocean Engineering Conference Proceedings*', 25-28th September, Gold Coast, Australia.

Glamore, W. (2003) Evaluation and analysis of acid sulphate soils impacts via tidal restoration. PhD Thesis, University of Wollongong.

Goldhabar, M. B. and Kaplan, I.R. (1982) Controls and consequence of sulphate reduction rates in recent marine sediments. In J. A Kittrick, D.S. Fanning and L.R. Hossner (eds.) Acid Sulfate Weathering, pp. 19-36. Soil Science Society of America Special Publication No. 10, Madison, WI, USA.

van Host, A.F and Westerveld, G.J.W. (1973) Corrosion of concrete foundations in (potential) acid sulphate soils and subsoils in the Netherlands. In H. Dost (ed.) Acid sulphate soils. Proceedings of the International Symposium, International Institute for Land Reclamation and Improvement Publication No.18, Vol 2, pp. 373-381, Wageningen, Netherlands.

Hilton, I.C. (1975) Classification of grout: Classification by Engineering Performance for Grout Selection. In: Bell, F.G. (ed) Methods of Treatment of Unstable Ground, Newnes-Butterworths, London.

Indraratna, B. (1983) The properties of grouts and the application of grouting with special reference to dam foundations, MSc, University of London.

Indraratna, B. (1996) Utilization of lime, slag and fly ash for improvement of a collluvial soil in New South Wales, Australia, *Geotechnical and Geological Engineering*, **14**, 169-191.

Indraratna, B. and Blunden, B. (1997) Remediation of acid sulphate soils by management of groundwater table. In 'Proceedings Second International Green Symposium on Geotechnics and the Environment'. (Ed. Sarsby), pp. 516-524 Thomas Telford Publishers, Krakow, Poland.

Indraratna, B., Nutalaya, P. and Kuganenthira, N. (1991) Stabilization of a dispersive soil by blending with fly ash, *Quarterly Journal of Engineering Geology*, **24**, 275-290.

Indraratna, B., Balasubramaniam, A.S. and Khan, M.J. (1995) Effect of fly ash with lime and cement on the behaviour of a soft clay, *Quarterly Journal of Engineering Geology*, **28** (2), 131-142.

Indraratna, B., Sullivan, J. and Nethery, A. (1995) Effect of groundwater table on the formation of acid sulphate soils. *Minewater and the Environment*, **14**, 71-84.

Indraratna, B. Tularam, G.A. and Blunden, B. (2001) Reducing the impact of acid sulphate soils at a site in Shoalhaven Floodplain of New South Wales, Australia, *Quarterly Journal of Engineering Geology and Hydrogeology*, **34**, 333-346.

Indraratna, B., Glamore, W., and Tularam, G.A. (2002). The Effects of Tidal Buffering on Acid Sulphate Soil Environments in Coastal Areas of NSW. *International. Journal of Geotechnical & Geological Engineering*, **20**(3): 181-199.

Ischy, E. and Glossop, R. (1962) An Introduction to Alluvial Grouting, *The Institution of Civil Engineers*, Paper No. 6598, pp. 449-474.

Jaynes, D.B., Rogowski, A.S. and Pionke, H.B. (1984) Acid Mine Drainage from Reclaimed Coal Strip Mines 1. Model Description, *Water Resources Research*, **21**(2): 233-242.

Joshi, R.C. and Wright (1978) In Situ Soil Improvement by Lime and Lime Fly Ash Slurry Injection Process, Proceedings of the Symposium on Soil Reinforcing and Stabilizing Techniques in Engineering Practice, The New South Wales Institute of Technology, Sydney Australia, October 16-19, 1978, pp. 545-558.

Kayes, I., Nissen, D. and Adamson, J (2000) Stabilisation of Rail Track Formation and Embankments, CORE2000, May 21-23.

Kepler, D.A. and McCleary, E.C. (1994) Successive alkalinity producing systems (SAPS) for the treatment of acidic mine drainage. In 'Proceedings of International Land Reclamation and Mine Drainage Conference and third International Conference on the Abatement of Acidic Drainage', United States Department of the Interior, pp. 195-204.

Kitsugi, K. and Azakami, H. (1982) Lime-column techniques in the improvement of clay ground, Symposium on Soil and Rock Improvement Techniques including Geotextiles, Reinforced Earth and Modern Piling Methods, 29 Nov – 3 Dec.

Kraus, M.J. (1998) Development of potential acid sulphate paleosols in Paleocene floodplains, Bighorn Basin, Wyoming, USA. *Palaeogeography, Palaeoclimatology, and Palaeoecology*, **144**, 203-224.

Lambe, T.W. (1962) Soil Stabilization. In: Leonards, G.A. (ed) Foundation Engineering, McGraw-Hill, New York.

Lin, C. and Melville, M.D. (1992) Mangrove soil: A potential contamination source to estuarine ecosystems of Australia, *Wetlands*, **11**, pp. 68-74.

Lin, C. and Melville, M.D. (1993) Controls on soils acidification by fluvial sedimentation in an estuarine floodplain, eastern Australia. *Sedimentary Geology*, **85**, 1-13.

Lin, C. and Melville, M.D. (1994) Acid sulphate soil-landscape relationships in the Pearl River Delta, southern China, *Catena*, **22**, 105-120.

Lin, C., Melville, M.D. and Hafer, S. (1995a) Acid sulphate soil-landscape relationships in an undrained, tide-dominated estuarine floodplain, Eastern Australia, *Catena*, **24**, 177-194.

Lin, C., Melville, M.D., White, I. And Wilson. B (1995b) Human and natural controls on the accumulation, acidification and drainage of pyritic sediments: contrasts

between the Pearl River Delta, China and coastal NSW. *Australian Geographical Studies*, **33**, 77-88.

Lin, C., Melville, M.D., Islam, M.M., Wilson, B.P., Yang, X., van Oploo, P. (1998) Chemical controls on acid discharge from acid sulfate soils under sugarcane cropping in an eastern Australian estuarine floodplain. *Environmental Pollution*, **103**, 269-276.

Lin, C., Bush, R.T. and McConchie, D. (2001a) Impeded acidification of acid sulphate soils in an intensively drained sugarcane land. *Pedosphere*, **11**

Lin, C., Rosicky, M., McConchie, D., Sullivan, L.A. and Lancaster, G. (2001b) Coastal land scalding in NSW, Australia: Soil chemical characteristics and their implications for remediation of the scaled lands. *Land Degradation and Development*, 12: 293-303.

Malouf, E.E. and Prater, J.D. (1961) Role of Bacteria in the Alteration of Sulfide Minerals, *Journal of Metals*, May, 353-356.

Moses, C., Nordstrom, D., Herman, J and Mills, A. (1987) Aqeous pyrite oxidation by dissolved oxygen and by ferric iron. *Geochimica et Cosmochimica Acta*, **51**, 1561-1571.

Mulvey, P. (1993) Pollution, prevention and management of sulfuric clays and sands. In '*Proceedings of the National Conference on Acid Sulfate Soils*'. (Ed. R. Bush). 24-25 June 1993 Coolangatta.

Munfakh, G.A. and Wylie, D.C. (2000) Ground improvement engineering – issues and selection. In 'GeoEng2000 An International Conference on Geotechnical and Geological Engineering Vol. 1: Invited Papers', 19-24 November 2000 Melbourne, Victoria.

Naftz, D., Morrison, S.J., Fuller, C.C. and Davis, J.A. (Eds) (2002) Handbook of groundwater remediation using permeable reactive barriers – Applications to radionuclides, trace metals and nutrients. Academic Press, San Diego, California.

Narasimha Rao, S. and Rajasekaran, G. (1994) Lime injection technique to improve the behaviour of soft marine clays.

Naylor, S., Chapman, G., Atkinson, G., Murphy, C., Tulau, M., Flewin, T., Milford, H. and Moran, D. (1995) Guidelines for the use of acid sulphate soils risk maps. Soil Conservation Service. Sydney.

Nonveiller, E. (1989) Grouting Theory and Practice, Elsevier Science Publishers, Amsterdam.

Nordstrom, D. (1982) The effect of sulfate on aluminium concentrations in natural waters: some stability relations in the system Al_2O_3-SO_3-H_2O at 298 K. *Geochimica et Cosmochimica Acta*, **46**, 681-692.

Nriagu, J. (1978) Dissolved silica in pore waters of Lake Ontario, Eire and Superior sediments. *Limnology and Oceanography*, **23**, 53-67.

Pantelis, G. and Ritchie, A.I.M. (1992) Rate-Limiting Factors in Dump Leaching of Pyritic Ores, *Applied Mathematical Modelling*, **16**(10): 553-560.

Pease, M. (1994) Acid Sulfate Soils and acid drainage Lower Shoalhaven Floodplain, NSW. Unpublished MSc (Hons) thesis. University of Wollongong.

Pekrioglu, A., Doven, A.G. and Tumay, T. In: Johnson, L.F., Bruce, D.A. and Byle, M.J (Eds.) *Grouting and Ground Treatment, Proceedings of the Third International Conference*, Feb 10-12, 2003, New Orleans, Louisiana, Vol 2, Geo-Institute of the American Society of Civil Engineers, Deep Foundations Institute.

Playle, R.C. and Wood, C.M. (1991) Mechanisms of Aluminum Extraction and Accumulation at the Gills of Rainbow-Trout, Oncorhynchus-Mykiss (Walbaum), in Acidic Soft-Water, *Journal of Fish Biology*, **38**(6): 791-805.

Pons, L. (1973) Outline of genesis, classification and improvement of acid sulfate soils. In 'Acid Sulfate Soils: Proceedings of the International Symposium' 13-20 August. IRRI Publication 18 Wageningen, The Netherlands.

Pons, L., van Breeman, N. and Driessen, P.M. (1982) Physiography of coastal sediments and development of potential soil acidity. In J. A. Kittrick, D.S. Fanning and L.R. Hossner (eds) Acid Sulfate Weathering, pp. 1-18. Soil Science Society of America Special Publication No. 10, Madison, WI, USA.

Raffle, J.F. and Greenwood, D.A. (1961) The relation between the rheological characteristics of grouts and their capacity to permeate soil, Proceedings of the 5th International Conference on Soil Mechanics and Foundation Engineering Vol 2.

Rajasekaran, G. and Narasimha Rao, S. (1996) Lime Migration studies in Marine Clay, *Ocean Engineering*, **23**(4): 325-355.

Rajasekaran, G. and Narasimha Rao, S. (2002) Permeability characteristics of lime treated marine clay, *Ocean Engineering*, **29**, 113-127.

Ritsema, C.J., van Mensvoort, M.E.F., Dent, D.L., Tan, Y., van den Bosch, H., and van Wijk, A.L.M. (2000) Acid Sulfate Soils. In 'Handbook of Soil Science' (Ed. Sumner, M.E), CRC Press, Boca Raton.

Rogers. C.D.F. and Glendinning, S. (1997) Improvement of clay soils *in situ* using lime piles in the UK, *Engineering Geology*, pp. 243-257.

Roy, P. (1984) New South Wales estuaries: their origin and evolution. In 'Coastal Geomorphology in Australia'. (Ed. Thom). Academic Press Australia. Sydney.

Roy, P., Thom, B. and Wright, L. (1980) Holecene sequences on an embayed high-energy coast: an evolutionary model. *Sedimentary Geology*, **26**, 1-19.

Rudens, C. (2001) The role of biotic oxidation on acid production in potential acid sulfate soils in the Shoalhaven Floodplain. Unpublished BE (Environmental) thesis. University of Wollongong.

Sammut, J. (1994). A Brief Overview of Acid Sulfate Soils and their Impacts: The Lower Richmond River, Northern New South Wales. Report for the ASSMAC Technical Committee, 8 pp.

Sammut, J., Melville, M.D., Callinan, R. and Fraser, G. (1995) Estuarine acidification: impacts on aquatic biota of draining acid sulfate soils. *Australian Geographicl Studies*, **33**, 89-100.

Sammut, J., White, I. and Melville, M.D. (1996) Acidification of an Estuarine Tributary in Eastern Australia due to Drainage of Acid Sulfate Soils, *Marine Freshwater Research*, **47**, 669-84.

Scheetz, B.E., Silsbee, M.R., Fontana, C., Zhao, X. and Schueck, J. (1993) Properties and potential applications of large volume use of fly ash-based grouts for acid mine drainage abatement, 15th Annual Meeting of the Association of Abandoned Mine Land Programs, Jackson, Wyoming, September 13-15 1993.

Shearer (2001) What are Acid Sulphate Soils, NSW Department of Agriculture.

Shroff, A.V. and Shah, D.L. (1993) Grouting Technology in Tunnelling and Dam Construction, A.A. Balkema, Rotterdam.

Singh, A. (1975) Soil Engineering in Theory and Practice, Volume 1, Fundamentals and General Principles, Asia Publishing House, Bombay.

Simpson, H.J. and Pedini, M. (1985) Brackishwater Aquaculture in the Tropics: The Problem of Acid Sulphate Soils, *Fisheries Circular No. 791*, Food and Agriculture Organisation of the United Nations, Rome, August, p.32.

Skousen, J.G. (1997) Overview of passive systems for treating acid mine drainage. *Green Lands*, **27**(4): 34-43.

Sowers, G.B. and Sowers, G.F. (1970) Soil Mechanics and Foundations, 3rd Edition, Collier-Macmillan Limited, London.

Stone, Y., Ahern, C. and Blunden, B. (1998) NSW Acid Sulfate Soil Manual. NSW Government. Sydney.

Stumm, W. and Morgan, J.J. (1996) *Aquatic Chemistry* (3rd edn). John Wiley and Sons, New York.

Taylor, J.R., Waring, C.L., Murphy, N.C. and Leake, M.J. (1997) An overview of acid mine drainage control and treatment options including recent advances. In 'Proceedings of the 3rd Australian Workshop on Acid Mine Drainage', Darwin, Australia, pp. 147-160.

Thom, B.G. and Chappell, J. (1975) Holocene sea levels relative to Australia, *Search*, **6**, 90-93.

Thong, L.J. (1998) Management of acid sulphate soils in column experiments, Unpublished BE thesis, University of Wollongong.

Umitsu, M., Buman, M., Kawase, K. and Woodroffe, C. (2001) Holocene palaeocology and formation of the Shoalhaven River deltaic-estuarine plains, southeast Australia. *The Holocene*, **11**(4): 407-418.

van Breeman N. (1973) Soil forming processes in acid sulphate soils. In 'Acid Sulphate Soils: Proceedings of the International Symposium on Acid Sulphate'. (Ed. H. Dost) pp 66-129. ILRI, Wageningen, The Netherlands.

van Breeman N. (1980) Acid sulphate soils. Problem Soils: their reclamation and management. Land Reclamation and water management. ILRI Pub. 27, Wageningen, pp. 53-57.

van der Kevie, W. (1973) Morphology, genesis, occurrence, and agricultural potential of acid sulphate soils in Central Thailand. *Thailand Journal of Agricultural Science*, **5**, pp. 162-182.

van Impe, W.F. (1989) Soil Improvement Techniques and their Evolution, A.A. Balkema, Rotterdam.

Walker, P. (1972) Seasonal and stratigraphic controls in coastal floodplain soils. *Australian Journal Soil Research*, **10**, 127-142.

Watzlaf, G.R., Schroeder, K.T. and Kairies, C.L. (2000) Long-term performance of alkalinity-producing passive systems for the treatment of mine drainage. In: 'Proceedings 2000 National Meeting of the American Society for Surface Mining and Reclamation', Tampa, Fl. American Society for Surface Mining and Reclamation, pp. 262-274.

White, I. And Melville, M. (1993) Treatment and Containment of Acid Sulfate Soils. Technical Report 53, Centre for Environmental Mechanics, CSIRO, Canberra.

White, I., Melville, M., Sammut, J. and Lin, C. (1996) Hydrology and drainage of acid sulfate soils. Proceedings 2nd National Conference on Acid Sulphate Soils. (Eds. Smith and Smith). Pp. 103-108. Coffs Harbour.

White, I., Melville, M., Sammut, J. and Wilson, B. (1997) reducing acidic discharges from coastal wetlands in eastern Australia. *Wetlands Ecology and Management*, **5**, pp. 55-72.

Willett, I.R. and Walker, P.H. (1982) Soil Morphology and Distribution of Iron and Sulphur Fractions in a Coastal Flood Plain Toposequence, *Australian Journal of Soil Research*, **20**, p283-294.

Wilson, B. (1995) Soil and hydrological relations to drainage from sugarcane on acid sulfate soils. Unpublished PhD thesis, University of New South Wales, Sydney.

Woodroffe, C., Buman, M., Kawase, K. and Umitso, M. (2000) Estuarine infill and formation of deltaic plains, Shoalhaven River. *Wetlands (Austrlia)*, **18**(2), 72-84.

Yamanouchi, T. (1992) Soil-Lime Stabilisation in particular reference to its developments in Japan, Applied Ground Improvement Techniques, Southeast Asian Geotechnical Society (SEAGS) Asian Institute of Technology, Bangkok, Thailand.

Ziemkiewicz, P.F., Skousen, J.G., Brant, D.L., Sterner, P.L. and Lovett, R.J. (1997) Acid Mine Drainage Treatment with Armored Limestone in open Limestone Channels, *Journal of Environmental Quality*, **26**, July-August, p1017-1024.

Appendix A: Field and Laboratory Soil Data

A.1 Calculation of time lag for Transect A Piezometers using Penman Formulae and Assumed Permeability

Transect A Piezometer No.1:

$$t = 3.3e^{-6} \times \frac{d^2 \ln\left[L/D + \sqrt{1+(L/D)^2}\right]}{kL}$$

When: $k = 1e^{-6}$ cm/s

d = 20 cm

D = 10 cm

L = 25 cm

$$t = 3.3e^{-6} \times \frac{(20)^2 \ln\left[25/10 + \sqrt{1+(25/10)^2}\right]}{1e^{-6} \times 25}$$

$$= 3.3e^{-6} \times \left[\frac{400 \ln 5.192582404}{0.000025}\right]$$

$$= 3.3e^{-6} \times 26355698.34$$

$$= 86.97380453$$

$$= 0.87 days$$

Transect A Piezometer No.2:

Time lag the same as Transect A Piezometer No.1.

0.87 days

Transect A Piezometer No.3:

$$t = 3.3e^{-6} \times \frac{d^2 \ln\left[L/D + \sqrt{1+(L/D)^2}\right]}{kL}$$

$$t = 3.3e^{-6} \times \frac{(20)^2 \ln\left[27.5/10 + \sqrt{1+(27.5/10)^2}\right]}{1e^{-6} \times 27.5}$$

$$= 3.3e^{-6} \times \left[\frac{400 \ln 5.676174978}{0.0000275}\right]$$

$$= 3.3e^{-6} \times 25254946.71$$

$$= 83.34132415$$

$$= 0.83 days$$

Transect A Piezometer No.4:

Time lag the same as Transect A Piezometers 1 and 2.

0.87 days

Transect A Piezometer No.5:

$$t = 3.3e^{-6} \times \frac{d^2 \ln\left[L/D + \sqrt{1+(L/D)^2}\right]}{kL}$$

$$t = 3.3e^{-6} \times \frac{(20)^2 \ln\left[26.2/10 + \sqrt{1+(26.2/10)^2}\right]}{1e^{-6} \times 26.2}$$

$$= 3.3e^{-6} \times \left[\frac{400 \ln 5.424353758}{0.0000262}\right]$$

$$= 3.3e^{-6} \times 25815248.39$$

$$= 85.19031968$$

$$= 0.85 days$$

A.2: Total Actual Acidity (TAA), Sulphur, pH, Electrical Conductivity (EC), Chloride and Sulphate soil Data

Depth (cm)	Elevation (m AHD)	TAA (moles H^+/tonne)	Sulphur (%)	pH ($CaCl_2$)	EC (mg/kg)	Chloride (mg/kg)	Sulphate (mg/kg)	Cl:SO_4
5	0.82	82	0.016	4.33	0.63	130	220	0.5909
20	0.67	250	0.034	3.74	0.55	180	320	0.5625
65	0.22	370	0.045	3.31	0.61	180	340	0.5294
85	0.02	160	0.023	3.38	0.36	74	140	0.5285
125	-0.38	230	0.76	3.04	1.35	270	1200	0.225
155	-0.68	120	3.00	3.55	1.50	100	610	0.1639

Appendix B: Bureau of Meteorology Data

B.1: Precipitation Data

Date	Day Number	Precipitation (mm)
1-Aug-03	0	0
2-Aug-03	1	0
3-Aug-03	2	0
4-Aug-03	3	0
5-Aug-03	4	0
6-Aug-03	5	3
7-Aug-03	6	0
8-Aug-03	7	0
9-Aug-03	8	0
10-Aug-03	9	0
11-Aug-03	10	7.4
12-Aug-03	11	0.3
13-Aug-03	12	0
14-Aug-03	13	3.2
15-Aug-03	14	0.5
16-Aug-03	15	0
17-Aug-03	16	0
18-Aug-03	17	0.6
19-Aug-03	18	0.5
20-Aug-03	19	1.4
21-Aug-03	20	1
22-Aug-03	21	0.4
23-Aug-03	22	2.6
24-Aug-03	23	12.2
25-Aug-03	24	0
26-Aug-03	25	0
27-Aug-03	26	0
28-Aug-03	27	0
29-Aug-03	28	0
30-Aug-03	29	0
31-Aug-03	30	0
1-Sep-03	31	0
2-Sep-03	32	0
3-Sep-03	33	0
4-Sep-03	34	0
5-Sep-03	35	0
6-Sep-03	36	0

7-Sep-03	37	0
8-Sep-03	38	0
9-Sep-03	39	0
10-Sep-03	40	0
11-Sep-03	41	0
12-Sep-03	42	7
13-Sep-03	43	0.3
14-Sep-03	44	0.3
15-Sep-03	45	0.3
16-Sep-03	46	0
17-Sep-03	47	0
18-Sep-03	48	0
19-Sep-03	49	0.8
20-Sep-03	50	0.8
21-Sep-03	51	0.8
22-Sep-03	52	0
23-Sep-03	53	0.3
24-Sep-03	54	0.1
25-Sep-03	55	0
26-Sep-03	56	0
27-Sep-03	57	0.6
28-Sep-03	58	0.6
29-Sep-03	59	0.6
30-Sep-03	60	2
1-Oct-03	61	0
2-Oct-03	62	11.2
3-Oct-03	63	25.2
4-Oct-03	64	1
5-Oct-03	65	1.1
6-Oct-03	66	0.5
7-Oct-03	67	2
8-Oct-03	68	0
9-Oct-03	69	13
10-Oct-03	70	2
11-Oct-03	71	1
12-Oct-03	72	0
13-Oct-03	73	4
14-Oct-03	74	0
15-Oct-03	75	0
16-Oct-03	76	0
17-Oct-03	77	0
18-Oct-03	78	0
19-Oct-03	79	0
20-Oct-03	80	13.5

21-Oct-03	81	0
22-Oct-03	82	0.3
23-Oct-03	83	0
24-Oct-03	84	0
25-Oct-03	85	3
26-Oct-03	86	1
27-Oct-03	87	4
28-Oct-03	88	0
29-Oct-03	89	4.8
30-Oct-03	90	0
31-Oct-03	91	0
1-Nov-03	92	0.5
2-Nov-03	93	12.4
3-Nov-03	94	11.7
4-Nov-03	95	0.1
5-Nov-03	96	0
6-Nov-03	97	0
7-Nov-03	98	1.2
8-Nov-03	99	0.1
9-Nov-03	100	0.1
10-Nov-03	101	0.5
11-Nov-03	102	0
12-Nov-03	103	0
13-Nov-03	104	0
14-Nov-03	105	0
15-Nov-03	106	2.9
16-Nov-03	107	2.9
17-Nov-03	108	8
18-Nov-03	109	2
19-Nov-03	110	0
20-Nov-03	111	0
21-Nov-03	112	5.8
22-Nov-03	113	27
23-Nov-03	114	25
24-Nov-03	115	58
25-Nov-03	116	33.2
26-Nov-03	117	12.6
27-Nov-03	118	6
28-Nov-03	119	0.1
29-Nov-03	120	0
30-Nov-03	121	0
1-Dec-03	122	0
2-Dec-03	123	16.6
3-Dec-03	124	1.4

4-Dec-03	125	14
5-Dec-03	126	6.5
6-Dec-03	127	1.4
7-Dec-03	128	1.4
8-Dec-03	129	1.4
9-Dec-03	130	0
10-Dec-03	131	0
11-Dec-03	132	0
12-Dec-03	133	3.6
13-Dec-03	134	0
14-Dec-03	135	0
15-Dec-03	136	0
16-Dec-03	137	0
17-Dec-03	138	0
18-Dec-03	139	0
19-Dec-03	140	0
20-Dec-03	141	0
21-Dec-03	142	0
22-Dec-03	143	0.8
23-Dec-03	144	0
24-Dec-03	145	0
25-Dec-03	146	1.6
26-Dec-03	147	1.6
27-Dec-03	148	2
28-Dec-03	149	1.6
29-Dec-03	150	1.6
30-Dec-03	151	1.6
31-Dec-03	152	1.6
1-Jan-04	153	0
2-Jan-04	154	0
3-Jan-04	155	0
4-Jan-04	156	0
5-Jan-04	157	0
6-Jan-04	158	0.4
7-Jan-04	159	1.2
8-Jan-04	160	0
9-Jan-04	161	0
10-Jan-04	162	0
11-Jan-04	163	0
12-Jan-04	164	0.2
13-Jan-04	165	0
14-Jan-04	166	20.2
15-Jan-04	167	0.6
16-Jan-04	168	0.4

17-Jan-04	169	0.4
18-Jan-04	170	0.4
19-Jan-04	171	0.4
20-Jan-04	172	0.4
21-Jan-04	173	0
22-Jan-04	174	8.4
23-Jan-04	175	3.2
24-Jan-04	176	12.2
25-Jan-04	177	13.4
26-Jan-04	178	14.8
27-Jan-04	179	0
28-Jan-04	180	1.8
29-Jan-04	181	0.5
30-Jan-04	182	0
31-Jan-04	183	1.2
1-Feb-04	184	0
2-Feb-04	185	0
3-Feb-04	186	10
4-Feb-04	187	0
5-Feb-04	188	0
6-Feb-04	189	0
7-Feb-04	190	0
8-Feb-04	191	0
9-Feb-04	192	0
10-Feb-04	193	6.4
11-Feb-04	194	0
12-Feb-04	195	13
13-Feb-04	196	0
14-Feb-04	197	0
15-Feb-04	198	0
16-Feb-04	199	0
17-Feb-04	200	0
18-Feb-04	201	0
19-Feb-04	202	0
20-Feb-04	203	0
21-Feb-04	204	0
22-Feb-04	205	0
23-Feb-04	206	0
24-Feb-04	207	8.4
25-Feb-04	208	23
26-Feb-04	209	11.8
27-Feb-04	210	0
28-Feb-04	211	0
29-Feb-04	212	0

1-Mar-04	213	0
2-Mar-04	214	0
3-Mar-04	215	0
4-Mar-04	216	0
5-Mar-04	217	0
6-Mar-04	218	0
7-Mar-04	219	36.4
8-Mar-04	220	0
9-Mar-04	221	0
10-Mar-04	222	0
11-Mar-04	223	1.6
12-Mar-04	224	0
13-Mar-04	225	0.1
14-Mar-04	226	0.1
15-Mar-04	227	0.1
16-Mar-04	228	18.2
17-Mar-04	229	0
18-Mar-04	230	0
19-Mar-04	231	0.2
20-Mar-04	232	0
21-Mar-04	233	0
22-Mar-04	234	4.4
23-Mar-04	235	9.6
24-Mar-04	236	0.1
25-Mar-04	237	0
26-Mar-04	238	0
27-Mar-04	239	0
28-Mar-04	240	0
29-Mar-04	241	0
30-Mar-04	242	0
31-Mar-04	243	0
1-Apr-04	244	0
2-Apr-04	245	0.6
3-Apr-04	246	0
4-Apr-04	247	4
5-Apr-04	248	70.8
6-Apr-04	249	41
7-Apr-04	250	0.4
8-Apr-04	251	0.6
9-Apr-04	252	0
10-Apr-04	253	0.6
11-Apr-04	254	0
12-Apr-04	255	0.6
13-Apr-04	256	0

14-Apr-04	257	0
15-Apr-04	258	0
16-Apr-04	259	0
17-Apr-04	260	0
18-Apr-04	261	0
19-Apr-04	262	0
20-Apr-2004	263	0
21-Apr-2004	264	0
22-Apr-2004	265	0
23-Apr-2004	266	0
24-Apr-2004	267	0
25-Apr-2004	268	0
26-Apr-2004	269	0
27-Apr-2004	270	0
28-Apr-2004	271	2.4
29-Apr-2004	272	0.5
30-Apr-2004	273	1
1-May-2004	274	0
2-May-2004	275	0
3-May-2004	276	0
4-May-2004	277	0
5-May-2004	278	0
6-May-2004	279	0
7-May-2004	280	0
8-May-2004	281	3.8
9-May-2004	282	0
10-May-2004	283	0
11-May-2004	284	0
12-May-2004	285	0.4
13-May-2004	286	13.6
14-May-2004	287	0
15-May-2004	288	0
16-May-2004	289	0
17-May-2004	290	0
18-May-2004	291	0
19-May-2004	292	0
20-May-2004	293	0
21-May-2004	294	0
22-May-2004	295	0
23-May-2004	296	0
24-May-2004	297	0
25-May-2004	298	0
26-May-2004	299	1.4
27-May-2004	300	0

28-May-2004	301	0
29-May-2004	302	0
30-May-2004	303	0
31-May-2004	304	0
1-Jun-2004	305	0
2-Jun-2004	306	0
3-Jun-2004	307	1.4
4-Jun-2004	308	0
5-Jun-2004	309	0
6-Jun-2004	310	0
7-Jun-2004	311	0
8-Jun-2004	312	0
9-Jun-2004	313	0
10-Jun-2004	314	0
11-Jun-2004	315	6.8
12-Jun-2004	316	0
13-Jun-2004	317	0
14-Jun-2004	318	0
15-Jun-2004	319	0
16-Jun-2004	320	0
17-Jun-2004	321	4
18-Jun-2004	322	0
19-Jun-2004	323	0
20-Jun-2004	324	0
21-Jun-2004	325	0
22-Jun-2004	326	0
23-Jun-2004	327	0
24-Jun-2004	328	0
25-Jun-2004	329	0
26-Jun-2004	330	0
27-Jun-2004	331	0
28-Jun-2004	332	0
29-Jun-2004	333	0
30-Jun-2004	334	0
1-Jul-2004	335	
2-Jul-2004	336	
3-Jul-2004	337	
4-Jul-2004	338	
5-Jul-2004	339	
6-Jul-2004	340	
7-Jul-2004	341	
8-Jul-2004	342	
9-Jul-2004	343	
10-Jul-2004	344	

11-Jul-2004	345	
12-Jul-2004	346	
13-Jul-2004	347	
14-Jul-2004	348	
15-Jul-2004	349	
16-Jul-2004	350	
17-Jul-2004	351	
18-Jul-2004	352	
19-Jul-2004	353	
20-Jul-2004	354	
21-Jul-2004	355	
22-Jul-2004	356	
23-Jul-2004	357	
24-Jul-2004	358	
25-Jul-2004	359	
26-Jul-2004	360	
27-Jul-2004	361	
28-Jul-2004	362	
29-Jul-2004	363	
30-Jul-2004	364	
31-Jul-2004	365	
1-Aug-2004	366	0
2-Aug-2004	367	0
3-Aug-2004	368	0.4
4-Aug-2004	369	0.4
5-Aug-2004	370	0
6-Aug-2004	371	0
7-Aug-2004	372	0
8-Aug-2004	373	0
9-Aug-2004	374	0
10-Aug-2004	375	0
11-Aug-2004	376	0
12-Aug-2004	377	0
13-Aug-2004	378	0
14-Aug-2004	379	0
15-Aug-2004	380	0
16-Aug-2004	381	0
17-Aug-2004	382	7
18-Aug-2004	383	6
19-Aug-2004	384	28
20-Aug-2004	385	0
21-Aug-2004	386	0
22-Aug-2004	387	0
23-Aug-2004	388	0

24-Aug-2004	389	0
25-Aug-2004	390	0
26-Aug-2004	391	0
27-Aug-2004	392	0
28-Aug-2004	393	0
29-Aug-2004	394	0
30-Aug-2004	395	0.8
31-Aug-2004	396	0
1-Sep-2004	397	
2-Sep-2004	398	
3-Sep-2004	399	
4-Sep-2004	400	
5-Sep-2004	401	0
6-Sep-2004	402	
7-Sep-2004	403	
8-Sep-2004	404	
9-Sep-2004	405	
10-Sep-2004	406	
11-Sep-2004	407	
12-Sep-2004	408	
13-Sep-2004	409	
14-Sep-2004	410	
15-Sep-2004	411	
16-Sep-2004	412	
17-Sep-2004	413	
18-Sep-2004	414	
19-Sep-2004	415	
20-Sep-2004	416	
21-Sep-2004	417	
22-Sep-2004	418	
23-Sep-2004	419	
24-Sep-2004	420	
25-Sep-2004	421	
26-Sep-2004	422	
27-Sep-2004	423	
28-Sep-2004	424	
29-Sep-2004	425	
30-Sep-2004	426	
1-Oct-2004	427	
2-Oct-2004	428	
3-Oct-2004	429	
4-Oct-2004	430	
5-Oct-2004	431	
6-Oct-2004	432	

7-Oct-2004	433	0
8-Oct-2004	434	0
9-Oct-2004	435	0
10-Oct-2004	436	0
11-Oct-2004	437	0
12-Oct-2004	438	0
13-Oct-2004	439	0
14-Oct-2004	440	0

B.2: Monthly Long Term Averages

Month	Monthly rainfall (mm)	Long term average (mm)
Aug-03	33.1	
Sep-03	14	81
Oct-03	35.8	
Nov-03	210	100
Dec-03	47	113
Jan-04	78	139
Feb-04	97	150
Mar-04	71	160
Apr-04	123	137
May-04	8	
Jun-04	12	136
Jul-04	48	
Aug-04	43	86
Sep-04	26.5	

B.3: Southern Oscillation Index Data

Month (Study Period)	SOI
Aug-03	-1.8
Sep-03	-2.2
Oct-03	-1.9
Nov-03	-3.4
Dec-03	9.8
Jan-04	-11.6
Feb-04	8.6
Mar-04	0.2
Apr-04	-15.4
May-04	13.1
Jun-04	-14.4
Jul-04	-6.9
Aug-04	-7.6
Sep-04	-2.8

Appendix C: Water Quality Data – Lime-fly ash barrier Site

C.1: Water Quality Data (pH, electrical conductivity, groundwater table elevation, temperature), Anion and Cation Results

Day Number	Sample	pH	Electrical Conductivity (mS)	Groundwater Table (m AHD)	Temp. (C)	Total Fe (mg/L)	Al3+ (mg/L)	Ca2+ (mg/L)	Mg2+ (mg/L)	Cl (mg/L)	SO4 (mg/L)	Cl:SO4
0	OH1	3.22	1.22	0.2	14.6	30.9	8.6	27	42	109.4	435	0.2515
	OH2	3.10	1.21	0.26	14.7	54.9	40.8	19	72.3	155.9	412	0.3784
	OH3	3.04	1.29	0.24	14.4	48.5	35	29.7	103.7	99.2	455	0.218
	OH4	3.28	1.20	0.28	14.7	77.5	40.1	11.9	66.7	98.01	471	0.2081
	OH5	3.30	1.27	0.25	14.7	135.4	16.3	11.8	40	98.47	553	0.1781
	OH6	2.90	1.34	0.28	14.5	86.8	17.6	12.8	46	94.58	558	0.1695
	OH7	3.28	1.28	0.26	14.6	60.6	30.4	27.5	42	108.6	596	0.1822
	OH8	2.94	1.55	-0.31	14.5	169	82.8	8.1	81.6	94.42	539	0.1752
	OH9	3.02	1.30	0.28	14.6	119.1	67.9	11.7	97	110.2	724	0.1523
	OH10	2.87	1.62	0.34	14.7	98.8	52.5	7.4	68.5	93.43	464	0.2014
	OH11	2.96	1.24	0.36	14.7	65.8	49.8	27	82.9	94.62	500	0.1892
	OH12	3.00	1.37	0.35	14.7	82.4	38.7	27.8	45	119	675	0.1763
	OH13	3.00	1.53	0.34	14.7	115.5	137	6.4	98.2	92.56	725	0.1277
	OH14	3.18	1.19	0.28	14.6	117.6	78.7	27	89.9	94.24	510	0.1848

	OH15	*3.45*	1.14	0.26	14.6	195	108.1	2.5	83.4	94.09	535	0.1759
	OH16	3.12	1.14	0.28	14.6	89.9	65.2	4.7	82.3	96.49	439	0.2198
	OH17	3.08	1.16	0.32	14.4	51.9	36.1	21.2	31	96.04	411	0.2337
	OH18	3.21	1.18	0.3	14.7	45.2	34.9	11.1	31	92.78	425	0.2183
	OH19	2.96	1.22	0.33	14.6	67.6	48.9	20.4	106.9	92.87	424	0.219
	OH20	3.18	1.18	0.31	14.4	45.1	36.8	37.8	37	90.86	507	0.1792
	OH21	3.55	1.05	0.32	14.4	57.1	12.7	20.7	35	103.5	391	0.2648
	OH22	3.28	1.12	0.31	14.2	55.2	59	10.7	55.9	114	457	0.2495
	OH23	3.03	1.33	0.29	14.4	57.9	47	15.1	36	106.9	496	0.2155
	OH24	3.07	1.21	0.34	14.2	87.5	47	17.3	36	107.7	404	0.2665
	OH25	3.20	1.14	0.29	14.4	~	~	~	~	~	~	~
	OH26	3.84	0.98	0.08	17.6	90.8	65.2	8.8	33	77.15	405	0.1905
	OH27	3.69	1.05	-0.19	13.9		233	1.5	88.9	93.5	393	0.2379
	OH28	3.51	0.86	-0.48	13.1	90	136	11.3	37	93.89	109	0.8614
	Drain -u/s	3.03	1.26	~	9.9	38.9	34.1	10.1	33	117.7	487	0.2416
	Drain - mid	2.96	1.26	~	10.3	41.2	20.3	9.9	33	97.35	499	0.1951
	Drain - d/s	2.88	1.32	~	10.7	83.2	37.3	8.8	31	5550	652	8.512
14	OH1	3.06	1.30	0.25	13.9	12.1	55.6	5.9	52.6	157.8	462	0.3416
	OH2	2.92	1.48	0.26	14.1	34	76.9	12	36.7	142.7	443	0.3222
	OH3	2.88	1.50	0.27	13.9	45.8	67.7	15.5	38.1	114.4	474	0.2413

	OH4	3.13	1.35	0.28	14.3	82.5	38.6	13.6	52.8	144.3	450	0.3206
	OH5	3.34	1.24	0.25	14.4	57.4	88.2	5	31.9	190.6	461	0.4135
	OH6	3.05	1.38	0.27	14.3	81.4	69.7	13.8	49.7	125.6	471	0.2667
	OH7	3.11	1.35	0.31	14.4	58	46.1	73	48.2	116.4	451	0.258
	OH8	2.80	1.67	0.32	13.9	132	125	25.8	85.9	163.4	625	0.2615
	OH9	3.28	1.25	0.3	14.1	41.5	36.1	7.5	89.2	109.3	444	0.2462
	OH10	2.86	1.46	0.29	14.1	32.4	40.7	8.4	39.3	114.6	525	0.2182
	OH11	2.99	1.39	0.26	14.2	108	87.3	12.2	62.1	192	440	0.4364
	OH12	2.93	1.41	0.28	14.3	24.6	43.4	11.6	41.4	1110	447	2.4842
	OH13	2.94	1.66	0.29	14.5	11.5	30.3	17.1	39.5	146.3	490	0.2986
	OH14	2.99	1.37	0.255	14.1	24	39	39	65.3	109.8	418	0.2627
	OH15	3.18	1.34	0.26	14.2	75.4	178.6	14.8	45.7	132.2	441	0.2997
	OH16	3.25	1.16	0.24	14.4	62.1	64.6	8.4	53.2	108.4	251	0.4318
	OH17	3.12	1.20	0.29	14.4	29.5	46.6	7.9	44.6	105.3	451	0.2335
	OH18	3.16	1.26	0.28	14.4	7.2	25.8	20.1	39.9	114.1	457	0.2496
	OH19	2.98	1.26	0.3	14.4	33.9	52	31	77.1	108.7	427	0.2546
	OH20	2.87	1.55	0.29	14.1	14.2	29.1	8.8	41.3	125.5	528	0.2378
	OH21	3.21	1.20	0.32	14.1	10.9	10.9	41	55.7	108.5	388	0.2795
	OH22	3.08	1.36	0.315	14.4	8.4	23.1	31.2	59.5	124.1	444	0.2796
	OH23	2.86	1.74	0.27	14.0	9.7	16.5	17.8	42.3	171	532	0.3215

	OH24	2.87	1.45	0.29	14.1	16.1	20.3	27.2	50.2	121.1	447	0.2709
	OH25	2.92	1.38	0.26	14.1	15	17.5	30.2	57.4	125.8	396	0.3176
	OH26	3.53	0.99	0.48	11.9	58.4	101.3	4.7	44.9	129.5	370	0.35
	OH27	3.87	1.44	0.315	14.3	68.9	81.6	111	67.2	131.6	403	0.3265
	OH28	3.35	0.92	0.37	12.4	31.3	48.3	8.8	53.4	91.31	366	0.2495
	Drain -u/s	3.01	1.50	~	10.9	60.4	39.9	10.2	57.5	201.1	529	0.3802
	Drain - mid	2.84	1.66	~	9.3	57.3	48.2	11.2	64.1	427.6	512	0.8351
	Drain - d/s	2.87	2.00	~	11.2	70.8	43.2	14.2	93.6	251.5	519	0.4847
28	OH1	3.88	1.38	0.25	10.5	70	66.9	20	50	168.8	478	0.3531
	OH2	4.42	0.60	0.26	11.4	158	115.2	4	36	81.11	245	0.3311
	OH3	4.50	0.49	0.26	11.0	6	18.9	14	28	68.16	72.4	0.9414
	OH4	4.20	0.51	0.28	10.4	103	25.7	13	33	~	~	~
	OH5	3.41	0.76	0.25	10.2	105	29.4	13	36	61.64	264	0.2335
	OH6	3.80	0.61	0.26	10.2	103	30.7	13	37	60.15	193	0.3117
	OH7	3.95	0.62	0.31	10.5	91	111.3	5	44	70.99	251	0.2828
	OH8	4.88	0.62	0.29	10.6	14	33.5	15	33	36.94	74.5	0.4959
	OH9	4.33	0.56	0.30	10.5	16	38.9	17	35	48.54	108	0.4495
	OH10	4.05	0.76	0.29	10.4	138	97.8	16	57	204.7	441	0.4643
	OH11	4.30	0.79	0.26	10.2	16	39.9	17	41	80.15	138	0.5808
	OH12	4.63	0.63	0.27	10.3	9	38.9	17	40	~	~	~

	OH13	4.67	0.61	0.29	10.2	22	48.6	16	40	56.34	151	0.3731
	OH14	3.52	0.90	0.25	10.1	59	123.6	22	62	102.8	425	0.242
	OH15	3.44	1.07	0.25	10.5	12	54.3	70	60	114.4	450	0.2542
	OH16	3.31	0.93	0.25	10.7	29	64.5	14	54	124.6	357	0.3491
	OH17	3.41	0.94	0.29	10.7	24	66	12	56	97.76	373	0.2621
	OH18	3.15	1.07	0.25	10.9	28	68	22	58	106.4	384	0.2772
	OH19	3.37	0.95	0.38	10.9	19	71.9	17	57	97.94	379	0.2584
	OH20	3.37	1.18	0.36	11.0	31	80.5	21	65	125.4	488	0.2569
	OH21	3.42	0.98	0.37	10.9	10.8	12.8	41	33.8	107.1	379	0.2825
	OH22	3.64	1.00	0.40	10.5	20	72.8	28	63	117.5	438	0.2683
	OH23	3.44	1.30	0.27	10.4	30	71.9	80	71	185.2	540	0.3429
	OH24	3.61	1.08	0.42	10.4	25	75.1	25	64	172.9	447	0.3868
	OH25	3.21	1.10	0.28	10.6	20	79.1	20	61	173.9	414	0.4199
	OH26	5.75	0.49	0.38	10.6	3	69.1	27	51	41.25	141	0.2926
	OH27	5.98	2.04	0.34	10.6	17	71.5	80	80	232.5	448	0.519
	OH28	3.49	0.91	0.23	10.8	4	91.2	20	64	111.6	365	0.3058
	OH29	3.81	0.87	0.24	10.7	20	87.5	19	62	160.9	322	0.4998
	OH30	3.67	0.83	0.22	10.8	20	85.4	21	61	88.18	348	0.2534
	OH31	4.00	0.97	0.26	10.7	36	89.5	24	65	101.9	380	0.2682
	Drain -u/s	3.12	1.08	~	8.5	65.9	30.4	13.2	38.4	106.9	492	0.2173

	Drain - mid	*2.99*	1.15	~	8.4	119.3	39.1	4.9	26.4	107	503	0.2128
	Drain - d/s	2.94	1.20	~	8.5	46.1	32.1	12.7	34	126.8	450	0.2818
42	OH1	3.08	1.21	0.20	11.0	34.4	15.4	22	34	488.9	445	1.0986
	OH2	3.64	1.17	0.16	10.6	48.5	24.9	15.6	48.8	972.3	433	2.2455
	OH3	3.23	0.86	0.22	10.5	7.4	11.7	16.8	24.8	164.9	280	0.589
	OH4	3.91	0.92	0.18	10.7	44.6	21.7	12.8	31.2	245.3	377	0.6507
	OH5	3.63	1.21	0.21	10.7	43.1	27.6	10.4	36.4	590.7	410	1.4407
	OH6	3.69	1.12	0.20	10.7	46.6	26.2	11.1	36.5	325.2	391	0.8317
	OH7	3.87	0.90	0.21	11.0	51.7	28.8	11.8	33.1	129.1	408	0.3165
	OH8	4.29	1.06	0.19	11.0	50.7	8.2	21.9	34.6	258	397	0.6499
	OH9	4.06	0.98	0.23	11.1	48.3	24.8	15.2	38.9	213.6	410	0.521
	OH10	3.67	1.03	0.19	11.1	73	32.1	15.3	45.3	544.1	532	1.0227
	OH11	3.66	0.98	0.23	11.1	24.7	25.6	10.9	35.8	140.7	391	0.3597
	OH12	3.61	0.94	0.23	11.0	25.1	21.3	13	34.7	124.1	392	0.3167
	OH13	3.64	0.98	0.19	11.0	14.4	16.4	24.1	46.5	123.3	336	0.367
	OH14	3.61	1.03	0.22	11.0	16.7	31.3	20.2	41.8	207.2	409	0.5065
	OH15	3.48	1.00	0.21	11.2	8.6	17.7	25.7	39.3	511.5	414	1.2356
	OH16	3.48	0.94	0.21	11.3	25.4	29.6	10.6	40	164.6	381	0.4319
	OH17	3.38	0.97	0.24	11.2	20.1	25.3	10	35.9	122.7	370	0.3317
	OH18	3.24	1.01	0.20	11.2	11.1	19.6	15.1	36.3	345	400	0.8624

	OH19	3.25	0.98	0.25	11.3	13	22.6	9.2	34.7	370.1	398	0.9299
	OH20	3.36	1.17	0.24	11.2	16.9	21.5	19.4	46.2	114.7	467	0.2455
	OH21	3.46	0.97	0.25	11.2	12.6	13.1	21	38.3	65.18	364	0.1791
	OH22	3.42	1.06	0.24	11.0	12.8	24.4	19	42.9	100.9	416	0.2426
	OH23	3.61	1.29	0.22	11.4	39.1	48.3	17.7	51.5	484.6	588	0.8241
	OH24	3.20	1.14	0.19	11.4	23.2	19.9	17.7	42.6	305.3	463	0.6595
	OH25	3.50	1.03	0.23	11.4	40.8	40.2	12.2	41.8	131	423	0.3098
	OH26	4.13	0.62	0.28	11.4	4.6	6.9	20.2	32.4	47.26	234	0.2019
	OH27	3.65	0.98	0.19	11.4	10.5	16.7	24.6	43.7	145.6	454	0.3208
	OH28	3.48	0.86	0.18	11.5	16.1	37.9	7.5	34.9	104.7	369	0.2838
	OH29	3.07	1.08	0.17	11.3	17.1	20.6	12.8	43	567.9	371	1.5307
	OH30	3.22	0.83	0.13	11.4	8.5	11.4	12	35.1	67.71	275	0.2462
	OH31	3.06	1.03	0.17	11.4	11.2	22.1	16.4	45.8	78.73	393	0.2003
	Drain -u/s	2.54	4.48	~	11.4	49.8	29.8	63	138.4	2105	651	3.2339
	Drain - mid	2.55	5.49	~	11.7	48	24.7	76	397	3508	715	4.9063
	Drain - d/s	2.51	5.45	~	11.6	99.1	30.9	64	147.6	905	671	1.3487
56	OH1	3.88	4.30	0.20	14.0	113.8	29	21	110.2	1379	584	2.3612
	OH2	3.90	6.82	0.16	12.3	67.8	43.7	63	581	3783	715	5.2906
	OH3	3.88	6.72	0.19	11.8	91.7	39.4	47	514	2377	578	4.1128
	OH4	3.85	5.78	0.16	11.4	79.9	57.5	86	693	5462	953	5.7312

	OH5	3.74	7.13	0.18	11.3	94.1	55.2	57	629	4184	703	5.9515
	OH6	3.83	5.53	0.21	11.3	82.4	54	49	598	3718	737	5.0443
	OH7	3.94	2.89	0.20	11.4	75.2	53.3	45	340	3002	729	4.1176
	OH8	4.33	2.07	0.19	11.6	103.7	17.6	34	198	370.1	640	0.5782
	OH9	3.83	5.88	0.20	11.4	82.2	43.9	25.9	134.5	1897	636	2.9831
	OH10	3.68	6.17	0.18	11.5	71.2	58.7	42	600	3834	715	5.3623
	OH11	3.67	6.59	0.21	11.5	82.8	57.3	40	592	~	~	~
	OH12	3.82	5.28	0.22	11.6	90.8	46	25.4	141.6	1907	602	3.1686
	OH13	4.02	3.38	0.18	11.6	76.6	47.5	26	151.5	~	~	~
	OH14	3.79	4.19	0.20	11.4	90.2	23.5	30	233	3437	627	5.4817
	OH15	3.78	2.32	0.18	11.5	44	16.2	32	222	~	~	~
	OH16	3.60	5.28	0.19	11.5	74	52.7	20.5	138.3	2260	565	4.0009
	OH17	3.66	4.73	0.23	11.5	84.1	54.5	21	526	2417	585	4.1315
	OH18	3.73	3.21	0.20	11.7	89.4	41.1	23.1	128.3	1688	556	3.0359
	OH19	3.54	7.03	0.18	11.5	70.4	48.3	24	381	~	~	~
	OH20	3.71	3.14	0.21	11.5	83.5	25.7	17.5	79.1	~	~	~
	OH21	3.77	3.41	0.17	11.4	114.9	39.3	37	369	~	~	~
	OH22	3.66	6.12	0.23	11.4	80.7	32.1	22	309	~	~	~
	OH23	3.77	4.37	0.20	11.6	128.8	26.8	49	140	1875	676	2.7744
	OH24	3.66	8.69	0.20	11.7	158	85.7	17	565	~	~	~

	OH25	3.55	7.49	0.19	11.7	95.9	46.9	34	589	~	~	~
	OH26	4.10	1.24	0.18	11.5	29.1	13.4	24	268	~	~	~
	OH27	3.88	1.60	0.16	11.7	29.9	20.8	17	284	~	~	~
	OH28	3.71	1.35	0.17	11.8	39.2	26.7	7.3	53.1	~	~	~
	OH29	3.52	5.00	0.17	12.2	71.1	53.8	19.7	136.5	~	~	~
	OH30	3.71	2.77	0.02	12.1	67.4	26.2	13.8	73	765.8	375	2.0421
	OH31	3.51	4.06	0.16	12.3	73.3	32.5	13.8	76.3	768.6	449	1.7119
	Drain -u/s	2.96	14.86	~	12.3	31.9	20.1	201	613	7902	1190	6.6399
	Drain - mid	2.90	15.54	~	13.8	35	17	178	572	9179	1230	7.4629
	Drain - d/s	2.75	15.10	~	14.6	24.1	17.3	169	578	8564	1210	7.0776
70	OH1	3.98	5.92	0.20	12.3	100.9	48.2	70	215	3087	648	4.7645
	OH2	3.77	6.68	0.16	11.0	96	69.4	87	329	4410	706	6.2458
	OH3	3.92	5.15	0.22	10.8	123	63.5	70	268	3017	631	4.781
	OH4	3.90	6.47	0.18	10.7	83	53.1	45	197	1678	483	3.4734
	OH5	3.72	6.15	0.22	10.7	86	56.6	38	194	1577	540	2.9195
	OH6	3.82	4.61	0.23	11.0	~	~	~	~	1048	454	2.3088
	OH7	3.87	4.72	0.21	11.0	83	55	55	229	1925	610	3.1559
	OH8	4.13	3.01	0.19	11.0	68.1	11.3	55	171	~	~	~
	OH9	3.87	3.74	0.22	11.0	51	41.2	36	158	777.5	397	1.9586
	OH10	3.72	4.18	0.19	11.2	85	59.1	40	230	1575	609	2.5859

	OH11	3.90	5.49	0.23	11.1	65	52.3	39	206	1260	516	2.4411
	OH12	3.89	3.81	0.22	11.4	102	50.2	56	236	1501	578	2.5973
	OH13	3.99	3.93	0.19	11.0	33	24.3	94	185	471.9	345	1.3677
	OH14	3.91	2.72	0.21	11.3	94	42.3	60	218	966.1	592	1.632
	OH15	3.86	2.35	0.21	11.4	88	29.1	78	195	545.3	517	1.0548
	OH16	3.69	3.07	0.19	11.3	53	45.4	42	223	1207	453	2.6645
	OH17	3.68	4.07	0.24	11.2	73	57.8	48	248	1508	578	2.6088
	OH18	3.77	3.14	0.20	11.4	85	39.9	75	237	1061	579	1.8331
	OH19	3.61	4.83	0.21	11.2	63	47.4	59	248	1234	527	2.3411
	OH20	3.68	4.19	0.22	11.2	93	40.8	54	262	1026	577	1.7776
	OH21	3.74	3.91	0.20	11.3	142	49.3	64	298	1777	594	2.9914
	OH22	3.61	5.72	0.23	11.0	86	56.2	131	285	1797	594	3.0247
	OH23	3.79	5.86	0.24	10.9	123	39.7	159	314	1862	710	2.6219
	OH24	3.71	6.72	0.22	11.0	123	75.3	79	405	3144	745	4.22
	OH25	3.61	6.72	0.21	11.3	126.6	60.1	73	191	3223	724	4.4513
	OH26	3.91	1.50	0.23	11.0	68.1	11.3	55	171	198.9	448	0.444
	OH27	3.76	1.96	0.19	11.0	31.4	24.8	47	160	346.7	513	0.6759
	OH28	3.75	1.32	0.19	11.2	39	22.6	16	176	330.2	427	0.7732
	OH29	3.51	5.63	0.17	11.4	74.4	49	50	276	2340	627	3.7314
	OH30	3.49	5.37	0.17	11.5	84.3	56.5	40	290	1779	568	3.1328

	OH31	3.47	5.13	0.16	11.3	64.5	46.6	32	218	1266	505	2.5072
	Drain -u/s	2.94	11.36	~	12.2	81.7	56.8	104	316	5127	829	6.1842
	Drain - mid	2.93	9.06	~	11.7	72.3	77	90	290	4116	751	5.4812
	Drain - d/s	2.78	9.31	~	11.7	56.3	75.3	66	327	4499	744	6.0466
84	OH1	3.92	6.44	0.08	12.7	98.3	50.3	61	374	2685	622	4.317
	OH2	3.82	6.42	0.06	12.6	83.6	59.3	57	364	2965	672	4.4116
	OH3	3.98	4.94	0.08	12.3	132.5	47.2	64	167	2058	607	3.3908
	OH4	3.84	4.97	0.08	12.3	132.7	43.3	76	203	2597	625	4.1552
	OH5	3.80	5.77	0.06	12.3	77.7	49.9	54	391	2793	652	4.2841
	OH6	3.75	4.63	0.09	12.2	95.4	49.6	52	167	1893	610	3.1033
	OH7	3.95	3.58	0.11	12.2	89.4	37.7	77	146	1302	647	2.0129
	OH8	4.11	2.96	0.09	12.3	127.7	23.4	74	136	958.1	671	1.4278
	OH9	3.87	3.22	0.13	12.3	111.9	44.1	55	152	1230	636	1.9339
	OH10	3.79	3.67	0.09	12.4	81.1	43.3	51	184	1053	553	1.9043
	OH11	4.06	3.79	0.07	12.3	101.2	30.2	46	187	1147	562	2.0404
	OH12	3.91	3.58	0.07	12.4	159.8	40.3	42	205	1245	619	2.0113
	OH13	4.34	3.07	0.09	12.4	51.2	26.1	35	304	980.3	500	1.9606
	OH14	3.90	2.86	0.05	12.4	72.3	24.8	42	266	866.2	534	1.6221
	OH15	3.91	2.66	0.06	12.3	122.9	22.8	82	147	743.4	528	1.408
	OH16	3.74	2.65	0.05	12.3	54	31.1	26	374	938.1	454	2.0664

	OH17	3.77	3.32	0.11	12.3	66	9	29	344	1166	483	2.4135
	OH18	3.75	2.89	0.08	12.3	92.4	33.8	44	209	857	512	1.6739
	OH19	3.76	3.88	0.11	12.3	103.6	63.5	44	203	1436	505	2.8429
	OH20	3.93	3.89	0.11	12.2	123.3	1.5	27	383	1372	553	2.4817
	OH21	3.88	3.93	0.11	12.3	129.4	38	42	238	1390	497	2.7961
	OH22	3.77	5.34	0.10	12.1	95.4	59.2	38	283	1588	502	3.1625
	OH23	3.97	5.79	0.07	12.3	106.7	18.5	63	466	1952	607	3.215
	OH24	3.85	6.75	0.18	12.2	82.3	20.8	53	486	2625	619	4.2399
	OH25	3.84	6.30	0.06	12.2	130.1	60.8	60	288	3650	604	6.043
	OH26	3.99	1.74	0.08	12.3	82	52.9	56	144	275.7	479	0.5756
	OH27	3.89	1.75	0.03	12.3	29	19	26	408	308.3	453	0.6805
	OH28	3.86	1.24	0.02	12.5	59.9	24.3	21	124	181.5	391	0.4641
	OH29	3.70	6.58	0.07	12.5	115.7	12	50	282	2949	613	4.8104
	OH30	3.67	6.62	0.02	12.7	130.1	54.6	65	288	2563	611	4.1946
	OH31	3.61	5.26	0.06	12.6	103.6	47.8	32	458	2038	509	4.0046
	Drain -u/s	3.04	10.20	~	13.6	68.5	52.5	57	435	4337	925	4.689
	Drain - mid	2.90	13.92	~	15.2	64.3	26.3	140	562	6691	1220	5.4846
	Drain - d/s	2.92	13.22	~	15.2	43.3	41.3	88	560	6278	1050	5.9793
99	OH1	3.79	6.57	0.02	14.2	268	76.3	94	279	2792	617	4.5246
	OH2	3.88	6.27	-0.04	12.9	206	90.7	75	330	3397	665	5.1079

	OH3	3.92	4.44	0.03	12.6	245	91.7	49	275	1785	552	3.2333
	OH4	3.96	4.82	-0.02	12.4	121	57.6	49	219	2394	586	4.0846
	OH5	3.73	5.39	0.02	12.4	169	82.3	52	291	2689	641	4.1958
	OH6	3.77	4.01	0.03	12.4	191	75.2	52	304	509.3	627	0.8123
	OH7	3.80	3.29	0.01	12.5	175	50.2	37	191	1148	586	1.9587
	OH8	4.13	2.95	0.00	12.6	196	34.6	49	185	908.7	613	1.4824
	OH9	3.74	2.95	0.03	12.6	161	44.6	54	193	1056	641	1.6469
	OH10	3.92	2.79	0.00	12.6	166	66.7	27	223	1464	585	2.5021
	OH11	3.85	3.51	0.04	12.6	123	47.6	29	179	1251	530	2.3608
	OH12	3.89	3.32	0.03	12.6	165	48.1	36	186	125.9	602	0.2091
	OH13	4.54	2.82	-0.01	12.6	127	26.3	68	182	883.4	572	1.5444
	OH14	3.89	2.79	0.01	12.6	180	52.2	29	178	2776	553	5.019
	OH15	3.93	2.70	0.01	12.6	143	17	77	168	1159	529	2.1902
	OH16	3.92	2.51	0.02	12.6	96	45.9	18	178	1151	482	2.3876
	OH17	3.85	3.10	0.04	12.8	145	41.6	33	192	1098	512	2.1441
	OH18	4.10	2.57	0.03	12.8	123	26.4	25	181	1004	542	1.8529
	OH19	3.86	3.51	0.05	12.7	118	56.4	29	212	1997	535	3.7331
	OH20	3.46	3.96	0.06	12.7	201	52.1	44	229	1892	566	3.3431
	OH21	3.72	3.64	0.02	12.6	304	147.8	25	481	1941	539	3.6016
	OH22	3.90	4.90	0.04	12.6	88.9	47.4	43	469	2796	550	5.0829

	OH23	3.84	5.62	0.04	12.6	144.1	36.9	66	275	3416	661	5.1683
	OH24	3.53	6.73	0.04	12.7	250	50	76	324	4971	646	7.6944
	OH25	3.35	6.16	0.01	12.7	193	39.7	54	272	4522	576	7.8499
	OH26	4.05	1.80	0.03	12.6	90.8	15.1	54	427	347.1	519	0.6689
	OH27	4.44	1.63	-0.01	13.0	72.6	34.5	36	178	319.7	496	0.6445
	OH28	4.08	1.22	0.00	13.0	60.4	17.8	20	155	173.7	416	0.4177
	OH29	3.59	6.90	-0.01	13.1	110.4	53.1	54	575	6489	622	10.432
	OH30	4.20	6.73	-0.02	13.0	201	53	35	337	5542	606	9.1453
	OH31	4.02	5.71	-0.01	13.0	152.9	50.9	43	238	4410	542	8.1373
	Drain -u/s	3.43	10.05	~	15.9	37.6	36.8	1	255	8966	681	13.166
	Drain - mid	2.10	6.13	~	16.8	~	~	~	~	9439	1650	5.7207
	Drain - d/s	3.13	14.03	~	16.2	250	14.2	94	743	7739	1310	5.9073
125	OH1	4.46	3.51	0.48	19.2	105.4	44.6	37	347	1741	511	3.4068
	OH2	5.04	1.26	0.41	19.4	26.9	6.2	29	150	240.6	188	1.2796
	OH3	5.43	0.93	0.49	18.9	12.6	0.8	18	262	123.2	134	0.9193
	OH4	4.68	0.84	0.48	19.0	29.9	12.8	10	276	193.4	296	0.6535
	OH5	4.60	0.53	0.48	18.8	3.1	4.2	10	115	~	~	~
	OH6	4.54	1.01	0.53	18.6	31.1	16	20	142	68.45	123	0.5565
	OH7	4.89	0.75	0.53	18.6	12.4	9.8	13	287	157.9	306	0.516
	OH8	6.10	0.55	0.51	18.4	8.9	1.2	24	131	144.1	210	0.6861

	OH9	4.85	0.79	0.54	18.9	13.1	7.7	22	149	45.54	101	0.4509
	OH10	4.60	0.87	0.54	18.6	28.1	18	14	152	101	214	0.472
	OH11	5.03	0.78	0.56	19.0	31.2	10.7	19	154	122.8	316	0.3887
	OH12	5.52	0.71	0.55	18.8	26.1	2.5	21	151	129.7	162	0.8006
	OH13	5.46	0.68	0.54	18.9	4	1.9	19	148	60.05	77.9	0.7709
	OH14	4.78	0.88	0.53	19.2	27.2	15.3	21	179	130.6	360	0.3627
	OH15	4.99	0.99	0.51	19.3	11.8	5.1	56	173	94.93	314	0.3023
	OH16	4.65	0.76	0.54	19.2	2.8	7.1	42	301	70.59	200	0.353
	OH17	4.59	1.34	0.54	19.0	31.4	20.7	7	189	114.9	354	0.3246
	OH18	5.22	1.08	0.52	19.0	13.7	1.8	77	192	110	296	0.3715
	OH19	5.09	0.92	0.55	19.0	7.6	4	40	303	106.2	286	0.3714
	OH20	4.59	1.49	0.55	19.0	1.9	1.1	47	186	68.4	220	0.3109
	OH21	5.31	0.83	0.54	19.5	7.7	1.2	56	189	80.84	257	0.3145
	OH22	4.30	1.80	0.54	19.0	2.3	0.9	44	300	95.94	281	0.3414
	OH23	4.81	1.29	0.51	19.0	1.5	0.2	37	181	66.82	194	0.3444
	OH24	4.50	3.21	0.55	18.8	9.6	6.5	33	298	180.3	222	0.8123
	OH25	5.14	1.63	0.51	19.2	8.6	2.5	30	309	196.8	154	1.2777
	OH26	5.40	0.81	0.53	19.0	6.6	1.9	15	95	38.11	109	0.3497
	OH27	4.31	1.35	0.55	18.9	3.8	9.6	20	318	113.2	300	0.3773
	OH28	4.51	0.89	0.57	19.1	38.8	17.8	8	198	85.84	335	0.2562

	OH29	4.25	2.33	0.47	18.9	59.8	21.4	19	231	677	386	1.7539
	OH30	4.22	2.88	0.42	18.8	~	~	~	~	850.4	397	2.142
	OH31	4.14	3.72	0.49	18.9	88.8	36.9	28	522	720.8	488	1.477
	Drain -u/s	5.20	0.50	~	22.1	11.5	7.2	5	318	61.37	119	0.5157
	Drain - mid	5.18	0.40	~	22.2	19.5	6.7	9	193	65.42	123	0.5318
	Drain - d/s	5.13	0.39	~	22.2	163.2	51.1	67	568	109.7	158	0.694
140	OH1	3.77	4.14	0.25	20.2	135.40	34.20	40.00	257.00	1,325	493	2.69
	OH2	3.88	2.33	0.19	19.4	73.50	12.20	16.00	157.00	657	409	1.61
	OH3	4.03	1.66	0.24	19.2	45.00	15.00	28.00	137.00	223	376	0.59
	OH4	3.90	1.29	0.22	19.4	~	~	~	~	174	332	0.52
	OH5	3.72	1.91	0.25	19.2	39.80	19.10	15.00	147.00	262	378	0.69
	OH6	3.70	1.55	0.24	19.4	43.70	16.40	14.00	157.00	293	404	0.72
	OH7	4.15	1.65	0.21	19.2	91.70	8.60	40.00	169.00	439	522	0.84
	OH8	4.31	1.43	0.21	19.4	32.70	9.10	16.00	144.00	159	295	0.54
	OH9	3.77	1.32	0.26	19.4	80.50	11.90	4.00	113.00	140	380	0.37
	OH10	3.67	1.50	0.23	19.4	33.40	22.30	16.00	167.00	136	354	0.38
	OH11	3.78	1.47	0.26	19.5	50.50	13.00	20.00	121.00	214	413	0.52
	OH12	4.25	1.96	0.26	19.4	58.60	10.50	18.00	149.00	255	414	0.62
	OH13	4.02	1.50	0.22	19.5	18.50	16.80	33.00	169.00	105	332	0.32
	OH14	3.78	1.63	0.25	19.7	28.60	9.80	13.00	129.00	202	406	0.50

	OH15	3.82	1.79	0.26	19.8	37.80	9.90	29.00	111.00	185	393	0.47
	OH16	3.52	1.19	0.24	20.0	32.40	14.40	12.00	137.00	106	379	0.28
	OH17	3.77	1.87	0.32	20.0	43.90	14.40	16.00	143.00	170	399	0.43
	OH18	3.95	1.74	0.38	19.8	66.70	13.70	24.00	185.00	256	434	0.59
	OH19	3.75	1.57	0.32	20.0	21.80	10.00	19.00	127.00	128	354	0.36
	OH20	3.60	2.50	0.29	20.0	27.10	8.90	27.00	123.00	296	323	0.92
	OH21	3.77	1.64	0.27	20.4	39.80	10.60	18.00	169.00	145	333	0.44
	OH22	3.49	2.01	0.31	22.0	27.00	17.70	24.00	186.00	325	359	0.90
	OH23	3.61	3.65	0.27	21.9	73.30	23.60	30.00	210.00	790	423	1.87
	OH24	3.74	3.62	0.29	20.1	57.30	14.70	27.00	202.00	496	334	1.49
	OH25	3.03	2.69	0.28	20.4	83.20	13.20	29.00	161.00	925	415	2.23
	OH26	3.45	1.03	0.25	20.2	39.80	9.10	21.00	196.00	98	276	0.36
	OH27	4.46	1.37	0.21	20.1	39.30	19.50	23.00	212.00	171	438	0.39
	OH28	4.55	1.38	0.22	20.1	39.00	30.40	12.00	145.00	99	359	0.27
	OH29	3.40	4.15	0.27	20.0	94.50	21.10	23.00	191.00	1,262	497	2.54
	OH30	3.56	3.72	0.22	20.0	81.70	30.40	29.00	237.00	762	449	1.70
	OH31	3.30	4.75	0.26	19.8	114.20	40.10	24.00	245.00	1,182	304	3.89
	Drain -u/s	5.11	3.41	~	23.6	611.00	40.70	14.00	148.00	684	503	1.36
	Drain - mid	5.46	5.17	~	25.2	1405.00	65.20	17.00	212.00	1,833	760	2.41
	Drain - d/s	3.29	1.92	~	24.2	778.00	0.40	14.00	140.00	411	666	0.62

210	OH1	3.85	3.26	0.1	20.7	175	19.6	33	332	1094	500	2.1885
	OH2	4.10	2.29	0.07	20.7	158.9	24.1	111	441	439.7	389	1.1303
	OH3	4.10	1.9	0.14	20.5	143.4	4.6	28	224	457.4	437	1.0467
	OH4	3.87	1.61	0.05	20.4	82.5	2.1	26	231	488.3	343	1.4237
	OH5	3.85	1.68	0.1	20.6	105.3	8.1	21	233	446.7	452	0.9883
	OH6	~	~	0.96	~	~	~	~	~	~	~	~
	OH7	5.52	2.42	0.12	20	20.5	5.7	30	214	129.8	336	0.3863
	OH8	4.54	1.87	0.1	20.4	104.2	3.8	24	234	252.7	442	0.5717
	OH9	3.82	1.63	0.13	20.4	40.4	21.1	2	285	127.8	397	0.3218
	OH10	3.61	1.64	0.1	20.4	135.1	15.4	22	244	346.9	647	0.5361
	OH11	4.24	1.98	0.12	20.2	116.7	5.7	32	259	396.9	549	0.7229
	OH12	4.39	1.91	0.1	20.3	129	7.4	22	244	284.3	493	0.5766
	OH13	3.82	1.37	0.09	21	33.1	11.7	38	278	101.3	399	0.2539
	OH14	4.27	2	0.085	20.6	129	18	30	304	285	493	0.5781
	OH15	3.72	1.54	0.07	20.5	120.8	10.4	32	290	275.2	494	0.5571
	OH16	3.66	1.28	0.09	20.8	50.1	16.1	21	293	156.8	386	0.4063
	OH17	3.93	1.68	0.13	20.7	81.8	12.8	18	296	188.4	421	0.4474
	OH18	3.43	1.23	0.1	21.7	46.3	14.3	25	291	147.8	457	0.3234
	OH19	4.31	1.5	0.13	21.6	16.8	11	34	282	132.8	326	0.4074
	OH20	3.75	1.63	0.14	21	31.3	15.6	23	297	194.7	370	0.5261

	OH21	3.93	1.64	0.14	21	36.2	12.8	24	298	123.4	376	0.3281
	OH22	3.78	1.78	0.135	20.9	103.7	12	15	301	329.8	426	0.7743
	OH23	4.18	2.25	0.1	20.7	108.9	6.2	28	323	459.7	398	1.1551
	OH24	4.03	2.95	0.14	21	76	9.4	19	323	350.6	472	0.7429
	OH25	4.23	2.94	0.1	21	122.4	12.6	20	331	645.3	417	1.5475
	OH26	4.02	1.51	0.09	20.7	132.8	5.4	26	323	158	478	0.3306
	OH27	4.63	1.47	0.055	21	68.3	14.7	20	226	167.1	452	0.3697
	OH28	4.74	1.28	0.05	21	96.3	14.2	18	230	168.9	473	0.3571
	OH29	3.89	2.66	0.08	21.7	153.7	3.7	34	369	951.7	380	2.5044
	OH30	3.68	2.68	-0.17	21.5	~	~	~	~	~	~	~
	OH31	4.05	3.75	0.12	21.7	267	16.8	31	393	1224	523	2.3413
	Drain -u/s	~	~	~	~	~	~	~	~	~	~	~
	Drain - mid	3.61	6.18	~	22.3	184	7.8	52	400	1591	666	2.3884
	Drain - d/s	~	~	~	~	~	~	~	~	~	~	~
251	OH1	4.12	~	0.4	~	78.10	18.10	173.00	104.00	527	459	1.15
	OH2	4.30	~	0.34	~	2.90	1.90	180.00	74.00	84	130	0.64
	OH3	5.11	~	0.41	~	9.40	2.20	222.00	96.00	68	217	0.31
	OH4	3.90	~	0.38	~	14.20	13.70	109.00	109.00	79	273	0.29
	OH5	4.32	~	0.4	~	2.70	4.20	73.00	103.00	61	170	0.36
	OH6	~	~	0.96	~	~	~	~	~	~	~	~

	OH7	4.35	~	0.41	~	55.50	12.00	69.00	117.00	150	384	0.39
	OH8	6.05	~	0.39	~	3.90	3.20	131.00	108.00	18	32	0.56
	OH9	4.41	~	0.42	~	2.10	2.50	107.00	119.00	20	110	0.19
	OH10	4.37	~	0.39	~	9.10	6.70	170.00	136.00	52	164	0.32
	OH11	4.31	~	0.44	~	11.00	8.40	138.00	119.00	53	194	0.28
	OH12	5.26	~	0.43	~	3.10	1.20	112.00	110.00	18	56	0.32
	OH13	5.16	~	0.39	~	4.20	3.30	76.00	130.00	28	96	0.29
	OH14	4.00	~	0.415	~	2.50	16.90	309.00	154.00	81	330	0.25
	OH15	4.10	~	0.42	~	10.90	15.70	190.00	159.00	94	380	0.25
	OH16	3.86	~	0.43	~	6.10	6.60	99.00	145.00	49	179	0.27
	OH17	3.97	~	0.44	~	25.00	18.10	170.00	172.00	87	349	0.25
	OH18	4.05	~	0.44	~	51.20	20.20	97.00	167.00	119	412	0.29
	OH19	4.32	~	0.45	~	2.60	6.40	154.00	167.00	98	359	0.27
	OH20	4.34	~	0.42	~	2.50	2.10	94.00	155.00	70	293	0.24
	OH21	4.26	~	0.42	~	2.40	3.60	133.00	162.00	72	270	0.27
	OH22	3.86	~	0.435	~	16.90	14.50	200.00	194.00	142	432	0.33
	OH23	4.31	~	0.44	~	9.40	4.60	190.00	161.00	89	250	0.36
	OH24	4.37	~	0.41	~	45.50	6.60	110.00	173.00	178	371	0.48
	OH25	4.76	~	0.41	~	6.10	0.40	151.00	159.00	53	130	0.41
	OH26	4.24	~	0.38	~	40.90	7.00	329.00	185.00	60	310	0.19

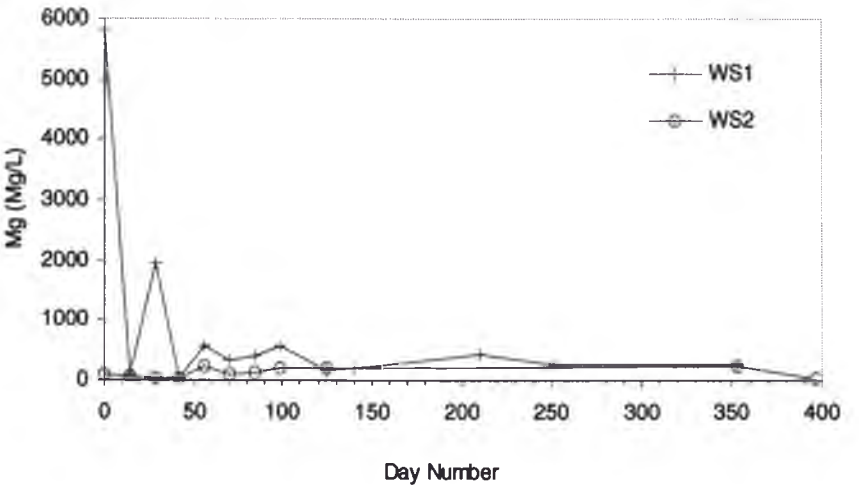

Figure 8.39: Soluble magnesium concentrations in groundwater at the Weir Sites

8.4.5 Anion concentrations

As previously mentioned, low concentrations of chloride in the groundwater at the floodgate and weir sites indicate the chloride that was present at the time of deposition of the pyrite and other estuarine clays has been removed from the soil as a result of freshwater flushing. High chloride concentrations can occur as a result of saline intrusion. Sulphate in groundwater is directly linked to pyrite oxidation.

8.4.5.1 Chloride concentrations

Dissolved chloride concentrations in groundwater at the floodgate sites are presented in Figure 8.40. The average soluble Cl^- concentration in groundwater ranged from 616.5 mg/L at FG4 to 7693 mg/L at FG1. High chloride concentrations were found in the groundwater at FG1 (8993 mg/L), due to its close proximity to the floodgate and salt water intrusion. The lowest soluble Cl^- concentration in groundwater was measured at FG4 (73.69 mg/L). Soluble Cl^- in the soil would have been leached into the drain as a result of freshwater flushing and the lack of saline intrusion into this flood mitigation drain would explain this low soluble Cl^- concentration.

	OH27	4.98	~	0.385	~	23.40	14.40	260.00	175.00	86	345	0.25
	OH28	4.64	~	0.41	~	4.10	25.40	56.00	179.00	67	321	0.21
	OH29	3.98	~	0.37	~	44.00	19.80	86.00	183.00	231	410	0.56
	OH30	3.76	~	0.34	~	44.60	13.80	184.00	193.00	235	375	0.63
	OH31	3.82	~	0.36	~	83.00	11.80	82.00	193.00	351	454	0.77
	Drain -u/s	3.71	~	~	~	122.90	25.30	72.00	181.00	92	284	0.32
	Drain - mid	5.73	~	~	~	243.00	6.00	142.00	206.00	387	247	1.57
	Drain - d/s	3.51	~	~	~	11.80	11.40	200.00	210.00	97	225	0.43
273	OH1	3.92	1.98	0.23	15.4	~	~	~	~	~	~	~
	OH2	3.97	1.32	0.18	15.7	~	~	~	~	~	~	~
	OH3	3.6	1.15	0.24	15.5	~	~	~	~	~	~	~
	OH4	~	~	0.94	~	~	~	~	~	~	~	~
	OH5	3.49	0.94	0.24	15.6	~	~	~	~	~	~	~
	OH6	-	~	0.96	~	~	~	~	~	~	~	~
	OH7	3.61	1.09	0.24	15.7	~	~	~	~	~	~	~
	OH8	4.15	0.81	0.24	15.7	~	~	~	~	~	~	~
	OH9	3.4	1.02	0.26	15.7	~	~	~	~	~	~	~
	OH10	3.89	0.58	0.23	15.8	~	~	~	~	~	~	~
	OH11	3.5	1	0.32	15.7	~	~	~	~	~	~	~
	OH12	3.57	1.2	0.26	15.8	~	~	~	~	~	~	~

	OH13	3.67	1	0.24	15.8	~	~	~	~	~	~	~
	OH14	3.33	1.14	0.235	15.9	~	~	~	~	~	~	~
	OH15	3.37	1.25	0.25	16	~	~	~	~	~	~	~
	OH16	3.42	1.13	0.25	16.1	~	~	~	~	~	~	~
	OH17	3.23	1.23	0.3	16.1	~	~	~	~	~	~	~
	OH18	3.3	1.28	0.27	16.1	~	~	~	~	~	~	~
	OH19	3.46	1.11	0.27	16.1	~	~	~	~	~	~	~
	OH20	4.08	1.17	0.28	16.1	~	~	~	~	~	~	~
	OH21	3.25	1.115	0.27	16.3	~	~	~	~	~	~	~
	OH22	5.11	1.56	0.285	16.1	~	~	~	~	~	~	~
	OH23	4.68	1.39	0.27	16	~	~	~	~	~	~	~
	OH24	3.1	1.83	0.29	16	~	~	~	~	~	~	~
	OH25	3.16	1.54	0.25	16.1	~	~	~	~	~	~	~
	OH26	4	0.76	0.25	15.8	~	~	~	~	~	~	~
	OH27	3.85	0.89	0.215	15.7	~	~	~	~	~	~	~
	OH28	4.77	1.03	0.22	16.4	~	~	~	~	~	~	~
	OH29	3.91	2.53	0.21	16	~	~	~	~	~	~	~
	OH30	3.82	1.41	0.22	15.8	~	~	~	~	~	~	~
	OH31	4.39	1.73	0.21	15.8	~	~	~	~	~	~	~
	Drain -u/s	3.12	1.67	~	14.1	~	~	~	~	~	~	~

	Drain - mid	3.07	1.67	~	13.6	~	~	~	~	~	~	~
	Drain - d/s	3.06	1.85	~	12.7	~	~	~	~	~	~	~
294	OH1	2.93	2.2	0.24	15.9	~	~	~	~	~	~	~
	OH2	3.16	1..25	0.17	14.8	~	~	~	~	~	~	~
	OH3	3.13	1.33	0.23	14.4	~	~	~	~	~	~	~
	OH4	~	~	0.94	~	~	~	~	~	~	~	~
	OH5	3.42	1.2	0.24	15	~	~	~	~	~	~	~
	OH6	~	~	0.96	~	~	~	~	~	~	~	~
	OH7	~	~	0.93	~	~	~	~	~	~	~	~
	OH8	3.12	1.27	0.21	14.8	~	~	~	~	~	~	~
	OH9	3.18	1.14	0.24	14.5	~	~	~	~	~	~	~
	OH10	3.13	1.3	0.19	14.5	~	~	~	~	~	~	~
	OH11	3.15	1.24	0.25	14.6	~	~	~	~	~	~	~
	OH12	3.23	1.32	0.25	14.6	~	~	~	~	~	~	~
	OH13	3.29	1.2	0.22	14.5	~	~	~	~	~	~	~
	OH14	3.1	1.33	0.235	14.6	~	~	~	~	~	~	~
	OH15	3.01	1.4	0.25	14.7	~	~	~	~	~	~	~
	OH16	3.2	1.29	0.24	14.9	~	~	~	~	~	~	~
	OH17	3.09	1.38	0.28	14.9	~	~	~	~	~	~	~
	OH18	3.01	1.53	0.25	14.9	~	~	~	~	~	~	~

	OH19	3.19	1.26	0.25	14.9	~	~	~	~	~	~	~
	OH20	3.04	1.63	0.26	14.8	~	~	~	~	~	~	~
	OH21	3.01	1.4	0.27	14.9	~	~	~	~	~	~	~
	OH22	3.04	1.67	0.285	14.8	~	~	~	~	~	~	~
	OH23	3.01	1.89	0.25	14.5	~	~	~	~	~	~	~
	OH24	2.96	1.97	0.28	14.6	~	~	~	~	~	~	~
	OH25	2.97	1.85	0.25	14.7	~	~	~	~	~	~	~
	OH26	3.28	1.01	0.23	13.9	~	~	~	~	~	~	~
	OH27	4.97	1.03	0.205	14.6	~	~	~	~	~	~	~
	OH28	4.76	1.09	0.22	15.2	~	~	~	~	~	~	~
	OH29	3.8	1.34	0.21	14.9	~	~	~	~	~	~	~
	OH30	3.78	1.36	0.22	14.3	~	~	~	~	~	~	~
	OH31	3.17	1.73	0.26	14.5	~	~	~	~	~	~	~
	Drain -u/s	3.03	1.64		11.8	~	~	~	~	~	~	~
	Drain - mid	3.16	1.57		12.5	~	~	~	~	~	~	~
	Drain - d/s	3.15	1.79		12	~	~	~	~	~	~	~
300	OH1	3.33	2.41	~	12.7	~	~	~	~	~	~	~
	OH2	3.15	1.46	~	13.5	~	~	~	~	~	~	~
	OH3	3.36	1.27	~	13.9	~	~	~	~	~	~	~
	OH4	-	-	~	-	~	~	~	~	~	~	~

	OH5	3.87	1.17	~	13.5	~	~	~	~	~	~	~
	OH6	-	-	~	-	~	~	~	~	~	~	~
	OH7	-	-	~	-	~	~	~	~	~	~	~
	OH8	3.25	1.2	~	14.1	~	~	~	~	~	~	~
	OH9	3.26	1.17	~	14.1	~	~	~	~	~	~	~
	OH10	3.45	0.58	~	13.4	~	~	~	~	~	~	~
	OH11	3.29	1.25	~	13.6	~	~	~	~	~	~	~
	OH12	3.25	1.35	~	14.1	~	~	~	~	~	~	~
	OH13	3.29	1.21	~	13.8	~	~	~	~	~	~	~
	OH14	3.12	1.34	~	14.1	~	~	~	~	~	~	~
	OH15	3.21	1.35	~	14.3	~	~	~	~	~	~	~
	OH16	3.24	1.26	~	14.7	~	~	~	~	~	~	~
	OH17	3.04	1.42	~	14.5	~	~	~	~	~	~	~
	OH18	2.97	1.61	~	14.4	~	~	~	~	~	~	~
	OH19	3.15	1.3	~	14.7	~	~	~	~	~	~	~
	OH20	3.03	1.75	~	14.5	~	~	~	~	~	~	~
	OH21	3	1.45	~	14.8	~	~	~	~	~	~	~
	OH22	3.07	1.67	~	14.5	~	~	~	~	~	~	~
	OH23	3.03	2.03	~	14.4	~	~	~	~	~	~	~
	OH24	2.94	2.07	~	14.1	~	~	~	~	~	~	~

	OH25	2.95	1.99	~	14.3	~	~	~	~	~	~	~
	OH26	3.25	1.05	~	13.8	~	~	~	~	~	~	~
	OH27	4.98	1.11	~	14.5	~	~	~	~	~	~	~
	OH28	4.8	1.28	~	14.1	~	~	~	~	~	~	~
	OH29	3.89	1.11	~	14	~	~	~	~	~	~	~
	OH30	3.91	1.3	~	14.1	~	~	~	~	~	~	~
	OH31	3.22	1.74	~	13.8	~	~	~	~	~	~	~
	Drain -u/s	3.21	1.45		10.5	~	~	~	~	~	~	~
	Drain - mid	3.34	1.8		10.4	~	~	~	~	~	~	~
	Drain - d/s	2.98	1.48		10.3	~	~	~	~	~	~	~
329	OH1	3.23	2.83	0.1	13.1	~	~	~	~	~	~	~
	OH2	3.47	2.1	0.06	12.7	~	~	~	~	~	~	~
	OH3	3.4	1.5	0.09	12.7	~	~	~	~	~	~	~
	OH4					~	~	~	~	~	~	~
	OH5	3.59	1.38	0.07	12.8	~	~	~	~	~	~	~
	OH6					~	~	~	~	~	~	~
	OH7			0.93		~	~	~	~	~	~	~
	OH8	3.32	1.54		12.8	~	~	~	~	~	~	~
	OH9	3.25	1.31	0.13	13.1	~	~	~	~	~	~	~
	OH10	3.26	1.38	0.09	12.9	~	~	~	~	~	~	~

	OH11	3.22	1.52	0.1	12.9	~	~	~	~	~	~	~
	OH12	3.53	1.3	0.11	13.2	~	~	~	~	~	~	~
	OH13	5.54	2.14	0.09	13.6	~	~	~	~	~	~	~
	OH14	4.83	1.26	~	13.2	~	~	~	~	~	~	~
	OH15	3.35	1.34	0.08	13.5	~	~	~	~	~	~	~
	OH16	5.12	1.16	0.07	13.4	~	~	~	~	~	~	~
	OH17	3.24	1.35	0.13	13.5	~	~	~	~	~	~	~
	OH18	3.09	1.63	0.1	13.5	~	~	~	~	~	~	~
	OH19	4.91	0.96	0.2	13.3	~	~	~	~	~	~	~
	OH20	3.24	1.62	0.14	13.1	~	~	~	~	~	~	~
	OH21	3.13	2.45	0.13	13.1	~	~	~	~	~	~	~
	OH22	3.27	2.41	0.135	13.5	~	~	~	~	~	~	~
	OH23	3.1	2.22	0.11	13.2	~	~	~	~	~	~	~
	OH24	3.32	1.13	0.14	13	~	~	~	~	~	~	~
	OH25	4.5	1.26	0.1	13.6	~	~	~	~	~	~	~
	OH26	4.53	1.17	0.08	13.8	~	~	~	~	~	~	~
	OH27	4.92	1.38	0.055	12.7	~	~	~	~	~	~	~
	OH28	4.75	1.58	0.03	13.3	~	~	~	~	~	~	~
	OH29	~	~	0.09	~	~	~	~	~	~	~	~
	OH30	~	~	0.03	~	~	~	~	~	~	~	~

	OH31	3.37	2.52	0.08	13.1	~	~	~	~	~	~	~
	Drain -u/s	~	~	~	~	~	~	~	~	~	~	~
	Drain - mid	~	~	~	~	~	~	~	~	~	~	~
	Drain - d/s	~	~	~	~	~	~	~	~	~	~	~
353	OH1	3.27	2.4	0.2	11.4	21.5	14.9	21	78	425.3	398	1.0685
	OH2	3.27	1.13	0.11	11.9	16.1	24.3	7.6	74	94.53	71.6	1.3203
	OH3	3.42	1.38	0.14	11.7	10.5	19.2	30.8	78	155.9	228	0.6836
	OH4	3.54	1.1	~	11.9	53.7	20.6	22.4	86	130.8	287	0.4557
	OH5	3.42	1.41	0.15	12.2	61.2	20.2	12.7	89	164	222	0.7389
	OH6	3.47	1.45	~	12	58	22.9	17.2	97	185.8	286	0.6495
	OH7	3.31	1.32	~	12.2	59.3	27.9	10.1	109	131.8	213	0.6186
	OH8	3.25	1.46	0.17	12.4	20.5	19.9	16.2	101	176	277	0.6352
	OH9	3.23	1.29	0.21	12.3	6.7	3.1	29.6	81	117	185	0.6325
	OH10	3.42	1.21	0.09	12.1	53.9	25.8	12.2	100	126.5	176	0.7189
	OH11	3.22	1.38	0.23	12.2	31.3	21.4	20.7	100	140.3	154	0.9111
	OH12	3.45	1.31	0.22	12.2	71.1	24.9	15.8	106	135.5	229	0.5919
	OH13	3.61	1.31	0.09	12.4	19.5	28.6	18	117	143.6	177	0.8111
	OH14	4.46	~	0.175	12.4	21.2	21.3	21.3	114	141.1	143	0.9867
	OH15	3.45	1.26	0.18	13	55.3	22.7	13.2	114	138.9	185	0.7509
	OH16	3.45	1.2	0.15	12.5	59.3	23	11.7	110	124.1	279	0.4449

	OH17	3.18	1.37	0.22	12.5	23	21.7	14.5	121	188.8	147	1.284
	OH18	3.18	1.41	0.19	12.6	33	21.1	21.5	133	178.6	243	0.7351
	OH19	5.52	0.93	0.2	12.4	15.9	2.4	79.9	117	104.5	136	0.7685
	OH20	3.79	1.69	0.19	12.9	17.9	14.2	27.4	142	284.5	269	1.0575
	OH21	3.25	1.34	0.18	12.5	19.3	22.5	18.3	146	197.3	210	0.9394
	OH22	3.35	1.57	0.235	12.1	12.6	18.1	18.3	141	210.1	317	0.6628
	OH23	3.32	2.03	0.25	12.5	46.4	14.7	28.5	161	408	262	1.5572
	OH24	3.14	1.91	0.2	12.2	22.5	19.3	19.9	149	333.2	330	1.0097
	OH25	3.42	1.66	0.17	12	35.8	17.4	21.7	154	336.5	248	1.3567
	OH26	3.38	1.07	0.18	12.2	13.5	22.2	49.4	147	100.7	319	0.3156
	OH27	4.28	0.98	0.195	12.4	14.7	26.2	15	149	117.3	362	0.3241
	OH28	4.47	1.21	0.21	12.8	62.5	24.7	8.3	150	117.7	361	0.3259
	OH29	3.68	1.48	0.16	11.3	64.4	15.5	19.5	161	213.7	373	0.573
	OH30	3.71	1.64	0.08	11.7	97	16.3	27.9	175	277.5	391	0.7098
	OH31	3.26	2.23	0.16	12	21.8	18.5	18.9	176	460.1	374	1.2303
	Drain -u/s	~	~	~	~	5.5	4	13.6	153	107.6	114	0.9434
	Drain - mid	~	~	~	~	16.2	5.1	16.2	155	121.2	134	0.9042
	Drain - d/s	~	~	~	~	7.7	8.3	22.9	176	399.8	367	1.0893
378	OH1	3.24	1.82	0.1	11.2	~	~	~	~	~	~	~
	OH2	3.76	1.92	0.06	11.3	~	~	~	~	~	~	~

	OH3	3.52	1.53	0.09	11.4	~	~	~	~	~	~	~
	OH4	4.58	1.29	0.03	11.6	~	~	~	~	~	~	~
	OH5	3.25	1.5	0.05	11.6	~	~	~	~	~	~	~
	OH6	4.61	1.42	0.08	11.9	~	~	~	~	~	~	~
	OH7	4.73	1.38	0.06	11.9	~	~	~	~	~	~	~
	OH8	4.45	1.61	0.09	11.7	~	~	~	~	~	~	~
	OH9	3.86	1.29	0.13	11.7	~	~	~	~	~	~	~
	OH10	3.86	1.26	0.04	12.1	~	~	~	~	~	~	~
	OH11	3.37	1.25	0.11	12.1	~	~	~	~	~	~	~
	OH12	3.85	1.29	0.05	111.9	~	~	~	~	~	~	~
	OH13	5.88	1.85	0.09	11.9	~	~	~	~	~	~	~
	OH14	3.53	1.54	0.035	12	~	~	~	~	~	~	~
	OH15	5.25	1.44	0.06	12.2	~	~	~	~	~	~	~
	OH16	3.46	1.33	0.09	12.4	~	~	~	~	~	~	~
	OH17	4	1.29	0.14	12.2	~	~	~	~	~	~	~
	OH18	3.02	1.3	0.1	12.2	~	~	~	~	~	~	~
	OH19	5.57	0.89	0.15	12.1	~	~	~	~	~	~	~
	OH20	3.51	1.61	0.16	12.2	~	~	~	~	~	~	~
	OH21	3.05	1.37	0.12	12	~	~	~	~	~	~	~
	OH22	3.24	1.51	0.135	12.1	~	~	~	~	~	~	~

	OH23	3.08	2.16	0.12	11.6	~	~	~	~	~	~	~
	OH24	3.19	2.07	0.14	11.6	~	~	~	~	~	~	~
	OH25	3.24	1.7	0.11	11.8	~	~	~	~	~	~	~
	OH26	3.19	1.16	0.08	11.9	~	~	~	~	~	~	~
	OH27	4.75	1.29	0.015	12.3	~	~	~	~	~	~	~
	OH28	4.56	1.05	-0.03	12.6	~	~	~	~	~	~	~
	OH29	4.04	1.28	0.02	11.2	~	~	~	~	~	~	~
	OH30	4.1	1.37	0.02	11.9	~	~	~	~	~	~	~
	OH31	3.27	2.06	0.11	11.7	~	~	~	~	~	~	~
	Drain -u/s	3.14	1.66	~	8.2	~	~	~	~	~	~	~
	Drain - mid	~	~	~		~	~	~	~	~	~	~
	Drain - d/s	~	~	~		~	~	~	~	~	~	~
397	OH1	3.53	2.07	0.1	11.5	~	~	~	~	~	~	~
	OH2	4.65	1.53	0.11	11.4	52.5	37.5	~	46	~	~	~
	OH3	3.59	1.14	0.14	11.6	14.1	11.5	90	43	~	~	~
	OH4	3.67	1.18	0.08	11.8	74	25.2	58	49	~	~	~
	OH5	3.86	1.34	0.1	11.7	57.8	17.9	69	96	~	~	~
	OH6	3.7	1.33	0.13	11.9	62.3	28.1	62	81	~	~	~
	OH7	3.71	1.25	0.11	11.9	64.2	20.9		49	~	~	~
	OH8	4.08	1.45	0.04	11.9	27.1	26.4	69	48	~	~	~

	OH9	3.58	1.27	0.23	11.8	~	22.1	72	60	~	~	~
	OH10	3.82	1.28	0.09	11.8	57.2	24.2	49	36	~	~	~
	OH11	3.68	1.32	0.16	11.9	55.9	27.9	54	31	~	~	~
	OH12	3.73	1.27	0.15	12	86.3	29	54	44	~	~	~
	OH13	5.51	2.05	0.14	12.2	7.6	4.5	75	44	~	~	~
	OH14	3.79	1.26	0.185	12	~	26.5	62	37	~	~	~
	OH15	4.98	1.3	0.16	12.2	~	22.2	82	44	~	~	~
	OH16	3.87	1.26	0.09	12.1	67.8	25.6	22	24.5	~	~	~
	OH17	4.17	1.29	0.19	12.2	13.9	1	40	13.9	~	~	~
	OH18	3.57	1.38	0.15	12.2	37.8	20.7	68	22.5	~	~	~
	OH19	5.65	0.97	0.2	11.9	11.7	5.9	98	12.5	~	~	~
	OH20	3.3	1.55	0.16	12.1	20.1	13.4	83	39.5	~	~	~
	OH21	3.21	1.33	0.17	12	~	23.5	58	35.2	~	~	~
	OH22	3.68	1.53	0.185	11.8	19.3	23	66	31.9	~	~	~
	OH23	3.68	1.97	0.17	11.9	47	11.7	87	35	~	~	~
	OH24	4.03	1.93	0.19	11.8	24.8	17.1	72	32	~	~	~
	OH25	3.3	1.62	0.16	11.8	17.3	19.4	77	32.6	~	~	~
	OH26	3.15	1.14	0.13	11.9	25.2	24.5	58	23.1	~	~	~
	OH27	4.27	1.1	0.115	12.2	14.9	21.2	51	21.6	~	~	~
	OH28	3.79	1.03	0.12	12.6	70.1	24.9	40	21.4	~	~	~

	OH29	5.18	1.34	0.17	11.4	88.3	18.6	57	29.7	~	~	~
	OH30	3.78	1.3	0.07	11.9	68.9	11	67	23.9	~	~	~
	OH31	4.42	1.65	0.16	11.6	42.3	20.8	50	32.6	~	~	~
	Drain -u/s	3	1.66	~	11.2	77.1	33.2	58	31.3	~	~	~
	Drain - mid	~	~	~	~	73	7.4	78	29.4	~	~	~
	Drain - d/s	~	~	~	~	~	8.7	73	36.7	~	~	~
435	OH1	4.26	1.64	0.3	12.6	~	~	~	~	~	~	~
	OH2	5.67	2.62	0.26	12.3	~	~	~	~	~	~	~
	OH3	5.01	1.12	0.32	12.4	~	~	~	~	~	~	~
	OH4	4.23	1.18	0.26	12.5	~	~	~	~	~	~	~
	OH5	5.16	1.45	0.3	12.5	~	~	~	~	~	~	~
	OH6	4.61	1.4	0.33	12.5	~	~	~	~	~	~	~
	OH7	4.65	1.54	0.36	12.6	~	~	~	~	~	~	~
	OH8	~	~	~	~	~	~	~	~	~	~	~
	OH9	4.64	0.95	0.36	12.6	~	~	~	~	~	~	~
	OH10	~	~	~	~	~	~	~	~	~	~	~
	OH11	5.02	1.32	0.36	12.6	~	~	~	~	~	~	~
	OH12	4.79	1.49	0.35	12.7	~	~	~	~	~	~	~
	OH13	5.68	2.21	0.34	12.7	~	~	~	~	~	~	~
	OH14	4.79	1.42	0.335	12.6	~	~	~	~	~	~	~

	OH15	4.39	1.39	0.33	12.7	~	~	~	~	~	~	~
	OH16	4.32	1.26	0.34	12.8	~	~	~	~	~	~	~
	OH17	4.52	1.28	0.36	12.7	~	~	~	~	~	~	~
	OH18	~	~	~	~	~	~	~	~	~	~	~
	OH19	5.23	1.03	0.35	12.6	~	~	~	~	~	~	~
	OH20	4.18	1.57	0.35	12.7	~	~	~	~	~	~	~
	OH21	4.19	1.19	0.36	12.8	~	~	~	~	~	~	~
	OH22	4.51	1.53	0.355	12.6	~	~	~	~	~	~	~
	OH23	5.1	1.92	0.35	12.5	~	~	~	~	~	~	~
	OH24	4.51	2.04	0.38	12.5	~	~	~	~	~	~	~
	OH25	4.21	1.82	0.31	12.5	~	~	~	~	~	~	~
	OH26	3.67	1.14	0.29	12.4	~	~	~	~	~	~	~
	OH27	4.21	1.1	0.315	12.8	~	~	~	~	~	~	~
	OH28	3.87	1.17	0.32	13.1	~	~	~	~	~	~	~
	OH29	5.18	1.32	0.31	12.2	~	~	~	~	~	~	~
	OH30	4.88	1.53	0.24	12.3	~	~	~	~	~	~	~
	OH31	4.74	2.09	0.34	12.8	~	~	~	~	~	~	~
	Drain -u/s	3.42	0.96	~	11.6	~	~	~	~	~	~	~
	Drain - mid	3.22	1.14	~	12.4	~	~	~	~	~	~	~
	Drain - d/s	3.17	1.41	~	11.6	~	~	~	~	~	~	~

Appendix D: Water Quality Data – Floodgate and Weir Sites

D.1: Floodgate Sites
Note: ~ reading not taken; n/a reading not applicable

		FG1			FG2			FG3			FG4		
Day Number	**Species**	**C/W**	**D/W**	**G/W**	**C/W**	**D/W**	**G/W**	**C/W**	**D/W**	**G/W**	**C/W**	**D/W**	**G/W**
0	Total Fe (mg/L)	3.4	28.4	~	5.05	5.63	~		3.37	821	28.3	29.9	~
	Al3+ (mg/L)	3.3	4.5	~	3.7	15.6	~		11.6	639	4.1	45.9	~
	Ca2+ (mg/L)	75	77	~	95	76	~		36	28	56	28.6	~
	Mg2+ (mg/L)	410	400	~	480	370	~		240	713	5850	116	~
	Cl (mg/L)	4,936.2	~	~	6,406	4510.3	~	3647.5	1,825	1347.6	6078.2	1461. 3	~
	SO4 (mg/L)	500	~	~	637	745	~	466	353	571	1050	965	~
	Cl:SO4	9.872			10.057	6.054		7.827	5.169	2.360	5.789	1.514	
	pH	7.29	6.99	~	6.56	3.88	~	6.48	5.61	4.28	4.43	2.73	~
	Conductivity (mS)	15.17	14.03	~	17.5	13.1	~	10.52	9.1	2.45	16.9	a	~
	Groundwater table elevation (m below ground surface)	n/a	n/a	-1.7	n/a	n/a	-2.2	n/a	n/a	-1	n/a	n/a	~

	Temperature (C)	11.4	11.5	a	13.5	11.2	a	11.4	12.1	12.2	11.7	9.5	
14	Total Fe (mg/L)	4.9	6	53.5	4.5	13.2	133.2	5.2	3.5	17.9	6.1	31.5	20.7
	Al3+ (mg/L)	4.9	7.2	10.1	4.1	15	18.2	3.8	13	66.2	4.2	27.9	49.2
	Ca2+ (mg/L)	43	54	70	58	47	64	2	1	23	102	43	38
	Mg2+ (mg/L)	7360	7320	6880	8710	970	7510	8240	441	48.4	10200	9410	8870
	Cl (mg/L)	4963.7	6183.9	5073.7	8050.8	6543.4	1950.9	8237.6	5805.2	134.2	8722.4	5040.1	2547.5
	SO4 (mg/L)	590	739	1650	994	1020	618	1040	506	1130	1310	1080	505
	Cl:SO4	8.413	8.368	3.075	8.099	6.415	3.157	7.921	11.473	0.119	6.658	4.667	5.045
	pH	6.37	5.71	5.55	6.27	3.62	5.71	7.8	5.99	6.17	6.03	5.85	3.69
	Conductivity (mS)	a	16.99	17.25	20.41	17.35	5.99	a	10.65	9.23	20.36	6.58	2.07
	Groundwater table elevation (m below ground surface)	n/a	n/a	-2.45	n/a	n/a	-2.15	n/a	n/a	-2.4	n/a	n/a	-1.7
	Temperature (C)	9.7	12.1	14.1	11.2	11.9	14.1	14.1	13.5	17	13.2	12.4	13.7
28	Total Fe (mg/L)	5.8	4.2	22.7	30.3	18.4	160	3.6	70.1	54.1	3.8	7.7	334
	Al3+ (mg/L)	10.4	11.3	14.2	19.8	19.4	25.5	17.4	43	21.5	23.5	28.1	54.7
	Ca2+ (mg/L)	137	281	15	197	241	165	213	131	137	179	148	59
	Mg2+ (mg/L)	516	956	1660	755	891	1410	1940	523	465	2020	2040	1800
	Cl (mg/L)	7,328	6,362	7,041	8,169	7,584	2,098	10,071	4,367	2,858	7,884	6,288	74
	SO4 (mg/L)	783	1,040	1,690	1,200	1,210	667	1,420	1,130	490	1,320	772	1,790
	Cl:SO4	9.359	6.118	4.166	6.807	6.268	3.145	7.092	3.865	5.833	5.973	8.145	0.041

	pH	7.06	6.93	5.98	6.86	4	3.75	6.9	3.2	7.1	6.96	5.63	3.98
	Conductivity (mS)	11.8	12.1	11.84	10.23	8.48	3.18	13.28	10.45	5.95	14.95	12.29	1.69
	Groundwater table elevation (m below ground surface)	n/a	n/a	-1.5	n/a	n/a	-1.5	n/a	n/a	-1.55	n/a	n/a	-1.7
	Temperature (C)	11	11.3	12.3	8.8	7.9	9.8	13.6	5.95	16.1	13.4	12.4	12.9
42	Total Fe (mg/L)	2.5	3.4	108	2.2	3.3	107	1.8	11.2	2.9	2.4	3.7	226
	Al3+ (mg/L)	1	1	1.7	1.4	3.9	8.8	1	10.4	1.4	1.4	2.9	52.5
	Ca2+ (mg/L)	195	206	282	236	192	167	200	134	102	188	202	85
	Mg2+ (mg/L)	65.9	68.6	13.3	75.2	67.9	14.1	18.8	55.6	38	20.3	21.7	16.8
	Cl (mg/L)	9410.8	12438.3	7483.9	11019.3	10335.7	1364	10864.6	10000.1	248.8	10124.9	8296.6	2856.2
	SO4 (mg/L)	1310	1520	2330	1350	1540	620	1960	1980	1380	1540	1340	473
	Cl:SO4	7.184	8.183	3.212	8.162	6.711	2.200	5.543	5.051	0.180	6.575	6.192	6.038
	pH	6.89	6.66	5.48	6.99	4.1	5.88	6.95	5.62	6.91	6.72	6.08	3.72
	Conductivity (mS)	10.88	9.62	7.52	2.91	1.94	0.71	13.6	12.1	6.14	10.89	10.12	1.61
	Groundwater table elevation (m below ground surface)	n/a	n/a	-1.95	n/a	n/a	-1.6	n/a	n/a	-1.03	n/a	n/a	-1.8
	Temperature (C)	12.7	12.7	12.1	11.4	10.4	11.7	13.6	13.5	13.9	14.3	14.3	13
56	Total Fe (mg/L)	1.1	1.6	143	1.2	3	5	1.3	3.1	10.7	1.5	134	302
	Al3+ (mg/L)	0.4	1	12.4	0.8	0.7	5.8	0.6	4.1	13.3	1.6	47.7	354

	Ca2+ (mg/L)	319	215	270	299	228	169	308	144	242	296	240	22
	Mg2+ (mg/L)	926	716	686	925	783	417	970	471	806	980	903	260
	Cl (mg/L)	9760.9	~	8170.9	11013.5	8401.1	2749.9	10428	3012.9	8810	9799.7	9026.3	~
	SO4 (mg/L)	2100	~	2080	2080	1450	605	1870	497	1510	1580	1610	~
	Cl:SO4	4.648	~	3.928	5.295	5.794	4.545	5.576	6.062	5.834	6.202	5.606	~
	pH	7.01	6.73	5	7.24	5.19	5.96	7.24	3.25	7.07	6.88	6.36	4.56
	Conductivity (mS)	20.45	19.74	13.33	18.36	15.41	5.39	22.9	16.86	8.44	20.97	19.64	1.77
	Groundwater table elevation (m below ground surface)	n/a	n/a	-1.9	n/a	n/a	-2.1	n/a	n/a	-0.95	n/a	n/a	-1.85
	Temperature (C)	~	~	~	~	~	~	~	~	~	~	~	~
70	Total Fe (mg/L)	2.2	123.3	5	4.6	76.1	80.7	3.8	2.5	2.8	1	15.6	248
	Al3+ (mg/L)	0.2	10.5	17.7	10.9	3	14.3	11.1	2.9	0.6	0.6	16.3	110.5
	Ca2+ (mg/L)	204	317	219	171	118	138	233	288	170	214	163	204
	Mg2+ (mg/L)	665	542	586	603	570	230	680	930	360	658	619	724
	Cl (mg/L)	9527.6	9446.5	7237.5	9754.1	10127.4	1818.3	11180.4	10,754	2839.2	10344.2	9315.5	105.9
	SO4 (mg/L)	1570	1710	2080	1730	1880	658	2150	2,060	529	1600	1680	1180
	Cl:SO4	6.069	5.524	3.480	5.638	5.387	2.763	5.200	5.220	5.367	6.465	5.545	0.090
	pH	6.96	6.95	5.05	7.49	6.16	6.05	6.97	3.77	7	6.75	6.04	4.94
	Conductivity (mS)	16.5	16.93	13.25	14.5	14.74	5.45	19.87	11.86	8.23	18.65	15.67	1.82

	Groundwater table elevation (m below ground surface)	n/a	n/a	-1.95	n/a	n/a	-1.6	n/a	n/a	-1	n/a	n/a	-1.8
	Temperature (C)	11.8	13.2	13	10.2	10.7	11.8	12.8	12	12.6	14.1	14	11.7
84	Total Fe (mg/L)	3.1	4.4	115.8	2.4	362	80.4	~	10.2	~	~	0.6	~
	Al3+ (mg/L)	7.9	1	18.2	0.5	44.2	8.8	35.2	10.4	11.6	9.3	0.6	19.4
	Ca2+ (mg/L)	213	163	284	163	51	136	~	180	~	~	131	~
	Mg2+ (mg/L)	761	797	543	802	129	303	~	670	~	~	486	~
	Cl (mg/L)	10,333	10,423	7,703	11,509	10,271	1,999	11,488	10,359	29.187	10,095	10,075	110
	SO4 (mg/L)	1,500	1,690	2,050	1,620	1,520	617	1,640	1,540	526	1,370	1,400	1,110
	Cl:SO4	6.889	6.167	3.757	7.105	6.757	3.240	7.005	6.727	0.055	7.368	7.196	0.099
	pH	6.74	6.52	3.87	7.18	6.03	4.04	6.63	4.29	6.26	6.15	5.64	2.83
	Conductivity (mS)	18.16	18.54	13.77	19.36	15.42	4.16	23.46	19.92	8.55	20.15	18.37	1.89
	Groundwater table elevation (m below ground surface)	n/a	n/a	-1.64	n/a	n/a	-1.7	n/a	n/a	-0.89	n/a	n/a	-1.9
	Temperature (C)	~	15.3	13.5	15.2	12.2	11.7	16	16.2	14.4	17.1	16.2	12.6
99	Total Fe (mg/L)	5.2	134.2	195	0.7	542	5.7	2.7	3.7	4.4	0.1	433	67.4
	Al3+ (mg/L)	5.9	61.4	8.6	5.2	27.5	7.2	5.2	5.9	6.3	0.5	159	3.1
	Ca2+ (mg/L)	168	281	164	191	216	184	223	226	93	241	19	136
	Mg2+ (mg/L)	560	761	747	712	830	698	915	917	352	791	240	277

	Cl (mg/L)	11350.1	9903.1	8167.1	9950	9590.7	3411.5	12459.7	12299.8	5030.9	12103.1	11619.6	90.4
	SO4 (mg/L)	1500	1990	1810	1860	2470	594	2090	2350	548	1920	1510	1100
	Cl:SO4	7.567	4.976	4.512	5.349	3.883	5.743	5.962	5.234	9.181	6.304	7.695	0.082
	pH	6.05	6.46	3.66	7.18	3.38	4.82	6.86	6.67	5.06	5.45	5.93	5.31
	Conductivity (mS)	19.33	18.14	13.62	17.25	15.07	3.93	23.84	23.44	8.23	19.26	15.47	1.39
	Groundwater table elevation (m below ground surface)	n/a	n/a	-1.74	n/a	n/a	-1.7	n/a	n/a	-0.97	n/a	n/a	-1.9
	Temperature (C)	15.9	15.6	13.7	15.4	13.3	12.3	17.5	~	17.5	17.3	~	~
125	Total Fe (mg/L)	7.4	10.2	85.6	4.3	8.7	84.2	16.2	18.2	0.52	~	1	17
	Al3+ (mg/L)	14.9	11.7	61.3	2.2	19.3	8.6	16.8	19.6	2.8	~	5.2	69.4
	Ca2+ (mg/L)	12	12	222	15	39	81	17	42	106	~	9.3	44
	Mg2+ (mg/L)	117	95	729	152	182	244	210	194	563	~	219	264
	Cl (mg/L)	207	193	8,745	499	752	1,073	873	1,294	2,839	~	66	88
	SO4 (mg/L)	207	225	1,570	103	531	867	161	639	595	~	95	788
	Cl:SO4	1.001	0.859	5.570	4.845	1.416	1.238	5.422	2.025	4.771	~	0.694	0.112
	pH	4.81	4.46	4.81	6.75	4.3	5.19	6.63	4.1	7.38	~	5.6	4.15
	Conductivity (mS)	0.94	11.45	1.41	1.27	2.22	2.23	2.24	3.52	6.79	~	0.36	1.11
	Groundwater table elevation (m below ground surface)	n/a	n/a	-1.79	n/a	n/a	-1.09	n/a	n/a	-0.7	n/a	n/a	-1.3

	Temperature (C)	21.9	21.4	20.4	20.7	20.6	19	23.2	23.2	20.9	~	24	21.9
140	Total Fe (mg/L)	5.5	68.4	73.3	0.66	6.9	65.3	139.9	3.2	1.27	35.5	2	119.3
	Al3+ (mg/L)	58.2	62.5	108.5	40.4	0.8	7.7	25.2	149.6	6.8	1.2	13	67.8
	Ca2+ (mg/L)	90	49	176	107	55	77	122	102	75	50	85	58
	Mg2+ (mg/L)	482	384	731	585	363	382	699	584	414	427	528	310
	Cl (mg/L)	5,982	3,979	8,994	6,014	3,614	1,119	7,470	8,085	3,335	4,154	4,208	87
	SO4 (mg/L)	676	616	1,570	993	577	952	909	1,080	579	678	544	1,080
	Cl:SO4	8.85	6.46	5.728	6.056	6.263	1.175	8.217	7.486	5.760	6.127	7.736	0.080
	pH	6.18	4.11	3.93	6.59	4.73	4.37	~	~	~	~	~	~
	Conductivity (mS)	11.99	8.65	14.25	12.54	7.53	3.41	~	~	~	~	~	~
	Groundwater table elevation (m below ground surface)	n/a	n/a	-1.64	n/a	n/a	-1.39	n/a	n/a	-0.8	n/a	n/a	-1.63
	Temperature (C)	26.4	24.7	21.6	24.4	23.5	19.4	~	~	~	~	~	~
210	Total Fe (mg/L)	13.9	1.8	145	~	~	~	1.24	18.8	1.41	1.5	1.74	131.2
	Al3+ (mg/L)	26.3	3.5	5.7	~	~	~	2.7	5.9	3	3.9	3.8	21
	Ca2+ (mg/L)	12	194	250	~	~	~	18	137	112	11	1	87
	Mg2+ (mg/L)	353	993	979	~	~	~	363	796	569	326	310	403
	Cl (mg/L)	1,224	9,741	8,153	~	~	~	1,373	201	3,052	670	7,674	91
	SO4 (mg/L)	157	1,500	1,840	~	~	~	176	71	514	109	1,220	1,240
	Cl:SO4	7.797	6.494	4.431	~	~	~	7.800	2.825	5.938	6.143	6.290	0.073

	pH	6.81	5.92	4.6	~	~	~	~	~	~	~	~	~
	Conductivity (mS)	4.18	17.92	16.12									
	Groundwater table elevation (m below ground surface)	n/a	n/a	1.74	n/a	n/a	0.87	n/a	n/a	1.6	n/a	n/a	1.02
	Temperature (C)	21.1	21.8	20.9	~	~	~	~	~	~	~	~	~
251	Total Fe (mg/L)	7	6.2	96.1	~	~	~	3.5	4.1	5.5	~	~	~
	Al3+ (mg/L)	3.6	3.4	0.7	~	~	~	0.9	1.4	0.3	~	~	~
	Ca2+ (mg/L)	103	125	241	~	~	~	96	227	170	~	~	~
	Mg2+ (mg/L)	180	197	734	~	~	~	191	214	509	~	~	~
	Cl (mg/L)	105	120	8,327	~	~	~	251	373	3,130	~	~	~
	SO4 (mg/L)	23	26	1,140	~	~	~	44	74	497	~	~	~
	Cl:SO4	4.644	4.597	7.305	~	~	~	5.76	5.073	6.297	~	~	~
	pH	6.59	6.38	5.05	~	~	~	6.58	6.32	6.56	~	~	~
	Conductivity (mS)	~	~	~	~	~	~	~	~	~	~	~	~
	Groundwater table elevation (m below ground surface)	n/a	n/a	-1.64	n/a	n/a	~	n/a	n/a	-0.67	n/a	n/a	~
	Temperature (C)	~	~	~	~	~	~	~	~	~	~	~	~
353	Total Fe (mg/L)	4.6	4.4	95.8	3.9	8.5	102.4	48.1	64.7	6.4	4.1	16.4	~
	Al3+ (mg/L)	1.9	9.4	3.8	0.2	0.9	9.1	86	8.3	0.3	1.2	18.6	~

Ca2+ (mg/L)	266.1	107.8	203.3	260.1	269.6	86.5	256.4	325.2	137.4	211.1	78.2	~
Mg2+ (mg/L)	962	407	626	950	958	289	1016	1172	430	763	351	~
Cl (mg/L)	10,175	4,997	7,224	12,221	10,166	1,330	12,363	8,322	3,101	8,658	1,537	116
SO4 (mg/L)	1,560	911	1,180	1,720	1,480	563	1,950	2,040	555	1,060	582	2,040
Cl:SO4	6.522	5.485	6.122	7.105	6.869	2.363	6.34	4.08	5.588	8.168	2.64	0.057
pH	6.74	4.69	4.04	6.84	7.32	5.96	6.99	6.81	7.02	~	~	~
Conductivity (mS)	~	14.31	19.72	~	~	5.46	~	~	9.47	~	~	~
Groundwater table elevation (m below ground surface)	~	~	-2.25	~	~	-1.04	~	~	-0.9	~	~	-1.9
Temperature (C)	7.6	7.5	13.5	8	5.9	11.2	8.2	9.2	12.8	~	~	~

D.2: Weir Sites
Note: ~ reading not taken; n/a reading not applicable

		WS1		WS2	
Day Number	**Species**	**D/W**	**G/W**	**D/W**	**G/W**
0	Total Fe (mg/L)	23.4	365	5.22	435
	Al3+ (mg/L)	22.9	299	3.6	1222
	Ca2+ (mg/L)	2.8	2.2	21.5	0.2
	Mg2+ (mg/L)	21	5820	88	86
	Cl (mg/L)	1,288	384	43.8	122.5
	SO4 (mg/L)	575	1,320	20.6	1190
	Cl:SO4	2.241	0.291	2.126	0.103
	pH	2.94	3.56	6.35	3.66
	Conductivity (mS)	4.41	1.81	0.32	0.97
	Groundwater table elevation (m below ground surface)	n/a	-1.7	n/a	-1.6
	Temperature (C)	14.3	15.9	12.1	13.7
14	Total Fe (mg/L)	23.3	33	7.7	94.3
	Al3+ (mg/L)	52.8	134.5	47.5	5.9
	Ca2+ (mg/L)	23	14.6	47	158
	Mg2+ (mg/L)	125.6	112.3	8930	57.8
	Cl (mg/L)	1922.3	2554.9	91.9	141.9
	SO4 (mg/L)	574	586	27.9	716
	Cl:SO4	3.349	4.360	3.294	0.198
	pH	2.77	3.06	6.44	3.47
	Conductivity (mS)	6.14	8.65	0.34	1.82
	Groundwater table elevation (m below ground surface)	n/a	-1.1	n/a	-1.3
	Temperature (C)	12.1	14.3	11	13.2
28	Total Fe (mg/L)	36	111.4	12.2	79.1
	Al3+ (mg/L)	43.2	80.8	32	71
	Ca2+ (mg/L)	49	42	14	14
	Mg2+ (mg/L)	368	1970	1920	34.4
	Cl (mg/L)	1,692	2,426	77	87
	SO4 (mg/L)	491	588	38	699

	Cl:SO4	3.446	4.126	2.046	0.125
	pH	3.02	3.04	6.97	3.33
	Conductivity (mS)	4.7	5.55	0.34	1.62
	Groundwater table elevation (m below ground surface)	n/a	-1.1	n/a	-1.25
	Temperature (C)	12	12.1	9.1	12.6
42	Total Fe (mg/L)	274	84.5	5.7	45.4
	Al3+ (mg/L)	26.6	60.4	3.1	52.8
	Ca2+ (mg/L)	112	73	17	22
	Mg2+ (mg/L)	52	18	33.2	18.4
	Cl (mg/L)	5455.4	3488.7	240.8	317.9
	SO4 (mg/L)	793	707	55.9	754
	Cl:SO4	6.879	4.935	4.309	0.422
	pH	2.79	2.86	6.22	3.19
	Conductivity (mS)	6.54	5.46	0.41	1.8
	Groundwater table elevation (m below ground surface)	n/a	-1.15	n/a	-1.3
	Temperature (C)	12	12.3	10.7	11.3
56	Total Fe (mg/L)	30.3	56.2	~	58.1
	Al3+ (mg/L)	31	109.8	~	61.9
	Ca2+ (mg/L)	184	93	~	23
	Mg2+ (mg/L)	723	579	~	225
	Cl (mg/L)	6673.5	8,313	~	248.2
	SO4 (mg/L)	1150	1,280	~	694
	Cl:SO4	5.803	6.494	~	0.358
	pH	3.19	3.1	~	3.32
	Conductivity (mS)	15.25	13.26	~	2.11
	Groundwater table elevation (m below ground surface)	n/a	-1.1	~	-1.4
	Temperature (C)	~	~	~	~
70	Total Fe (mg/L)	20.8	110.9	4.9	103.1
	Al3+ (mg/L)	23.5	104.3	13.8	60.5
	Ca2+ (mg/L)	144	73	10	18
	Mg2+ (mg/L)	714	335	85	103
	Cl (mg/L)	7705.1	6116.6	100.4	115.2

	SO4 (mg/L)	1020	1000	90.8	775
	Cl:SO4	7.554	6.117	1.105	0.149
	pH	3.08	3.19	5.99	3.73
	Conductivity (mS)	13.38	11.25	0.4	1.91
	Groundwater table elevation (m below ground surface)	n/a	-1.1	n/a	-1.3
	Temperature (C)	11.7	11.3	9.7	11.7
84	Total Fe (mg/L)	~	151	35	131.5
	Al3+ (mg/L)	14.1	84.4	21.3	68.5
	Ca2+ (mg/L)	~	118	21	18
	Mg2+ (mg/L)	~	400	133	134
	Cl (mg/L)	880	466	95	128
	SO4 (mg/L)	1,240	1,030	284	866
	Cl:SO4	0.710	0.453	0.334	0.147
	pH	3.36	3.08	3.58	3.42
	Conductivity (mS)	15.47	11.77	0.68	1.92
	Groundwater table elevation (m below ground surface)	n/a	-1.08	n/a	-1.4
	Temperature (C)	14.3	13.3	12.6	12.3
99	Total Fe (mg/L)	29.9	206	156.6	145
	Al3+ (mg/L)	4.4	54.1	21.1	47.3
	Ca2+ (mg/L)	195	163	29	23
	Mg2+ (mg/L)	614	570	113	191
	Cl (mg/L)	8320.89	5929.9	95.8	170.5
	SO4 (mg/L)	1700	1220	469	913
	Cl:SO4	4.895	4.861	0.204	0.187
	pH	2.8	3.34	4.37	4.73
	Conductivity (mS)	14.85	12.54	0.06	0.8
	Groundwater table elevation (m below ground surface)	n/a	-1.13	n/a	-1.4
	Temperature (C)	21.7	~	~	~
125	Total Fe (mg/L)	~	161.1	33.5	30.1
	Al3+ (mg/L)	~	13.9	29.4	65.3
	Ca2+ (mg/L)	~	43	4	9
	Mg2+ (mg/L)	~	181	156	189